# UNIVERSITÉ DE STRASBOURG

*ÉCOLE DOCTORALE 414 : Sciences de la vie et de la santé*

**Architecture et Réactivité de l'ARN – IBMC Strasbourg**

# THÈSE présentée par :

**Laura ANTOINE**

Soutenue le : 21 juillet 2021

Pour obtenir le grade de : **Docteur de l'université de Strasbourg**

Discipline/ Spécialité : Aspects Moléculaires et Cellulaires de la Biologie

# Caractérisation des modifications post-transcriptionnelles des ARN non codants chez *Staphylococcus aureus* en réponse à divers stress environnementaux : analyse dynamique et fonctionnelle

**THÈSE dirigée par :**
**M. MARZI Stefano** — CR1, CNRS, Université de Strasbourg

**RAPPORTEURS :**
**Mme TISNÉ Carine** — DR1, CNRS, Université de Paris
**M HELM Mark** — Associate Professor (W2), Johannes Gutenberg University (JGU), Mainz

**EXAMINATEUR INTERNE:**
**Mme FRUGIER Magali** — DR2, CNRS, Université de Strasbourg

*A la mémoire de Clément,*

# Remerciements

*Je tiens tout d'abord à remercier les membres du jury d'avoir accepté d'évaluer mon travail ; Carine Tisné, Mark Helm et surtout Magali Frugier, qui suit l'évolution de ma thèse depuis le début. Merci à toi et à Philippe Giegé pour votre disponibilité et vos conseils.*

*Pascale, merci pour ta patience et ta gentillesse. Merci à toi ainsi qu'à Eric Westhof de m'avoir laissé ma chance et accueillie au sein de l'unité, pour votre soutien et les nombreuses discussions, toujours passionnantes et instructives.*

*Merci à Stefano de m'avoir encadrée, encouragée et pour les conversations toujours enrichissantes. Merci d'avoir eu la patience de m'expliquer un nombre incalculable de trucs, d'avoir écouté mes suggestions et surtout, merci pour ta bienveillance à toute épreuve, même quand je rate l'avion pour Krakow.*

*Les membres du labo 436, merci pour les conversations pendant les tea-time et tous les bons moments passés au labo avec vous.*
*Merci beaucoup à Isa et Papy pour les conseils de microbiologistes, votre disponibilité et votre écoute. Merci Papy Chulo pour la miniature du clip !*
*Merci beaucoup à Emma d'avoir été là, de m'avoir soutenue et conseillée depuis le tout début du master. Et surtout merci de m'avoir rappelé à chaque fois qu'il y avait des inscriptions à faire ou des papiers à rendre ça m'a sauvé plus d'une fois*
*Noémie, merci pour les pauses clopes à m'écouter me plaindre et parler de mes animaux et de mes plantes. Et merci aussi d'avoir gardé mon chat quand je n'étais pas là le weekend.*
*Lucas, merci d'être l'homme de la situation, l'homme du ribosome profiling, qui a retiré les tubes bloqués dans le rotor ! Quel homme ce Lucas ! Merci de m'avoir aidé !*
*Laura B, merci d'avoir tué la plante que je t'ai offert à noël. Tu n'es plus Laura 2 maintenant, profites bien de ton nouveau statut d'unique Laura du labo ;).*
*Hiroki and Roberto, it was a pleasure to work with you, I hope I helped with your tRNA and ribosome purifications. Thank you Hiroki for the conversations about french pastries. Thank you Roberto for the conversations during evenings in the lab.*

*Je remercie également Philippe Wolff de m'avoir mis le pied à l'étrier et formée à la spectrométrie de masse des ARN. Merci de m'avoir supportée et conseillée dès de début de mon stage de master. Merci également à tous les membres de la plateforme protéomique pour leur soutien et leur aide pour les analyses de protéines*

*Merci aussi à tous les phD de l'unité pour les phD seminars et les phDrink. Merci surtout à José et Luc pour leur amitié et leur soutien. Merci aussi pour les soirées et les débats devant des russes blancs*

*Je remercie aussi les personnes de la promo du master chimie-bio de Strasbourg pour leur accueil incroyable et leur soutien. Merci à Najet, Mike, Juline pour les soirées. Merci à Marine et Camille pour les brunchs du dimanche au restaurant végétarien et merci à Jérémy pour les poissons et les soirées tartes flambées au gîte. Merci à Stéphane pour les randos ensemble et les soirées à l'o'brien.*

*Merci à Myriam Seemann et Philippe Chaignon pour m'avoir pris pour mon premier stage, m'avoir appris les enzymes à cluster et m'avoir encouragée comme vous l'avez fait.*

*Un grand merci à OC, Mika et surtout Nanoo, merci pour tout, merci d'avoir été là, même de loin, depuis plus de 20ans !*

*Merci à la famille, les cousins et cousines, les oncles et tantes pour leur soutien infaillible et les moments inoubliables au cabaret vert et bon courage Solweig pour ta thèse, que du bonheur, tu verras !*
*Merci également à Jérémy et aux parents, spécialement à maman, merci pour tout Maman. Je t'aime.*

*Enfin merci à Nemo d'être à mes côtés depuis 15 ans maintenant, de m'avoir soutenue et supportée depuis toutes ces années et surtout d'avoir été si gentil et si patient avec moi ces derniers mois (ou ces dernières années ?). Je t'aime.*

# Résumé de la thèse

## Caractérisation des modifications post-transcriptionnelles des ARN non codants chez *Staphylococcus aureus* en réponse à divers stress environnementaux : analyse dynamique et fonctionnelle

**Introduction :**

Les ARN non codants jouent un rôle essentiel pour la cellule, notamment lors de la traduction. En effet, les ribosomes sont constitués essentiellement d'ARN ribosomiques (ARNr) et les ARN de transfert (ARNt) assurent le décodage des ARN messagers (ARNm). Le processus de traduction des ARNm en protéines peut être régulé par d'autres ARN non codants appelés petits ARN régulateurs (sARN).

Les modifications post-transcriptionnelles influencent la structure de l'ARN et les propriétés chimiques des nucléosides. Les ARNt et les ARNr présentent le plus grand nombre de modifications, qui par conséquent jouent un rôle prépondérant pour leurs fonctions, pour l'efficacité et pour la vitesse de la traduction. Par exemple, la modification en position 34 (la base « wobble ») des ARNt est indispensable tant pour le décodage de différents codons correspondant à un même acide aminé que pour la discrimination de codons proches[1]. Pour les bactéries pathogènes, ces modifications post-transcriptionnelles sont impliquées dans l'adaptation à l'environnement, dans l'expression de gènes de virulence[2] et dans les interactions avec l'hôte lors d'infections. La présence de modification en position 34 des ARNt est liée à la virulence chez *Streptococcus pyogenes*[3]. Par ailleurs, la présence ou l'absence d'une modification sur les ARNr peut conférer une résistance aux antibiotiques ciblant le ribosome[4].

Dans ce contexte, cette étude a porté sur *Staphylococcus aureus*, une bactérie commensale de l'Homme présente chez 1 individu sur 3 et aussi un pathogène opportuniste responsable d'infections nosocomiales et communautaires [5]. L'émergence de souches multi-résistantes aux antibiotiques est un véritable problème de santé publique, notamment dans le milieu hospitalier. En tant qu'opportuniste, *S. aureus* possède une grande capacité d'adaptation en réponse aux changements environnementaux. Cette capacité lui permet, via la régulation très fine de l'expression des facteurs de virulence, d'être à l'origine de nombreuses infections pouvant être très graves. A ce jour, le rôle des modifications post-transcriptionnelles dans les processus adaptatifs et l'infection par *S. aureus* reste encore inconnu.

A l'aide d'analyses de spectrométrie de masse associées à différentes méthodes de séquençage à haut débit des ARN (RNA-Seq), cette étude consiste à établir une cartographie des modifications post-transcriptionnelles des ARN non codant chez *S. aureus*. Elle vise ensuite à déterminer leurs potentielles variations en fonction de conditions de stress mimant l'environnement durant une infection afin de mieux comprendre leur impact sur la croissance bactérienne, les réponses aux stress et dans la virulence.

**Résultats :**

Afin de caractériser les modifications post-transcriptionnelles des ARNt de *S. aureus*, j'ai mis en place, en collaboration avec Philippe Wolff (UPR 9002, responsable de l'analyse de spectrométrie de masse appliquée aux ARN), une méthode de purification et d'identification par chromatographie liquide couplée à la spectrométrie de masse UPLC-MS/MS (Ultra Performance Liquid Chromatography Tandem Mass Spectrometry)[6,7]. La cartographie réalisée par spectrométrie de masse dans les ARNt de *S. aureus* étant partielle, elle a été complétée et confirmée par différentes méthodes de RNA-Seq telles que le Psi-Seq, le RiboMethSeq et l'Alkaniline-Seq[8], en collaboration avec le Pr Yuri Motorin et la Dr Virginie Marchand de la plateforme Epitranscriptomique et Séquençage (EpiRNA-Seq) de Nancy. Les données RNA-Seq ont également permis d'obtenir des informations sur les modifications présentes sur les ARNr (**Figure 1**). Celles détectées dans les ARNt de *S. aureus* sont très proches de celles caractérisées chez d'autres bactéries à Gram positif tel que *Lactococcus lactis*[9]. De façon inattendue, mon étude a également révélé des éléments uniques aux ARNt de *S. aureus*. Précisément, les ARNt de la glycine qui en plus d'être impliqués dans la traduction des protéines, participent également à la formation du pont pentaglycine présent dans la paroi cellulaire des Staphylocoques. Les ARNt responsables du transport de la glycine vers la paroi ont été analysés et ne possèdent pas les modifications spécifiques des ARNt impliqués dans l'incorporation des glycines dans les protéines, specifiquement au niveau de leurs anticodons. De plus, la présence d'une modification dont la masse ne correspond à aucune modification connue à ce jour a pu être détectée en position 37 de l'ARNt de la lysine. Ces résultats ont conduit à un nouveau projet d'étude dans le laboratoire pris en charge par un chercheur post-doctorant afin de déterminer le rôle des modifications (ou leur absence) dans la discrimination des $ARNt_{Gly}$.

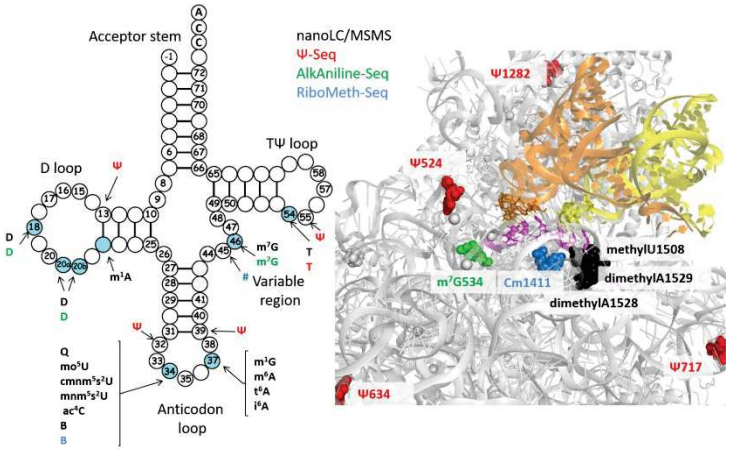


**Figure 1.** Modifications cartographiées par différentes méthodes dans les ARNt à gauche et l'ARNr 16S de *S. aureus* à droite

Une fois la cartographie établie en condition normale de croissance en laboratoire, différentes conditions de stress mimant ceux rencontrés lors de l'infection et les interactions avec l'hôte (augmentation de la température, privation de nutriments, hypoxie, stress oxydant ou nitrique et présence d'antibiotiques) ont été réalisés. Plusieurs de ces conditions, montrent des variations flagrantes dans le profil de migration des ARNt sur gel de polyacrylamide qui peut résulter de changements dans les modifications (**Figure 2A**). Dans certaines conditions, tel que le stress induit par l'oxyde nitrique (NO), une analyse complète de spectrométrie de masse ainsi que de RNA-Seq de chaque ARNt sera nécessaire pour déterminer si un changement a lieu. Cependant, une condition spécifique qui a montré clairement une variation de migration d'ARNt est le stress oxydant induit par l'addition de méthylviologen entrainant la formation d'espèces réactives de l'oxygène (ROS). La production de ROS est une des défenses principales du système immunitaire contre les infections. Les macrophages produisent des anions superoxydes, du peroxyde d'hydrogène ainsi que des oxydes nitriques en réponse à la phagocytose de bactéries. De plus, ces espèces réactives de l'oxygène et de

l'azote sont impliquées dans l'inflammation et les lésions tissulaires qui sont également hypoxiques[10]. Dans ce contexte, j'ai donc décidé d'étudier l'impact du stress oxydant induit par le méthylviologen sur les modifications des ARNt ainsi que les conséquences qu'une modification différentielle peut avoir sur le processus de traduction.

L'analyse des modifications des ARNt par UPLC-MS/MS montre un clivage par la RNase T1 de l'ARNt$_{TyrGUA}$ en 3' de la queuosine en position 34 qui n'a pas lieu en absence de l'agent oxydant (**Figure 2A**). Cet effet suggère que la queuosine, modification complexe et importante impliquée dans le décodage de l'ARNm lors de la traduction, est absente en condition de stress oxydant. L'absence de queuosine dans les bactéries cultivées en en condition de stress oxydant a été confirmée dans les quatre ARNt (ARNt Tyr, His, Asp et Asn) contenant cette modification par électrophorèse d'affinité au boronate et par analyse UPLC-MS/MS des ARNt purifiés. Pour l'électrophorèse d'affinité, des ARN totaux provenant d'une souche de *S. aureus* n'exprimant pas l'enzyme Tgt, responsable du transfert de l'intermédiaire preQ1 sur l'ARNt ont été également utilisés (**Figure 2B**). Grâce à cette méthode, j'ai également montré qu'il était possible de restaurer la présence de queuosine par l'ajout du preQ1 dans le milieu de culture des bactéries soumises au stress oxydant (**Figure 2B**) indiquant une possible inactivation d'une des enzymes impliquées dans la voie de biosynthèse du preQ1 lors du stress.

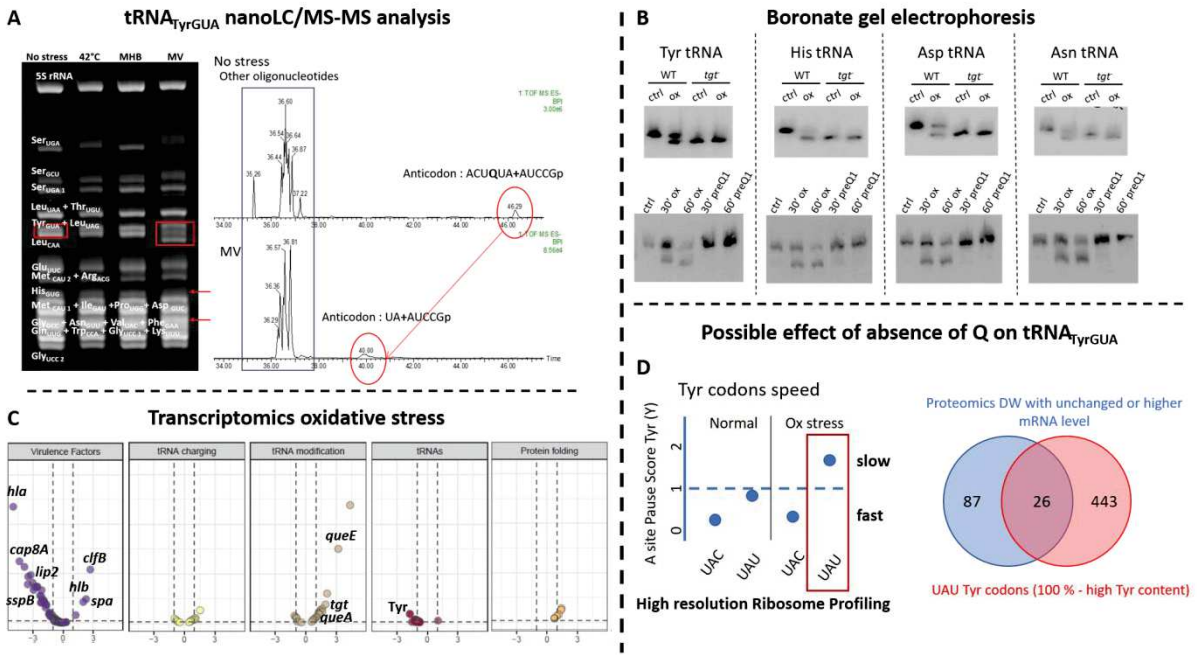


**Figure 2. A. Analyse des ARNt dans différentes conditions de stress environnementaux**, à gauche : gel de polyacrylamide (12,5%, 8 M urée) des ARNt de *S. aureus* cultivés en conditions normales (no stress), à 42°C (augmentation de la température), en milieu MHB (Mueller-Hinton Broth : privation de nutriments) ou stress oxydant (MV : méthylviologen). Les ARN présents dans chaque bande ont été identifiés par UPLC-MS/MS. A droite : chromatogrammes obtenus à partir des bandes encadrées en rouge contenant l'ARNt$^{Tyr}_{GUA}$, encerclés en rouge les pics correspondants aux anticodons, non clivé par la RNase T1 pour l'ARNt issu de la culture non stressée, clivé pour celui issu de la culture soumise au stress oxydant. Q: queuosine; +: N6-isopentyl Adénosine. **B. Electrophorèse d'affinité au boronate,** ligne du haut : profil de migration des 4 ARNt contenant la queuosine de la souche WT en condition normale et en condition de stress oxydant et de ces ARNt sans queuosine provenant de la souche n'exprimant pas le gène *tgt*. Ligne du bas : profil de migrations des ARNt en conditions de stress oxydant et après addition de l'intermédiaire de la queuosine preQ1. **C. Volcano plot représentant la transcription différentielle de plusieurs types de gènes** tels que les facteurs de virulence, ceux impliqués dans le repliement des protéines et dans les fonctions des ARNt en conditions de stress oxydant. **D. Impact de l'absence de queuosine de l'ARNt$^{Tyr}$ sur la traduction.** A gauche : taux de pause des deux codons UAC et UAU de la tyrosine montrant un décodage plus lent du codon UAU en condition de stress oxydant. A droite : diagramme de Venn indiquant les gènes sous exprimés en protéomique pour lesquels le niveau de transcription ne change pas, voire augmente et dont les ARNm sont riches en codons UAU.

Une altération de la queuosine en position 34 implique d'inévitables conséquences au niveau de l'efficacité de la traduction. L'absence de cette modification peut impacter la vitesse et la finesse de la reconnaissance des codons par l'ARNt, ainsi que la fidélité d'incorporation des acides aminés, entrainant la production de protéines anormales. Afin d'étudier les possibles causes et conséquences de l'anomalie de queuosine en position 34, des analyses protéomiques et transcriptomiques ont été réalisées montrant d'importantes variations dans l'expression des gènes marqueurs du stress oxydant mais également de nombreux facteurs de virulence impliqués dans la dissémination et la protection contre le système immunitaire (**Figure 2C**). Ces résultats sont à corréler avec une analyse de « high resolution ribosome profiling » (hRibo-seq) pour étudier la vitesse de traduction codon par codon. Les résultats préliminaires obtenus, montrent que durant le stress oxydant, les codons UAU nécessitent la présence de la queuosine en 34 de l'ARNt$^{Tyr}$ pour être décodés efficacement. En effet, ils présentent une diminution importante de leur vitesse de décodage, tandis que celle des codons UAC ne semble pas être impactée par l'absence de queuosine (**Figure 2D**). De manière remarquable, l'analyse protéomique en condition de stress oxydant révèle une dérégulation de la traduction pour de nombreux gènes alors que les niveaux d'ARNm demeurent inchangés, voire augmentent. Certains de ces ARNm présentent une composition particulièrement riche en codon UAU. L'analyse de hRibo-seq a été répétée en condition de stress oxydant mais aussi en présence de preQ1 pour discriminer plus clairement les effets exclusivement dus à l'absence de queuosine sur les 4 ARNt concernés. Cette étude est actuellement en cours.

**Conclusions et perspectives :**

La mise en place de L'UPLC-MS/MS en association avec les méthodes de RNA-Seq a permis d'établir les cartographies partielles des modifications présentes dans les ARN non codants de *S. aureus* afin d'étudier leurs variations, en particulier dans les ARNt lors de stress environnementaux mimant les conditions rencontrées lors de l'infection. J'ai ainsi mis en évidence, d'une part une altération de la queuosine des 4 ARNt possédant cette modification en position wobble de l'anticodon et d'autre part étudié l'impact sur la traduction de l'absence de cette modification. L'expérience de hRibo-Seq complète est en cours afin d'élucider la fonction de la queuosine sur le décodage de l'ensemble des codons nécessitant cette modification. Cette étude est réalisée en parallèle avec une analyse de la composition en nucléosides modifiés des ARNt afin de déterminer l'impact du stress oxydant sur les autres modifications post-transcriptionnelles présentes sur les ARNt totaux. Les données d'analyses de RNA-Seq de ribosomes provenant de bactéries soumises au stress oxydant induit par le méthylviologen sont en cours d'analyse. L'étude structurale de l'impact des variations de modifications des ARNt et ARNr sur l'ensemble de la machinerie traductionnelle se déroule en collaboration avec Roberto Bahena, qui est actuellement en première année de thèse.
Pour compléter l'étude de l'épitranscriptome de *S. aureus*, 4 sARN régulateurs (RsaA, C, G et I) ont également été analysés par RNA-Seq. Cependant, les résultats n'ont pas montré la présence de modifications post-transcriptionnelles. Des analyses UPLC-MS/MS seront nécessaires afin de confirmer l'absence de modifications dans ces sARN.
Cette approche que j'ai mise en place pour l'étude des variations des modifications des ARN en réponse au stress oxydant et de leur impact traductionnel, pourra être appliquée à l'adaptation de la bactérie à d'autres conditions environnementales rencontrées lors de l'infection pour lesquelles des profils différents de migration des ARNt ont été observés.
Bibliographie :

1. Rozov A, Demeshkina N, Khusainov I, Westhof E, Yusupov M, Yusupova G. Novel base-pairing interactions at the tRNA wobble position crucial for accurate reading of the genetic code. Nat Commun. 2016;7:10457. doi:10.1038/ncomms10457

2. Koh CS, Sarin LP. Transfer RNA modification and infection – Implications for pathogenicity and host responses. Biochim Biophys Acta BBA - Gene Regul Mech. 2018;1861(4):419-432. doi:10.1016/j.bbagrm.2018.01.015

3. Cho KH, Caparon MG. tRNA Modification by GidA/MnmE Is Necessary for Streptococcus pyogenes Virulence: a New Strategy To Make Live Attenuated Strains. Infect Immun. 2008;76(7):3176-3186. doi:10.1128/IAI.01721-07

4. Stojković V, Noda-Garcia L, Tawfik DS, Fujimori DG. Antibiotic resistance evolved via inactivation of a ribosomal RNA methylating enzyme. Nucleic Acids Res. 2016;44(18):8897-8907. doi:10.1093/nar/gkw699

5. Lowy FD. Staphylococcus aureus Infections. N Engl J Med. 1998;339(8):520-532. doi:10.1056/NEJM199808203390806

6. Antoine L, Wolff P. Mapping of Posttranscriptional tRNA Modifications by Two-Dimensional Gel Electrophoresis Mass Spectrometry. Methods Mol Biol Clifton NJ. 2020;2113:101-110. doi:10.1007/978-1-0716-0278-2_8

7. Antoine L, Wolff P, Westhof E, Romby P, Marzi S. Mapping post-transcriptional modifications in Staphylococcus aureus tRNAs by nanoLC/MSMS. Biochimie. 2019;164:60-69. doi:10.1016/j.biochi.2019.07.003

8. Motorin Y, Helm M. Methods for RNA Modification Mapping Using Deep Sequencing: Established and New Emerging Technologies. Genes. 2019;10(1):35. doi:10.3390/genes10010035

9. Puri P, Wetzel C, Saffert P, et al. Systematic identification of tRNAome and its dynamics in Lactococcus lactis. Mol Microbiol. 2014;93(5):944-956. doi:10.1111/mmi.12710

10. Eltzschig HK, Carmeliet P. Hypoxia and inflammation. N Engl J Med. 2011;364(7):656-665. doi:10.1056/NEJMra0910283

# Liste des Abbreviations

Acides nucléiques :

ADN : acide désoxyribonucléique

ARN : acide ribonucléique

ARNm : ARN messager

ARNr : ARN ribosomique

ARNt : ARN de transfert

Composés chimiques et milieux de cultures

NO : oxyde nitrique

ROS : espèces réactives de l'oxygène

APB : Acide phénylboronique

BHI : Brain heart infusion : infusion cœur cerveau

MV : Méthylviologen

TEA-Cl : chlorure de tetraéthyl ammonium.

Bactéries

*S. aureus : Staphylococcus aureus*

*B. subtilis : Bacillus subtilis*

*L. lactis : Lactococcus lactis*

*E. coli : Escherichia coli*

MRSA : Methicillin Resistant *S. aureus* (résistante à la méthicilline)

Protéines et facteurs de virulence :

Ahp : Alkyl hydroperoxyde réductase

Clf: Clumping factor (facteur d'agglutinement)

Efb : Extracellular fibrinogen binding protéine (protéine de liaison au fibrinogène extracellulaire)

Fnbp : Fibronectin binding protein (Protéine de liaison à la fibronectine)

Isd : Iron-Regulated Surface Determinant

MSCRAMM : microbial surface components recognizing adhesive matrix molecules (composants de la surface microbienne reconnaissant les molécules adhésives de la matrice)

PSM : Phenol Soluble Modulins

Sod : Superoxyde dismutase

SpA : Staphylococcal protein A (protéine staphylococcique A)

TSST : Toxic shock syndrome toxin (toxine du syndrome de choc toxique)

Techniques

LC : chromatographie liquide

MS : Spectrométrie de masse

# Table des Matières

Remerciements ..... 1

Résumé de la thèse ..... 5

Liste des Abbreviations ..... 11

Table des Matières ..... 12

I. Introduction ..... 15

1. Rôle des modifications post-transcriptionnelles chez bactéries pathogènes ..... 15

2. *Staphylococcus aureus* ..... 40

3. L'oxydation comme défense contre les pathogènes ..... 43

4. *S. aureus* et son adaptation au stress oxydant ..... 44

5. Objectifs de la thèse ..... 46

II. Résultats : ..... 47

1. Mise en place de la méthode d'analyse des ARN par gel en 2 dimensions et NanoLC-MS/MS ..... 47

*2.* Cartographie des modifications post-transcriptionnelles des ARNt de *S.aureus* ..... 58

3. Analyse de RNA-Seq des ARN non codants de *S.aureus* ..... 70

4. Réponse au stress oxydant : ..... 71

i. Analyse transcriptomique et protéomique ..... 72

ii. Dynamique des modifications des ARNt en réponse au stress oxydant ..... 74

iii. Analyse des ARNt contenant la Q34 issus de cultures stressées ..... 75

iv. Le précurseur preQ1 restaure la queuosine dans les 4 ARNt contenant la Q34 ..... 76

III. Discussion ..... 77

1. Mise en place de la méthode et cartographie des modifications ..... 77

i. Limites et méthodes complémentaires : le pouvoir de la coopération ..... 77

ii. Cartographie des modifications des ARN non codants de *S. aureus* ..... 78
2. Réponse globale de *S. aureus* au stress oxydant ..... 81
i. Système SOS de réparation de l'ADN et gènes phagiques ..... 81
ii. Détoxification des espèces réactives de l'oxygène ..... 82
iii. Métabolisme des acides aminés ..... 83
iv. Homéostasie du fer ..... 83
v. La voie de respiration en anaérobie ..... 83
vi. L'implication des ARNt et des enzymes de modifications ..... 84
vii. La persistance de la bactérie privilégiée au détriment de la dissémination et de l'infection aiguë ..... 85
3. Modifications des ARNt et stress oxydant ..... 85
i. Dynamique des modifications des ARNt durant le stress ..... 85
ii. Causes de l'absence de queuosine ..... 86
iii. Conséquences traductionnelles de l'absence de Q34 ..... 89
IV. Conclusions ..... 91
V. Matériels et méthodes ..... 93
1. Produits et sondes utilisés ..... 93
2. Souches bactériennes et conditions de culture ..... 93
i. Souches ..... 93
ii. Conditions de culture ..... 94
3. Analyse par NanoLC-MS/MS de l'ARNr 16S ..... 95
4. Analyse transcriptomique ..... 96
5. Analyse protéomique ..... 96
6. Gel d'acide phénylboronique et Northern blot ..... 97
7. Purification des ARNt ..... 97
8. Digestion à la RNAse U2 des ARNt purifiés. ..... 98

9. Modèlisation des structures de QueE et QueF de *S. aureus* ..... 98

10. Ribosome profiling à haute résolution ..... 98

Références bibliographiques ..... 100

Annexes ..... 111

Annexe 1 : Tableau de la transcription différentielle durant le stress oxydant ..... 111

Annexe 2 : Tableau de l'expression différentielle des protéines durant le stress oxydant : ..... 125

Annexe 3 : Tableau de l'expression différentielle selon les voies métaboliques impliquées. ..... 134

# I. Introduction

## 1. Rôle des modifications post-transcriptionnelles chez bactéries pathogènes

Les modifications post-transcriptionnelles des ARN sont impliquées dans de nombreux processus biologiques et sont présentes dans toutes les classes d'ARN. Ces modifications sont constitutives ou modulées en réponse à des processus adaptatifs. Elles remplissent de nombreuses fonctions puisqu'elles peuvent impacter l'appariement des bases, la reconnaissance par les protéines, le décodage ainsi que la structure et la stabilité des ARN. Cependant, leurs rôles dans les adaptations aux stress environnementaux ainsi que durant les infections causées par des bactéries pathogènes commencent juste à être appréciées. Avec le développement de technologies modernes de spectrométrie de masse et de séquençage, des exemples récents de modifications régulant les interactions hôte-pathogène ont été étudiés. Ils révèlent comment les modifications des ARN peuvent réguler la réponse immunitaire, la résistance aux antibiotiques, l'expression des gènes de virulence et la persistance bactérienne. Dans la revue suivante, écrite avec l'aide de Roberto Bahena, Stefano Marzi, Pascale Romby, ainsi que 3 étudiants de master, nous illustrons quelques-unes de ces découvertes et soulignons les stratégies utilisées pour caractériser les modifications des ARN et leur potentiel pour de nouvelles applications thérapeutiques. La revue sera soumise à Genes pour le numéro spécial "Functions and Dynamics of RNA Modifications".

*Review*

# RNA modifications in pathogenic bacteria: Impact on host adaptation and virulence

**Laura Antoine [1], Roberto Bahena-Ceron [1], Heemee Devi Bunwaree[1], Martin Gobry[1], Victor Loegler [1], Pascale Romby [1] and Stefano Marzi [1,*]**

[1] Université de Strasbourg, CNRS, Architecture et Réactivité de l'ARN, UPR 9002, F-67000 Strasbourg, France.

* Correspondence: s.marzi@ibmc-cnrs.unistra.fr

Received: date; Accepted: date; Published: date

**Abstract (200 words max: 138 words):**

RNA modifications are involved in numerous biological processes and are present in all classes of RNA. These modifications are constitutive or modulated in response to adaptive processes. RNA modifications play multiple functions since they can impact RNA basepairings, recognition by proteins, decoding, as well as RNA structure and stability. However, their roles in stress, environmental adaptation and during infections caused by pathogenic bacteria have just started to be appreciated. With the development of modern technologies in mass spectrometry and deep sequencing, recent examples of modifications regulating host-pathogen interactions have been demonstrated. They show how RNA modifications can regulate immune responses, antibiotic resistance, expression of virulence genes, and bacterial persistence. Here, we illustrate some of these findings, and highlight the strategies used to characterize RNA modifications, and their potential for new therapeutic applications.

**Keywords:** RNA modifications 1; pathogenic bacteria 2; host-adaptation 3; stress adaptation 4; ribosomal RNA 5; tRNA 6; small non coding RNA 7; mRNA 8;

## 1. Introduction

Bacteria are remarkably versatile organisms, which can survive and grow in numerous environmental niches on the planet. They modulate the expression of their genes to respond and adapt their growth to environmental stress such as temperature and pH shifts, nutrient availability, antimicrobials or dangerous chemical reactive species. This is particularly the case for pathogenic bacteria, which must adapt their metabolism to the host environment and ensure their survival facing the human/animal immune systems and antibiotic therapies. Bacteria can sense the environment directly via the effect that physical and chemical stresses might have on different macromolecules, or via signaling systems, very often two-component systems (TCS), transducing the stress signal from a specific sensor histidine kinase to a corresponding response regulator [1]. The responses are aimed at eliminating the stressor or its effects, at repairing damages or at inducing the escape from the stress, but sometime the external stimuli are signals for switching to programmed life-style changes. They produce profound changes in cell physiology and behaviors, and affect gene expression at transcriptional, post-transcriptional, translational, and post-translational levels. In these processes, an interplay between various TCS, transcriptional protein regulators, and regulatory RNAs orchestrates complex regulatory networks in order to link metabolism adaptation and virulence [2]. Because RNAs, occupy a central position in translation (tRNAs, rRNAs, mRNAs), they actively contribute to these regulatory networks.

In bacteria, the rate of translation is modulated by multiple signals present in mRNAs affecting translation initiation, elongation, termination, and ribosome recycling [3-6]. The mRNA translation initiation signals can be masked or liberated by the binding of proteins or small regulatory RNAs (sRNAs), or by structural rearrangements occurring in response to metabolite binding or to physical cues changes, which also directly affect transcription and RNA folding [7-12]. Besides, codon usage specific for each gene (codon bias) is used in relation to variation of the tRNA pool to fine tune gene expression [13]. Moreover, many studies have emphasized the physiological importance of ribosome heterogeneity to rapid modulation of selective gene expression in response to environmental conditions [14, 15]. These mechanisms are influenced by base or ribose modifications present in RNAs [16] adding another sophisticated layer of regulation. In fact, stresses can alter RNA modification states of various RNA species (i.e., rRNA, tRNA, sRNA and mRNA) with effect on translation rates, on RNA regulatory properties, or on codon recoding.

The number of newly detected modifications enhances at a constant pace [17]. They can be very simple like methylation or deamination, or be more complicated. Some of them require the consecutive action of several modification enzymes and cofactors [18]. These modifications modulate

the chemical and physical properties of the nucleotides and in turn the RNA functions (for a review see [19]). They might change any of the nucleotide interacting edges, which can potentially affect Watson-Crick base-pairing and non-canonical interactions [20]. For example, the A-form RNA helix, favored by C3′-*endo* sugar pucker, is stabilized by 2′-OH methylation of ribose [21, 22] while dihydrouridine (D) significantly destabilizes the C3′-*endo* sugar conformation, providing structure flexibility [23]. Interestingly, D is predominantly found in psychrophile bacteria and archaea [23]. Methylation on the bases can influence hydrogen-bonding and stacking interactions [24]. Pseudouridine (Ψ) can shift between *syn*/*anti* conformations with relatively greater ease [25]. The dynamic nature and the regulatory functions of some of these RNA modifications [26] have generated a new field referred to 'epitranscriptomics' [27]. The detection of the bacterial epitranscriptome relies on cutting edge methodologies involving combination of mass spectroscopy (LC/MSMS) and RNA-seq based methodologies. Nevertheless, identification of the epitranscriptome of pathogenic bacteria and its modulation upon stress and during the infection process is only in its infancy.

In this review, we illustrate several examples of the involvement of RNA modifications on the expression of virulence genes and in stress responses of different pathogenic bacteria. Even though these studies provide mechanistic explanations for only few cases, they already reveal a multitude of strategies developed by pathogenic bacteria to survive, persist, and fight against host immune defenses based upon the modulation of RNA modifications.

## 2. Technological advances: Detecting RNA modifications

A prerequisite to analyze the functions of RNA modifications is obviously to be able to detect the modified nucleosides, to quantify them, to map their localization within specific RNA. A detailed description of the available methods is outside the scope of the review. We will give here a summary of the most employed approaches with their limits and advantages (**Table 1**), and details will be found in more specific articles.

Mapping of post-transcriptional RNA modifications using mass spectrometry (MS) existed for over 30 years [28]. The precise measurement of molecular masses (less than 1 Da) provided the possibility to characterize known modified residues in tRNAs using liquid chromatography coupled to mass spectrometry (LC/MSMS). Two complementary MS approaches are routinely used to get a complete repertoire of modified nucleosides obtained either from tRNA extracts in a single experiment [29-31], or from tRNA fragments produced from specific endoribonuclease digestion to determine both the nature of modifications and their location in the tRNA sequence [32, 33]. The analysis of a pure RNA or a class of RNAs hydrolyzed into nucleosides allows precise characterization and quantification of modifications, while oligonucleotide analysis allows precise localization of

modified sites on sequence, but no quantification can be achieved. Moreover, the method does not allow complete sequence coverage and the use of RNases with different sequence specificity can increase it. Capillary electrophoresis coupled to MS (CE/MSMS) allows precise analysis of a wide range of molecules (reviewed in [34]), and can also be used for the characterization of tRNA modifications with the two approaches. Because capillary electrophoresis allows analysis of small oligonucleotide fragments, the combination of LC/MSMS and CE/MSMS leads to a better sequence coverage on pure tRNAs [35]. Nevertheless, one of the major limitations of these MS methods is the detection of Ψ, which is an isomer of uridine and for this reason is a mass-silent modification. The MS analysis of Ψ can be done because they can be selectively modified by 1-cyclohexyl-(2-morpholinoethyl)carbodiimide metho-p-toluene sulfonate (CMCT) [36]. The carbodiimide (CMC) moiety of CMCT modifies the N1 of guanosine, the N3 of uridine, and the N1 and N3 of Ψ, but alkaline treatment at pH 10.3 easily removes it from them, with the exception of the N3 of Ψ, therefore producing a detectable mass increment of 252 Da [37]. More recently, pseudouridines have been also detected directly in RNA fragments by pseudo-$MS^3$ (MS/MS/MS) analysis [38] thanks to the specific signature ion at *m*/*z* 207.041 for double dehydrated Ψ [39].

Various high throughput sequencing methods are often used to characterize specific modifications by Reverse Transcriptase (RT) signatures after chemical treatment. These methods do not need to purify the RNA prior to the analysis but they need bioinformatics data treatment and statistical evaluation of errors. NGS-based methods are often not quantitative, have high false-positive rates [40] and require multiple ligation steps and extensive polymerase chain reaction amplification during the library preparation, introducing undesired biases in the sequencing data [41]. Currently, customized protocols must be optimized for each RNA modification type, leading to experimental designs in which the RNA modification type to be studied is chosen beforehand, limiting the ability to characterize the plasticity of the epitranscriptome in a systematic and unbiased manner. A recent review described in details the RNAseq based approaches [42]. We will just mention here the very recent development of single molecule direct RNA sequencing methods developed by Oxford Nanopore Technologies (ONT), which are promising for the analysis of modification landscape on a specific RNA sequence [43-46].

Combination of these highly complementary methods allows a precise localization and characterization of post-transcriptional modifications and their dynamics, a prerequisite to a better understanding of the roles of RNA modification in bacterial adaptation.

| Methods | | | Modifications detected | Quantification | Genome wide | Positional information | Remarks (Pros/Cons) |
|---|---|---|---|---|---|---|---|
| Structure determination | X-ray Cristallography | | All modifications | ✗/✓ | ✗ | ✓ | Difficult to obtain crystals |
| | Cryo Electron Microscopy | | | | | | Heterogeneous resolution |
| | Nuclear Magnetic Resonance | | | | | | Size limit |
| LC/MSMS | Nucleoside analysis | DMRM [28] | Known modifications | ✓ | ✓ | ✗ | Fragmentation pattern and retention time of modifications must be known |
| | | NLS [28] | Various modifications | ✓ | ✓ | ✗ | NLS is less suitable for quantification than DMRM |
| | Fragment analysis | With a reference (SILNAS/CARD/SILCARD) [47, 48] | Known modifications | ✓ | ✗ | ✓ | Relative quantification can be assessed with reference *in vitro* RNA |
| | | Without reference (RNase digests) [33] | Known modifications | ✗ | ✗ | ✓ | Determination of base composition and localization by comparing mass-spectrometry results with expected RNase fragments |
| NGS-based methods | RNA deep-sequencing direct method | | A-to-I [49] | ✓ | ✓ | ✓ | To be accompanied by DNA sequencing to distinguish editing events from SNPs |
| | | | Methylations [50] | ✗ | ✗ | | Based on RT stops or missincorporations |
| | Nanopore RNA sequencing [51, 52] | | $m^6A$, $m^5C$, A-to-I, Ψ and others | ✓ | ✓ | | Based on the use of systematic base-calling 'errors' caused by the presence of RNA modifications. Software is still in development |
| | Indirect methods: chemical treatments | ICE-Seq [53, 54] | A-to-I | ✓ | ✓ | | No need of DNA seq |
| | | Bisulfite-Seq [55] | $m^5C$ | | | | |
| | | Riboxi-Seq [56] | Nm | | | | |
| | | RiboMethSeq[57, 58] | | | | | |
| | | Pseudo-Seq[59] | Ψ | | | | |
| | | Ψ-Seq | | | | | |
| | | PSI-Seq[60] | | | | | |
| | | HydraPsi-Seq [61] | | | | | |
| | | SLAM-Seq[62] | $s^4U$ | | | | |
| | | ARM-Seq[63] | $m^1A$, $m^3C$, $m^1G$ | | | | |
| | | TRAC-Seq[64] | $m^7G$ | | | | |
| | | AlkAniline-Seq[65] | $m^7G$, $m^3C$, D | | | | |
| | Indirect methods: IP | miCLIP[66] | Methylation | ✓ | ✓ | | |
| | | $m^6A$-Seq[67] | $m^6A$ | | | | |
| | | meRIP-Seq[68] | | | | | |
| | | $m^6A$-LAIC-Seq[69] | | | | | |
| | | Nm-Seq / 2OMe-Seq[70] | Nm | | | | |
| | | acRIP-Seq[71] | $ac^4C$ | | | | |
| | | NAD capture-Seq[72] | 5'-NAD cap | | | | |
| Affinity gel electrophoresis | Mercury-sulfur affinity[73] | | $s^2U$, $s^4U$ | ✗? | ✗ | ✗ | APM treatment (Acrylo-aminophenylmercuric chloride) |
| | Boronate affinity[74] | | NAD- or FAD-modified RNAs | ✓ | ✓ | ✗ | APB treatment (Acryloylaminophenyl boronic acid); fast screening (easy and quick); quantification possible as per intensity of bands |

**Table 1. Summary of main techniques for the detection of RNA modifications.**

## 3. Impact of RNA Modifications on Pathogenic Bacteria Stress Responses and Host Adaptation

### *3.1. rRNA Modifications*

The ribosome is a powerful molecular machine and a huge ribonucleoprotein complex (2.3 MDa in bacteria), which performs the crucial task of translating the genetic information into proteins. The ribosome is also a ribozyme with its catalytic centers made by RNAs [75]. To carry out translation, the ribosome needs to balance between speed and accuracy and rRNA base modifications participate to fine tune ribosome structure and function. Indeed, *in vitro* reconstituted *E. coli* ribosomes lacking rRNA modifications were severely defective in catalytic activity [76] and the ribosome assembly was also altered (Ofengand's lab). Numerous studies showed that the loss of rRNA modifications perturbs the active site structures [77, 78], and causes altered rates and accuracy of translation [79]. In bacterial ribosomes, there are three major types of rRNA modifications: Ψ, methylation of the 2'-hydroxyl group of riboses (Nm), and methylation of base (mN) [80]. Even if specific role for several of these modifications was not yet attributed, they confer specific properties to the nucleotides. For instance, they can induce enhanced (Ψ) or decreased (D) base stacking, structure rigidity (Ψ and Nm) or flexibility (mN) to both single- and double-stranded regions with possible altered hydrogen-bonding [25, 81]. These modifications are clustered in highly conserved areas devoted to decoding, peptidyl transfer, binding sites of A- and P- tRNAs, the peptide exit tunnel, and inter-subunit bridges [82, 83](**Fig. 1A and 1B**).

Bacterial rRNA modifications have been investigated by Mass Spectrometry (MS), Reverse Transcriptase extension (RT), RNAseq, and structure analysis. Several high-resolution structures of 70S ribosomes have been achieved both by cryo-EM and X-ray studies. However, cryo-EM structures can be non-uniform in local resolution and confident assignment of modifications is often possible on their most structurally stable core. Assignment of 35 modifications on bacterial rRNAs was first obtained on the cryo-EM structure of *E. coli* 70S-EF-Tu-tRNA complex solved at 2.65-2.9 Å resolution [84]. This study provides clues on their roles in fine-tuning ribosome structure and function and in modulating the action of antibiotics. In this structure, the methyl group of nucleosides could be clearly visualized as extra densities, as well as the non-planar dihydrouridine at position 2449 of 23S rRNA, while Ψs were identified indirectly by polar residues within hydrogen-bonding distance of the N1 position. Besides, the rRNA modifications were unambiguously identified in the *T. thermophilus* and *E. coli* crystal structures at 2.3-2.5-Å resolution, respectively [85, 86]. More recently, sub-stoichiometric modified nucleotides, like $m^7$G527 and $m^6$A1519 of the 16S rRNA, could be assigned on the structure of *E. coli* 70S solved at 2 Å resolution, and some antibiotic resistance mechanisms could be proposed [82] (**Fig. 1A**). In the past three years, cryo-EM analyses of 70S [83] and 50S [87] from *S. aureus* allowed the placing of 10 rRNA modifications (**Fig. 1B**).

Because the literature about the functions of rRNA modifications is very rich, we have chosen specific examples in different bacteria, which illustrate the variety of their functional impact. For clarity, we refer to the *E. coli* numbering of the 16S and 23S rRNA sequences. In the decoding region of the small 30S subunit, several modified nucleotides contact tRNA or mRNA, or are close to positions known to be important for translation, contributing to the building of the decoding site. For example, the *E. coli* $m^2G966$ contacts the P-site tRNA through stacking with nucleotide at position 34 of the tRNA [88]. Particularly, they stabilize the binding of initiator fMet-$tRNA^{fMet}$ to the 30S pre-initiation complex prior to start codon recognition [89]. The correct folding of the 16S rRNA around the initiator tRNA helps to discriminate the initiator tRNA against other tRNAs. In this context, $m^2G966$, $m^{6}{}_2A1518$ and $m^{6}{}_2A1519$ monitor the characteristic presence of the three consecutive GC pairs of the anticodon stem of the initiator tRNA [90]. In addition, $m^4Cm1402$ and $m^3U1498$ contact the P-site mRNA codon and play a role in fine-tuning the shape and function of the P-site [82] to increase initiation decoding fidelity [91]. In *S. aureus*, the $m^4Cm1402$ modifications are important for infection since *rsmI* and *rsmH* genes encoding the two methylases of C1402 protect *S. aureus* from oxidative stress and restore translational fidelity [92].

On the large ribosomal subunit, *E. coli* Gm2251 and Um2552 are located in the P- and A-loops, respectively, to establish interactions with the CCA end of tRNAs in P- and A- sites. Gm2251 is conserved in all three kingdoms of life [93], whereas Um2552 is present in many bacteria except that in some Bacillus species, like *B. subtilis* and *B. stearothermophilus,* methylation at the neighboring G2553 was observed [94]. Absence of Um2552 modification (*rlmE*-deficient mutant) increases the flexibility of the nucleotides next to it, and induces 50S maturation delay, slower subunit association, and slower translocation rate [95]. Surprisingly, translation with unmethylated U2552 appears to be more accurate suggesting that a certain degree of recoding provided by methylation of this residue is important for cell physiology [96].

The ribosome and more generally the translation apparatus are main targets of antibacterial therapies [97-100]. However, bacteria are continuously evolving resistance mechanisms for antibiotics. Acquisition of additional rRNA modifications is one of the most direct marks of antibiotic resistance. For example, aminoglycosides target the 30S subunit to prevent translocation and A-site tRNA binding, and promotes miscoding (**Fig. 1C**), while macrolides bind to the nascent peptide exit tunnel on the 50S subunit to prevent peptide bond formation and translocation [101, 102] (**Fig. 1D**). Methylation of their rRNA target sites inhibits antibiotics binding [103]. Interestingly, the modification enzymes responsible for the resistance are often inducible and only synthetized when necessary for survival. For example, in *S. aureus* sub-inhibitory concentrations of the macrolide erythromycin (**Fig. 1D**) stall ribosomes on the leader peptide for the methylase (*ermC*) responsible for the dimethylation

of A2058 at the ribosomal peptide exit tunnel of the 50S subunit [104] (**Fig. 1D**). This pausing induces the transcript to form a structure in which the Shine and Dalgarno sequence for *ermC* is exposed, allowing translation of *ermC* [104]. ErmC induced-dimethylation of A2058 prevents erythromycin binding (**Fig. 1D**), but also results in inefficient translation of selected polypeptides [104]. It is interesting to note that, *S.* aureus strains bearing $m^6{}_2$A2058 are not only erythromycin-resistant, but can also better escape host immune system, avoiding recognition by specific Toll-like receptors [105]. Other mechanisms of modifications inducing resistance but compromising bacterial fitness involve methylations of G1405 and A1408 in 16S rRNA, which are required for aminoglycoside resistance in Gram-negative bacteria (**Fig. 1C**). In fact, these additional modifications interfere with the natural methylation at the neighboring C1407 residue ($m^5$C1407) and decrease translation accuracy [106]. Conversely, antibiotic resistance could also arise from the lack of modifications at naturally occurring sites. Indeed, mutation of the *ksgA* gene encoding methyltransferase, causes a defect of modifications at A1518 and A1519 in the 16S rRNA, and induces kasugamycin resistance [107] accompanied by assembly defects and a cold sensitive phenotype [108]. Similarly, loss of methylation at $m^7$G527, which is located near the mRNA decoding site has been shown to confer low-level streptomycin and neomycin resistance [109, 110].

Finally, induction of rRNA modifications has been reported to be a key step in the ribosome reactivation during resuscitation of persistence state [111]. Indeed, antibiotic stresses together with a myriad of other stresses, are sometimes inducing the differentiation of a subpopulation of cells, which become dormant and multi-stress tolerant (persisters) [112]. This transient phenotype, which does not involve genetic changes, can be reverted via different mechanisms to re-activate ribosomes [113-115]. For instance, it has been recently shown by single-cell studies, that in *E. coli* cells resuscitate and ribosome activity is resumed by the action of the RluD enzyme, which is responsible of 23S rRNA pseudouridine (5-ribosyl-uracil) modification at positions 1911, 1915, and 1917 [111].

### *3.1. tRNA Modifications*

tRNAs are key molecules in translational process, their main purpose is to participate to protein synthesis by decoding the mRNA codons into the corresponding amino acids. They contain the largest number of modifications and the widest chemical diversity. Their modifications are known to improve tRNA decoding capacity, to decrease codon sensitivity, and to dictate codon choice and the maintenance of reading frame. Their localization concentrates in two hotspots - the anticodon loop and the tRNA core region, where the D- and TΨ -loops interact with each other (**Fig. 2**) (reviewed in [116, 117]).

Modifications in the tRNA core are important for the stability of tRNA structure and can contribute to temperature adaptation in thermophilic as well as in psychrophilic organisms [118]. Because they are involved in the tertiary interactions maintaining the L-shape, they are also expected to influence the binding of several proteins to the tRNA (i.e. EF-Tu, aminoacyl-tRNA synthetases, and anticodon modification enzymes) [119-121]. Different mutagenesis studies have demonstrated the role of these modifications in tRNA structure stabilization and their consequences on bacterial physiology during stress adaptation and on pathophysiology. The 2′-O methylation of Gm18, present on several tRNAs and common to all Gram-negative bacteria, is lacking in most Gram-positive species despite the presence of putative *trmH*-like genes. Methylation of the ribose stabilizes G18 in its C3′-endo form increasing its rigidity [122, 123] and promotes Gm18-Ψ55 base pairing (**Fig. 2**). The 5-methylation of U54 and the isomerization of U55 into Ψ55 enhance base stacking and stabilize the tRNA [124-126]. In the mesophilic *E. coli*, lack of the modification enzymes coded by the genes *trmH* (Gm18), *trmA* ($m^5U54$) and *truB* (Ψ55), reduces growth rate particularly at high temperature [127]. In the thermophilic *T. thermophilus*, adaptation to low temperature requires maintaining a sufficient flexibility of tRNAs. In this condition, methylation of the ribose of G18 is prevented but only if Ψ55 is present [128]. Moreover, the lack of some of these modifications induces changes in decoding and modulates frameshifting. In the pathogenic bacteria *Shigella flexneri*, Ψ55 is linked to the expression of several virulence factors, which are responsible of shigellosis, an intestinal infection causing diarrhea. Deletions of *trmH*, *trmA*, and *truB* genes in *S. flexneri* are associated with a reduction of the hemolytic activity and a decrease of the secretion system expression [127]. Furthermore, Gm18 is known to be responsible for TLR-7 dependent suppression of the immune response of dendritic cells, allowing a better tolerance of several enterobacteria by the host immune system [129-131].

The anticodon loop (ASL) is the other hotspot for modifications, which affect the geometry and physicochemical determinants governing the decoding process [132, 133]. The anticodon regions of all tRNAs bind to their cognate mRNA codons on the ribosome with similar affinities, despite diverse codon−anticodon pairings that should exhibit differences in basepairing strengths [134]. The modifications in the tRNA anticodon loop compensate for potential binding differences and ensures uniform affinities of all tRNAs to their cognate codons [135]. Perturbations of these modifications selectively alter the spectrum of proteins during adaptation via rare codon usage and translational frameshifting [136]. Specifically, modifications of nucleotide at position 37 and at the position 34 (wobble) have a strong impact on maintaining the reading frame [136, 137]. Modifications at positions 32 and 38, the first and last nucleotides of the loop, have also important consequences in modulating the affinity for specific codons, by inducing 32-38 basepairing and reducing the size of the loop [138]. This interaction is coordinated with the identity of codons. Strong GC-rich codon−anticodon

interactions are always balanced by a weaker 32–38 pairing and conversely, a weak AU-rich codon−anticodon interaction is coupled with a stronger 32–38 pairing [138]. Several studies have analyzed the link between modifications of anticodon loop residues and gene expression regulation. For example, the introduction of queuosine (Q) in the $tRNA^{Tyr}_{GUA}$, $tRNA^{Asn}_{GUU}$, $tRNA^{Asp}_{GUC}$ and $tRNA^{His}_{GUG}$ at the wobble position (G34) in Eukaryotes and Bacteria, permits efficient recognition of both NAC and NAU codons. This Q modification allows fine-tuning of translation and has been correlated with low-level translation of *Shigella* virulence factors, including the main transcriptional regulator VirF [139]. Its efficient translation depends on the presence of Q34 and 2-methylthio-N6-isopentenyladenosine ($ms^2i^6A37$) tRNA modifications. Deletion of either *tgt* (tRNA-guanine transglycosylase, for Q) or *miaA* (tRNA dimethylallyltransferase, for $ms^2i^6A$) genes leads to a less efficient synthesis of VirF in *S. flexneri* and reduces its pathogenicity [139]. In *E. coli*, it has been shown that $ms^2i^6A$ is important for translation of RpoS, the general stress response alternative sigma factor, which is particularly rich in UUX-Leu codons over CUX-Leu codons [140]. Similarly, *S. flexneri virF* contains a high proportion of UUX-Leu codons [141]. Although the mechanism by which Q induces *virF* translation is not known, it is noticeable that putrescine or a combination of methionine and arginine metabolically related to putrescine, restore VirF expression of *S. flexneri tgt* mutant [142]. Since polyamine like putrescine can modulate translational fidelity and maintenance of reading frame [143, 144], it is possible that translation misreading of *virF* could occur in absence of Q.

Studies on U34 hypermodifications reveal the central role of wobble U modifications and associated enzymes in bacterial adaptation to environmental conditions and virulence in pathogens. Even if the precise mechanism remains unclear, in the absence of modifications, frameshift occurs resulting in the expression of alternate proteins [136, 145]. Deletion of *gidA* and *mnmE*, encoding two enzymes of the 5-methylaminomethyl-2-thiouridine ($mnm^5s^2U34$) modification pathway, was shown to significantly reduce the colonization of *Salmonella Typhimurium* in liver and spleen, accompanied by decreased invasion of epithelial cells and compromised ability to survive and replicate inside macrophages [146]. This effect can be explained in part by the fact that several colonization genes important for host cell invasion, including the T3SS genes *invAEG*, *spaPQ*, and *prgHJ* were downregulated in the attenuated mutants [147]. In addition, in this strains it has been also observed the repression of several other proteins as the oxidoreductase Ygh, and the thiol peroxidase Tpx, which promote the survival of *S. Typhimurium* under the stressful conditions experienced within host macrophages [148]. The modified nucleotide $mnm^5s^2U34$ is also important for virulence in other bacteria. In *Streptococcus* species, Gram-positive bacteria responsible for a wide range of infections from skin infection to sepsis, GidA/MnmE modification enzymes are essential for acid stress and high temperature adaptation [149], for pathogenicity [150], reduced ability of adhesion and invasion in

epithelial cells, and increased sensitivity to phagocytosis [151]. Transposon mutagenesis in GidA gene is leading to sensitivity to acidic conditions also in *Cronobacter sakazakii*, an opportunist pathogen causing neonatal meningitis, enterocolitis, septicemia, bloody diarrhea and brain abscesses, decreasing its ability to growth in host digestive system [152]. One of the best-characterized example of host adaptation via the induction of specific tRNA modification at U34 to selectively translate codon-biased mRNAs for persistence genes, has been described for *Mycobacterium bovis* [153]. When mycobacteria species infect host lungs, they are phagocytized by alveolar macrophages, which are unable to kill and digest them. Consequently, the bacteria multiply and promote the formation of granulomas, which are symptomatic of chronic infections. Human granulomas lacking endothelial and blood vessel are highly hypoxic [154], and mycobacteria enter a quiescent state in which cell replication is halted or slowed [155]. In this condition, DosR, the master regulator of hypoxic bacteriostasis, mediates the expression of approximately 50 genes necessary for dormancy survival [156]. Translation activation of DosR requires shifting from $mo^5U$, presents at U34 in $tRNA^{Thr}_{UGU}$ in aerobic conditions, to $cmo^5U$ and $mcmo^5U$. This change of modification type, facilitates decoding of ACG codons, particularly abundant in *dosR* transcript [153]. The rationale for this decoding has been described by structural analysis [157]. The presence of $cmo^5U34$ induces a classical Watson-Crick base-pairing geometry involving the wobble position, which allows better stacking between U34 and purine 35, and as a consequence increases the stability of the codon-anticodon interaction.

In addition to wobble position, 2′-O-methylations of A, C, and U at position 32 by methyltransferases of the Trm family, have been shown to confer resistance to oxidative stress in *P. aeruginosa*, allowing its survival during infection [158]. Hypomethylation of the 2′-O-ribose moiety at position 32, linked to reduced catalase activity, perturbs codon-anticodon interaction and results in translation insufficiency and transcript misreading [159, 160]. Thiolation of cytidine at position 32 catalyzed by TtcA, a [Fe-S] cluster enzyme, has been shown to play a role in the response to oxidative stress during infections caused by *P aeruginosa* [161].

Finally, modifications of nucleotides in the variable loop have been shown to contribute to host adaptation. For example, $m^7G46$ catalyzed by tRNA guanine-N7-methyltransferase (*trmB*) is important for decoding efficiency of $tRNA^{Asp}_{GUC}$ and $tRNA^{Phe}_{GAA}$. In *P. aeruginosa*, loss of *trmB* has a strong negative effect on the translation of Phe- and Asp-enriched mRNAs, including those coding for the major peroxide detoxifying enzymes, the catalases KatA and KatB, resulting in oxidative stress-sensitive phenotype [162]. Using tRNA-seq and mass spectrometry performed on *Vibrio cholera* revealed specific modifications in various tRNAs that were not described in *E. coli* tRNAs [163]. These modifications include an acetylated acpU at either position 20 in the D-loop and at positions 46 or 47 in the variable loop. More interestingly, an editing process C-to- Ψ was for the first time identified at

position 32 of the anticodon loop of $tRNA^{Tyr}$. Although the physiological consequences of these specific features have to be defined, it is tempting to propose that RNA modifications contribute to the speciation of the bacteria and to the adaption of the organism to its specific niches.

*3.1. sRNA Modifications*

Small trans-acting regulatory RNAs (sRNAs) belong to a very heterogeneous class of RNAs regulating several processes including virulence gene expression, stress adaptation, and quorum sensing [164]. They exert their functions through specific interactions with diverse targets such as mRNAs, sRNAs, tRNA precursors, proteins or even with the ribosome [165]. The sRNAs are very different in length, sequence, structure and regulate gene expression using various mechanisms. So far only few examples of RNA modifications have been reported in bacterial sRNAs [166].

The best examples of regulatory RNAs, where modifications have been identified, are tmRNA and Y RNA, both mimicking the tRNA structure (**Fig. 3**). The tmRNA together with the small protein B (SmpB) is involved in trans-translation, the major and ubiquitous ribosome rescue system in bacteria [4]. This mechanism is taking place when ribosomes and tRNAs are stalled on problematic and often truncated mRNAs, which can lead to reduced translation [167]. Ribosome halting resulted from i) chemical mRNA damages produced by environmental stresses, ii) rare codons or problematic polypeptide stretches, iii) drugs inducing translational misreading, non-programmed frameshifting, or stop codons readthrough, and from iv) spurious RNase activity or cleavage of the mRNA in the A-site by RelE in response to starvation stress [168-172]. In these situations, trans-translation operates to liberate the ribosome, and simultaneously to degrade the nascent truncated peptide [4]. A vacant ribosomal A-site is the signal recognized by tmRNA/SmpB complex, which is delivered to the ribosome by the translation elongation factor EF-Tu. The tmRNA is characterized by two functional domains embedded into a conserved and complex structure, which are a tRNA-like domain (TLD) specifically aminoacylated with alanine and a mRNA-like domain (MLD) encoding a peptide tag targeting proteolysis [173, 174]. TLD presents a typical tRNA TΨ-loop with two Ψs and one $m^5U$ [175]. These modifications most probably enhance tRNA structural mimicry and its use in translation as a canonical tRNA (**Fig. 3**). Most probably that $m^5U54$ in tmRNA is introduced by the SAM-dependent methyltransferase TrmA as it is for the tRNAs [176]. Although tmRNA has been shown to be essential for the expression of virulence factors during *S. Typhimurium* infection [177], to our knowledge no studies have been conducted to establish the role of its modifications in bacterial adaptation or infection.

The non-coding Y RNAs are present in both eukaryotes and in several bacteria including some pathogens [178]. Bacterial Y RNA, known as YrlA (Y RNA-like A) RNA, is a modular RNA of variable

length (between 90 and 150 nucleotides) characterized by a large stem involving pairings between nucleotides at the 5′ and 3′ ends (**Fig. 3**) and a tRNA-like domain [179]. This domain shows high similarities to the D, TΨ and acceptor arms of tRNA (**Fig. 3**). Due to this structure similarity, YrlA is a substrate for two tRNA modification enzymes DusA and TruB, which introduce a dihydrouridine and a Ψ in the D and TΨ loops, respectively [180]. The basal stem of YrlA tethers the monomeric ring Rsr protein similar to eukaryotic Ro60 protein, while the effector tRNA-like domain binds the ring-shaped 3′ to 5′ exoribonuclease polynucleotide phosphorylase (PNPase), forming a double-ringed RNA degradation machine called RYPER [179]. Although the functions and mechanism of RYPER are still under investigation, Rsr and YrlA have been shown to alter PNPase substrate specificity to preferentially direct the degradation of structured RNAs (including rRNAs) [179, 181]. By altering the levels of specific RNA populations, RYPER has been proposed to be involved in stress responses, such as UV irradiation or prolonged stationary phase [182, 183]. In *Salmonella enterica*, expression of YrlA appears to be confined to certain infection stages [184]. Surprisingly, it was reported that lupus autoimmunity might be triggered and sustained by commensal bacteria expressing Rsr RNPs [185]. Noteworthy, in some bacteria including *S. Typhimurium*, *rsr* and Y RNA genes are located within an "RNA repair" operon together with the *rtcA* encoding RNA cyclase and *rtcB* encoding RNA ligase [179], which transcription is activated by tRNA fragments resulting from the SOS response to DNA damage [186]. tRNA fragments also accumulate when tRNAs are hypomodified, such as in *ΔtruA* strain where Ψ at positions 38, 39, and 40 in the anticodon arm of some tRNAs cannot be introduced anymore [187]. Since tRNA fragments are both natural substrates of PNPase and of RtcB religation, it is possible that assembly of RYPER protects them from degradation and that the expression of RtcB could restore tRNAs from halves and translation [186]. Interestingly, in *E. coli* RtcB re-ligates a 16S rRNA 3′ fragment containing the anti-Shine-Dalgarno sequence cleaved by the MazF toxin [188]. This indicates a tight link between RNA modification levels, translation regulation, and RNA metabolism in response to stress.

Another example of sRNA modification in pathogenic bacteria derives from a transcriptome-wide profiling of $m^6A$ distribution in *Pseudomonas aeruginosa*. Methylation sites were found present in two major sRNAs, RsmY and RsmZ [189], which sequester the regulatory protein RsmA to control its activity which is associated with acute and chronic virulence phenotypes [12, 190]. The involvement of these modifications in the regulatory mechanisms of RsmY/Z has not been studied yet.

Recently, one of the best characterized sRNA in *S. aureus*, an opportunistic pathogen causing a large variety of infections, has been shown to contain at its 5'end a peculiar modification which is co-transcriptionally introduced [191]. The expression of RNAIII is under the control of a two-component system, which senses bacterial cell density, to orchestrate the regulation of virulence gene expression

[192, 193]. This dual RNA codes for the cytotoxic δ-hemolysin peptide, while its 5′ and 3′ UTRs act as antisense RNA to regulate at the post-transcriptional level the expression of virulence genes associated with infectious diseases [193]. Hence, through basepairing interactions with its target mRNAs, it represses several cell wall associated proteins involved in adhesion and tissue colonization, and the transcriptional repressor of toxins Rot while it activates directly or indirectly the synthesis of many secreted proteins and toxins required for infection dissemination. A new RNAseq based approach has been developed to detect the incorporation of NAD, the nicotinamide-adenine dinucleotide, at the 5 ends of RNA transcripts [194]. This study found only few *S. aureus* transcripts containing this 5′ cap, including RNAIII. In Gram-negative bacteria, NAD has been reported to have a stabilization effect protecting the RNA from the 5′ processing enzyme RppH, which produces monophosphate at the end of RNAs that are substrates of RNase E [194]. In *Bacillus subtilis*, NAD protects RNAs from the exonucleolytic activity of RNase J1/J2 [195]. In *S. aureus*, the presence of NAD in RNAIII does not induce its stabilization nor affects its structure, but it has important consequences on pathophysiology. By a yet unknown mechanism, the NAD modified RNAIII leads to a decreased expression of δ-hemolysin and reduced cytotoxicity [191].

*3.1. mRNA Modifications*

Besides the classical 5′-cap $m^7G$ modification of eukaryotic mRNAs, other modifications have been described, including the 6-methyladenosine ($m^6A$), the 5-methylcytosine ($m^5C$), inosine (I) derived from adenine deamination and pseudouridine (Ψ). These modifications, which are present within 5′- and 3′-untranslated regions (UTRs) and the coding sequences of mRNAs, contribute to fine tune gene regulation [196-202]. In bacteria, the presence and the roles of mRNA modifications is relatively unexploited in pathogenic bacteria. In bacterial mRNAs, the presence of non-canonical 5′ ends has recently been reported for a subset of mRNAs. As described above, co-transcriptionally introduced 5′ NAD cap has also been detected in some *E. coli* mRNAs and is thought to modulate mRNA stability and translation efficiency [194, 203]. Recently, NAD cap has been found in mRNAs expressed in *B. subtilis* spores, a dormant state developed in response to different stresses [204]. Its role in these mRNAs remains to be analyzed. Other studies have shown additional types of 5′ capping directly incorporated into mRNAs during transcription initiation, which might increase mRNA stability. For example, dinucleoside tetraphosphates, very often Np4A, have been reported in *E. coli* [205]. Interestingly, the incorporation of such dinucleosides depends on their cellular concentration, which increases in some stress conditions such as heat shock [206] and oxidative stress [207].

Bacterial mRNAs can also contain post-transcriptional modifications. In *E.* coli, Ψs have been detected in some mRNAs. They can be located at specific codons and as a consequence they alter

translation speed or mRNA decoding [208], and at stop codons to induce nonsense suppression [209, 210]. Ψs have been proposed to influence the kinetics of RNase E-directed degradation in Gram-negative bacteria [211]. Another abundant mRNA modification is $m^6A$, which has been detected in genes involved in energy metabolism in Gram-negative bacteria, including pathogenic *P. aeruginosa* [189]. Very recently, it has been shown that $m^6A$ reduces both sense and stop codon reading accuracy [212, 213]. The molecular explanation for this decoding perturbation could be due to the formation of less stable codon-anticodon interactions with cognate tRNAs [212]. Indeed, when compared with unmodified A, $m^6A$ forms less stable basepairing with uridine (U) and destabilizes local RNA structures and short duplexes [214, 215]. It remains to be studied whether these modifications in mRNAs vary significantly in response to metabolic changes or stress.

Adenosine deamination is most probably the major modification in mRNAs, which can directly influence the activity of the synthesized protein. Adenosine-to-inosine (A-to-I) mRNA editing is catalyzed by the tRNA adenosine deaminase enzyme TadA, which recognizes stem-loop structures resembling the anticodon arm of $tRNA^{Arg}$ [216]. Because inosine (I) is recognized as guanosine (G) by the translational machinery, A-to-I editing expands the decoding rules resulting in protein diversification. In *E. coli* and in the two pathogenic bacteria *Klebsiella pneumonia* and *Yersinia enterocolitica*, recoding tyrosine (UAC) to cysteine (UGC) has been reported in mRNAs encoding self-killing toxins like HokB, increasing its toxicity [216]. HokB induces cellular growth arrest in response to starvation as a function of cellular density, via membrane depolarization. By doing so, it was found to mediate antibiotic tolerance leading to persistence [217]. Since bacteria persistence is characterized by the existence of sub-populations of bacteria that are tolerant to an antibiotic treatment with a fitness cost [218], the heterogeneous RNA editing levels of *hokB* mRNA could promote non-genetic cell heterogeneity [219].

*3.2. Figures and Table*

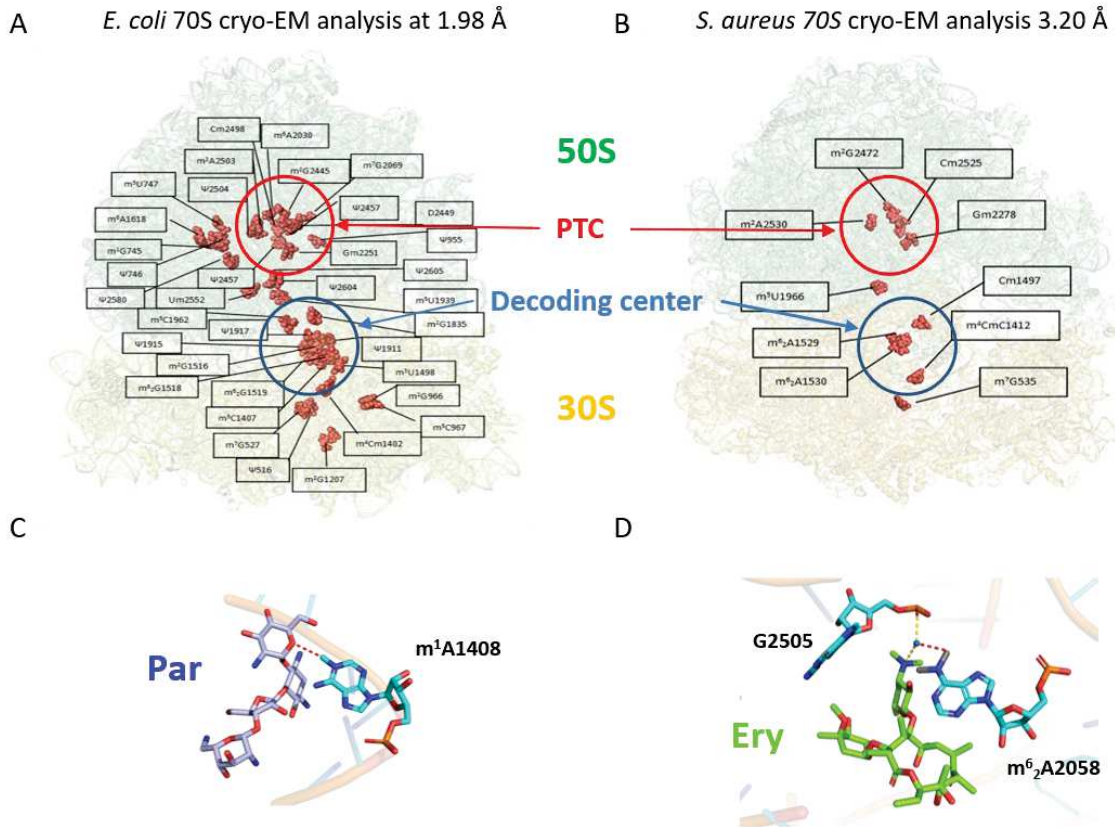


**Figure 1. Natural ribosomal RNA modifications and additionally modification implicated in antibiotic resistance mechanisms as indicated by structural analyses.** (**A**) Cryo-EM structure at 1.98 Å of *E. coli* 70S ribosome (pdb file 7K00). 11 and 24 RNA modifications (red spheres) could be visualized in the 30S (16S rRNA) and 50S (23S rRNA) subunits, respectively [82]. (**B**) Cryo-EM structure at 3.20 Å of *S. aureus* 70S ribosome (pdb file 6YEF). The limited resolution allowed the visualization of 4 RNA modifications in the 16S rRNA and 6 in 23S rRNA [83]. PTC, Peptidyl Transferase Center on the large 50S subunit. (**C**) Mechanism of aminoglycoside (Par, paromomycin) resistance induced by methylation of A1408 (pdb file 5ZEJ [220]). The presence of the methyl group directly perturbs antibiotic interaction. (**D**) Mechanism of macrolide (Ery, erythromycin) resistance induced by dimethylation of A2058 (pdb file 6XHV [221]). The two methyl groups on A2058 prevent the coordination of a water molecule with G2505, which stabilizes erythromycin binding.

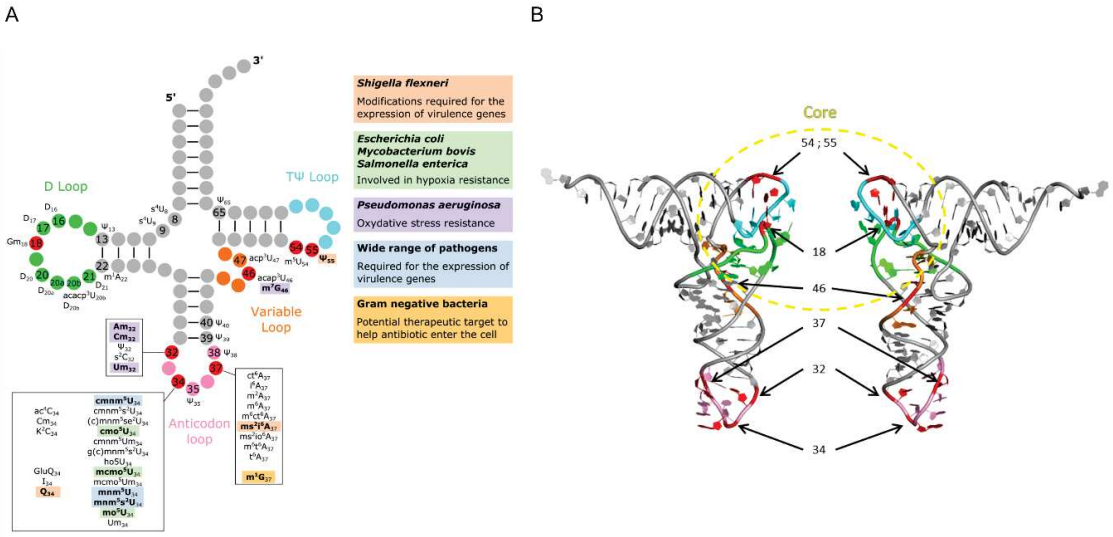


**Figure 2. Pathogenic bacteria tRNA modifications involved in virulence and stress adaptation.** (**A**) Secondary structure of tRNA. The nucleotides in the loops, where the majority of modifications accumulate, are colored as follow: D loop in green, anticodon loop in pink, variable loop in orange, and TΨ loop in light blue. The nucleotides for which the modifications are associated with a specific phenotype specified in the figure are in red. (**B**) Tertiary L-shape structure of tRNA. The 3D model corresponded to the crystal structure of *Saccharomyces cerevisiae* $tRNA^{Phe}_{GAA}$ (pdb file 1EHZ [222]). The same color code is used for the secondary (A) and tertiary (B) tRNA structures. The core domain of the tRNA comprises the D-, TΨ- and variable loops.

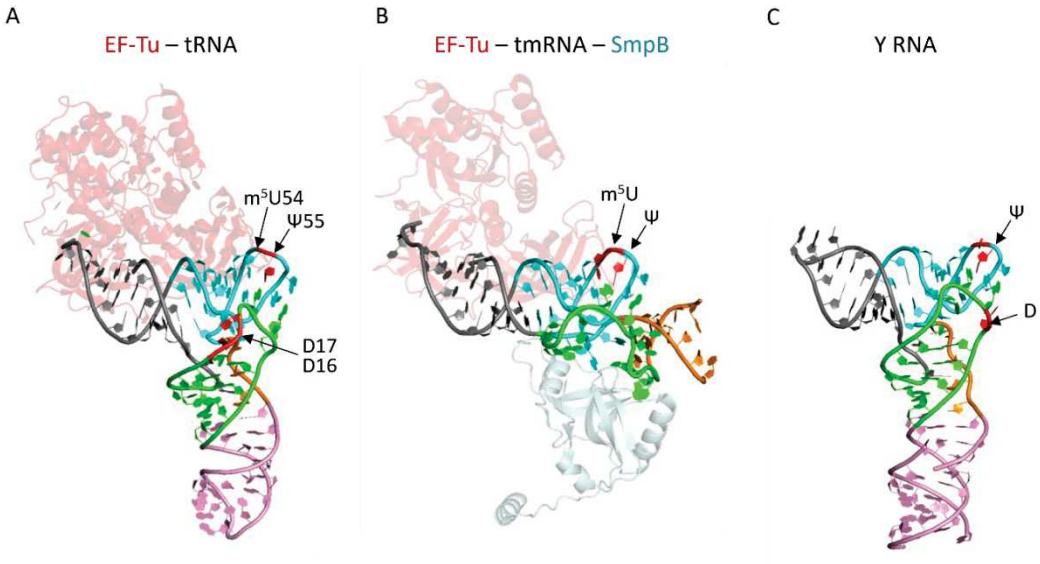


**Figure 3. The structures of tmRNA and Y RNA mimic part of the tRNA structure.** (**A**) The structure of EF-Tu-tRNA$^{Phe}$ complex (with GDPNP, GTP analog) from *Thermus aquaticus* (pdb file 1TTT [223]). Each domain of the tRNA is colored: acceptor am in grey, TY-arm in light blue, the variable region in orange, the D-arm in green, and the anticodon-arm in pink. EF-Tu structure is represented in light pink. (**B**) The structure of the tmRNA fragment in complex with EF-Tu (with GDP and kirromycin antibiotic, in light pink) and SmpB (in light grey) from *Thermus thermophilus* (pdb file 4V8Q [224]). The regions of tmRNA mimicking tRNA are shown with the same color code as for the tRNA. (**C**) *Salmonella Typhimurium* Y RNA (YrlA, pdb file 6CU1 [225]). The regions of YrlA mimicking tRNA are shown with the same color code as for the tRNA.

## 4. Conclusion and perspectives

The review presented several examples, which unveiled the diversity of functions of RNA modifications in translation and RNA degradation in bacterial pathogens. Because technologies are constantly improving, it is expected that the whole set of modifications will be mapped in RNA molecules as well as their quantifications. This will be the prerequisite to better study their dynamics upon stress or during bacterial infection. Further works correlating the modifications with the characterization of their protein co-factors (referred as writers, readers, and erasers) will be another step necessary to get an in-depth overview of their functions and the physiological consequences on bacterial pathogens. Many questions still remain to be addressed: what is the extent of chemical modifications diversity and complexity among evolutionary distant bacteria? Are there specific classes of bacterial sRNAs and mRNAs that could be modified extensively as it is for tRNAs and rRNAs? What are the consequences of RNA modification defects on bacterial physiology and pathogenesis? Some of the data suggested that some tRNA modifications are species-specific. Hence, it is expected that modifications might contain some metabolites issued from specific metabolic pathways resulting from the bacterial adaption to its ecological niches. Meanwhile during the infection process, the pathogens have to face metabolic burden and should counteract the host defenses mechanisms. It would not be so surprising that some of the modifications might be acquired or disrupted during the infection process with consequences on the bacterial proteome. The functional studies of the modification enzymes might also led to biotechnological applications, to design gene reprogramming or new tools for RNA studies, or to select novel anti-microbial strategies. Many of these studies will require the development of more simple technologies, such as the direct RNA sequencing methodologies, to facilitate the mapping and the discovery of RNA modifications among bacterial species. Although many studies have been done on tRNA and rRNA modifications, we are still far to fully appreciate the impact of modifications on RNA functions. We are only at the beginning of the tip of the iceberg.

**Author Contributions:** All authors have contributed to the review, searching the literature, writing the text and preparing the figures. All authors have read and agreed to the published version of the manuscript.

**Funding:** This work was supported by the Centre National de la Recherche Scientifique (CNRS). This work of the Interdisciplinary Thematic Institute IMCBio, as part of the ITI 2021-2028 program of the University of Strasbourg, CNRS and Inserm, was supported by IdEx Unistra (ANR-10-IDEX-0002) and by SFRI-STRAT'US project, and

EUR IMCBio (IMCBio ANR-17-EURE-0023) under the framework of the French Investments for the Future Program.

**Acknowledgments:**

**Conflicts of Interest:** The authors declare no conflict of interest.

References

1.Papon, N. and A.M. Stock, Curr Biol, 2019. 29(15): p. R724-R725.
2.Beier, D. and R. Gross, Curr Opin Microbiol, 2006. 9(2): p. 143-52.
3.Samatova, E., et al., Front Microbiol, 2020. 11: p. 619430.
4.Müller, C., C. Crowe-McAuliffe, and D.N. Wilson, Front Microbiol, 2021. 12: p. 652980.
5.Duval, M., et al., Biochimie, 2015. 114: p. 18-29.
6.Tollerson, R., 2nd and M. Ibba, J Biol Chem, 2020. 295(30): p. 10434-10445.
7.Loh, E., et al., Microbiol Spectr, 2018. 6(2).
8.Ignatova, Z. and F. Narberhaus, Curr Opin Microbiol, 2017. 36: p. 14-19.
9.Giuliodori, A.M., et al., Mol Cell, 2010. 37(1): p. 21-33.
10.Geissmann, T., S. Marzi, and P. Romby, RNA Biol, 2009. 6(2): p. 153-60.
11.Marzi, S., et al., Biol Chem, 2008. 389(5): p. 585-98.
12.Pourciau, C., et al., Front Microbiol, 2020. 11: p. 601352.
13.Quax, T.E., et al., Mol Cell, 2015. 59(2): p. 149-61.
14.Sauert, M., H. Temmel, and I. Moll, Biochimie, 2015. 114: p. 39-47.
15.Kurylo, C.M., et al., Cell Rep, 2018. 25(1): p. 236-248 e6.
16.Grosjean, H., Nucleic Acids Are Not Boring Long Polymers of Only Four Types of Nucleotides: A Guided Tour, in DNA and RNA Modification Enzymes: Structure, Mechanism, Function and Evolution, H. Grosjean, Editor. 2009, Landes Bioscience: Austin. p. 1-18.
17.Boccaletto, P., et al., Nucleic Acids Research, 2017. 46(D1): p. D303-D307.
18.Shetty, S. and U. Varshney, J Biol Chem, 2020. 296.
19.Frye, M., et al., Nat Rev Genet, 2016. 17(6): p. 365-72.
20.Motorin, Y. and M. Helm, Biochemistry, 2010. 49(24): p. 4934-44.
21.Davis, D.R., Biophysical and Conformational Properties of Modified Nucleosides in RNA (Nuclear Magnetic Resonance Studies), in Modification and Editing of RNA. 1998. p. 85-102.
22.Yokoyama, S., K. Watanabe, and T. Miyazawa, Adv Biophys, 1987. 23: p. 115-47.
23.Dalluge, J.J., et al., Nucleic Acids Res, 1996. 24(6): p. 1073-9.
24.Song, Q., et al., Structural Chemistry, 2013. 24(1): p. 55-65.
25.Charette, M. and M.W. Gray, IUBMB Life, 2000. 49(5): p. 341-51.
26.Yue, Y., J. Liu, and C. He, Genes Dev, 2015. 29(13): p. 1343-55.
27.Meyer, K.D. and S.R. Jaffrey, Nat Rev Mol Cell Biol, 2014. 15(5): p. 313-26.
28.Thuring, K., et al., Methods, 2016. 107: p. 48-56.
29.Edmonds, C.G., et al., J Bacteriol, 1991. 173(10): p. 3138-48.
30.Pomerantz, S.C. and J.A. McCloskey, Methods Enzymol, 1990. 193: p. 796-824.
31.Russell, S.P. and P.A. Limbach, J Chromatogr B Analyt Technol Biomed Life Sci, 2013. 923-924: p. 74-82.
32.Pomerantz, S.C., J.A. Kowalak, and J.A. McCloskey, J Am Soc Mass Spectrom, 1993. 4(3): p. 204-9.
33.Kowalak, J.A., et al., Nucleic Acids Res, 1993. 21(19): p. 4577-85.

34.Stolz, A., et al., ELECTROPHORESIS, 2019. 40(1): p. 79-112.
35.Lechner, A., et al., Anal Chem, 2020. 92(10): p. 7363-7370.
36.Addepalli, B. and P.A. Limbach, J Am Soc Mass Spectrom, 2011. 22(8): p. 1363-72.
37.Ho, N.W. and P.T. Gilham, Biochemistry, 1971. 10(20): p. 3651-7.
38.Raska, C.S., et al., J Am Soc Mass Spectrom, 2002. 13(9): p. 1034-41.
39.Yamauchi, Y., et al., Nucleic Acids Res, 2016. 44(6): p. e59.
40.Anreiter, I., et al., Trends Biotechnol, 2021. 39(1): p. 72-89.
41.Lahens, N.F., et al., Genome Biol, 2014. 15(6): p. R86.
42.Motorin, Y. and V. Marchand, Genes (Basel), 2021. 12(2).
43.Begik, O., et al., Nat Biotechnol, 2021.
44.Gao, Y., et al., Genome Biol, 2021. 22(1): p. 22.
45.Ramasamy, S., et al., bioRxiv, 2021: p. 2020.05.19.105338.
46.Begik, O., et al., bioRxiv, 2021: p. 2020.07.06.189969.
47.Paulines, M.J. and P.A. Limbach, Methods Mol Biol, 2017. 1562: p. 19-32.
48.Taoka, M., et al., Nucleic Acids Res, 2015. 43(18): p. e115.
49.Bahn, J.H., et al., Genome Res, 2012. 22(1): p. 142-50.
50.Vandivier, L.E., Z.D. Anderson, and B.D. Gregory, Methods Mol Biol, 2019. 1870: p. 51-67.
51.Garalde, D.R., et al., Nat Methods, 2018. 15(3): p. 201-206.
52.Workman, R.E., et al., Nat Methods, 2019. 16(12): p. 1297-1305.
53.Sakurai, M., et al., Genome Res, 2014. 24(3): p. 522-34.
54.Suzuki, T., et al., Nat Protoc, 2015. 10(5): p. 715-32.
55.Schaefer, M., et al., Nucleic Acids Res, 2009. 37(2): p. e12.
56.Zhu, Y., S.P. Pirnie, and G.G. Carmichael, RNA, 2017. 23(8): p. 1303-1314.
57.Marchand, V., et al., Nucleic Acids Res, 2016. 44(16): p. e135.
58.Ayadi, L., Y. Motorin, and V. Marchand, Methods Mol Biol, 2018. 1649: p. 29-48.
59.Carlile, T.M., et al., Nature, 2014. 515(7525): p. 143-6.
60.Schwartz, S., et al., Cell, 2014. 159(1): p. 148-162.
61.Marchand, V., et al., Nucleic Acids Res, 2020. 48(19): p. e110.
62.Herzog, V.A., et al., Nat Methods, 2017. 14(12): p. 1198-1204.
63.Cozen, A.E., et al., Nat Methods, 2015. 12(9): p. 879-84.
64.Lin, S., et al., Nat Protoc, 2019. 14(11): p. 3220-3242.
65.Marchand, V., et al., Angew Chem Int Ed Engl, 2018. 57(51): p. 16785-16790.
66.Hussain, S., et al., Cell Rep, 2013. 4(2): p. 255-61.
67.Dominissini, D., et al., Nature, 2012. 485(7397): p. 201-6.
68.Meyer, K.D., et al., Cell, 2012. 149(7): p. 1635-46.
69.Molinie, B., et al., Nat Methods, 2016. 13(8): p. 692-8.
70.Dai, Q., et al., Nat Methods, 2017. 14(7): p. 695-698.
71.Arango, D., et al., Cell, 2018. 175(7): p. 1872-1886 e24.
72.Winz, M.L., et al., Nat Protoc, 2017. 12(1): p. 122-149.
73.Igloi, G.L., Biochemistry, 1988. 27(10): p. 3842-9.
74.Nübel, G., F.A. Sorgenfrei, and A. Jäschke, Methods, 2017. 117: p. 14-20.
75.Cech, T.R., Science, 2000. 289(5481): p. 878-9.
76.Baxter-Roshek, J.L., A.N. Petrov, and J.D. Dinman, PLoS One, 2007. 2(1): p. e174.
77.Demirci, H., et al., RNA, 2010. 16(12): p. 2319-24.
78.Desaulniers, J.P., et al., Org Biomol Chem, 2008. 6(21): p. 3892-5.
79.Liang, X.H., Q. Liu, and M.J. Fournier, Mol Cell, 2007. 28(6): p. 965-77.
80.Decatur, W.A. and M.J. Fournier, Trends Biochem Sci, 2002. 27(7): p. 344-51.
81.Arnez, J.G. and T.A. Steitz, Biochemistry, 1994. 33(24): p. 7560-7.
82.Watson, Z.L., et al., Elife, 2020. 9.
83.Golubev, A., et al., FEBS Lett, 2020. 594(21): p. 3551-3567.

84.Fischer, N., et al., Nature, 2015. 520(7548): p. 567-70.
85.Polikanov, Y.S., et al., Nat Struct Mol Biol, 2015. 22(4): p. 342-344.
86.Noeske, J., et al., Nat Struct Mol Biol, 2015. 22(4): p. 336-41.
87.Halfon, Y., et al., Sci Rep, 2019. 9(1): p. 11460.
88.Jenner, L.B., et al., Nat Struct Mol Biol, 2010. 17(5): p. 555-60.
89.Burakovsky, D.E., et al., Nucleic Acids Res, 2012. 40(16): p. 7885-95.
90.Das, G., et al., EMBO J, 2008. 27(6): p. 840-51.
91.Kimura, S. and T. Suzuki, Nucleic Acids Res, 2010. 38(4): p. 1341-52.
92.Kyuma, T., et al., FEBS J, 2015. 282(13): p. 2570-84.
93.Sergeeva, O.V., A.A. Bogdanov, and P.V. Sergiev, Biochimie, 2015. 117: p. 110-8.
94.Hansen, M.A., et al., RNA, 2002. 8(2): p. 202-13.
95.Wang, W., et al., Proc Natl Acad Sci U S A, 2020. 117(27): p. 15609-15619.
96.Widerak, M., et al., Gene, 2005. 347(1): p. 109-14.
97.Francklyn, C.S. and P. Mullen, J Biol Chem, 2019. 294(14): p. 5365-5385.
98.Ho, J.M., et al., RNA Biol, 2018. 15(4-5): p. 667-677.
99.Lin, J., et al., Annu Rev Biochem, 2018. 87: p. 451-478.
100.Wilson, D.N., Nat Rev Microbiol, 2014. 12(1): p. 35-48.
101.Doi, Y., J.I. Wachino, and Y. Arakawa, Infect Dis Clin North Am, 2016. 30(2): p. 523-537.
102.Vázquez-Laslop, N. and A.S. Mankin, Trends Biochem Sci, 2018. 43(9): p. 668-684.
103.Gupta, P., et al., Nat Commun, 2013. 4: p. 1984.
104.Arenz, S., et al., Mol Cell, 2014. 56(3): p. 446-52.
105.Oldenburg, M., et al., Science, 2012. 337(6098): p. 1111-5.
106.Lioy, V.S., et al., RNA, 2014. 20(3): p. 382-91.
107.Helser, T.L., J.E. Davies, and J.E. Dahlberg, Nat New Biol, 1972. 235(53): p. 6-9.
108.Sharma, H. and B. Anand, Nucleic Acids Res, 2019. 47(21): p. 11368-11386.
109.Okamoto, S., et al., Mol Microbiol, 2007. 63(4): p. 1096-106.
110.Mikheil, D.M., et al., J Antibiot (Tokyo), 2012. 65(4): p. 185-92.
111.Gutgsell, N.S., M.P. Deutscher, and J. Ofengand, RNA, 2005. 11(7): p. 1141-52.
112.Van den Bergh, B., M. Fauvart, and J. Michiels, FEMS Microbiol Rev, 2017. 41(3): p. 219-251.
113.Kim, J.S., et al., Environ Microbiol, 2018. 20(6): p. 2085-2098.
114.Yamasaki, R., et al., iScience, 2020. 23(1): p. 100792.
115.Wood, T.K., S. Song, and R. Yamasaki, J Microbiol, 2019. 57(3): p. 213-219.
116.Helm, M. and J.D. Alfonzo, Chem Biol, 2014. 21(2): p. 174-85.
117.Jackman, J.E. and J.D. Alfonzo, Wiley Interdiscip Rev RNA, 2013. 4(1): p. 35-48.
118.Lorenz, C., C.E. Lunse, and M. Morl, Biomolecules, 2017. 7(2).
119.Eargle, J., et al., J Mol Biol, 2008. 377(5): p. 1382-405.
120.Zhang, J. and A.R. Ferre-D'Amare, Life (Basel), 2016. 6(1).
121.Giege, R. and M. Springer, EcoSal Plus, 2016. 7(1).
122.Kawai, G., et al., Nucleic Acids Symp Ser, 1991(25): p. 49-50.
123.Kawai, G., et al., Biochemistry, 1992. 31(4): p. 1040-6.
124.Davanloo, P., et al., Nucleic Acids Res, 1979. 6(4): p. 1571-81.
125.Davis, D.R., Nucleic Acids Res, 1995. 23(24): p. 5020-6.
126.Wang, S. and E.T. Kool, Biochemistry, 1995. 34(12): p. 4125-32.
127.Urbonavicius, J., J.M. Durand, and G.R. Björk, J Bacteriol, 2002. 184(19): p. 5348-57.
128.Ishida, K., et al., Nucleic Acids Res, 2011. 39(6): p. 2304-18.
129.Gehrig, S., et al., J Exp Med, 2012. 209(2): p. 225-33.
130.Jockel, S., et al., J Exp Med, 2012. 209(2): p. 235-41.
131.Rimbach, K., et al., J Innate Immun, 2015. 7(5): p. 482-93.
132.Grosjean, H. and E. Westhof, Nucleic Acids Res, 2016. 44(17): p. 8020-40.
133.Rozov, A., et al., Trends Biochem Sci, 2016. 41(9): p. 798-814.

134.Fahlman, R.P., T. Dale, and O.C. Uhlenbeck, Mol Cell, 2004. 16(5): p. 799-805.
135.Gromadski, K.B., T. Daviter, and M.V. Rodnina, Mol Cell, 2006. 21(3): p. 369-77.
136.Gustilo, E.M., F.A. Vendeix, and P.F. Agris, Curr Opin Microbiol, 2008. 11(2): p. 134-40.
137.Agris, P.F., F.A. Vendeix, and W.D. Graham, J Mol Biol, 2007. 366(1): p. 1-13.
138.Olejniczak, M. and O.C. Uhlenbeck, Biochimie, 2006. 88(8): p. 943-50.
139.Durand, J.M., et al., Mol Microbiol, 2000. 35(4): p. 924-35.
140.Aubee, J.I., M. Olu, and K.M. Thompson, RNA, 2016. 22(5): p. 729-42.
141.Thompson, K.M. and S. Gottesman, J Bacteriol, 2014. 196(4): p. 754-61.
142.Durand, J.M. and G.R. Björk, Mol Microbiol, 2003. 47(2): p. 519-27.
143.Jelenc, P.C. and C.G. Kurland, Proc Natl Acad Sci U S A, 1979. 76(7): p. 3174-8.
144.Matsufuji, S., et al., Cell, 1995. 80(1): p. 51-60.
145.Bregeon, D., et al., Genes Dev, 2001. 15(17): p. 2295-306.
146.Shippy, D.C., et al., Microb Pathog, 2013. 57: p. 1-9.
147.Shippy, D.C. and A.A. Fadl, Int J Mol Sci, 2014. 15(10): p. 18267-80.
148.Shippy, D.C., et al., Microb Pathog, 2011. 50(6): p. 303-13.
149.Li, D., et al., Appl Environ Microbiol, 2014. 80(1): p. 97-103.
150.Gao, T., et al., Front Cell Infect Microbiol, 2019. 9: p. 173.
151.Gao, T., et al., Front Cell Infect Microbiol, 2016. 6: p. 44.
152.Alvarez-Ordóñez, A., et al., Int J Food Microbiol, 2014. 178: p. 21-8.
153.Chionh, Y.H., et al., Nat Commun, 2016. 7: p. 13302.
154.Tsai, M.C., et al., Cell Microbiol, 2006. 8(2): p. 218-32.
155.Chao, M.C. and E.J. Rubin, Annu Rev Microbiol, 2010. 64: p. 293-311.
156.Voskuil, M.I., K.C. Visconti, and G.K. Schoolnik, Tuberculosis (Edinb), 2004. 84(3-4): p. 218-27.
157.Weixlbaumer, A., et al., Nat Struct Mol Biol, 2007. 14(6): p. 498-502.
158.Jaroensuk, J., et al., Nucleic Acids Res, 2016. 44(22): p. 10834-10848.
159.Pintard, L., et al., EMBO J, 2002. 21(7): p. 1811-20.
160.Guy, M.P., et al., RNA, 2012. 18(10): p. 1921-33.
161.Romsang, A., et al., Sci Rep, 2018. 8(1): p. 11882.
162.Thongdee, N., et al., Nucleic Acids Res, 2019. 47(17): p. 9271-9281.
163.Kimura, S., P.C. Dedon, and M.K. Waldor, Nat Chem Biol, 2020. 16(9): p. 964-972.
164.Desgranges, E., et al., Microbiol Spectr, 2019. 7(2).
165.Dutta, T. and S. Srivastava, Gene, 2018. 656: p. 60-72.
166.Felden, B. and D. Gilot, Genes (Basel), 2018. 10(1).
167.Moore, S.D. and R.T. Sauer, Mol Microbiol, 2005. 58(2): p. 456-66.
168.Abo, T., et al., Genes Cells, 2002. 7(7): p. 629-38.
169.Ueda, K., et al., Genes Cells, 2002. 7(5): p. 509-19.
170.Bandyra, K.J. and B.F. Luisi, RNA Biol, 2013. 10(4): p. 627-35.
171.Thomas, E.N., et al., Elife, 2020. 9.
172.Christensen, S.K., et al., Proc Natl Acad Sci U S A, 2001. 98(25): p. 14328-33.
173.Rae, C.D., Y. Gordiyenko, and V. Ramakrishnan, Science, 2019. 363(6428): p. 740-744.
174.Karzai, A.W., E.D. Roche, and R.T. Sauer, Nat Struct Biol, 2000. 7(6): p. 449-55.
175.Felden, B., et al., EMBO J, 1998. 17(11): p. 3188-96.
176.Ranaei-Siadat, E., et al., RNA Biol, 2013. 10(4): p. 572-8.
177.Julio, S.M., D.M. Heithoff, and M.J. Mahan, J Bacteriol, 2000. 182(6): p. 1558-63.
178.Sim, S. and S.L. Wolin, Microbiol Spectr, 2018. 6(4).
179.Chen, X., et al., Cell, 2013. 153(1): p. 166-77.
180.Chen, X., et al., RNA, 2014. 20(11): p. 1715-24.
181.Chen, X., et al., Genes Dev, 2007. 21(11): p. 1328-39.
182.Chen, X., A.M. Quinn, and S.L. Wolin, Genes Dev, 2000. 14(7): p. 777-82.
183.Wurtmann, E.J. and S.L. Wolin, Proc Natl Acad Sci U S A, 2010. 107(9): p. 4022-7.

184.Westermann, A.J., et al., Nature, 2016. 529(7587): p. 496-501.
185.Greiling, T.M., et al., Sci Transl Med, 2018. 10(434).
186.Hughes, K.J., et al., Cell Rep, 2020. 33(12): p. 108527.
187.Cortese, R., et al., J Biol Chem, 1974. 249(4): p. 1103-8.
188.Temmel, H., et al., Nucleic Acids Res, 2017. 45(8): p. 4708-4721.
189.Deng, X., et al., Nucleic Acids Res, 2015. 43(13): p. 6557-67.
190.Marzi, S. and P. Romby, Mol Microbiol, 2012. 83(1): p. 1-6.
191.Morales-Filloy, H.G., et al., J Bacteriol, 2020. 202(6).
192.Novick, R.P., Mol Microbiol, 2003. 48(6): p. 1429-49.
193.Bronesky, D., et al., Annu Rev Microbiol, 2016. 70: p. 299-316.
194.Cahová, H., et al., Nature, 2015. 519(7543): p. 374-7.
195.Frindert, J., et al., Cell Rep, 2018. 24(7): p. 1890-1901 e8.
196.Pan, T., Trends Biochem Sci, 2013. 38(4): p. 204-9.
197.Anders, M., et al., Life Sci Alliance, 2018. 1(4): p. e201800113.
198.Squires, J.E., et al., Nucleic Acids Res, 2012. 40(11): p. 5023-33.
199.Nombela, P., B. Miguel-López, and S. Blanco, Mol Cancer, 2021. 20(1): p. 18.
200.Kumar, S. and T. Mohapatra, Front Cell Dev Biol, 2021. 9: p. 628415.
201.Bazak, L., et al., Genome Res, 2014. 24(3): p. 365-76.
202.Palladino, M.J., et al., Cell, 2000. 102(4): p. 437-49.
203.Vvedenskaya, I.O., et al., Mol Cell, 2018. 70(3): p. 553-564 e9.
204.Craft, D.L., et al., FEMS Microbiol Lett, 2020. 367(17).
205.Luciano, D.J. and J.G. Belasco, Proc Natl Acad Sci U S A, 2020. 117(7): p. 3560-3567.
206.Lee, P.C., B.R. Bochner, and B.N. Ames, Proc Natl Acad Sci U S A, 1983. 80(24): p. 7496-500.
207.Bochner, B.R., et al., Cell, 1984. 37(1): p. 225-32.
208.Eyler, D.E., et al., Proc Natl Acad Sci U S A, 2019. 116(46): p. 23068-23074.
209.Fernández, I.S., et al., Nature, 2013. 500(7460): p. 107-10.
210.Karijolich, J. and Y.T. Yu, Nature, 2011. 474(7351): p. 395-8.
211.Islam, M.S., et al., bioRxiv, 2021: p. 2021.05.23.445298.
212.Ieong, K.W., et al., Nucleic Acids Res, 2021. 49(5): p. 2684-2699.
213.Choi, J., et al., Nat Struct Mol Biol, 2016. 23(2): p. 110-5.
214.Roost, C., et al., J Am Chem Soc, 2015. 137(5): p. 2107-15.
215.Micura, R., et al., Nucleic Acids Res, 2001. 29(19): p. 3997-4005.
216.Bar-Yaacov, D., et al., Genome Res, 2017. 27(10): p. 1696-1703.
217.Verstraeten, N., et al., Mol Cell, 2015. 59(1): p. 9-21.
218.Harms, A., E. Maisonneuve, and K. Gerdes, Science, 2016. 354(6318).
219.Bar-Yaacov, D., Y. Pilpel, and O. Dahan, RNA Biol, 2018. 15(7): p. 863-867.
220.Kanazawa, H., et al., Nucleic Acids Res, 2017. 45(21): p. 12529-12535.
221.Svetlov, M.S., et al., Nat Chem Biol, 2021. 17(4): p. 412-420.
222.Shi, H. and P.B. Moore, RNA, 2000. 6(8): p. 1091-105.
223.Nissen, P., et al., Science, 1995. 270(5241): p. 1464-72.
224.Neubauer, C., et al., Science, 2012. 335(6074): p. 1366-9.
225.Wang, W., et al., Structure, 2018. 26(12): p. 1635-1644 e3.

## 2. *Staphylococcus aureus*

Les Staphylocoques sont des coques à Gram positif commensales de l'Homme, dont plusieurs espèces sont des pathogènes opportunistes. Parmi elles, *Staphylococcus aureus* représente l'espèce la plus virulente, responsable d'un grand nombre d'infections de gravité variable et touchant un large éventail de tissus, allant des infections cutanées bénignes à la pneumonie, l'endocardite, voire la septicémie. *S. aureus* est aussi capable de s'adapter pour persister à la surface et à l'intérieur de tissus humains. Elle est présente sur la peau et dans le nez chez environ 30% de la population (Wertheim *et al.*, 2005). La colonisation de la peau inclus l'implantation de la bactérie à sa surface en tant que constituant du microbiome (Oh *et al.*, 2016). Mais également l'insertion entre les couches de l'épiderme (Nakatsuji *et al.*, 2013), la modulation de la réponse immunitaire et la persistance dans les cellules immunitaires, endothéliales et épithéliales (Soong et al., 2015). Cette internalisation lui permet d'échapper complètement aux défenses immunitaires de celui-ci.

L'émergence de souches multi résistantes aux antibiotiques est une préoccupation majeure de santé publique, particulièrement en milieu hospitalier, les souches MRSA (*S. aureus* résistante à la méthicilline) provoquant des infections nosocomiales graves et difficiles à traiter. La diversité des symptômes cliniques provoqués et les mécanismes de résistance aux traitements dépendent de l'expression de nombreux facteurs de virulence et des voies de réponse au stress.

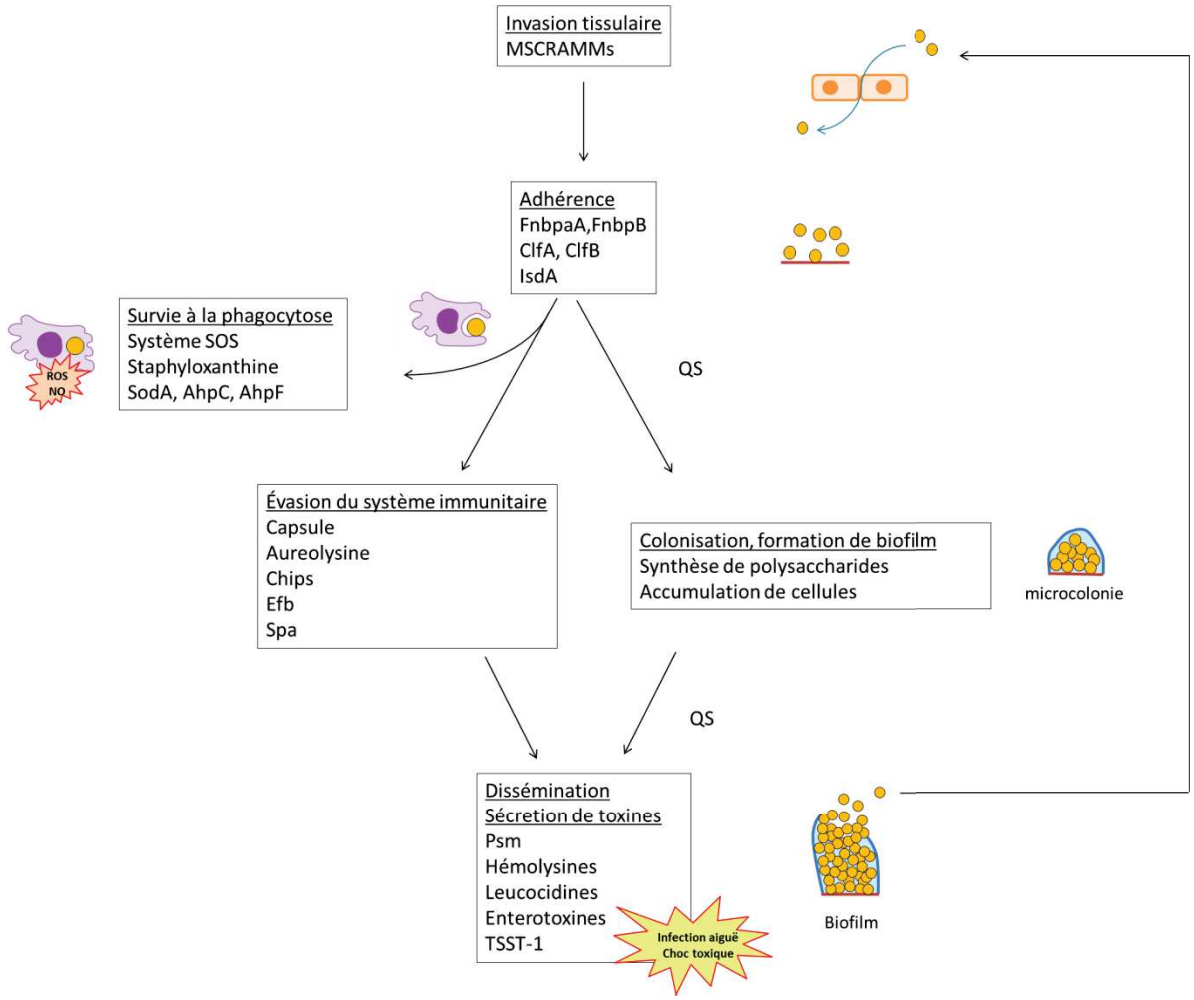


**Figure 1 : Schéma représentant les étapes de l'infection de *S. aureus*.** La colonisation des tissus amorce l'infection grâce aux adhésines permettant aux bactéries de se fixer sur différents types cellulaires. Au sein des tissus, les bactéries sont confrontées aux défenses immunitaires de l'hôte. Elles doivent donc échapper aux cellules immunitaires, former des colonies et entrer dans une phase de croissance grâce à la formation du biofilm les protégeant des stress environnementaux. Lorsque les colonies sont assez grandes, la phase de dissémination est déclenchée par la production de toxines et exoprotéines (nucléases et protéases) entrainant la rupture du biofilm et conduisant à une infection aiguë ou un choc toxique. En cas de phagocytose, la bactérie est capable de résister au stress généré dans les phagosomes grâce aux systèmes de détoxification et de réparation, elle va ainsi survivre sous forme quiescente. Les flèches annotées « QS » présentent des transitions entre les étapes du cycle d'infection qui sont réalisées sous le contrôle du Quorum Sensing, système à deux composants permettant à la bactérie de détecter la densité cellulaire et moduler l'expression de nombreux facteurs de virulences grâce à l'ARNIII. Cet ARN régulateur permettant simultanément de réprimer les facteurs impliqués dans l'adhérence et la colonisation et activer l'expression des toxines et exoprotéines

Le cycle de l'infection par *S. aureus* est assez précisément établi. A chaque étape du cycle, la bactérie va s'adapter grâce à la production d'un arsenal de facteurs de virulence dont l'expression est coordonnée en fonction de son environnement (**Fig. 1**).

Lors de l'adhérence et l'invasion tissulaire, l'étape initiatrice fondamentale à l'infection, des protéines de la famille des MSCRAMM (microbial surface components recognizing adhesive

matrix molecules) sont produites. Parmi elles, les protéines de liaison à la fibronectine (FnbpA et FnbpB) ou les facteurs de liaisons au fibrinogène, les Clumping factor A et B (ClfA et ClfB) permettent à la bactérie de se fixer sur différents types cellulaires de l'hôte (Eidhin *et al.*, 1998; Heilmann *et al.*, 2004). De plus, la protéine SpA (Staphylococcal protein A) lui permet non seulement de se lier aux immunoglobulines mais également d'échapper aux défenses immunitaires de l'hôte (Falugi *et al.*, 2013).

Afin de se protéger de la phagocytose, *S. aureus* est capable de produire une capsule de polysaccharides (Luong and Lee, 2002). La production de protéases telles que la Staphopain B et l'Aureolysine lui permet de dégrader l'élastine de l'hôte et entrainer la mort des monocytes (Shaw *et al.*, 2004; Smagur *et al.*, 2009; Elmwall *et al.*, 2017). Les CHIPS (chemotaxis inhibitory proteins of *S.aureus*) et Efb (extracellular fibrinogen binding protein) sont également sécrétées afin d'empêcher le recrutement de neutrophiles et l'activation du système du complément (Postma *et al.*, 2004; Rooijakkers *et al.*, 2006).

Pour assurer la prolifération de la bactérie dans les tissus, une structure de protection est produite sous forme de biofilm. Cette structure permet aux cellules de résister aux antibiotiques, d'échapper aux défenses immunitaires de l'hôte et ainsi devenir persistantes en diminuant leur métabolisme. (Arciola *et al.*, 2015; Otto, 2018)

La dissémination de la bactérie est facilitée par la production de toxines et d'exoprotéines (nucléases, lipases et protéases) entrainant la dispersion du biofilm. Ces toxines induisant la lyse des cellules ciblées, telles que les hémolysines (Jarry *et al.*, 2008; Berube and Wardenburg, 2013), les leucocidines (Spaan *et al.*, 2017) et les PSM (phenol soluble modulins) permettent également la propagation de l'infection à d'autres tissus (Periasamy *et al.*, 2012). Elles stimulent la libération de cytokines pro-inflammatoires (IL-18) des kératinocytes et sont indispensables à l'induction de l'inflammation de la peau (Syed *et al.*, 2015). Les cytokines pro-inflammatoires sont importantes pour maintenir les macrophages dans leur rôle de nettoyage des pathogènes avec une production d'oxyde nitrique et d'espèces réactives de l'oxygène importante (Pidwill *et al.*, 2021). Ces toxines sont responsables d'infections aiguës, les entérotoxines par exemple causent des intoxications alimentaires et les TSST-1 (Toxic shock syndrome toxin-1) causent les chocs toxiques Staphylococciques. Il existe une dualité claire entre la production de toxines (infection aiguë)

et la tolérance de l'hôte (infection chronique) durant laquelle *S. aureus* évite de stimuler les processus inflammatoires.

L'expression de l'ensemble de ces facteurs de virulence est orchestrée en réponse à de nombreux signaux environnementaux tels que la densité cellulaire, la disponibilité des nutriments ainsi que les stress imposées par les mécanismes de défense de l'hôte. Des systèmes de quorum sensing, codés notamment par le gène *agr* (accessory gene regulator) chez *S. aureus* permettent cette régulation fine de la virulence de la bactérie (Wang and Muir, 2016).

## 3. L'oxydation comme défense contre les pathogènes

La production d'espèces réactives de l'oxygène (ROS) tel que les superoxydes ($O_2^-$) et les peroxydes ($H_2O_2$) fait partie de la première ligne de défense mise en place par l'hôte pour lutter contre les bactéries pathogènes. Les ROS sont produits au sein des neutrophiles et des macrophages grâce au complexe de la phagocyte NADPH oxidase (Fang, 2004). Les superoxydes et les peroxydes entrainent la libération d'un atome de fer des metalloenzymes contenant un cluster [4Fe-4S] catalytique, entrainant la destruction du cluster et l'inactivation de l'enzyme (Imlay, 2006). Ces enzymes à cluster [4Fe-4S] sont impliquées dans un grand nombre de mécanismes indispensables pour tous les organismes, notamment les modifications post-transcriptionnelles.

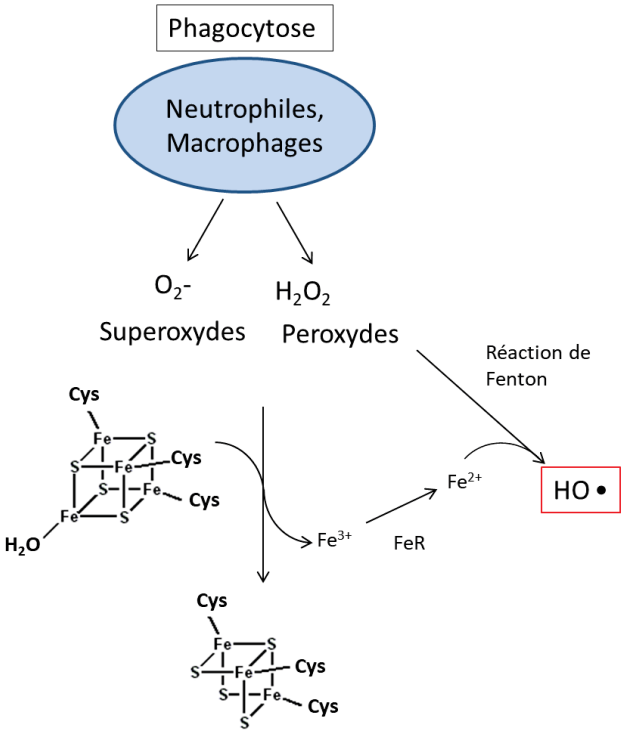


**Figure 2 : Schéma de la formation des radicaux hydroxyles induite par la destruction de centres [4Fe-4S] en présence de peroxyde.** L'ion ferreux libéré va réagir avec le peroxyde produit par les neutrophiles et macrophages entrainant la formation du HO•, encadré en rouge, par une réaction de Fenton.

Les radicaux hydroxyles (HO•) créés par des réactions de Fenton, sont fortement réactifs et interagissent avec toutes les molécules biologiques à proximité en causant des dommages parfois irréversibles. Les molécules les plus spécifiquement touchées sont les acides nucléiques, entrainant des mutations sur l'ADN (Keyer and Imlay, 1996). Les protéines sont également des cibles majeures des ROS, qui peuvent subir des modifications entrainant la formation d'agrégats (Davies, 2005, 2016). Les acides aminés contenant un groupement thiol (méthionine et cystéine) sont particulièrement sensibles à l'oxydation pouvant entrainer l'inactivation des protéines les contenant (Dean *et al.*, 1997; Grimaud *et al.*, 2001).

## 4. *S. aureus* et son adaptation au stress oxydant

*S. aureus* possède de nombreuses défenses pour s'adapter aux ROS, parmi lesquelles le pigment staphyloxanthine, responsable de sa couleur dorée caractéristique. Présents chez une grande partie des souches de *S. aureus* provenant d'infections humaines, ces pigments caroténoïdes sont connus pour désactiver les singulets d'oxygène. De par leur nombreuses

double-liaisons conjuguées, les caroténoïdes sont des molécules importantes pour la détoxification des ROS. La présence de staphyloxanthine confère ainsi une résistance aux ROS et améliore la survie de la bactérie lors d'infections (Liu *et al.*, 2005).

D'autres systèmes sont également connus pour réduire la concentration de ROS. Les superoxyde dismutases (SOD) sont des metalloenzymes de détoxification des ROS qui catalysent la dismutation du $O2^{-}$ en oxygène et $H_2O_2$, qui sera ensuite réduit en $H_2O$ par des catalases ou l'alkyl hydroperoxyde reductase (Clements *et al.*, 1999; Cosgrove *et al.*, 2007). *S. aureus* possède deux gènes codant pour des SOD, *sodA* et *sodM*. L'enzyme SOD majeure SodA dépend strictement du manganèse $Mn^{2+}$, tandis que l'enzyme alternative SodM est active lorsqu'elle est chargée en $Mn^{2+}$ ou en $Fe^{2+}$ (Treffon *et al.*, 2020).

L'homéostasie des ions métalliques, plus spécifiquement celle du fer, occupe donc une place importante dans la réponse des bactéries aux conditions oxydantes. De nombreux facteurs liés à l'apport du fer indispensable pour la survie de la cellule, sont mobilisés durant l'infection. Chez l'hôte, les ions $Fe^{2+}$ sont séquestrés au sein de complexes moléculaires les rendant très peu disponibles pour les pathogènes qui doivent mettre en place des stratégies afin de pouvoir acquérir le fer nécessaire à leur survie.

Chez *S. aureus*, les protéines du système Isd (Iron-Regulated Surface Determinant) sont des protéines exprimées lors d'un déficit de fer, ces protéines permettent l'utilisation du fer provenant de l'hème de l'hôte. (Clarke *et al.*, 2004; Muryoi *et al.*, 2008). Le système Isd est constitué de 10 protéines, permettant de capter l'hémoglobine et l'haptoglobine avec les recepteurs IsdB et IsdH (Dryla *et al.*, 2003; Torres *et al.*, 2006). L'hème est ensuite transféré à travers la paroi cellulaire via IspA et IspC (Liu *et al.*, 2008; Zhu *et al.*, 2008) vers le transporteur IsdDEF permettant son internalisation dans le cytoplasme. IsdDEF est un abc transporteur dans lequel IsdE est une lipoprotéine se liant à l'hème, IsdD est une ATPase et IsdF est une perméase. Enfin, la porphyrine est dégradée par IsdG ou IsdI qui sont des oxygènases produisant la staphylobiline (Skaar et al., 2004; Reniere et al., 2010). En plus de ce système Isd, la bactérie produit des staphyloferrines qui sont des sidérophores capables d'extraire le fer de la ferritine, les staphyloferrines A sont codés par les opérons *sfaABCD* (Beasley et al., 2009) et les staphyloferrines B par *sbnABCDEFGHI* (Park et al., 2005; Cheung et al., 2009)

Les systèmes de réparation de l'ADN tels que le système SOS est activé par la protéine RecA, impliquée dans la reconnaissance et la recombinaison de l'ADN simple brin qui est elle-même réprimée par la fixation de la protéine LexA. Lors de dommage sur l'ADN, LexA va être clivé, et permettre l'activation du système SOS (Cirz *et al.*, 2007; Butala *et al.*, 2009). L'opéron *rexBA* fait également partie de la réponse SOS également mis en place par la bactérie afin de survivre aux attaques des ROS produits par les défenses de l'hôte. Les protéines RexAB font partie de la famille des protéines AddAB hélicases-nucléases et sont indispensables pour la survie de la bactérie lors de l'infection. Elles sont impliquées dans la réparation des cassures du double brin (Chang *et al.*, 2006; Ha *et al.*, 2020b).

## 5. Objectifs de la thèse

La cartographie des modifications post-transcriptionnelles dans les ARN non codants de *S. aureus* reste encore peu connue ainsi que leurs implications dans l'adaptation de la bactérie à son environnement, notamment lors de l'infection.

Cette étude a pour but principal dans un premier temps d'établir une cartographie des modifications présentes dans les ARN non codants, plus spécifiquement dans les ARNt de *S. aureus*. Pour cela, une méthode d'analyse permettant de les isoler un à un et de caractériser les modifications présentes doit être mise en place et adaptée aux moyens matériels disponibles ainsi qu'à l'organisme étudié.

Dans un second temps, la cartographie établie pourra permettre une étude dynamique des modifications en adaptation à différentes conditions environnementales rencontrées par la bactérie durant les interactions avec l'hôte, plus spécifiquement les stress rencontrés durant l'infection.

Enfin, l'étude des causes et des conséquences traductionnelles des changements observés pourra être réalisée afin de déterminer le potentiel rôle des modifications post-transcriptionnelles dans l'adaptation aux stress

# II. Résultats :

## 1. Mise en place de la méthode d'analyse des ARN par gel en 2 dimensions et NanoLC-MS/MS

Le chapitre de Methods in molecular biology présente un protocole détaillé pour isoler les ARNt bactériens un a un par gel de polyacrylamide en 2 dimensions ainsi que l'identification des ARNt et la caractérisation des modifications post-trancriptionelles par l'analyse LC-MS/MS. Ce protocole mis en place au sein de l'unité pour l'analyse des ARNt de *E. coli* sera également appliqué sans modifications majeures à cette étude sur les ARNt de *S.aureus*.

# Chapter 8

## Mapping of Posttranscriptional tRNA Modifications by Two-Dimensional Gel Electrophoresis Mass Spectrometry

Laura Antoine and Philippe Wolff


### Abstract

RNA modification mapping by mass spectrometry (MS) is based on the use of specific ribonucleases (RNases) that generate short oligonucleotide digestion products which are further separated by nano-liquid chromatography and analyzed by MS and MS/MS. Recent developments in MS instrumentation allow the possibility to deeply explore posttranscriptional modifications. Notably, development of nano-liquid chromatography and nano-electrospray drastically increases the detection sensitivity and allows the identification and sequencing of RNA digested fragments separated and extracted from two-dimensional polyacrylamide gels, as long as the mapping and characterization of ribonucleotide modifications.


**Key words** 2D Gel isolation, Posttranscriptional tRNA modifications, Nano-LC-MS/MS

## 1 Introduction

RNA modification mapping recently experienced a renewed interest because of the development of new sensitive detection technologies and implication of RNA modifications in the deciphering of gene expression regulation or antibiotic resistance [1, 2]. In this chapter, we provide a detailed protocol for *E. coli* tRNA modification mapping. We present the sequencing by mass spectrometry of two tRNAs, tRNA Ser GCU and tRNA Leu CAG. To obtain the largest sequence coverage, three different nucleotide-specific RNases are used: RNase T1 (cleaves at 3′ end of G), RNase A (cleaves at 3′ end of U and C), and RNase U2 (cleaves at 3′ end of purine but preferably at 3′ end of A). The RNA modification mapping and data analysis workflow are shown in Fig. 1. This protocol had been applied successfully to different organisms such as bacteria, archaea, and eukaryotes.

The MS analysis procedure presents several caveats. First, as different tRNAs share similar sequences, it may be difficult to

Véronique Arluison and Frank Wien (eds.), *RNA Spectroscopy: Methods and Protocols*, Methods in Molecular Biology, vol. 2113, https://doi.org/10.1007/978-1-0716-0278-2_8, 

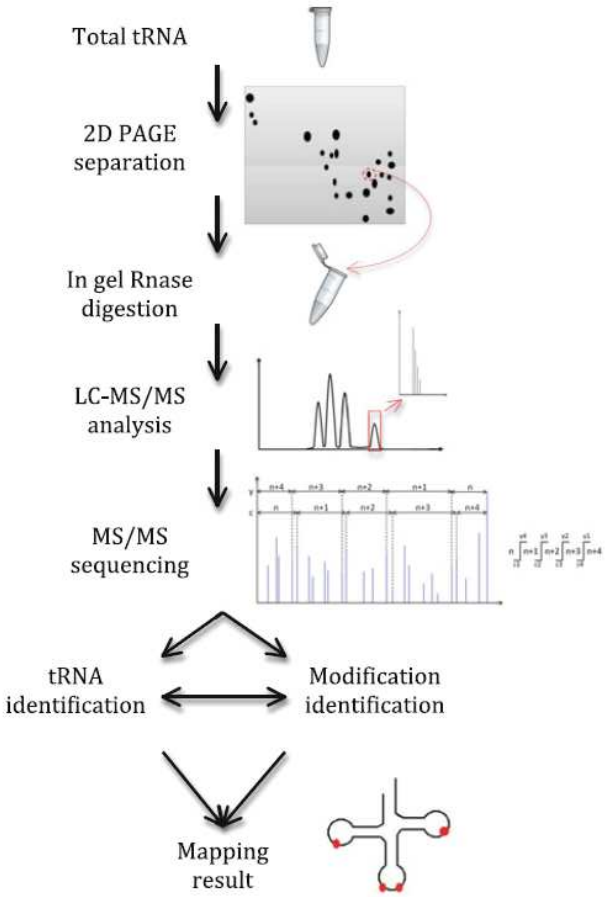


**Fig. 1** Workflow for posttranscriptional tRNA modifications mapping by two-dimensional gel electrophoresis followed by mass spectrometry analysis. tRNA is separated by 2D gel electrophoresis. Individual tRNA spots are sliced out and in-gel digested by nucleoside-specific RNases. RNase digests are sequenced by LC-MS/MS in order to identify tRNA and to localize modifications

unambiguously attribute such sequences to a single tRNA. Additionally, different sequences can have the same mass (same nucleotide composition) or similar mass (there is a difference of only 1 Da between cytosine and uridine). In those cases, there is often an isotopic pattern overlay, and it can be very difficult to sequence correctly MS/MS spectra. In order to simplify MS/MS analysis and tRNA identification, two-dimensional polyacrylamide gels (2D gels) were used to separate tRNAs (Fig. 2) [3, 4].

After "in-gel RNase digestion," oligonucleotide products (passively eluted from the gel) are separated by nano-ion-pair reversed-phase high-performance liquid chromatography (nano-IP-RP-HPLC) [5]. Eluted digests are directly injected in the spectrometer

| spot | tRNA |
|---|---|
| S02 | Ser GCU |
| S03 | Leu CAG |
| S05 | Leu CAA |
| S08 | Ile GAU |
| S08 | Asp GUC |
| S09 | Asn GUU |
| S11 | Glu UUC |
| S10 | Gln UUG |
| S10 | Gln CUG |
| S09 | Pro CGG |
| S09 | Ala UGC |
| S07 | Val UAC |
| S07 | Gly GCC |
| S06 | His GUG |
| S06 | Arg ACG |
| S06 | ProUGG |
| S13 | Leu UAG |
| S03 | Ser GGA |
| S14 | Tyr GUA |

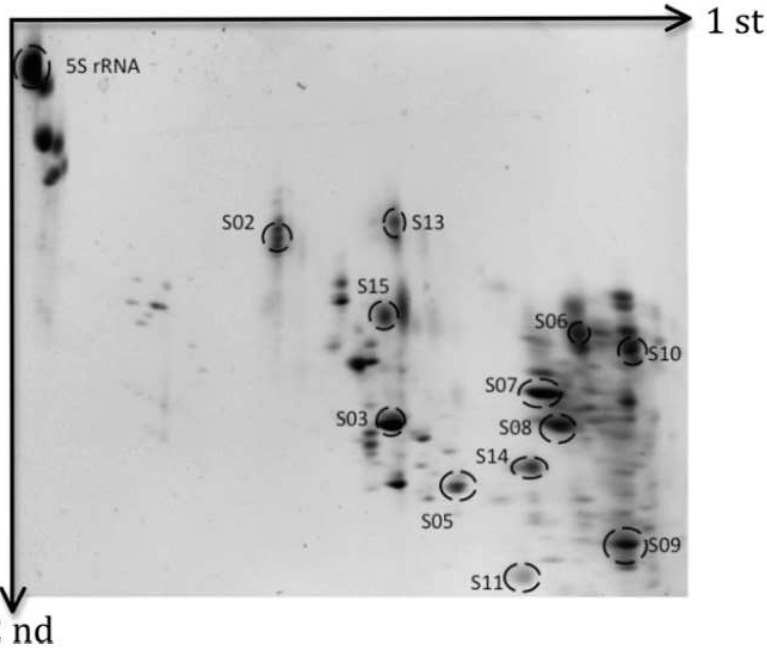


**Fig. 2** 2D polyacrylamide gel (20%) of *E. coli* total tRNA. 10 μg of total tRNA from *E. coli* were loaded; tRNA spots are revealed by ethidium bromide staining. The spots containing tRNA identified by MS/MS sequencing are indicated (black circles) and annotated in the table on the left

via a commercial NanoLockSpray ionization source to provide exact mass measurement. All oligonucleotides are fragmented by collision-induced dissociation (CID) and produce preferential fragments from y and c series for RNA sequencing [6]. Sequencing results are compared to genomic sequence in order to identify tRNA and to map RNA modifications in the sequence.

## 2 Materials

### *2.1 Instruments and Equipment*

1. Polyacrylamide gel electrophoresis (PAGE) apparatus for 50 cm glass plates, 1 mm spacers (first dimension).
2. Polyacrylamide gel electrophoresis (PAGE) apparatus for 30 cm glass plates, 1 mm spacers (second dimension).
3. Electrophoresis power supply.
4. UV transilluminator and UV safety glasses.
5. Sterile surgical blades.
6. SpeedVac vacuum concentrator.
7. NanoAcquity UPLC system (Waters, Manchester, UK).

8. Synapt G2-S mass spectrometer equipped with NanoLock-Spray ionization source (Waters, Manchester, UK).
9. MassLynx mass spectrometry software with MaxEnt3 module (Waters, Manchester, UK).
10. Acquity UPLC peptide BEH C18 column (130 Å, 1.7 μm, 75 μm × 200 mm) (Waters, Manchester, UK).
11. Basic laboratory materials (vortex, thermoblock, etc.)

***2.2 Two-Dimensional Gel Electrophoresis***

1. Total tRNA from *E. coli* used in this study was prepared by Gérard Keith (personal gift), but it is also commercially available.
2. 12.5% Acrylamide/bis-acrylamide (19:1), 8 M urea, 1× Tris-Borat-EDTA (TBE) (first dimension).
3. 20% Acrylamide/bis-acrylamide (19:1), 4 M urea, 1× TBE (second dimension).
4. Ethidium bromide (EtBr).

***2.3 In-Gel Digestion of Separated tRNA***

1. RNase T1 and A (Thermo Fischer Scientific).
2. RNase U2 was homemade prepared as described [7].
3. Ammonium acetate 100 mM.
4. ZIP Tip C18 (Millipore).

***2.4 Nano-liquid Chromatography***

1. Mobile phase A.
   - 200 mM Hexafluoropropanol (HFIP).
   - 7 mM Triethylamine (TEA).
   - 7.5 mM Triethylamine acetate (TEAA) pH 7.5.
2. Mobile phase B.
   - 100% Methanol LC-MS grade.

## 3 Methods

***3.1 Two-Dimensional Gel Electrophoresis (See Note 1)***

*3.1.1 First Dimension (Denaturing Conditions)*

1. Cast the first-dimensional, 12.5% acrylamide/bis-acrylamide, 8 M urea.
2. Pre-run the gel in 1× TBE buffer for 30 min at 30 W (constant power).
3. Load 10 μg per well of *E. coli* total tRNA in a minimum volume (less than 10 μL).
4. Run the gel for 7 h at 30 W (constant power).
5. Stain the gel with an EtBr solution (10 μg/L) for 10 min.

6. Visualize the bands containing tRNAs under UV light (302 nm). Beware of wearing appropriate protections for handling gel containing EtBr and manipulation under UV light.
7. Excise the gel fragments containing tRNAs with a clean razor blade.

*3.1.2 Second Dimension (Semi-denaturing Condition)*

1. Put the excised gel lanes on the top of the second polyacrylamide gel, and cast the second-dimensional gel 20% acrylamide/bis-acrylamide, 4 M urea. The excised gel fragment from the first electrophoresis should be embedded in the gel.
2. Run the gel for 24 h at 6 W (constant power).
3. Stain the gel with an EtBr solution (10 μg/L) for 10 min.
4. Using UV transilluminator, excise the spots containing tRNAs (Fig. 2). Beware of wearing appropriate protections for handling gel containing EtBr and manipulation under UV light.
5. Dry gel spots in Eppendorf tubes under vacuum for 10 min without heating.

### 3.2 In-Gel RNase Digestion

Rehydrate excised gel fragments with 20 μL of RNase T1 (1 U/μL) solution or 20 μL of RNase A (0.01 U/μL) solution in 100 mM ammonium acetate (pH is not adjusted), and incubate at 50 °C for 3 h, followed by 12 h at 37 °C.

For RNase U2 digestion, rehydrate gel fragments with 50 μL of RNase U2 at 0.3 ng $\mu L^{-1}$ in 100 mM ammonium acetate (pH is adjusted to 5.3), and incubate at 37 °C for 1 h.

### 3.3 RNA Digest Product Desalting

1. Prepare ZipTip C18 with 50% acetonitrile in water (3 × 10 μL).
2. Equilibrate the ZipTip for sample binding with 200 mM ammonium acetate (1 × 10 μL).
3. Bind the digested sample, and wash oligonucleotides with 200 mM ammonium acetate (5 × 10 μL).
4. Elute oligonucleotides with 10 μL of 50% acetonitrile in water.
5. Dry under vacuum for 20 min without heating.

### 3.4 LC-MS/MS

*3.4.1 Nano-liquid Chromatography*

Nano-LC is performed at a 0.3 μL/min flow rate for 1 h. RNase digestion products are eluted using a gradient from 15% to 35% B in 2 min followed by an increase of B to 50% in 20 min and then returning to 15% B in 25 min.

**Table 1**
**List of natural and modified nucleotides identified in this study**

| Name | Short name | Symbol | Nucleotide mass (Da) | $[M-H]^-$ Np (Da) | $[M-H]^-$ N > p (Da) | Neutral loss (Da) |
|---|---|---|---|---|---|---|
| Guanosine | G | G | 345 | 362 | 344 | |
| Cytidine | C | C | 305 | 322 | 304 | |
| Uridine | U | U | 306 | 323 | 305 | |
| Adenosine | A | A | 329 | 346 | 328 | |
| 2′-*O*-Methylguanosine | Gm | # | 359 | 376 | 358 | |
| 1-Methylguanosine | m1G | K | 359 | 376 | 359 | |
| 2′-*O*-Methylcytidine | Cm | B | 319 | 336 | 318 | |
| 5-Methyluridine | m5U | T | 320 | 337 | 319 | |
| Dihydrouridine | D | D | 308 | 325 | 307 | |
| N6-Threonylcarbamoyladenosine[a] | t6A | 6 | 329 | 346 | 328 | 145 |

A full list of modified nucleosides is available in the Modomics database (http://modomics.genesilico.pl/modifications/)
[a]Due to the neutral loss of threonylcarbamoyl, nucleotide mass fragmentation of t6A corresponds to the mass without modification. This modification occurs exclusively at position 37 in the anticodon loop

*3.4.2 Mass Spectrometry Analysis*

All experiments are performed in negative mode. The eluted RNase digests are injected on line into the mass spectrometer via Nano-LockSpray. Capillary voltage is set to 2.6 kV and sample cone to 30 V. Source is heated to 130 °C. For MS, a mass range from 500 to 1500 ($m/z$) is used, followed by collision-induced dissociation (CID) fragmentation of most intense signals using fast data directed acquisition (FastDDA) mode with a $m/z$ detection range of fragments from 50 to 2000. A collision energy ramp (18–28 V at $m/z$ 500 and 28–38 V at $m/z$ 1500) is applied in the trap collision cell to provide the maximum fragment ions.

### *3.5 Data Analysis*

All the fragment spectra are manually sequenced (*see* **Note 2**).

1. Deconvolute CID spectra by using MaxEnt3 software (*see* **Note 3**).
2. Using Table 1, listing the masses of the most common natural and modified nucleotides, reconstruct the sequence by following the y and/or c series (*see* **Note 4**). Three sequencing examples are shown in Fig. 3. Additionally, Fig. 4 gives a list of all the different masses obtained by nano-LC-MS/MS and the corresponding sequences.
3. Note that pseudouridine, an isomer of uridine, is a silent mass and cannot be detected by this method (*see* **Note 5**).

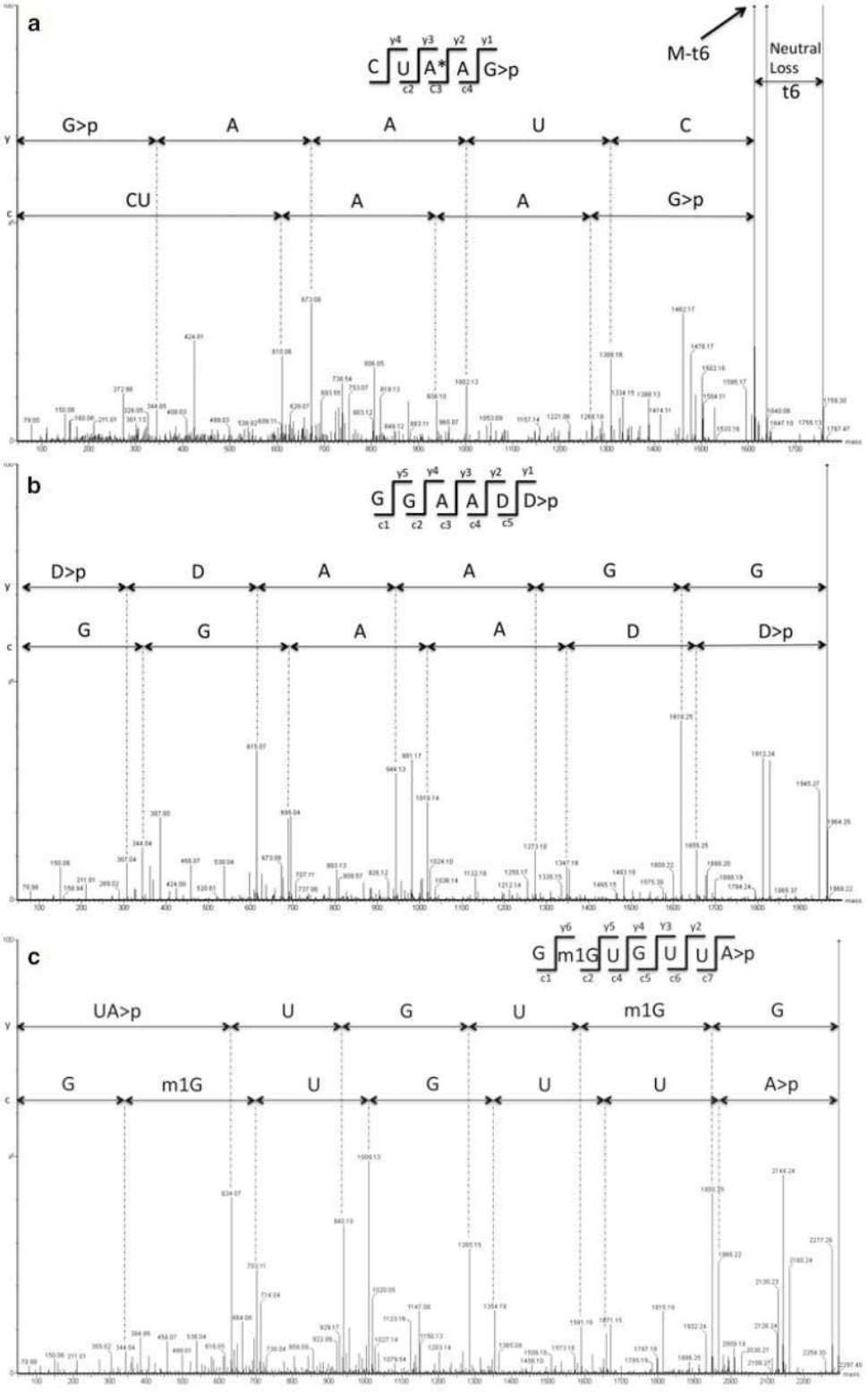


**Fig. 3** Typical MS/MS spectra of RNase digested tRNA fragments. Only series y and c have been sequenced. (**a**) MS/MS sequencing spectrum of CU**t6A**AG>p after RNase T1 digestion. In the case of t6A modification,

| theoretical m/z | observed m/z | z | molecular mass (Da) | sequence | tRNA | theoretical m/z | observed m/z | z | molecular mass (Da) | sequence | tRNA |
|---|---|---|---|---|---|---|---|---|---|---|---|
| RNase T1 | | | | | | | | | | | |
| 878,62 | 878,63 | -2 | 1758,3 | CU6AG>p | Ser GCU | 947,11 | 947,10 | -2 | 1895,2 | CUUCAG>p | Leu CAG |
| 946,62 | 946,62 | -2 | 1894,2 | CAUCCG>p | Ser GCU | 956,11 | 956,10 | -2 | 1913,2 | CUUCAGp | Leu CAG |
| 955,62 | 955,62 | -2 | 1912,2 | CAUCCGp | Ser GCU | 966,12 | 966,09 | -2 | 1933,2 | TUCAAG>p | Leu CAG |
| 1135,15 | 1135,13 | -2 | 2271,3 | UCAAAAG>p | Ser GCU | 975,13 | 975,10 | -2 | 1951,2 | TUCAAGp | Leu CAG |
| 1144,16 | 1144,13 | -2 | 2289,3 | UCAAAAGp | Ser GCU | 988,14 | 988,13 | -2 | 1977,3 | AADD#G>p | Leu CAG |
| 1240,14 | 1240,1 | -2 | 2481,2 | CUCCCCUG>p | Ser GCU | 997,15 | 997,13 | -2 | 1995,3 | AADD#Gp | Leu CAG |
| 1249,15 | 1249,12 | -2 | 2499,2 | CUCCCCUGp | Ser GCU | 1252,64 | 1252,60 | -2 | 2506,2 | UCCUUACG>p | Leu CAG |
| 1251,66 | 1251,63 | -2 | 2504,3 | CCUCACCG>p | Ser GCU | 1261,65 | 1261,62 | -2 | 2524,2 | UCCUUACGp | Leu CAG |
| 1263,66 | 1263,64 | -2 | 2528,3 | AAUCCCCG>p | Ser GCU | 1233,15 | 1233,11 | -3 | 3701,3 | UCCCCCCCCUCG>p | Leu CAG |
| 1272,67 | 1272,63 | -2 | 2546,3 | AAUCCCCGp | Ser GCU | 1239,15 | 1239,10 | -3 | 3719,3 | UCCCCCCCCUCGp | Leu CAG |
| RNase A | | | | | | | | | | | |
| 858,11 | 858,11 | -2 | 1717,2 | GGGGTp | Ser GCU | 662,09 | 662,09 | -2 | 1325,2 | AGACp | Leu CAG |
| 991,15 | 991,16 | -2 | 1983,3 | AAAAGCp | Ser GCU | 1326,18 | 1326,17 | -1 | 1326,2 | AAGUp | Leu CAG |
| 1007,14 | 1007,15 | -2 | 2015,3 | GAAGGCp | Ser GCU | 836,12 | 836,12 | -2 | 1673,2 | GGAADp | Leu CAG |
| 1179,66 | 1179,69 | -2 | 2360,3 | GAGAGGCp | Ser GCU | 981,13 | 981,14 | -2 | 1963,3 | GGAADD>p | Leu CAG |
| 1417,20 | 1417,18 | -2 | 2835,4 | 6AGGGAGUp | Ser GCU | 1007,63 | 1007,64 | -2 | 2016,3 | GAAGGUp | Leu CAG |
| 1046,47 | 1046,49 | -3 | 3141,5 | U6AGGGAGUp | Ser GCU | 1030,64 | 1030,64 | -2 | 2062,3 | GGGGGTp | Leu CAG |
| RNase U2 | | | | | | | | | | | |
| 706,10 | 706,1 | -2 | 1413,2 | CU6A>p | Ser GCU | 823,61 | 823,63 | -2 | 1648,3 | ADD#G>p | Leu CAG |
| 807,11 | 807,11 | -2 | 1615,2 | CDGAA>p | Ser GCU | 865,60 | 865,59 | -2 | 1732,2 | pGCGAA>p | Leu CAG |
| 915,15 | 915,15 | -2 | 1831,3 | CCGCCA | Ser GCU | 927,60 | 927,60 | -2 | 1856,2 | UCCUUA>p | Leu CAG |
| 966,62 | 966,62 | -2 | 1934,2 | GCUGCA>p | Ser GCU | 977,63 | 977,64 | -2 | 1956,3 | DD#GDA>p | Leu CAG |
| 1240,14 | 1240,14 | -2 | 2481,3 | CUCCCCUG>p | Ser GCU | 1142,16 | 1142,17 | -2 | 2285,3 | ADD#GDA>p | Leu CAG |
| 1388,19 | 1388,21 | -2 | 2777,4 | CU6AGGGA>p | Ser GCU | 1147,13 | 1147,13 | -2 | 2295,3 | GKUGUUA>p | Leu CAG |
| 1273,15 | 1273,16 | -3 | 3821,5 | GGCGCUCCCCUG>p | Ser GCU | 1425,66 | 1425,67 | -2 | 2852,3 | GUGUCCUUA>p | Leu CAG |
| | | | | | | 1479,21 | 1479,20 | -2 | 2959,4 | ADD#GDAGA>p | Leu CAG |
| | | | | | | 1233,15 | 1233,17 | -3 | 3701,5 | UCCCCCCCCUCG>p | Leu CAG |

tRNA Ser GCU
pGGUGAGGUGGCCGAGAGGCDGAAGGCGCUCCCCUGCU6AGGGAGUAUGCGGUCAAAAGCUGCAUCCGGGGTUCGAAU CCCCGCCUCACCGCCA
Sequence coverage 77%
tRNA Leu CAG
pGCGAAGGUGGCGGAADD#GDAGACGCGCUAGCUUCAGKUGUUAGUGUCCUUACGGACGUGGGGGTUCAAGUCCCCC CCCUCGCACCA
Sequence coverage 82%

**Fig. 4** List of all digested products experimentally observed for tRNA Ser GCU and Leu CAG, after individual digestion with RNases T1, A, and U2. The MS/MS sequenced products are indicated in red in the full tRNA sequences below the table. Although sequence coverage is close to 100%, some parts of the sequences are still missing. Thus, in the case of uncharacterized tRNA, modifications existing in vivo may be missed

4. For methyl groups, it is not possible to localize the group on the base and/or the ribose with this technique (*see* **Note 6**).
5. When a digested tRNA fragment is sequenced, the parent ion and the fragments' masses have to be checked using Mongo Oligo mass calculator (https://mods.rna.albany.edu/massspec/Mongo-Oligo). A maximum tolerance of 0.05 Da between the measured and calculated mass is routinely tolerated.
6. Comparison of the resulting sequences with *E. coli* genomic sequences (http://gtrnadb.ucsc.edu) identifies tRNA (*see* **Note 7**).

**Fig. 3** (continued) collision-induced dissociation (CID) fragmentation leads to a neutral loss of 145 Da corresponding to the leaving of the threonylcarbamoyl group. ∗ corresponds to the location of the neutral loss. (**b**) MS/MS sequencing spectra of GGAA**DD**>p after RNase A digestion. (**c**) MS/MS sequencing spectra of G**m1G**UGUUA>p after RNase A digestion

7. Map modifications on the tRNA sequence. Figure 4 shows a list of all digested tRNA fragments sequenced by MS/MS.

## 4 Notes

1. In the first-dimension electrophoresis, tRNAs are completely heat denatured due to the dual action of gel temperature (70 °C) and urea (8 M) and are separated by their length. In the second dimension, urea concentration was decreased to 4 M, and the gel is run at room temperature. Under these conditions, tRNAs are partially refolded, and the separation is based on the partial secondary conformation.
2. Software have been developed for interpretation and annotation of MS/MS data (Ariadne [8], RoboOligo [9]), but to obtain unambiguous localization of modifications, manual interpretation of MS/MS spectra is still required.
3. Electrospray spectrum produces multiple charged ions. Typically, RNase digest products are two or three times charged. Spectrum deconvolution allows to simplify spectrum reading by transforming multiple charges spectrum ($m/z$) to mono charge spectrum (mass).
4. Generally, the most intense series are y and c. Mongo Oligo online calculator (https://mods.rna.albany.edu/masspec/Mongo-Oligo) could be helpful to find and/or check ion series.
5. Pseudouridine may be specifically derivatized using *N*-cyclohexyl-*N*′-(2-morpholinoethyl)carbodiimide metho-*p*-toluenesulfonate (CMCT) in order to be detectable [10].
6. LC-MS/MS of digestion products allows the localization of methylation in the correct nucleotide but does not allow the localization on the ribose and/or on the base. Using known tRNA modification sequences, it could be possible to predict the type of methylation. Modomics tRNA database (http://modomics.genesilico.pl/sequences/list/tRNA/) [11] provides a large collection of modified tRNA sequences. Furthermore, based on phylogenetic conservation of modification locations, tRNAmodviz (http://genesilico.pl/trnamodviz/) [12], an online software tool, allows the visualization of modification pattern in tRNAs.
7. As with proteomics strategy, RNase digestion generates a set of oligonucleotides, specific to a unique tRNA. tRNA identification is possible by using a genomic tRNA database.

## Acknowledgments

The authors would like to thank Gérard Keith for the total *E. coli* tRNA preparation and Dominique Burnouf for critical reading of the manuscript and useful comments. We are grateful to Pascale Romby and Eric Westhof for their constant support. This work was supported by Labex NetRNA.

## References

1. Helm M, Motorin Y (2017) Detecting RNA modifications in the Epitranscriptome: predict and validate. Nat Rev Genet 18:275–291
2. Gaston KW, Limbach PA (2014) The identification and characterization of non-coding and coding RNAs and their modified nucleosides by mass spectrometry. RNA Biol 11:1568–1585
3. Fradin AH, Gruhl H, Feldmann H (1975) Mapping of yeast tRNAs by two-dimensional electrophoresis on polyacrylamide gels. FEBS Lett 50:185–189
4. Dong H, Nilsson L, Kurland GC (1996) Co-variation of tRNA abundance and codon usage in *Escherichia Coli* at different growth rates. J Mol Biol 260:649–663
5. Masato T, Ikumi M, Nakayama H, Masaki S, Matsuda R, Nobe Y, Yamauchi Y, Takeda J, Takahashi N, Toshiaki I (2010) In-gel digestion for mass spectrometric characterization of RNA from fluorescently stained polyacrylamide gels. Anal Chem 82:7795–7803
6. McLuckey SA, Van Berkel GJ, Glish GL (1992) Tandem mass spectrometry of small, multiply charged oligonucleotides. J Am Soc Mass Spectrom 3:60–70
7. Houser WM, Butterer A, Addepalli B, Limbach PA (2015) Combining recombinant Ribonuclease U2 and protein phosphatase for RNA modification mapping by liquid chromatography-mass spectrometry. Anal Biochem 478:52–58
8. Hiroshi N, Akiyama M, Taoka M, Yamauchi Y, Nobe Y, Ishikawa H, Takahashi N, Isobe T (2009) Ariadne: a database search engine for identification and chemical analysis of RNA using tandem mass spectrometry data. Nucleic Acids Res 37:e47
9. Sample PJ, Gaston KW, Alfonzo JD, Limbach PA (2015) RoboOligo: software for mass spectrometry data to support manual and de novo sequencing of post-transcriptionally modified ribonucleic acids. Nucleic Acids Res 43:e64
10. Durairaj A, Limbach PA (2008) Matrix-assisted laser desorption/ionization mass spectrometry screening for Pseudouridine in mixtures of small RNAs by chemical Derivatization, RNase digestion and signature products. Rapid Commun Mass Spectrom 22:3727–3734
11. Boccaletto P, Machnicka MA, Purta E, Piatkowski P, Baginski B, Wirecki TK, de Crécy-Lagard V (2018) MODOMICS: a database of RNA modification pathways. 2017 update. Nucleic Acids Res 46:D303–D307
12. Machnicka MA, Olchowik A, Grosjean H, Bujnicki JM (2014) Distribution and frequencies of post-transcriptional modifications in tRNAs. RNA Biol 11:1619–1629

## *2.* Cartographie des modifications post-transcriptionnelles des ARNt de *S.aureus*

La spectrométrie de masse est un outil puissant pour la caractérisation des modifications post-transcriptionnelles des ARN. La méthode de purification et d'analyse par NanoLC-MS/MS mise en place a ainsi permis d'établir une cartographie partielle des modifications présentes dans 40 ARNt de *S. aureus*. Les modifications spécifiques des bactéries à gram positives telles que le $mo^5U$ présente notamment dans les ARNt de *B. subtilis* a été localisé en position 34 des ARNt de *S. aureus*. La cartographie des ARNt établie permet l'étude dynamique des modifications des ARNt en réponse aux conditions environnementales rencontrées durant l'infection.

Biochimie 164 (2019) 60–69

Contents lists available at ScienceDirect

Biochimie

journal homepage: www.elsevier.com/locate/biochi

Research paper

# Mapping post-transcriptional modifications in *Staphylococcus aureus* tRNAs by nanoLC/MSMS

Laura Antoine [a, 1], Philippe Wolff [a, b, 1], Eric Westhof [a], Pascale Romby [a, **], Stefano Marzi [a, *]

[a] Université de Strasbourg, CNRS, Architecture et Réactivité de L'ARN, UPR 9002, F-67000, Strasbourg, France
[b] Plateforme Protéomique Strasbourg Esplanade, CNRS, FR1589, F-67000, Strasbourg, France

ARTICLE INFO

*Article history:*
Received 15 March 2019
Accepted 3 July 2019
Available online 8 July 2019

*Keywords:*
Post-transcriptional tRNA modifications
nanoLC/MSMS
*Staphylococcus aureus*
2D gel isolation

ABSTRACT

RNA modifications are involved in numerous biological processes. These modifications are constitutive or modulated in response to adaptive processes and can impact RNA base-pairing formation, protein recognition, RNA structure and stability. tRNAs are the most abundantly modified RNA molecules. Analysis of the roles of their modifications in response to stress, environmental changes, and infections caused by pathogens, has fueled new research areas. Nevertheless, the detection of modified nucleotides in RNAs is still a challenging task. We present here a reliable method to identify and localize tRNA modifications, which was applied to the human pathogenic bacteria, *Staphyloccocus aureus*. The method is based on a separation of tRNA species on a two-dimensional polyacrylamide gel electrophoresis followed by nano liquid chromatography-mass spectrometry. We provided a list of modifications mapped on 25 out of the 40 tRNA species (one isoacceptor for each amino acid). This method can be easily used to monitor the dynamics of tRNA modifications in *S. aureus* in response to stress adaptation and during infection of the host, a relatively unexplored field.



## 1. Introduction

### 1.1. A brief tour on the roles of tRNA modifications in bacteria

RNA modifications alter the chemical and physical properties of nucleotides and the biological functions of RNA. They are involved in numerous biological processes because they can impact RNA base-pairing formation, the structure of specific RNA motifs, protein recognition, translation and decoding properties, and RNA stability (for a review see Ref. [1]). RNA modifications can be present in many RNA species, but abundant noncoding RNAs such as tRNAs, rRNAs, and spliceosomal RNAs are the most heavily modified ones and depend on the modifications for their biogenesis and function. Today more than 170 modifications have been identified, primarily in tRNAs and rRNAs (http://modomics.genesilico.pl/modifications/) [2], and numerous RNA-modifying enzymes have been characterized [3–8]. The expression and activity of these enzymes can be modulated in response to environmental stresses, adding another layer of complexity in gene regulation. For example, in bacteria, deregulations of modifications in ribosomal RNAs (rRNA) can promote antibiotic resistance [9–11]. In tRNAs, modifications are central for folding, quality control, and efficient and accurate decoding. Also, they control gene expression during stress adaptation [12] and modulate interaction with human host [13].

tRNAs contain the largest number of modifications and the widest chemical diversity [2]. The complexity of tRNA modifications ranges from simple methylations on the base or the ribose to rather complex and large base hypermodifications, the synthesis of which generally depend on a cascade of enzymatic reactions [14]. Modifications have been shown to contribute to the highly conserved L-shaped structure, which is crucial for the interaction with a variety of proteins, the ribosome, and mRNAs. Interestingly, the distribution of the modified nucleotides along the tRNA molecule is conserved across evolution and reflects their two major functions in maintaining the tRNA structure and, ultimately, in decoding. Modified nucleotides concentrate in two hotspots - the anticodon loop and the tRNA core region, where the D- and

* Corresponding author.
** Corresponding author.
*E-mail address:* s.marzi@ibmc-cnrs.unistra.fr (S. Marzi).
[1] These authors contributed equally to this work.

https://doi.org/10.1016/j.biochi.2019.07.003
0300-9084/

**Abbreviations**

| | |
|---|---|
| LC | Liquid Chromatography |
| MS | Mass Spectrometry |
| BHI | Brain Heart Infusion |
| EtBr | Ethidium Bromide |
| TBE | Tris Borate EDTA |
| HFIP | Hexafluoro Isopropanol |
| TEA | Triethylamine |
| TEAA | Triethylamine Acetate |

TΨ-loops interact with each other (reviewed in Refs. [15,16]). tRNA modifications of the core are important for the stability of the tRNA structure. In this context, it was shown that they affect temperature adaptation in thermophilic as well as in psychrophilic organisms [17]. The modifications of the core region are also thought to be important for EF-Tu binding (U to T change at position 54 in the TΨ loop) [18] and since they are involved in the tertiary interactions maintaining the L-shape, they are expected to influence the binding of several proteins to the tRNA (i.e. aminoacyl tRNA synthetases and anticodon modification enzymes) [19,20]. tRNA modifications also facilitate tRNA-mediated transcriptional control through T-box riboswitches to sense intracellular availability of amino acids [21] and participate in quality control of tRNA integrity [22,23]. More recently, it was demonstrated that hypomodification of tRNAs in *Vibrio cholerae* induces their rapid decay mediated by the degradosome, demonstrating a new quality control mechanism [24].

Their major role in translation is due to their direct or indirect influence on the decoding process and fidelity of translation (i.e., [25]). Because the genetic code is degenerated, the 20 natural amino acids are encoded by 61 triplets that are recognized by 22–46 distinct tRNAs depending on the organism. Therefore, several tRNAs recognize more than one synonymous codon (i.e., the tRNA isoacceptors carry the same amino acid). The first nucleotide at position 34 of the anticodon (wobble base) can potentially form pairs non-complementary in the Watson-Crick sense (for a review see Refs. [26,27]). Detailed structural, physicochemical and kinetic studies of bacterial ribosomes associated with mRNA and aminoacyl-tRNAs have shown that the decoding center of the ribosome imposes specific constraints for the selection of a given codon by its cognate aminoacyl-tRNA by strongly favoring Watson-Crick pairs [25,28–34]. In miscoding induced by GU pairs, these pairs are in a Watson–Crick-like state promoted by tautomerization [27–29]. Interestingly, post-transcriptional modifications of nucleotide 34 can change the physicochemical behavior of the base (frequency of tautomerism), the spatial preference of the nucleotide (*syn/anti*, puckering of the ribose), the stability of codon-anticodon base-pairing and the structure of the anticodon loop itself, all contributing to the fidelity of the decoding process [25,35–40]. A typical example is given by $tRNATyr_{GUA}$, $tRNAAsn_{GUU}$, $tRNAAsp_{GUC}$ and $tRNAHis_{GUG}$, which can recognize both NAU and NAC codons, allowing G-C Watson-Crick base-pair with NAC codons and wobble G·U pair with NAU codons. These tRNAs (collectively harboring GUN anticodons), in eukaryotes and bacteria, present the Queuosine (Q) hypermodification on G34 [41]. Recently, Tuorto and colleagues [42] have demonstrated that, in mammals, the presence of Q affected translation speed. In the absence of Q modification, ribosomes pause on NAU codons, while NAC codons are much less affected [42]. Protein aggregation was observed for those genes enriched in NAU codons. This phenomenon seems to be species-specific since Q-modification in tRNAs in *S. pombe* has been shown to improve translation increasing the decoding speed of C-ending codons relative to U-ending codons [43]. Although not yet investigated, such deregulation based on mRNA codon content in response to the tRNA anticodon modification states, might take place in bacteria which display distinct codon usage bias (GtRNAdb [44]). Because tRNA modifications including the anticodon loop modifications can be modulated by various environmental changes, the proteome is expected to vary during adaptation [12]. To date, perturbations of tRNA modifications following physiological stress such as oxidation, temperature, pH, salinity, and nutrient starvation are well established in eukaryotes, but less well studied in bacteria [45,46].

### 1.2. Roles of tRNA modifications in pathogenic bacteria

During infection, pathogenic bacteria must adapt to the host environment, which is often scarce in nutrients and oxygen, and fastened with toxic metabolites and enzymes. They express virulence genes to interact with host tissues, to compete with the commensal flora, to avoid detection of the bacteria by the host immune system or to fight against it. Thus, pathogenic bacteria rapidly adapt to continuously changing environmental conditions and often regulate virulence gene expression at both the transcriptional and post-transcriptional levels. The analysis of the impact of RNA modifications in pathogenic bacteria during growth adaptation and infection has just started to be appreciated [47]. Recent studies in Gram-negative bacteria, have demonstrated that deletion of genes encoding RNA modification enzymes leaded to infection attenuation in mice, reduced colonization, decreased levels of the pro-inflammatory cytokines, reduced bacterial motility, replication in macrophages, and invasion of epithelial cells ([48] and references therein). For example, the deletion of the tRNA guanine transglycosylase gene (*tgt*) responsible for Q modifications reduces the translation of VirF, the transcription factor orchestrating *Shigella flexneri* virulence [49]. Moreover, tRNA modifications in pathogenic bacteria have been shown to modulate interaction with human host [13], or to regulate the expression of genes involved in the protection from oxidative stress, one of the main challenges that pathogenic bacteria must cope with during infection [50]. In mycobacteria, hypoxia modulates tRNA modification state to selectively translate codon-biased mRNAs for persistence genes [51]. In numerous Gram-negative (*Escherichia coli*, *Salmonella enterica*, *Aeromonas hydrophila*, *Pseudomonas fluorescens*, *P. aeruginosa* and *P. syringae*) and some Gram-positive pathogens (*Streptococcus pyogenes* and *S. suis*), the GidA/MnmE tRNA modification pathway, which leads to methylation of U34 in different tRNAs, has been implicated in the regulation of bacterial virulence [52]. Even if the precise mechanism remains unclear, an increased frequency of two-base frameshift has been reported [53]. Although these examples illustrate how the dynamic nature of tRNA modifications regulates virulence in various pathogenic bacteria, the roles of RNA modifications in *Staphylococcus aureus* have not been yet studied.

*S. aureus* is a Gram-positive opportunistic pathogen that is present in a third of the population on skin and in nostrils [54] as commensal bacteria, but is also responsible for a wide range of infections from minor skin abscesses to life-threatening diseases such as septicemia or toxic shock syndrome [55]. *S. aureus* represents a major health problem due to the insurgence of antibiotic multi-resistant strains in the hospital and community settings. Given the importance of tRNA modifications in several aspects of bacterial life, we decided to implement a rapid and easy method for their detection in *S. aureus* tRNAs for which little knowledge existed.

### 1.3. Analysis of tRNA modifications by mass spectrometry approaches

Mapping of post-transcriptional RNA modifications using mass spectrometry (MS) has existed for over 30 years [56]. The ability to get precise measure of molecular masses (less than 1 Da) provided the possibility to characterize modified residues in tRNAs using liquid chromatography coupled to mass spectrometry (LC/MSMS). Two complementary MS approaches have been developed. The first one implies total digest of tRNAs into nucleosides in order to identify the whole repertoire of modified nucleosides in one experiment [57]. The resulting nucleosides are thereby separated by reversed-phase high-performance liquid chromatography (HPLC) [58] and modifications detected using spectroscopy (e.g., UV) or by mass spectrometry [59]. The comparison of the HPLC chromatogram with known standard profiles and the characteristic measured mass-to-charge ratio ($m/z$) of the ionized nucleosides are contributing to the precise nucleoside identification. Atomic composition is finally obtained *via* collision induced dissociation (CID) tandem mass spectrometry (MSMS), providing a sensitive method for obtaining a survey of modified nucleosides in the tRNA sample. The second method is based on the generation of tRNA fragments produced from specific endoribonuclease digestion (e.g., RNase T1 cleaves every guanosine at their 3' side). The generated oligonucleotides with known 5′ and 3′-nucleotide identity [60] are then separated by HPLC and detected by MS. Fragments along the phosphodiester backbone by CID MSMS can be manually interpreted to localize the modification to a specific nucleotide. Thus, the mass and the sequence of each oligonucleotide is precisely identified by LC/MSMS allowing determination of the nature of each modification and their location in the tRNA sequence [61].

These two complementary methods have provided the first insights into tRNA modification dynamics following various stresses [56,62,63]. For nucleoside analysis, an ensemble of tRNAs can be studied to follow easily the changes of their modification patterns upon growth conditions while the LC/MSMS analysis of oligonucleotides requires purification of specific tRNA prior to digestion. This is usually done by affinity chromatography with a complementary DNA oligonucleotide linked to a solid resin or bead [63]. The recent development of Ultra-Performance LC (nanoLC) permits the careful separation of RNA fragments prior to the mass spectrometry analysis at very slow flow rates (hundreds of nL/min) in a column with a reduced resin diameter (<2 μm). This method requires smaller sample amounts, generates less chromatographic dilution and higher sensitivity. Because it is possible to detect very small amounts of tRNA-derived oligonucleotides, a two-dimensional gel electrophoresis (2D-PAGE) can be used to fractionate each tRNA species from bulk RNA extracts.

Here, we describe the use of this method and its application to the analysis of post-transcriptional modifications in *S. aureus* tRNAs. We also provide here for the first time a map of *S. aureus* tRNA modifications present in 26 out of the 40 tRNAs with different sequences, including at least one isoacceptor tRNA for each amino acid. We will also discuss applications to better address the roles of tRNA modifications in the physiopathology of *S. aureus*.

## 2. Material and methods

### 2.1. Bacterial growth

*S. aureus* HG001 strain, a derivative of RN1 (NCT8325) strain with restored *rbsU* (a positive activator of SigB), was used for tRNA isolation. The strain still contains a mutation at *tcaR*, a transcriptional regulator involved in teicoplanin susceptibility and biofilm [64]. *S. aureus* strain was manipulated under a specific hood in a dedicated room for manipulating class II pathogens. Stock culture in glycerol 25%, conserved at −80 °C were plated on a blood-agar Petri dish and grown at 37 °C overnight in Memmert model 100 incubator. One single clone was picked and grown in 2 mL Brain Heart Infusion (BHI from Sigma-Aldrich), incubated at 37 °C with a 180 rpm agitation overnight in a Stuart® orbital incubator S1600C. A preculture (100 μL) was added in 10 mL BHI medium ($OD_{600nm} = 0.05$), the bacterial growth was regularly checked until it reached an $OD_{600nm} = 3$ with a Thermospectronic Genesys 20 spectrophotometer (~4 h of culture at 37 °C stirring at 180 rpm).

### 2.2. Cell lysis and total RNA extraction

Cells were pelleted by centrifugation at 3750 rpm (3000 g) for 15 min at 4 °C in a Beckman Coulter Allegra X12-R centrifuge with a SX4750A rotor. Supernatant was carefully removed and the pellet (200 mg) was resuspended in 1 mL of RNAPro® Solution (MP Biomedicals, CA). Cells lysis was performed using a FastPrep®-24 with the 24 × 2 mL holder at 6 m/s speed in 2 mL FastPrep® tubes containing 0.1 mm zirconium silicate beads from FastRNA® pro blue kit (MP biomedicals, CA).

Total RNA purification followed the procedure described for the FastRNA Pro Blue Kit (MP Biomedicals, CA). RNA was further purified by adding 1/2 volume of chloroform:isoamyl alcohol (19:1), vortexed 10 s before precipitation of the RNA in the aqueous phase obtained by adding 3 vol of cold absolute ethanol (1.2 mL) in 2 mL Eppendorf tubes at −20 °C overnight. RNA was precipitated by centrifugation at 13000 rpm (18000 g) for 15 min at 4 °C using an Eppendorf 5417R centrifuge with a F45-30-11 rotor. The RNA pellet was washed with 500 μL of 80% cold ethanol and dried 20 min under vacuum in a Speed Vac® from Savant, before being resuspended in 200 μL of milliQ water. RNA concentration was determined by measuring absorbance at 260 nm with a Nanodrop ND-1000 spectrophotometer. Total RNA concentration was adjusted to 2 μg/μL. For phenol or chloroform extraction, work has to be done under a fume hood. Eppendorf tubes, tips, and buffers were RNase-free.

### 2.3. tRNA purification, 1st dimension PAGE

The first dimension gel electrophoresis was performed under denaturing conditions using 15% polyacrylamide gel (15% acrylamide:bisacrylamide 19:1 solution from Roth, 8 M urea, 1 × TBE buffer from Euromedex®) (Fig. 1A). Before loading the RNA sample, the gel was pre-run at 900 V for 20 min. One volume of urea-blue solution (urea 8 M, bromophenol blue and xylen cyanol 0.025%) was added to 5 μL containing 10 μg of total RNA. The sample was heated at 90 °C during 2 min before loading on the gel. After 15 h migration at 500 V at 20 °C, the gel was stained with 0.5 μg/mL EtBr solution (from Sigma-Aldrich) by soaking the gel during 5 min, then washed with milliQ water and visualized on a High performance 2UV™ transilluminator from UVP. The gel slice containing 5S rRNA and tRNAs was cut to perform the second dimension gel.

### 2.4. Individual tRNA purification, 2nd dimension PAGE

The second dimension was performed under semi-denaturing conditions. The first dimensional gel slice (see § 2.3) was first placed horizontally at the top and between two glass plates (20 × 20 cm). Then a solution containing 20% polyacrylamide (polyacrylamide-bisacrylamide 19:1), 4 M urea, 1X TBE and 0.06% of ammonium persulfate and TEMED was poured between the plates. Once polymerized, the gel was run at 6 W (200 V) for 24 h at 20 °C using BioRad Protean II xi Cell. The gel was stained with EtBr as described in paragraph § 2.3 before UV visualization (Fig. 1B). Gel

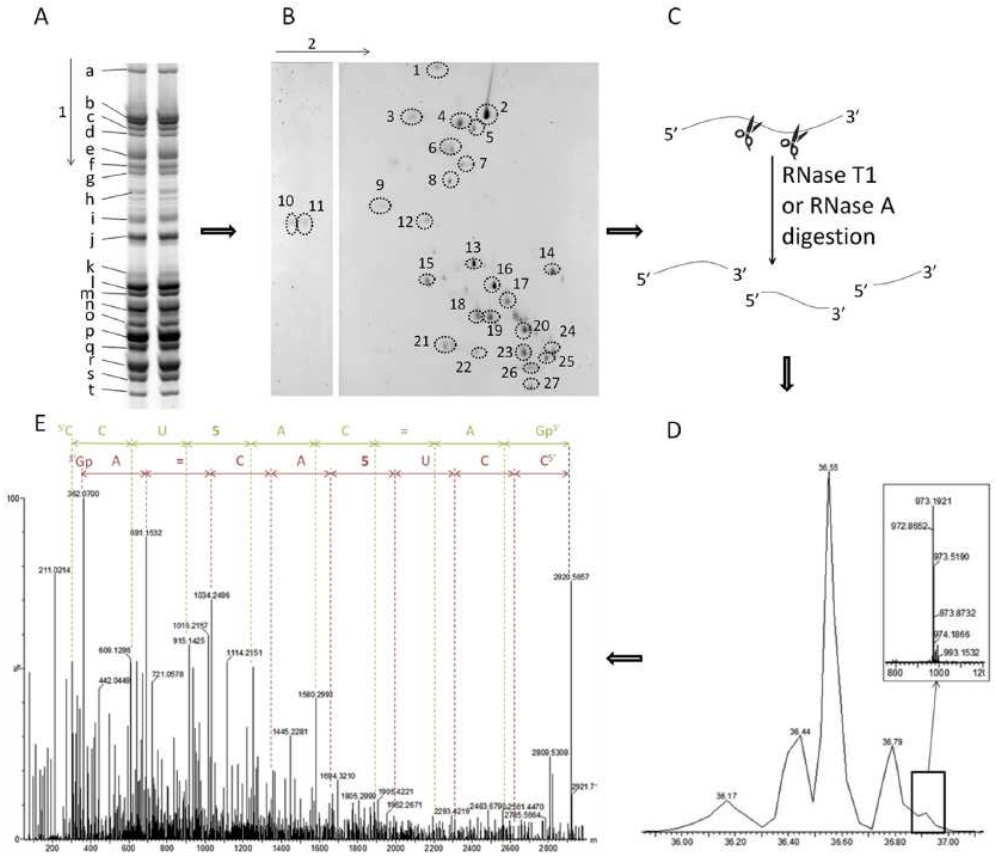


**Fig. 1. Complete protocol for nanoLC/MSMS analysis of *S. aureus* tRNAs from isolation to modification mapping.** The five main steps of the protocol are as follow. *A. First-dimension PAGE.* Total RNA was migrated on the first-dimension gel electrophoresis (denaturing 15% PAGE with 8 M Urea). The gel slice containing "tRNA-size" (25000–150000 Da) RNA species migrating close to 5S rRNA, was cut. Arrow 1 indicates the direction of gel migration. The gel slice containing the tRNAs is deposited on the top of the second-dimension gel. In parallel, the 21 visible bands (colored by Ethidium Bromide and named from *a* to *t*) were cut individually, digested with RNase T1 and analyzed by nanoLC/MSMS to determine which tRNAs are present in each band (see at the end of the legend). *B. Second-dimension PAGE.* Separation of the tRNAs from the first-dimension gel slice in the second-dimension gel electrophoresis (semi-denaturing 20% PAGE with 4 M Urea). Arrow 2 indicates the direction of migration. After staining, the gel was divided into three large areas to be analyzed by the Gel Doc™ EZ imager. Here only the middle (left) and bottom (right) parts are reported but the two pieces are coming from the same experiment. No spots were visible on the upper part of the gel (not shown). Each of the 23 spots (numbered from 1 to 23) was cut and used for the following steps. The identity of these spots, as obtained from the complete analysis is given at the end of the legend. *C. RNases in gel digestion.* The spots were subjected to RNase T1 or RNase A digestion, desalted, and used for the liquid chromatography separation of the fragments. *D. nanoLC (Ultra-Performant Liquid Chromatography) and MS analysis.* The RNase derived fragments from each 2D spot are separated on the BEH C18 column with a 300 nL/min flow rate. An example from spot 17 (tRNAVal$_{UAC1\text{-}2\text{-}3}$) digested with RNase T1 is given. Each peak is subjected to MS (insert) and MSMS (E) to determine its sequence and the presence of modifications. *E. MSMS analysis.* Electrospray-Ionization Collision-Induced Dissociation (ESI CID) spectrum obtained for the $^{5'}$CCU5UAC = AGp$^{3'}$ oligonucleotide ($m/z$ = 972.87, triple charged (-3H$^+$)) from the *S. aureus* tRNAVal$_{UAC1\text{-}2\text{-}3}$. The profile obtained from the MSMS (fragmentation) analysis is shown with its sequence given from its 5′ nucleotide (sequence in green, c ion series) or from its phosphorylated 3′ nucleotide (sequence in red, y ions series). The localization of a N6-methyladenosine ($m^6$A) is showed with its symbol " = ". **1D bands**: *a*: tRNASer$_{UGA3}$; *b*: 5S rRNA fragment + tRNASer$_{GCU}$; *c*: 5S rRNA fragment + tRNASer$_{UGA1}$; *d*: tRNATyr$_{GUA2}$; *e*: tRNALeu$_{UAG}$; *f*: tRNALeu$_{UAA1\text{-}2}$; *g*: tRNALeu$_{CAA}$; *h*: tRNAHis$_{GUG1\text{-}2}$; *i*: tRNAThr$_{UGU1\text{-}2\text{-}3}$ + tRNAHis$_{GUG1\text{-}2}$; *j*: tRNAArg$_{ACG1\text{-}2}$ + tRNAMet$_{CAU1}$; *k*: tRNAGly$_{GCC1\text{-}2p}$ (proteinogenic); *l*: tRNAAsp$_{GUC1\text{-}2\text{-}3\text{-}4}$ + tRNAIle$_{GAU1\text{-}2}$; *m*: tRNAMet$_{CAUI1}$; *n*: tRNAVal$_{UAC1\text{-}2\text{-}3}$; *o*: tRNAVal$_{UAC1\text{-}2\text{-}3}$ + tRNAGlu$_{UUC1}$; *p*: tRNAPro$_{UGG1\text{-}2}$ + tRNAAla$_{UGC1\text{-}2\text{-}3}$; *q*: tRNAAla$_{UGC1\text{-}2\text{-}3}$ + tRNAPhe$_{GAA}$; *r*: tRNAGly$_{UCC1\text{-}2p}$ + tRNAAsn$_{GUU1\text{-}2\text{-}3}$ + tRNALys$_{UUU2\text{-}3}$; *s*: tRNAGln$_{UUG1\text{-}2}$ + tRNATrp$_{CCA}$; *t*: tRNAGly$_{UCC1\text{-}3np}$ (non-proteinogenic). **2D spots**: 1: tRNASer$_{UGA3}$; 2: 5S rRNA fragment; 3: tRNASer$_{GCU}$; 4: tRNASer$_{UGA1}$; 5: tRNATyr$_{GUA2}$; 6: tRNALeu$_{UAG}$; 7: tRNALeu$_{UAA1\text{-}2}$; 8: tRNALeu$_{CAA}$; 9: tRNAHis$_{GUG1\text{-}2}$; 10: tRNAArg$_{ACG1\text{-}2}$; 11: tRNAThr$_{UGU1\text{-}2\text{-}3}$; 12: tRNAMet$_{CAU1}$; 13: tRNAGly$_{GCC1\text{-}2}$; 14: tRNAAsp$_{GUC1\text{-}2\text{-}3\text{-}4}$; 15: tRNAIle$_{GAU1\text{-}2}$; 16: tRNAMet$_{CAUI1}$; 17: tRNAVal$_{UAC1\text{-}2\text{-}3}$; 18: tRNAGlu$_{UUC1}$;: 19: tRNAPro$_{UGG1\text{-}2}$; 20: tRNAAla$_{UGC1\text{-}2\text{-}3}$; 21: tRNAPhe$_{GAA1}$; 22: tRNAGly$_{UCC1\text{-}2p}$ (proteinogenic); 23: tRNAAsn$_{GUU1\text{-}2\text{-}3}$; 24: tRNALys$_{UUU2\text{-}3}$; 25: tRNATrp$_{CCA}$; 26: tRNAGln$_{UUG1\text{-}2}$; 27: tRNAGly$_{UCC1\text{-}3np}$ (non-proteinogenic). 1D bands and 2D spots are also summarized in Table 1.

pictures were taken with a Gel Doc™ EZ imager with its corresponding 16 × 12 cm UV tray.

### 2.5. In gel RNase digestion

Gel spots containing tRNAs were excised with a blade scalpel and dried under vacuum for 10 min (Speed Vac®). Digestion of the tRNAs with specific RNase was carried out directly on the gel fragments. The gel spots were incubated with 20 μL of 1U/μL of RNase T1 from Thermo Fisher Scientific (cleavage at G residues) in ammonium acetate 100 mM (pH 6.8) and incubated at 50 °C for 3 h followed by a 37 °C overnight incubation under 300 rpm constant

agitation. Alternatively, 20 μL of 0.01 U/μL of RNase A from Thermo Fisher Scientific (cleavages at C and U residues) in ammonium acetate 100 mM were added to the gel spots and the samples were incubated at 60 °C during 3 h, followed by a 37 °C overnight incubation under 300 rpm constant agitation. The samples were stored at −20 °C or immediately desalted, after removal of the gels by centrifugation (10 min, at 18000 g, at 4 °C), using ZipTIP C18 (Millipore) prewet with acetonitrile 50% in milliQ water (3 × 10 μL) and 200 mM ammonium acetate (3 × 10 μL). The supernatant containing the digested tRNA fragments passively eluted from the gel, was loaded on the column, which was then washed with 200 mM ammonium acetate (7 × 10 μL) followed by milliQ water (5 × 10 μL). Finally, the fragments were eluted with 10 μL of 50% acetonitrile in milliQ water and dried for 25 min under vacuum (Speed Vac®) (Fig. 1C).

### 2.6. nanoLC/MSMS of RNA oligonucleotides

The pellet containing the oligonucleotides is resuspended in 3 μL of milliQ water. The oligonucleotides were then separated on nanoLC Acquity UPLC peptide BEH C18 column (130 Å, 1.7 μm, 75 μm × 200 mm) using a nanoAcquity UPLC system (Waters). The column was pre-equilibrated in Buffer A (200 mM HFIP (Hexafluoroisopropanol), 7 mM TEA (Triethylammonium), 7.5 mM TEAA (Triethylammonium acetate, pH 7.5) at a flow rate of 300 nL/min. After loading on the column, the RNase digestion products were eluted using a step gradient with two segments. The first consists of a gradient 15–35% of solution B (100% methanol (MeOH)) for 2 min, followed by the second step where the solution B reaches 50% (during 20 min at the same flow rate). Finally, the MeOH solution is decreased to 15% during 25 min. The column is then re-equilibrated in Buffer A during 20 min (Fig. 1D).

MS and MSMS analysis were performed using a SYNAPT G2-S HDMS from Waters equipped with a NanoLockSpray-ESI source in negative sensitivity mode with a capillary voltage set to 2.6 kV and sample cone to 30 V. Source was heated to 130 °C. For MS analysis, a mass range from 550 to 1500 ($m/z$) was used followed by Collision Induced Decay (CID) fragmentation of most intense signals with a $m/z$ detection range of fragments from 50 to 2000 with 1s scans (Fig. 1E).

### 2.7. Data analysis

Chromatograms and spectra were processed using the Masslynx software from Waters (V4.1). CID fragment spectra were deconvoluted by MaxEnt3 tool to convert the $m/z$ measured from multicharged ions into singly charged ones. Spectra were then manually sequenced using oligonucleotide fragmentation ion nomenclature [65]. Sequences are deduced by calculating mass difference between consecutive fragment ions singly charged. Typically, the most intense ion series (y and c) were used. Correct manual annotation was checked using MongoOligo online calculator (http://mods.rna.albany.edu/masspec/Mongo-Oligo), with a maximum tolerance of 0.05 Da between the calculated mass and the measured mass for parent and fragment ions. The tRNA genomic sequences were obtained from the HG001 genome [66].

## 3. Results and discussion

### 3.1. A global view of S. aureus tRNA modifications

The above protocol is fast and easily implementable. Briefly, the pool of tRNAs extracted from *S. aureus* cultures was isolated by collecting RNA species of sizes smaller than the 5S rRNA (118 nucleotides), which are clearly visible on a denaturing (8 M Urea) 1D gel (Fig. 1A). The tRNA samples were loaded on two different lanes on 1D gel. One lane was used for direct nanoLC/MSMS analysis and the other one was deposited on top of semi-denaturing gel for the second-dimension. The bands from the 1D gel were cut and analyzed by nanoLC/MSMS method to assign each tRNA (Fig. 1A). Several bands contained different RNA species (i.e., band *b* contains both a 5S fragment and $tRNASer_{GCU}$; and band *j* contains both $tRNAArg_{ACG1\text{-}2}$ and $tRNAMet_{CAU1}$). To assign unambiguously fragments to the different tRNAs, we then proceeded to a further purification step using the second-dimension gel electrophoresis under semi-denaturing conditions (4 M urea) (Fig. 1B). The 1D bands gave rise to several spots where tRNAs are migrating individually (i.e. band *b* was resolved into spots 2 and 3 containing 5S rRNA and $tRNASer_{GCU}$, respectively; and band *j* was resolved into spots 10 and 12 corresponding to $tRNAArg_{ACG1\text{-}2}$ and $tRNAMet_{CAU1}$, respectively). Each spot was subjected to the in-gel RNase T1 digestion (Fig. 1C) followed by nanoLC/MSMS analysis (Fig. 1D–E), which provided information on the sequences and on the presence of modifications.

Sixty-one tRNA genes are present in *S. aureus* HG001 [63]. They are transcribed from eleven *loci* as single genes ($tRNASer_{UGA1}$, $tRNAArg_{CCG}$, $tRNAArg_{UCU}$ and $tRNAGln_{UUG3}$) or organized into seven operons (I to VII, Fig. 2) sometimes together with rRNAs. The number of isoacceptor tRNAs varies between one (Cys, Trp and elongator tRNAMets) to seven (tRNAGly) (Fig. 2). With the exclusion of the non-proteinogenic tRNAGly and the tRNACys, we could determine fragments belonging to 25 different tRNAs (Table 1) representing 46 tRNA genes, at least one isoacceptor for each tRNA. Some isoacceptors have identical sequences and cannot be distinguished in our analysis (the three $tRNAAla_{UGC}$, the two $tRNAArg_{ACG}$, the three $tRNAAsn_{GUU}$, the four $tRNAAsp_{GUC}$, two of the three $tRNAGln_{UUG}$, the two $tRNAGly_{GCC}$, the two proteinogenic $tRNAGly_{UCC}$, two of the three non-proteinogenic $tRNAGly_{UCC}$, the two $tRNAIle_{GAU}$, the two $tRNALeu_{UAA}$, the two $tRNAPro_{UGG}$, the three $tRNAThr_{UGU}$ and the three $tRNAVal_{UAC}$). For the other tRNAs, we could determine exactly from which gene they were transcribed. Only fourteen tRNAs could not be detected (indicated with blue dots in Fig. 2; $tRNAGlu_{UUC2}$ and $tRNAGlu_{UUC3}$ are identical and therefore counted as single species). Three of them are transcribed from a single gene while the others belong to operons from which other tRNAs were isolated in our analysis. Since the most intense spots on the 2D-gel were all analyzed, it is possible that they are less abundant (less transcribed or more rapidly degraded) and more difficult to be detected. To complete the *S. aureus* tRNA analysis, it would be necessary to purify them individually using biotinylated oligonucleotides, which could specifically fish them from total RNA extracts [63].

Several modifications were detected on the tRNA fragments (Fig. 3) deriving from the core region (D and TΨ stem-loops), the variable region, and the anticodon loop. Modifications at nucleotides in the core region and variable loop include dihydrouridine (D), 1-methyladenosine ($m^1A$), 7-methylguanosine ($m^7G$), and thymidine (T). A high diversity of modifications was found in the anticodon loop and ten of them concentrate at positions 34 and 37 (Table 1, Fig. 3). Using the present strategy, pseudouridine (Ψ) cannot be detected since its mass is indistinguishable from that of uridine. In order to trace them, we use *N*-cyclohexyl-N′-β-(4-methylmorpholinium) ethylcarbodiimide *p*-tosylate (CMC) derivatization which modified only Ψ under alkaline conditions (at pH above 10) [67]. Although such modification can be visualized by mass spectrometry [68,69], we unfortunately lost it during the MSMS fragmentation step preventing the detection of any Ψ. This technical issue could be solved by the use of acrylonitrile, which is

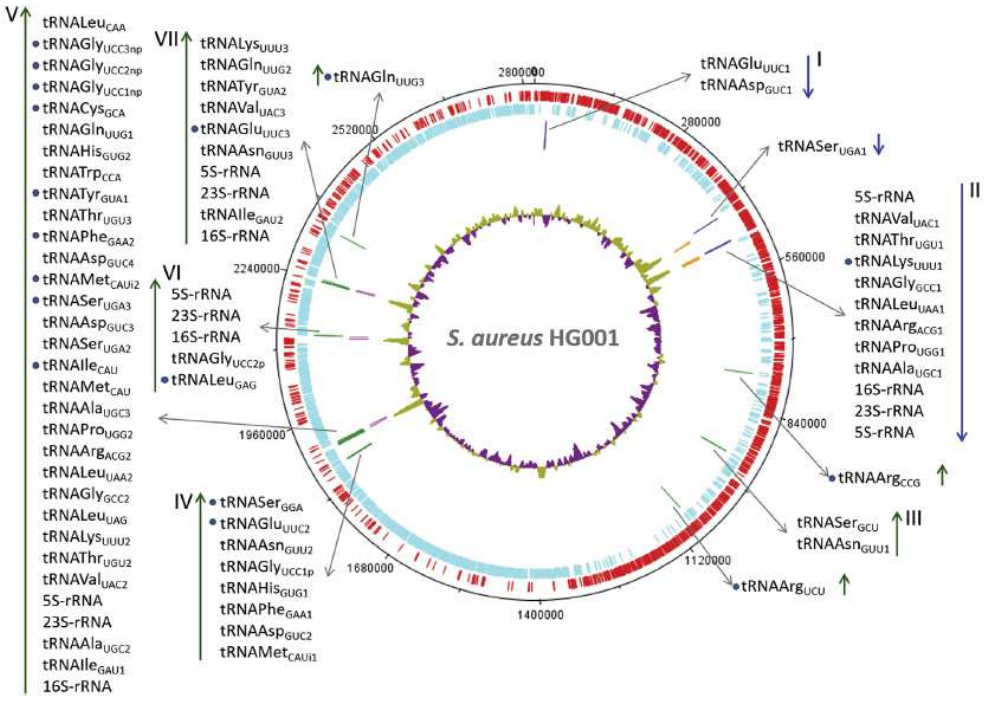


**Fig. 2.** ***Staphylococcus aureus*** **HG001 tRNA operons organization.** The sixty-one genes present in *S. aureus* HG001 [66] were placed on a circular genome representation using DNAPlotter [96]. The tRNA genes are expressed from eleven loci sometimes as single gene, and more often as operons, which also contain rRNA genes. tRNAs which were not detected in the present study are marked with a blue dot. tRNA genes on the positive and negative strands are represented as long blue and green tracks, respectively. rRNA genes on the positive and negative strands are represented as yellow and pink tracks, respectively. Coding sequences on the positive and negative strands are represented as red and cyan tracks, respectively. Mean centered GC% plot is represented in mustard (above-mean) and violet (below mean).

more resistant to the fragmentation [70].

Table 1 shows the regions that were probed for each analyzed tRNA. Four tRNAs are almost complete (coverage > 70% for the tRNASer$_{UGA3}$, the tRNAPro$_{UGG1\text{-}2}$, the tRNALys$_{UUU2\text{-}3}$ and the tRNAGlu$_{UUC1}$). On average almost 60% of the tRNA sequences were analyzed and, for most of the tRNAs, the core region and the anticodon loop were covered with the exception of tRNALeu$_{UAA1\text{-}2}$ and tRNATrp$_{CCA}$, for which we could not cover any nucleotide of the anticodon loop, and tRNAArg$_{ACG1\text{-}2}$ and tRNAGln$_{UUG1\text{-}2}$, for which we could not detect fragments including their anticodons (nucleotides 34–36). In this study, we used RNase T1 and RNase A since they are highly active enzymes able to hydrolyze RNA in the gel. RNase T1 cleaves specifically at guanosines while RNase A cleaves at pyrimidine residues. To enhance the coverage, we tested other RNases. We first used RNase MC1, which cleaves at the 5′ of uridine and pseudouridine [71] but no significant gel digestion of the tRNAs could be obtained (data not shown). We finally adapted RNase U2, which cleaves at purines with a slight specificity to adenosine [72], and preliminary data revealed that RNase U2 is able to digest RNAs contained in gel. By using multiple RNases with different base specificity, oligonucleotide fingerprints can be overlapped to provide full sequence coverage and to complete the mapping of tRNA modifications.

Overall, *S. aureus* tRNA modification types and their localization are similarly found in other Gram-positive bacteria such as *Bacillus subtilis* [2] and *Lactococcus lactis* [73] (Fig. S1). *S. aureus* specific features are discussed thereafter.

### 3.2. Individual tRNA modification maps

All modifications that were detected in the analyzed *S. aureus* tRNAs are detailed in Table 1. As expected, most of them were localized in the core regions and in the anticodon loops. In general, the modifications were also conserved in many other bacteria.

Our work highlights the possible roles of the modifications at position 34 and 37 in tRNA anticodons for fidelity maintenance, codon selection and discrimination in *S. aureus*. For instance, Q at position 34 of tRNATyr$_{GUA}$ was proposed to efficiently discriminate tyrosine codons (UAU and UAC) from stop codon during translation in eukaryotes (review in Ref. [14]) and to increase affinity for UAU codons [42] in bacteria. As expected, we could detect Q34 in tRNATyr$_{GUA2}$, but also in tRNAAsn$_{GUU1\text{-}3}$, tRNAAsp$_{GUC1\text{-}4}$ and tRNAHis$_{GUG1\text{-}2}$.

Modification at U34 is regularly found in tRNAs that read split codon-box families where the synonymous A- and G-ending codons encode a different amino acid than the U- and C-ending codons. We detected three major modifications at U34 (Table 1). The mo$^5$U (5-methoxyuridine (5)) [74] was present in eight *S. aureus* tRNAs. This modification is only found in Gram-positive bacteria and is believed to enhance translational fidelity by the ribosome [27,39,75]. We found cmnm$^5$s$^2$U (5-carboxymethylaminomethyl-2-thiouridine ($)) in the *S. aureus* tRNALys$_{UUU2\text{-}3}$. This hypermodification is ubiquitous in all bacteria and is usually detected in several tRNAs (Lys$_{UUU}$, Gln$_{UUG}$, Glu$_{UUC}$, Trp$_{UCA}$ or Leu$_{UAA}$). Finally, mnm$^5$s$^2$U (5-methylaminomethyl-2-thiouridine (S)) was observed

**Table 1**

**Characterization of RNA modifications in 26 *Staphylococcus aureus* tRNAs.** Sequences of characterized tRNAs are reported with their respective coverage percentages. In the sequences the color code is as follow: **red** nucleotides indicate oligonucleotides fragments obtained by RNase T1 digestion, **green** nucleotides indicate oligonucleotides fragments obtained by RNase A digestion (overlapping sequences are in red) while **black** nucleotides represent regions that could not be analyzed. The various regions of the tRNAs are visualized by colors according to the tRNA database http://trna.bioinf.uni-leipzig.de/as follow: sequences highlighted in orange are for the two complementary strands of the anticodon arm; sequences highlighted in green are for the two complementary strands of the D-stem; sequences highlighted in blue are for the two complementary strands of the acceptor-stem; sequences highlighted in pink are for the two complementary strands of the T-stem; sequences highlighted in light blue are for the CCA at the 3'. Modifications are indicated with symbols described in Fig. 3B.

| ID | 2D | A. A. | Anticc. | | Acc-stem | | D-stem | | D-loop | | D-stem | | Ac-stem | | Ac-loop | Ac-stem | V-region | T-stem | T-loop | T-stem | Acc-stem | | CCA | Cover. (%) | HG001 | Operon |
|---|---|---|---|---|---|---|---|---|---|---|---|---|---|---|---|---|---|---|---|---|---|---|---|---|---|---|
| | | | | -1 | 1 | | 8 | 10 | 14 | | 22 | 26 | 27 | | 32 | 39 | 44 | 49 | 53 | 61 | 66 | 73 | 74 | | | |
| p/q | 20. | Ala | UGC 1-2-3 | - | GGGGGCU | | UA | GCUC | AGCUGGGA | | GAGC | G | CCUGC | | UUSGCAC | GCAGG | AGGUC | AGCGG | UUCGAUC | CCGCU | AGUCUCC | A | CCA | 38 | 00443<br>01812<br>01823 | II<br>V<br>V |
| j | 10. | Arg | ACG 1-2 | - | GCGCCCG | | UA | GCUC | AAUDGGAUA | | GAGC | G | UUUGA | | CUACGKA | UCAAG | AG7UU | AUGGG | UUCGACU | CCUAU | CGGGCGC | G | CCA | 38 | 00441<br>01814 | II<br>V |
| r | 23. | Asn | GUU 1-2-3 | - | UCCACAG | | UA | GCUC | AGUGGUA | | GAGC | U | AUCGG | | CUQUU6A | CCGAU | CGGUC | GUAGG | UUCGAGU | CCUAC | CUGUGGA | G | CCA | 49 | 00874<br>01758<br>02198 | III<br>IV<br>VII |
| l | 14. | Asp | GUC 1-2-3-4 | - | GGUCUCG | | UA | GUGU | AGCGGDDA | | ACAC | G | CCUGC | | CUQUCAC | GCAGG | AGAUC | GCGGG | TUCGAUU | CCCGU | CGAGACC | G | CCA | 63 | 00021<br>01762<br>01805<br>01808 | I<br>IV<br>V<br>V |
| s | 26. | Gln | UUG 1-2 | - | UGGGCUA | | UA | GCCA | AGCGGUA | | AGGC | A | ACGGA | | CUUUGAC | UCCGU | CACUC | GUUGG | UUCGAAU | CCAGC | UAGCCCA | G | CCA | 27 | 01799<br>02194 | V<br>VII |
| o | 18. | Glu | UUC 1 | - | GGCUCCU | | UG | GUCA | AGCGGDDA | | "GAC | A | CCGCC | | CUSUCAC | GGCGG | UAAC | ACGGG | TUCGAGU | CCCGU | AGGAGUC | A | CCA | 85 | 00020 | I |
| k | 13. | Gly | GCC 1-2 | - | GCAGAAG | | UA | GUUC | AGCGGUA | | GAAU | A | CAACC | | UUGCCAA | GGUUG | GGGUC | GCGGG | UUCGAAU | CCCGU | CUUCUGC | U | CCA | 59 | 00439<br>01816 | II<br>V |
| r | 22. | Gly | UCC 1-2 p | - | GCGGGUG | | UA | GUUU | AAUGGCA | | AAAC | C | UCAGC | | CUSCCAA | GCUGA | UGUU | GUGGG | UUCGAUU | CCCAU | CACCCGC | U | CCA | 61 | 01759<br>02088 | IV<br>VI |
| i/h | 9. | His | GUG 1-2 | G | GCGGUUG | | UG | GUGA | AGUGGDDA | | "CAC | A | UCGGA | | UUQUQK/GU | UCCGA | CAUUC | GAGGG | TUCGAUC | CCCUU | CAGCCGC | C | CCA | 68 | 01760<br>01800 | IV<br>V |
| l | 15. | Ile | GAU 1-2 | - | GGGCCUA | | UA | GCUC | AGCUGGDDA | | GAGC | G | CACGC | | CUGAU6A | GCGUG | AGGUC | GGUGG | UUCGAGU | CCACU | UAGGCCC | A | CCA | 53 | 01824<br>02201 | V<br>VII |
| g | 8. | Leu | CAA | - | GCCGGUG | | UG | GCGG | AAUDGGCAG | | ACGC | G | CGGGA | | CUBAA+A | UCCCG | UUCCACUUGUGGAGU | GUCGG | UUCGACC | CCGAC | CACCGGU | A | CCA | 52 | 01794 | V |
| f | 7. | Leu | UAA 1-2 | - | GCCGGGG | | UG | GCGG | AACDGGCAG | | ACGC | A | CAGGA | | CUUAAAA | UCCUG | CGGUGAGAGAUCACCGU | ACCGG | TUCGAUU | CCGGU | CCUCGGC | A | CCA | 57 | 00440<br>01815 | II<br>V |
| e | 6. | Leu | UAG | - | GCGGGUG | | UG | GCGG | AAUDGGCAG | | ACGC | A | CUAGA | | CUSAGKA | UCUAG | CGCCUUACGGCGU | GGGGG | TUCGACU | CCCUU | CACCCGC | A | CCA | 66 | 01817 | V |
| r | 24. | Lys | UUU 2-3 | - | GAGCCAU | | UA | GCUC | AGUUGGUA | | GAGC | A | UCUGA | | CUS/SUU6/HA | UCAGA | GGGUC | AGAGG | TUCGAAU | CCUCU | AUGGCUC | A | CCA | 74 | 01818<br>02193 | V<br>VII |
| m | 16. | Met | CAU i1 | - | CGCGGGA | | UG | GAGC | AGUUCGGUA | | GCUC | G | UCGGG | | CUCAUAA | CCCGA | AGGUC | GGUGG | TUCAAAU | CCGCC | UCCCGCA | A | CCA | 44 | 01763 | IV |
| j | 12. | Met | CAU | - | GGCGGUG | | UA | GCUC | AGCUGGCDA | | GAGC | G | UACGG | | UUMAU=C | CCGUG | AGGUC | GGGGG | TUCGAUC | CCCUC | CACCGCC | A | CCA | 65 | 01811 | V |
| q | 21. | Phe | GAA 1 | - | GGUUCAG | | UA | GCUC | AGUUGGUA | | GAGC | A | AUGGA | | UUGAAKC | UCCAU | GUGUC | GGCAG | UUCGACU | CUGUC | CUGAACC | A | CCA | 45 | 01761 | IV |
| p | 19. | Pro | UGG 1-2 | - | CGGGAAG | | UA | GCUC | AGCUUGGUA | | GAGC | A | CUUG | | UUSGGKA | CCAAG | GGGmUC | GCAGG | TUCGAAU | CCUGU | CUUCCCG | A | CCA | 72 | 00442<br>01813 | II<br>V |
| b | 3. | Ser | GCU | - | GGAAACG | | UA | CUCA | AGUUGGCUGA | | "GAG | G | CGCCC | | CUGCU6A | GGGUG | UAGUCGCGAAAGCGGCGC | GAGGG | TUCGAAU | CCCUC | CGUUUCC | G | CCA | 66 | 00873 | III |
| c | 4. | Ser | UGA 1 | - | GGAGGAA | | UA | CCCA | AGUCCGGCUGA | | AGGG | A | UCGGU | | CUSGA+A | ACCGA | CAGGGGCUUAACGGCUCGC | GGGGG | UUCGAAU | CCCUC | UUCCUCC | G | CCA | 31 | 00383 | - |
| a | 1. | Ser | UGA 3 | - | GGAGGAA | | UA | CCCA | AGUCCGGCUGA | | "GGG | A | UCGGU | | CUSGA+A | ACCGA | CAGGGCCUUAACGGGCCGC | GGGGG | TUCGAAU | CCCUC | UUCCUCC | G | CCA | 70 | 01807 | V |
| i | 11. | Thr | UGU 1-2-3 | - | GCCGGCC | | UA | GCUC | AAUDGGUA | | GAGC | A | ACUGA | | CUSGU6A | UCAGU | AGGUU | GGGGG | TUCAAGU | CCUCU | GGCCGGC | A | CCA | 34 | 00437<br>01803<br>01819 | II<br>V<br>V |
| s | 25. | Trp | CCA | - | AGGGGCA | | UA | GUUC | AACGGUA | | GAAU | A | GAGGU | | CUCCAAA | ACCUU | UGGU | GUGGG | UUCGAUU | CCUAC | UGCCCCU | G | CCA | 45 | 01801 | V |
| d | 5. | Tyr | GUA 2 | - | GGAGGGG | | UA | GCGA | AGUGGCDAA | | "CGC | G | GCGGA | | CUQUA+A | UCCGC | UCCUUCGGGUUC | GGCAG | UUCGAAU | CUGCC | CCCCUCC | A | CCA | 64 | 02195 | VII |
| n/o | 17. | Val | UAC 1-2-3 | - | GGAGAAU | | UA | GCUC | AGCUGGGA | | GAGC | A | UCUGC | | CUSAC=A | GCAGA | GGGUC | GGCGG | UUCGAAC | CCGUC | AUUCUCC | A | CCA | 54 | 00436<br>01820<br>02196 | II<br>V<br>VII |

in tRNAGlu$_{UUC}$ and tRNALys$_{UUU}$ as shown in several Gram-negative bacteria like *Escherichia coli*. The hypermodifications (S and $) at U34 are primarily observed on tRNAs carrying U34 and U35 (Table 1). In fact, these two uridines are essential recognition determinants for the enzyme MnmA, which catalyzes the thiolation at position 2 of U34 [76]. Intriguingly, *S. aureus* tRNALys$_{UUU2-3}$ presented both "$" and "S" modifications at U34 (Fig. S2). Such heterogeneity was also observed at position 37 where $t^6A$ (N6-threonylcarbamoyladenosine (6)) was present on the same fragment presenting S at U34, while an unknown adenosine hypermodification (for a total mass of 530 Da for the nucleotide) was observed for the fragment containing $34. To estimate the relative abundance of the two different modification patterns of tRNALys$_{UUU2-3}$, the area of the peaks of the two distinct oligonucleotides in the mass chromatogram was determined (Figs. S2E–F). The comparison reveals that the oligonucleotide containing the anticodon with unknown modified adenosine (H) represents 34.6% of the total tRNALys$_{UUU2-3}$. Further analysis will be required to identify this novel modification, to carefully quantify its abundance and to understand the functional consequences of such heterogeneity in tRNALys.

The modification contents were also analyzed on the unique elongator tRNAMet$_{CAU}$ and one initiator tRNAMet$_{iCAU}$ species. The important determinants of the initiator tRNA in all bacteria are the absence of a Watson–Crick base pair between positions 1 and 72 in the acceptor stem and the presence of three conserved consecutive G:C base pairs in the anticodon stem [77]. The peculiarity of the acceptor stem accounts for the high specificity of the methionyl-tRNA$^{fMet}$ transformylase (FMT) for methionylated tRNAs over other aminoacylated species [78,79], while the anticodon stem-loop is important for IF3 discrimination of non-initiator tRNAs in the 30S translation initiation complex [80–83]. In addition, formylation of the methionine prevents misrecognition of the initiator tRNA by EF-Tu [84,85]. No modification could be detected in the anticodon of the initiator tRNAMet (Table 1). A search in the Modomics database (http://modomics.genesilico.pl [2,86]) shows that the absence of modification in the anticodon is a trait common to other bacterial initiator tRNAs (e.g., *Lactococcus lactis* and *Streptomyces griseus*), except that a methylation on the ribose at C32 was observed in *Thermus thermophilus* and in *E. coli*. The absence of modification for the initiator tRNA anticodon could be another peculiarity of the translation initiation complex in which decoding is monitored at level of the 30S subunit bound to the initiation factors IF1, IF2 and IF3 [87].

For the elongator tRNAMet$_{CAU}$, we identified a N4-acetylcytidine (M) at position 34 and a N6-methyladenosine (=) at position 37. Modifications at C34 and A37 are present in most of the bacterial elongator tRNAMet and believed to be important to maintain fidelity. For instance, the M34 modification in *E. coli* elongator tRNAMet was shown to prevent misreading of the AUA isoleucine codon [88]. Indeed, the NAU anticodons are particular because besides the tRNAMet, one tRNAIle isoacceptor also carries the anticodon CAU (Fig. 2). In addition, *S. aureus* encode two other tRNAIle isoacceptors with the GAU anticodons. In various

A

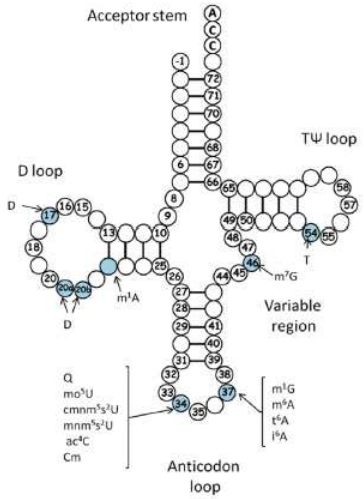


B

| Modification | Symbol | tRNA | position |
|---|---|---|---|
| Dihydrouridine | D | Leu UAA, Leu UAG, Leu CAA, Thr UGU, Arg ACG, Asp GUC, His GUG, Met CAU, Tyr GUA, Glu UUC | U 17 U 20a, b |
| 1-methyladenosine | " ($m^1A$) | His GUG, Tyr GUA, Glu UUC, Ser GCU, Ser UGA | A 22 |
| 2'-O-methylcytidine | B (Cm) | Leu CAA | C 34 |
| N4-acetylcytidine | M ($ac^4C$) | Met CAU | C 34 |
| Queuosine | Q | His GUG, Tyr GUA, Asn GUU, Asp GUC | G 34 |
| 5-methoxyuridine | 5 ($mo^5U$) | Gly UCC, Val UAC, Pro UGG, Ala UGC, Leu UAG, Thr UGU, Ser UGA | U 34 |
| 5-carboxymethylaminomethyl-2-thiouridine | Ş ($cmnm^5s^2U$) | Lys UUU | U 34 |
| 5-methylaminomethyl-2-thiouridine | S ($mnm^5s^2U$) | Glu UUC, Lys UUU | U 34 |
| 1-methylguanosine | K ($m^1G$) | His GUG, Pro UGG, Arg ACG, Leu UAG | G 37 |
| N6-methyladenosine | = ($m^6A$) | Met CAU, Val UAC | A 37 |
| N6-threonylcarbamoyladenosine | 6 ($t^6A$) | Ile GAU, Asn GUU, Thr UGU, Ser GCU | A 37 |
| N6-isopentenyladenosine | + ($i^6A$) | Tyr GUA, Ser UGA, Leu CAA | A 37 |
| Unknown modified adenosine | H (xA) | Lys UUU | A 37 |
| 7-methylguanosine | 7 ($m^7G$) | Arg ACG, Pro UGG | G 46 |
| 5-methyluridine | T ($m^5U$) | Met CAU, Asp GUC, Pro UGG, Leu UAG, Thr UGU, Glu UUC, Leu UAA, Ser GCU, Ser UGA | U 54 |

**Fig. 3. Atlas of modifications characterized on *S. aureus* tRNAs.** *A.* The different modifications observed on *S. aureus* tRNAs are reported on the typical cloverleaf two-dimensional structure of a tRNA. The acceptor stem, the variable region, the D, TΨ and anticodon loops are indicated. The nucleotide positions where the modifications were found are highlighted by light blue filled circles. *B.* Table summarizing the modifications with their abbreviations, the tRNAs for which each modification was found and its nucleotide position.

organisms, there are some variations in the tRNAIle content. Indeed, only in some bacteria, some tRNAIle have the UAU anticodons, common also in eukaryotes. Most eukaryotes have two isoacceptor tRNAIle, one with the anticodon IAU (I = inosine), which reads all three isoleucine codons (AUU, AUC and AUA) [89], while the other, with the anticodon ΨAΨ, is thought to read only AUA [90]. In bacteria, $tRNAIle_{GAU}$ reads two of the isoleucine codons (AUU and AUC) and carries a $t^6A$ modification at position 37, as it is also in *S. aureus* (Table 1). The other $tRNAIle_{CAU}$ reads the third isoleucine codon AUA and usually carries a lysidine residue (Lysine modified C at position 34). The enzyme TilS, responsible for this modification, is not only essential for the correct recognition of the AUA codon but also for the amino-acid specificity from methionine to isoleucine [91,92]. This modification enzyme is also present in the *S. aureus* genome suggesting that the lysidine modification is most likely present in $tRNAIle_{CAU}$ to maintain fidelity. Purification of this isoacceptor tRNAIle will be necessary to assert this hypothesis.

### 3.3. tRNA modification dynamics under different stress conditions

The protocol presented here can be easily applied to analyze specific stress conditions that might alter the modification state or the nature of modifications in tRNAs. The possibility to probe several tRNAs in one single experiment using 2D-gel isolation procedure, without the need of biotinylated probes to capture (single) tRNA, has removed one of the major bottlenecks for the LC/MSMS analyses. The recent advances in mass spectrometry technologies and software [93,94] now enable the routine sequence mapping of modifications from much less material than in the past. Prior to modification mapping on individual tRNAs, a complete nucleoside profile of total tRNAs would be complementary to screen for modification changes taking place under specific conditions. The analysis of the dynamics of tRNA modifications upon stress encountered during infection in *S. aureus* might reveal unexpected strategies developed by the pathogen to survive, persist, and fight against host immune defenses. The increase in the sensitivity of nanoLC/MSMS methodologies and the new development of high throughput RNA sequencing analysis [95] are promising developments amenable to gain a full picture of RNA modifications, opening new areas in the field of RNA regulatory functions in bacteria.


## Funding

This work was supported by the Agence Nationale de la Recherche (ANR, grant ANR-16-CE11-0007-01, RIBOSTAPH, to [P.R.] and ANR-15-CE11-0021-01 to [E.W.]), and from "Fonds Régional de Cooperation Pour la Recherche" (Région Grand Est, project EpiRNA). It has also been supported and published under the framework of the LABEX: ANR-10-LABX-0036 NETRNA as part of the investments for the future program and of ANR-17-EURE-0023 to [E.W. and P.R.] from the French National Research Agency. L.A. received the support for the Grand Est region and the labEx NetRNA for her PhD contract.


## Author contributions

LA conducted the experiments, analyzed the data and wrote the paper; PW developed the MS analysis approach, conducted the preliminary experiments, analyzed the data and wrote the paper; EW designed the research and wrote the paper; PR and SM designed the research, analyzed the data and wrote the paper; All authors have read and approved the manuscript.


## Acknowledgments

The authors thank P. Hammann, L. Kuhn and J. Chicher from the IBMC Proteomic Platform (Strasbourg), and all members of the team for their helpful discussions.

## Appendix A. Supplementary data

Supplementary data to this article can be found online at https://doi.org/10.1016/j.biochi.2019.07.003.

## References


[1] M. Frye, et al., RNA modifications: what have we learned and where are we headed? Nat. Rev. Genet. 17 (6) (2016) 365–372.
[2] P. Boccaletto, et al., MODOMICS: a database of RNA modification pathways. 2017 update, Nucleic Acids Res. 46 (D1) (2018) D303–D307.
[3] K. Chatterjee, et al., The archaeal COG1901/DUF358 SPOUT-methyltransferase members, together with pseudouridine synthase Pus10, catalyze the formation of 1-methylpseudouridine at position 54 of tRNA, RNA 18 (3) (2012) 421–433.
[4] B. Desmolaize, et al., A single methyltransferase YefA (RlmCD) catalyses both m5U747 and m5U1939 modifications in Bacillus subtilis 23S rRNA, Nucleic Acids Res. 39 (21) (2011) 9368–9375.
[5] M.P. Guy, et al., Yeast Trm7 interacts with distinct proteins for critical modifications of the tRNAPhe anticodon loop, RNA 18 (10) (2012) 1921–1933.
[6] M. Kempenaers, et al., New archaeal methyltransferases forming 1-methyladenosine or 1-methyladenosine and 1-methylguanosine at position 9 of tRNA, Nucleic Acids Res. 38 (19) (2010) 6533–6543.
[7] E. Purta, et al., YgdE is the 2'-O-ribose methyltransferase RlmM specific for nucleotide C2498 in bacterial 23S rRNA, Mol. Microbiol. 72 (5) (2009) 1147–1158.
[8] J.P. Wurm, et al., The ribosome assembly factor Nep1 responsible for Bowen-Conradi syndrome is a pseudouridine-N1-specific methyltransferase, Nucleic Acids Res. 38 (7) (2010) 2387–2398.
[9] S. Douthwaite, D. Fourmy, S. Yoshizawa, Nucleotide methylations in rRNA that confer resistance to ribosome-targeting antibiotics, in: Topics in Current Genetics, Fine-Tuning of RNA Functions by Modification and Editing, Springer-Verlag, Berlin, Heidelberg, 2005, pp. 285–307.
[10] L. Fernandez, R.E. Hancock, Adaptive and mutational resistance: role of porins and efflux pumps in drug resistance, Clin. Microbiol. Rev. 25 (4) (2012) 661–681.
[11] S.M. Toh, A.S. Mankin, An indigenous posttranscriptional modification in the ribosomal peptidyl transferase center confers resistance to an array of protein synthesis inhibitors, J. Mol. Biol. 380 (4) (2008) 593–597.
[12] E.M. Gustilo, F.A. Vendeix, P.F. Agris, tRNA's modifications bring order to gene expression, Curr. Opin. Microbiol. 11 (2) (2008) 134–140.
[13] S. Gehrig, et al., Identification of modifications in microbial, native tRNA that suppress immunostimulatory activity, J. Exp. Med. 209 (2) (2012) 225–233.
[14] B. El Yacoubi, M. Bailly, V. de Crecy-Lagard, Biosynthesis and function of posttranscriptional modifications of transfer RNAs, Annu. Rev. Genet. 46 (2012) 69–95.
[15] M. Helm, J.D. Alfonzo, Posttranscriptional RNA Modifications: playing metabolic games in a cell's chemical Legoland, Chem. Biol. 21 (2) (2014) 174–185.
[16] J.E. Jackman, J.D. Alfonzo, Transfer RNA modifications: nature's combinatorial chemistry playground, Wiley Interdiscip Rev RNA 4 (1) (2013) 35–48.
[17] C. Lorenz, C.E. Lunse, M. Morl, tRNA modifications: impact on structure and thermal adaptation, Biomolecules 7 (2) (2017).
[18] J. Eargle, et al., Dynamics of recognition between tRNA and elongation factor tu, J. Mol. Biol. 377 (5) (2008) 1382–1405.
[19] J. Zhang, A.R. Ferre-D'Amare, The tRNA elbow in structure, recognition and evolution, Life (Basel) 6 (1) (2016).
[20] R. Giege, M. Springer, Aminoacyl-tRNA synthetases in the bacterial world, EcoSal Plus 7 (1) (2016).
[21] J. Zhang, A.R. Ferre-D'Amare, Structure and mechanism of the T-box riboswitches, Wiley Interdiscip Rev RNA 6 (4) (2015) 419–433.
[22] R.K. Gudipati, et al., Extensive degradation of RNA precursors by the exosome in wild-type cells, Mol. Cell 48 (3) (2012) 409–421.
[23] S. Vanacova, et al., A new yeast poly(A) polymerase complex involved in RNA quality control, PLoS Biol. 3 (6) (2005) e189.
[24] S. Kimura, M.K. Waldor, The RNA degradosome promotes tRNA quality control through clearance of hypomodified tRNA, Proc. Natl. Acad. Sci. U. S. A. 116 (4) (2019) 1394–1403.
[25] H. Grosjean, E. Westhof, An integrated, structure- and energy-based view of the genetic code, Nucleic Acids Res. 44 (17) (2016) 8020–8040.
[26] P.F. Agris, F.A. Vendeix, W.D. Graham, tRNA's wobble decoding of the genome: 40 years of modification, J. Mol. Biol. 366 (1) (2007) 1–13.
[27] E. Westhof, M. Yusupov, G. Yusupova, The multiple flavors of GoU pairs in RNA, J. Mol. Recognit. (2019), e2782.
[28] A. Rozov, et al., Tautomeric G*U pairs within the molecular ribosomal grip and fidelity of decoding in bacteria, Nucleic Acids Res. 46 (14) (2018) 7425–7435.
[29] N. Demeshkina, et al., A new understanding of the decoding principle on the ribosome, Nature 484 (7393) (2012) 256–259.
[30] I. Wohlgemuth, et al., Evolutionary optimization of speed and accuracy of decoding on the ribosome, Philos. Trans. R. Soc. Lond. B Biol. Sci. 366 (1580) (2011) 2979–2986.
[31] R.P. Fahlman, T. Dale, O.C. Uhlenbeck, Uniform binding of aminoacylated transfer RNAs to the ribosomal A and P sites, Mol. Cell 16 (5) (2004) 799–805.
[32] J. Zhang, et al., Accuracy of initial codon selection by aminoacyl-tRNAs on the mRNA-programmed bacterial ribosome, Proc. Natl. Acad. Sci. U. S. A. 112 (31) (2015) 9602–9607.
[33] J.M. Ogle, et al., Selection of tRNA by the ribosome requires a transition from an open to a closed form, Cell 111 (5) (2002) 721–732.
[34] J.M. Ogle, V. Ramakrishnan, Structural insights into translational fidelity, Annu Rev Biochem 74 (2005) 129–177.
[35] J.W. Stuart, et al., Functional anticodon architecture of human tRNALys3 includes disruption of intraloop hydrogen bonding by the naturally occurring amino acid modification, t6A, Biochem. 39 (44) (2000) 13396–13404.
[36] V.Y. Vare, et al., Chemical and conformational diversity of modified nucleosides affects tRNA structure and function, Biomolecules 7 (1) (2017).
[37] F.V.t. Murphy, V. Ramakrishnan, Structure of a purine-purine wobble base pair in the decoding center of the ribosome, Nat. Struct. Mol. Biol. 11 (12) (2004) 1251–1252.
[38] F.V.t. Murphy, et al., The role of modifications in codon discrimination by tRNA(Lys)UUU, Nat. Struct. Mol. Biol. 11 (12) (2004) 1186–1191.
[39] A. Weixlbaumer, et al., Mechanism for expanding the decoding capacity of transfer RNAs by modification of uridines, Nat. Struct. Mol. Biol. 14 (6) (2007) 498–502.
[40] S. Kurata, et al., Modified uridines with C5-methylene substituents at the first position of the tRNA anticodon stabilize U.G wobble pairing during decoding, J. Biol. Chem. 283 (27) (2008) 18801–18811.
[41] F. Harada, S. Nishimura, Possible anticodon sequences of tRNA His , tRNA Asm , and tRNA Asp from Escherichia coli B. Universal presence of nucleoside Q in the first postion of the anticondons of these transfer ribonucleic acids, Biochem. 11 (2) (1972) 301–308.
[42] F. Tuorto, et al., Queuosine-modified tRNAs confer nutritional control of protein translation, EMBO J. 37 (18) (2018).
[43] M. Muller, et al., Queuine links translational control in eukaryotes to a micronutrient from bacteria, Nucleic Acids Res 47 (7) (2019) 3711–3727.
[44] P.P. Chan, T.M. Lowe, GtRNAdb 2.0: an expanded database of transfer RNA genes identified in complete and draft genomes, Nucleic Acids Res. 44 (D1) (2016) D184–D189.
[45] M. Vinayak, C. Pathak, Queuosine modification of tRNA: its divergent role in cellular machinery, Biosci. Rep. 30 (2) (2009) 135–148.
[46] T. Pan, Modifications and functional genomics of human transfer RNA, Cell Res. 28 (4) (2018) 395–404.
[47] C.N. Marbaniang, J. Vogel, Emerging roles of RNA modifications in bacteria, Curr. Opin. Microbiol. 30 (2016) 50–57.
[48] T. Kyuma, et al., Ribosomal RNA methyltransferases contribute to Staphylococcus aureus virulence, FEBS J. 282 (13) (2015) 2570–2584.
[49] J.M. Durand, et al., Transfer RNA modification, temperature and DNA superhelicity have a common target in the regulatory network of the virulence of Shigella flexneri: the expression of the virF gene, Mol. Microbiol. 35 (4) (2000) 924–935.
[50] L. Lan, et al., Pseudomonas aeruginosa OspR is an oxidative stress sensing regulator that affects pigment production, antibiotic resistance and dissemination during infection, Mol. Microbiol. 75 (1) (2010) 76–91.
[51] Y.H. Chionh, et al., tRNA-mediated codon-biased translation in mycobacterial hypoxic persistence, Nat. Commun. 7 (2016) 13302.
[52] D.C. Shippy, A.A. Fadl, tRNA modification enzymes GidA and MnmE: potential role in virulence of bacterial pathogens, Int. J. Mol. Sci. 15 (10) (2014) 18267–18280.
[53] D. Bregeon, et al., Translational misreading: a tRNA modification counteracts a +2 ribosomal frameshift, Genes Dev. 15 (17) (2001) 2295–2306.
[54] H. Grundmann, et al., Emergence and resurgence of meticillin-resistant Staphylococcus aureus as a public-health threat, Lancet 368 (9538) (2006) 874–885.
[55] F.D. Lowy, Staphylococcus aureus infections, N. Engl. J. Med. 339 (8) (1998) 520–532.
[56] K. Thuring, et al., Analysis of RNA modifications by liquid chromatography-tandem mass spectrometry, Methods 107 (2016) 48–56.
[57] C.G. Edmonds, et al., Posttranscriptional modification of tRNA in thermophilic archaea (Archaebacteria), J. Bacteriol. 173 (10) (1991) 3138–3148.
[58] S.C. Pomerantz, J.A. McCloskey, Analysis of RNA hydrolyzates by liquid chromatography-mass spectrometry, Methods Enzymol. 193 (1990) 796–824.
[59] S.P. Russell, P.A. Limbach, Evaluating the reproducibility of quantifying modified nucleosides from ribonucleic acids by LC-UV-MS, J Chromatogr B Analyt Technol Biomed Life Sci 923–924 (2013) 74–82.
[60] S.C. Pomerantz, J.A. Kowalak, J.A. McCloskey, Determination of oligonucleotide composition from mass spectrometrically measured molecular weight, J. Am. Soc. Mass Spectrom. 4 (3) (1993) 204–209.
[61] J.A. Kowalak, et al., A novel method for the determination of post-transcriptional modification in RNA by mass spectrometry, Nucleic Acids Res. 21 (19) (1993) 4577–4585.
[62] D. Su, et al., Quantitative analysis of ribonucleoside modifications in tRNA by HPLC-coupled mass spectrometry, Nat. Protoc. 9 (4) (2014) 828–841.
[63] R. Ross, et al., Sequence mapping of transfer RNA chemical modifications by liquid chromatography tandem mass spectrometry, Methods 107 (2016) 73–78.
[64] S. Herbert, et al., Repair of global regulators in Staphylococcus aureus 8325 and comparative analysis with other clinical isolates, Infect. Immun. 78 (6) (2010) 2877–2889.
[65] J. Wu, S.A. McLuckey, Gas-phase fragmentation of oligonucleotide ions, Int. J. Mass Spectrom. 237 (2) (2004) 197–241.

[66] I. Caldelari, et al., Complete genome sequence and annotation of the Staphylococcus aureus strain HG001, Genome Announc. 5 (32) (2017).
[67] N.W. Ho, P.T. Gilham, Reaction of pseudouridine and inosine with N-cyclohexyl-N'-beta-(4-methylmorpholinium)ethylcarbodiimide, Biochem. 10 (20) (1971) 3651–3657.
[68] K.G. Patteson, L.P. Rodicio, P.A. Limbach, Identification of the mass-silent post-transcriptionally modified nucleoside pseudouridine in RNA by matrix-assisted laser desorption/ionization mass spectrometry, Nucleic Acids Res. 29 (10) (2001). E49-9.
[69] A. Durairaj, P.A. Limbach, Matrix-assisted laser desorption/ionization mass spectrometry screening for pseudouridine in mixtures of small RNAs by chemical derivatization, RNase digestion and signature products, Rapid Commun. Mass Spectrom. 22 (23) (2008) 3727–3734.
[70] J. Mengel-Jorgensen, F. Kirpekar, Detection of pseudouridine and other modifications in tRNA by cyanoethylation and MALDI mass spectrometry, Nucleic Acids Res. 30 (23) (2002) e135.
[71] B. Addepalli, N.P. Lesner, P.A. Limbach, Detection of RNA nucleoside modifications with the uridine-specific ribonuclease MC1 from Momordica charantia, RNA 21 (10) (2015) 1746–1756.
[72] W.M. Houser, et al., Combining recombinant ribonuclease U2 and protein phosphatase for RNA modification mapping by liquid chromatography-mass spectrometry, Anal. Biochem. 478 (2015) 52–58.
[73] P. Puri, et al., Systematic identification of tRNAome and its dynamics in Lactococcus lactis, Mol. Microbiol. 93 (5) (2014) 944–956.
[74] K. Murao, T. Hasegawa, H. Ishikura, 5-methoxyuridine: a new minor constituent located in the first position of the anticodon of tRNAAla, tRNAThr, and tRNAVal from Bacillus subtilis, Nucleic Acids Res. 3 (10) (1976) 2851–2860.
[75] S. Okumura, et al., Codon recognition by tRNA molecules with a modified or unmodified uridine at the first position of the anticodon, Nucleic Acids Symp. Ser. (34) (1995) 203–204.
[76] T. Numata, et al., Snapshots of tRNA sulphuration via an adenylated intermediate, Nature 442 (7101) (2006) 419–424.
[77] J. Shepherd, M. Ibba, Bacterial transfer RNAs, FEMS Microbiol. Rev. 39 (3) (2015) 280–300.
[78] C.P. Lee, B.L. Seong, U.L. RajBhandary, Structural and sequence elements important for recognition of Escherichia coli formylmethionine tRNA by methionyl-tRNA transformylase are clustered in the acceptor stem, J. Biol. Chem. 266 (27) (1991) 18012–18017.
[79] J.M. Guillon, et al., Nucleotides of tRNA governing the specificity of Escherichia coli methionyl-tRNA(fMet) formyltransferase, J. Mol. Biol. 224 (2) (1992) 359–367.
[80] D. Hartz, et al., Domains of initiator tRNA and initiation codon crucial for initiator tRNA selection by Escherichia coli IF3, Genes Dev. 4 (10) (1990) 1790–1800.
[81] T. Meinnel, et al., Discrimination by Escherichia coli initiation factor IF3 against initiation on non-canonical codons relies on complementarity rules, J. Mol. Biol. 290 (4) (1999) 825–837.
[82] T. Hussain, et al., Large-scale movements of IF3 and tRNA during bacterial translation initiation, Cell 167 (1) (2016) 133–144 e13.
[83] D. Petrelli, et al., Translation initiation factor IF3: two domains, five functions, one mechanism? EMBO J. 20 (16) (2001) 4560–4569.
[84] J.M. Guillon, et al., Importance of formylability and anticodon stem sequence to give a tRNA(Met) an initiator identity in Escherichia coli, J. Bacteriol. 175 (14) (1993) 4507–4514.
[85] J.M. Guillon, et al., Interplay of methionine tRNAs with translation elongation factor Tu and translation initiation factor 2 in Escherichia coli, J. Biol. Chem. 271 (37) (1996) 22321–22325.
[86] M.A. Machnicka, et al., MODOMICS: a database of RNA modification pathways–2013 update, Nucleic Acids Res. 41 (2013) D262–D267. Database issue.
[87] A. Simonetti, et al., A structural view of translation initiation in bacteria, Cell. Mol. Life Sci. 66 (3) (2009) 423–436.
[88] L. Stern, L.H. Schulman, The role of the minor base N4-acetylcytidine in the function of the Escherichia coli noninitiator methionine transfer RNA, J. Biol. Chem. 253 (17) (1978) 6132–6139.
[89] C. Kohrer, et al., Life without tRNAIle-lysidine synthetase: translation of the isoleucine codon AUA in Bacillus subtilis lacking the canonical tRNA2Ile, Nucleic Acids Res. 42 (3) (2014) 1904–1915.
[90] B. Senger, et al., The modified wobble base inosine in yeast tRNAIle is a positive determinant for aminoacylation by isoleucyl-tRNA synthetase, Biochem. 36 (27) (1997) 8269–8275.
[91] A. Soma, et al., An RNA-modifying enzyme that governs both the codon and amino acid specificities of isoleucine tRNA, Mol. Cell 12 (3) (2003) 689–698.
[92] T. Muramatsu, et al., Codon and amino-acid specificities of a transfer RNA are both converted by a single post-transcriptional modification, Nature 336 (6195) (1988) 179–181.
[93] H. Nakayama, et al., Ariadne: a database search engine for identification and chemical analysis of RNA using tandem mass spectrometry data, Nucleic Acids Res. 37 (6) (2009) e47.
[94] P.J. Sample, et al., RoboOligo: software for mass spectrometry data to support manual and de novo sequencing of post-transcriptionally modified ribonucleic acids, Nucleic Acids Res. 43 (10) (2015) e64.
[95] D.R. Garalde, et al., Highly parallel direct RNA sequencing on an array of nanopores, Nat. Methods 15 (3) (2018) 201–206.
[96] T. Carver, et al., DNAPlotter: circular and linear interactive genome visualization, Bioinformatics 25 (1) (2009) 119–120.

**Supplementary file : Figure S1.**

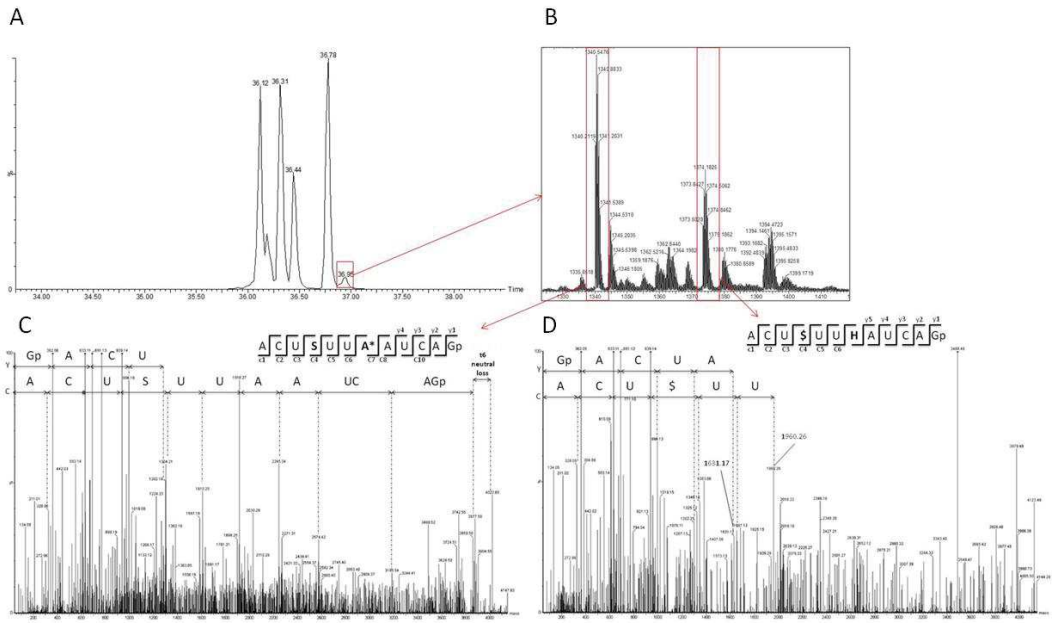


**Figure S1. nanoLC/MSMS analysis of spot n°24 containing Lys-tRNA$_{UUU2-3}$ after RNase T1 digestion.** *A.* Elution profile of the nanoLC of spot n°24 containing Lys-tRNA$_{UUU2-3}$ after T1 digestion. The different fragments are as follow: *a* acceptor stem (sequence $^{5'}$CUACACCA$^{3'}$ from position 70 to 76); *b* acceptor stem (sequence $^{5'}$CAUCUGp$^{3'}$ from position 25 to 30); *c* acceptor stem (sequence $^{5'}$CCAUUAGp$^{3'}$ from position 4 to 10); *d* TΨ loop and stem (sequence $^{5'}$AAUCCUCUAUGp$^{3'}$ from position 57 to 68); *e* anticodon loop (sequence $^{5'}$ACUUUUAAUCAG$^{3'}$ from position 31 to 42). *B.* MS spectrum of the peak *e* of the nanoLC chromatogram corresponding to the anticodon loop. The two main ions have been selected for further fragmentation. *C.* MSMS spectrum of anticodon loop corresponding to the sequence $^{5'}$ACUSUUA*AUCAGp$^{3'}$ with the 145 Da neutral loos specific of the t6A. A* is present at position 37, carrying the t6A modification. Measured m/z : 1340,19 (-3H$^+$). The specific bonds that fragment most often are the 5' P-O inter-nucleotide bond. Fragment ions where the charge is retained on the 5'-fragment are denoted as c-type fragment ions, and fragment ions where the charge is retained on the 3'-fragment are denoted as y-type fragment ions {McLuckey, 1992 #79}. *D.* MS/MS spectrum of anticodon loop corresponding to the sequence $^{5'}$ACU$UUHAUCAGp$^{3'}$ without neutral loss. Measured m/z : 1373,50 (-3H$^+$).

### 3. Analyse de RNA-Seq des ARN non codants de *S.aureus*

Afin de compléter la cartographie des modifications des ARNt (et ARNr), réalisée par NanoLC-MS/MS, des approaches complémentaires basées sur le RNA-Seq ont été combinées (**Fig 3.**). Les trois techniques qui ont été utilisées permettent de détecter les Ψ, $m^7G$, $m^3C$, D et 2'-O methylations. Les analyses RNA-Seq telles que l'HydraPsi-Seq (Marchand *et al.*, 2020), l'AlkAniline-Seq (Marchand *et al.*, 2018) et le RiboMeth-Seq (Marchand *et al.*, 2016; Ayadi *et al.*, 2018) ont été réalisées en collaboration avec le Pr. Yuri Motorin et la Dr. Virginie Marchand de la plateforme Epitranscriptomique et Séquençage (EpiRNA-Seq) de Nancy. Ces analyses ont été réalisées sur les ARNt totaux et sur les ARNr. Les résultats d'HydraPsi-Seq révèlent la présence de pseudouridines en position 13, 32 et 55 des ARNt et également en position 524, 634, 717 et 1282 de l'ARNr 16S. L'AlkAniline-Seq spécifique des $m^7G$, $m^3C$ et D, a confirmé la présence de modifications caractérisées pas NanoLC-MS/MS telles que les dihydrouridines localisées dans la boucle D et le $m^7G$ en position 46 dans la boucle variable de l'$ARNt^{Pro}_{UGG}$. Cette méthode à également permis la caractérisation d'un $m^7G$ en 534 de l'ARNr 16S. Le RiboMeth-Seq a confirmé la présence d'un 2'O-méthyl en position 34 de l'$ARNt^{Leu}_{CAA}$ mais a également révélé la présence d'un Gm en position 45 de l'$ARNt^{Val}_{UAC}$ ainsi que la présence d'un Cm en position 1411 de l'ARNr 16S.

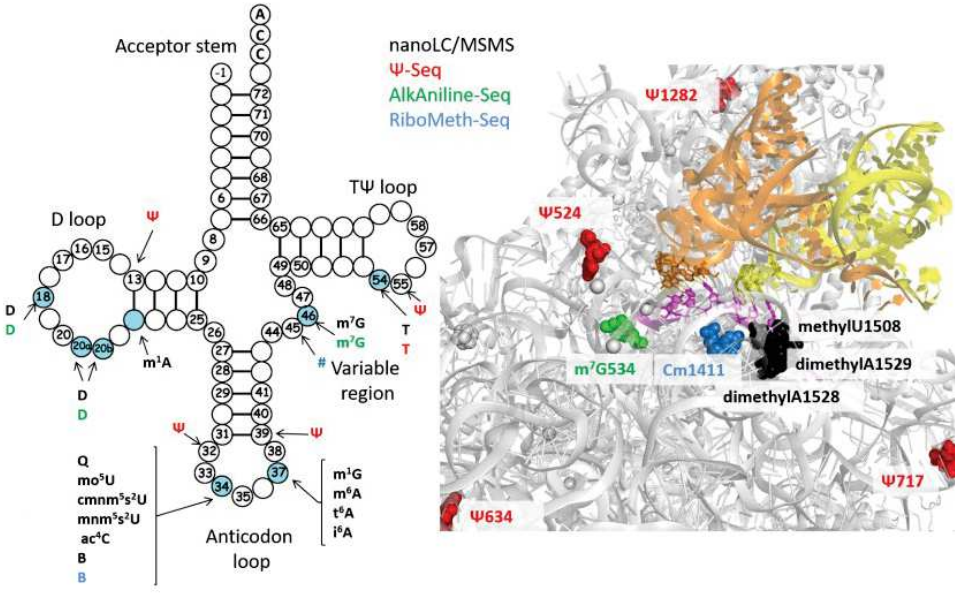


**Figure 3 :** Modifications cartographiées par différentes méthodes de NanoLC-MS/MS et RNA-Seq dans les ARNt à gauche et l'ARNr 16S de *S. aureus* à droite

## 4. Réponse au stress oxydant :

Après avoir caractérisé de nombreuses modifications sur des ARNt de *S. aureus*, leur dynamique en réponse à des conditions mimant les stress rencontrés pendant l'infection reste à déterminer. La production par les macrophages et les neutrophiles de ROS générant un stress oxydant est une des lignes de défense du système immunitaire. Tout d'abord, des analyses de transcriptomique différentielle et de protéomique sont réalisées afin de caractériser l'adaptation globale de la bactérie au stress oxydant avant de suivre les changements de modification des ARNt.

L'induction des ROS dans les cultures de S. aureus est réalisée par l'ajout de l'herbicide Méthylviologen (MV ; N,-N'-dimethyl-4,-4'-bipyridinium dichloride ; aussi appelé Paraquat). Le MV est une molécule communément utilisée pour étudier le stress oxydant chez les bactéries et les plantes. La réaction entre le radical du MV et le dioxygène ($O_2$) génère les espèces toxiques : le radical superoxyde ($O_2^-$) et le peroxyde d'hydrogène (Hassan, 1984).

## i. Analyse transcriptomique et protéomique

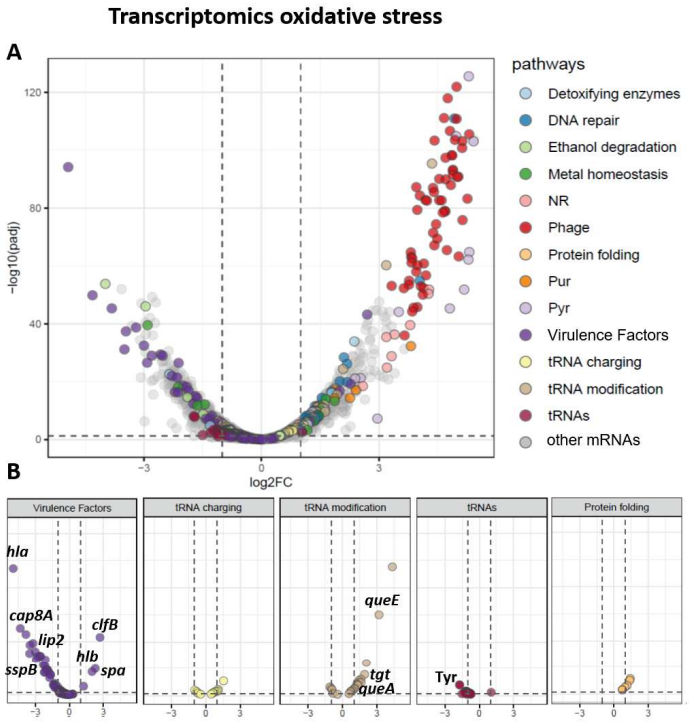


**Figure 4 : A)** Volcano plot représentant l'analyse transcriptomique différentielle de cultures de *S.aureus* HG001 soumises à un stress oxydant (**Annexe 1**.). Pyr et Pur représentent les voies de biosynthèse des désoxynucléotides et NR représente la voie de réduction des nitrites et des nitrates. **B)** Extraits du volcano plot.

L'analyse transcriptomique différentielle de cultures de *S. aureus* HG001 cultivées en conditions normales ou soumises au stress oxydant généré par le méthylviologen est réalisée en collaboration avec la plateforme EpiRNA-Seq. Ces résultats montrent une surexpression de gènes codants pour des protéines phagiques et des enzymes de détoxification. De même, des protéines impliquées dans les voies de synthèse des acides nucléiques (purines et surtout pyrimidines), de la réparation de l'ADN ainsi que de la réduction des nitrites et des nitrates sont plus exprimées chez les bactéries stressées (**Fig. 4A.**) La plupart des facteurs de virulence sont sous exprimés, notamment *cap8A* impliqués dans la synthèse de la capsule, la staphopain, la triacylglycerol lipase (*lip2*) et les toxines (l'alpha-hemolysin *hly*, la delta-hemolysin *hld* présente dans l'ARNII, les gamma-hemolysins *hlgABC* et les peptides PSM). Tandis que l'hémolysine B, le clumping factor B, la protéine A sont surexprimés en condition oxydante. Le niveau de tRNA semble également légèrement plus faible chez les bactéries

stressées, spécifiquement l'ARNt$^{Tyr}$. Les protéines chaperonnes semblent à l'inverse légèrement plus exprimées durant le stress (**Fig. 4B.**).

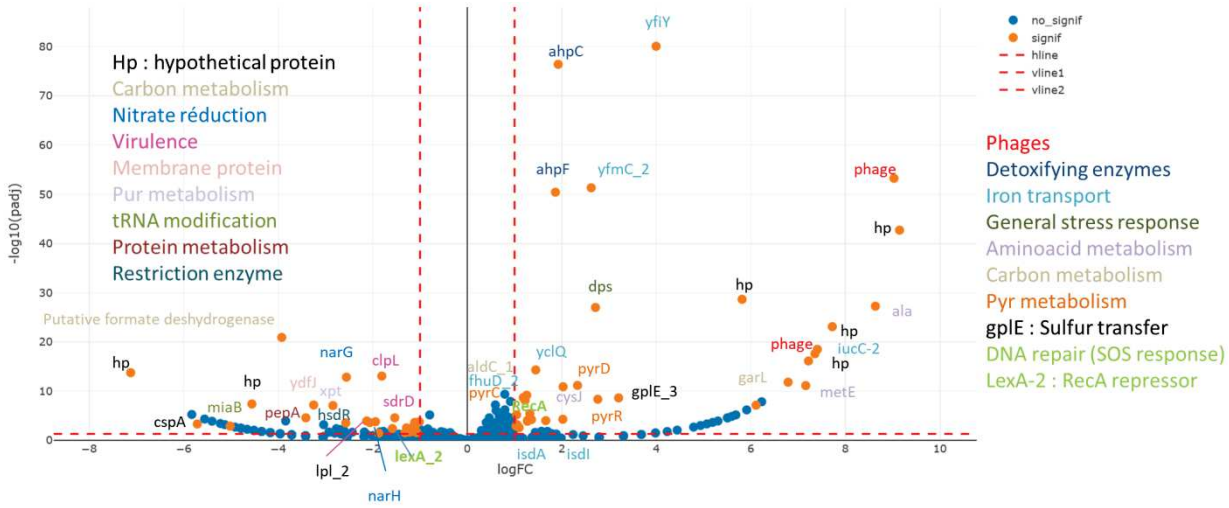


**Figure 5 :** Volcano plot représentant l'expression différentielle des protéines de cultures de *S.aureus* HG001 soumises à un stress oxydant (**Annexe 2.**).

Les données de protéomique ont été obtenues par analyse LC-MS/MS d'extraits de protéines totales issues de bactéries HG001 cultivées ou non en présence de MV, cette analyse est réalisée en collaboration avec la plateforme protéomique de l'Esplanade de Strasbourg. Cette analyse montre une activation de l'expression des gènes phagiques ainsi qu'une forte augmentation de l'expression de gènes codant pour des protéines de réponse générale au stress (Dps) ainsi que des sous unités C et F de l'alkyl hydroperoxide reductase (AhpC et AhpF). Plusieurs protéines impliquées dans l'import de fer provenant du milieu (YfiY, YfmC_2) ou de l'hôte (IsdI) sont également surexprimées lors du stress oxydant. De même, une protéine dont l'expression est influencée par la disponibilité du fer (IsdA) semble légèrement plus présente dans les bactéries stressées. La protéine de réparation de l'ADN RecA ainsi que des protéines impliquées dans le métabolisme des acides nucléiques, plus spécifiquement des pyrimidines sont surexprimées lors du stress oxydant alors que l'expression de la Xanthine phosphoribosyltransferase codée par le gène *xpt* est inhibée (**Fig. 5**.).

### ii. Dynamique des modifications des ARNt en réponse au stress oxydant

L'effet du stress oxydant sur les ARNt peut être caractérisé en analysant leur migration sur gel de polyacrylamide puis en analysant les modifications présentes par NanoLC-MS/MS. Différentes souches ont été utilisées, la souche de laboratoire HG001 mais aussi la souche clinique USA300 et une souche avec un gène *tgt* inactivé (Fey *et al.*, 2013) et ne présentant pas la queuosine.

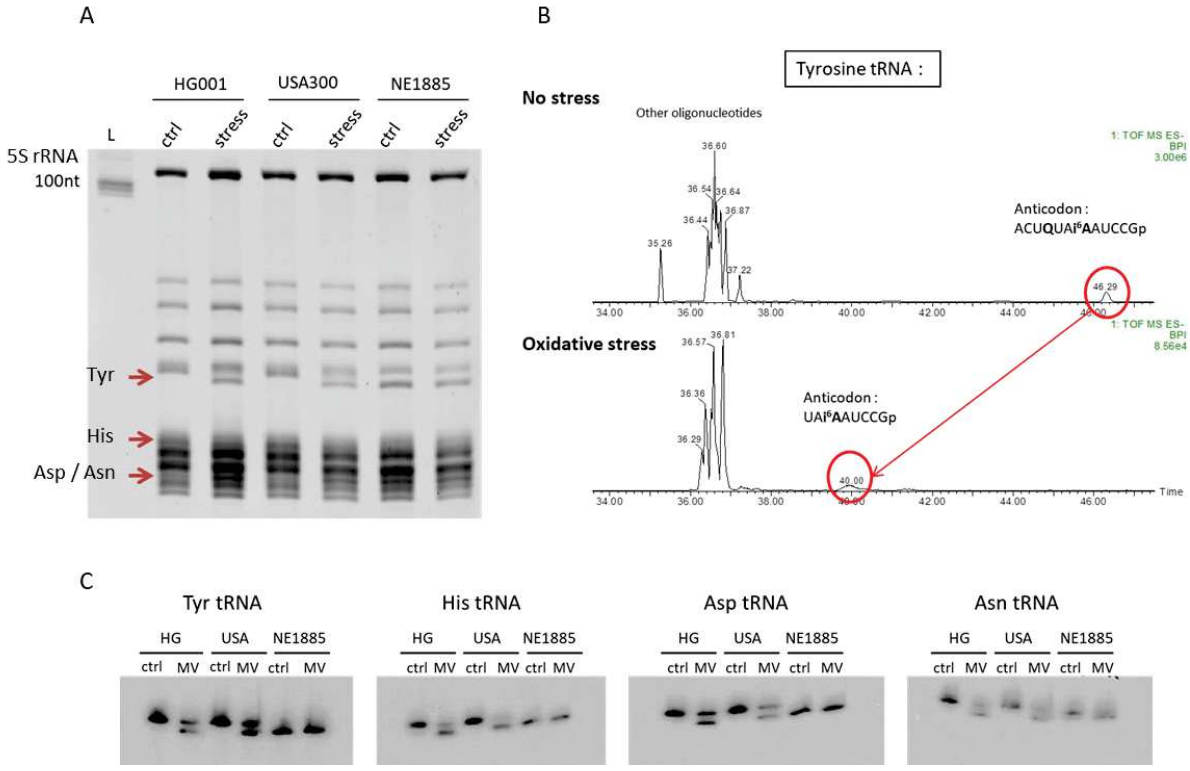


**Figure 6 : A)** Profil de migration sur gel (polyacrylamide 12%, 8M urée) des ARNt des souches HG001 (souche contrôle), USA300 (souche clinique) et NE1885 (souche possédant le gène *tgt* inactivé) de *S. aureus*. Les flèches rouges indiquent les positions sur le gel des ARNt connus pour posséder une Q en position 34 et correspondant aux bandes présentant un changement de comportement électrophorétique. **B)** Chromatogrammes obtenus à partir des bandes contenant l'ARNt$^{Tyr}_{GUA}$ issus de *S. aureus* HG001. Encerclés en rouge les pics d'élutions correspondants aux anticodons, non clivé par la RNase T1 pour l'ARNt issus de la culture non stressée, clivé pour celui issus de la culture soumise au stress oxydant. **C)** Northern blot sur gel de polyacrylamide et acide phénylboronique des 4 ARNt contenant une Q34 issus de cultures en présence (MV) ou en absence (ctrl) de stress oxydant.

Les profils électrophorétiques des ARNt issus de la souche de laboratoire HG001 sont similaires à ceux des ARNt de la souche clinique USA300. Les ARNt provenant de cellules soumises à un stress oxydant présentent 3 bandes shiftées correspondantes aux profils de

migration de l'ARNt de la Tyrosine, de l'Histidine ainsi que les ARNt de l'Aspartate et l'Asparagine (Antoine *et al.*, 2019). La souche NE1885 provenant de la Nebraska collection est dérivée de la souche USA300 avec le gène *tgt* impliqué dans la voie de biosynthèse de la Q inactivé (Fey *et al.*, 2013). Les ARNt extraits de cette souche montrent un profil de migration similaire à ceux issus des souches HG001 et USA300 soumises au stress oxydant (**Fig. 6A**). L'analyse LC-MS/MS de la bande présentant un changement de migration flagrant provenant de la culture de *S. aureus*, contenant l'ARNt$^{Tyr}$ révèle le clivage de l'anticodon par la RNase T1 en 3' de la Q34 de cet ARNt issus de la culture stressée. Ce clivage n'a pas lieu dans l'ARNt$^{Tyr}$ issus de la culture non stressée, dû à la présence de la modification, empêchant sa reconnaissance par la RNAse T1 (**Fig. 6B**). Les gels d'affinité contenant de l'acide phénylboronique (APB) qui interagit spécifiquement avec la queuosine, ralentissent la migration des ARNt modifiés (Igloi and Kössel, 1985). Le Northern blot des gels avec APB montre que les ARNt ne possédant pas de Q34 (NE1885) ont migré plus rapidement que les ARNt issus de cultures non stressées qui contiennent une Q34. La migration des ARNt issus des cultures stressées semble plus rapide, comparable à la migration des ARNt ne contenant pas de Q34 (**Fig. 6C**).

### iii. Analyse des ARNt contenant la Q34 issus de cultures stressées

Chacun des ARNt contenant une Q34 a été purifié par hybridation avec une sonde d'ADN biotinylée spécifique. L'analyse par LC-MS/MS après digestion avec la RNase U2 révèle la présence d'un G non modifié en position 34 pour 3 des 4 ARNt concernés. Les autres modifications telles que les dihydrouridines dans la boucle D, le m7G dans la boucle variable, la thymidine dans la boucle TΨ ainsi que les modifications en position 37 de l'anticodon ($t^6A$, $m^1G$ et $i^6A$) ne semblent pas impactées par le stress oxydant.

| Amino Acid | Anticodon | | Acc-stem | | D-stem | D-loop | D-stem | | Ac-stem | Ac-loop | Ac-stem | V-region | T-stem | T-loop | T-stem | Acc-stem | | CCA |
|---|---|---|---|---|---|---|---|---|---|---|---|---|---|---|---|---|---|---|
| Asp | GUC | - | GGUCUCG | UA | GUGU | AGCGGDDA | ACAC | G | CCUGC | CUGUCAC | GCAGG | AGAUC | GCGGG | TUCGGUU | CCCGU | CGAGACC | G | CCA |
| Asn | GUU | - | UCCACAG | UA | GCUC | AGUGGDA | GAGC | U | AUCGG | CUGUU6A | CCGAU | CG7UC | GUAGG | TUCGAGU | CCUAC | CUGUGGA | G | CCA |
| His | GUG | G | GCGGCUG | UG | GUGA | AGUGGDDA | AmCAC | A | UCGGA | UUGUGKU | UCCGA | CAUUC | GAGGG | UUCGAUC | CCCUU | CAGCCGC | C | CCA |
| Tyr | GUA | - | GGAGGGG | UA | GCGA | AGUGGCUAA | ACGC | G | GCGGA | CUGUA+A | UCCGC | UCCUUCGGGUUC | GGCAG | TUCGAAU | CUGCC | CCCCUCC | A | CCA |

**Tableau 1 :** Séquences des ARNt contenants une Q34 issus d'une culture de *S. aureus* HG001 soumise au stress oxydant. En bleu sont présentés les fragments séquencés par MS/MS après digestion avec la RNase U2.

### iv. Le précurseur preQ1 restaure la queuosine dans les 4 ARNt contenant la Q34

A partir des données d'analyses de protéomique et de transcriptomique, aucune des 8 enzymes (**Fig. 7A**) de la voie de synthèse de la queuosine ne présente de changement dans son expression. Cependant, le stress oxydant peut affecter directement l'activité des protéines. Afin de comprendre quelles enzymes sont susceptibles d'être inactivées, les cultures soumises au stress oxydant ont été supplémentées avec le précurseur de la queuosine preQ1. La cinétique d'incorporation de la queuosine a ensuite été vérifiée par électrophorèse d'affinité à l'APB. (**Fig. 7B**).

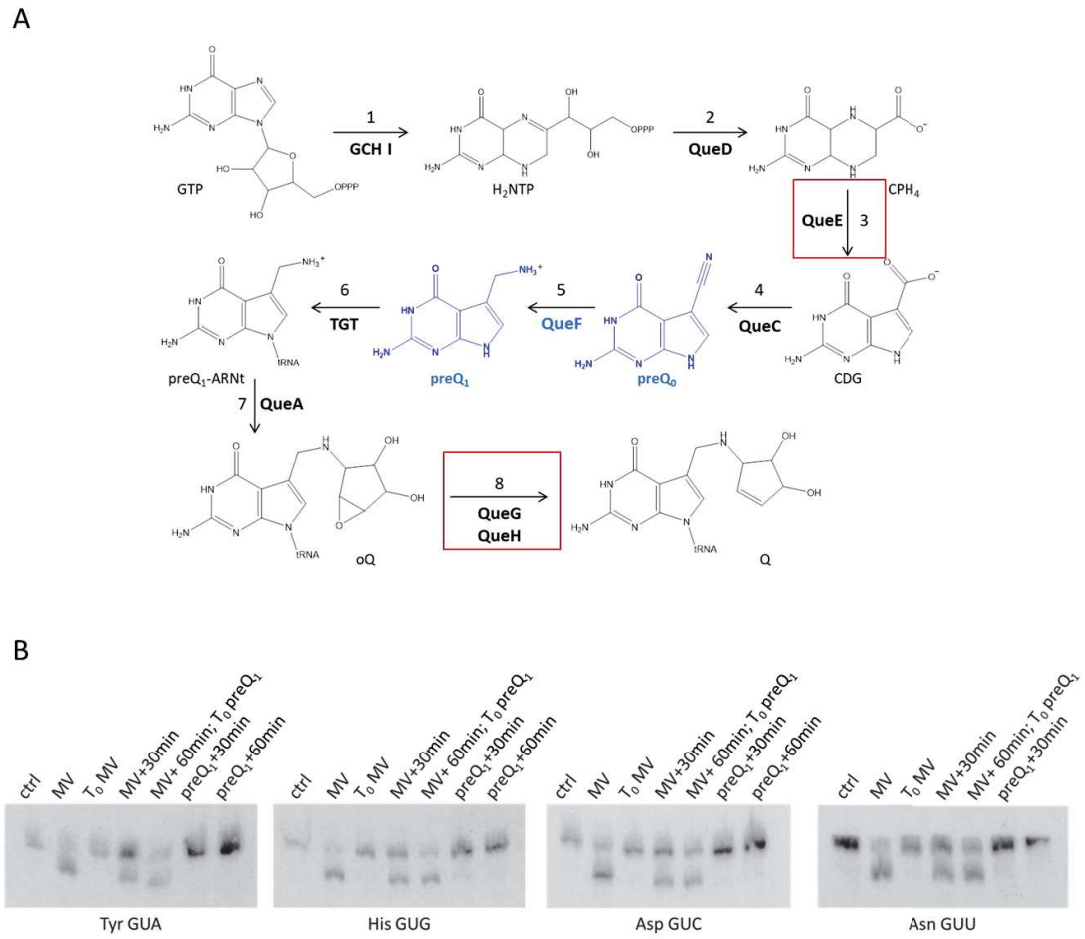


**Figure 7 : A)** Voie de biosynthèse de la queuosine (adapté de (Dowling *et al.*, 2016). En rouge sont encadrées les étapes catalysées par des enzymes à cluster [4Fe-4S], en bleu l'étape catalysée par la QueF convertissant le$preQ_0$ en $preQ_1$**. B)** Northern blot de gels APB des ARNt contenant une Q34 issus de *S.aureus* HG001 cultivées en condition oxydante. A $T_0$MV, le stress oxydant est appliqué à la culture et à $T_0preQ_1$, 60min après l'ajout de MV, l'intermédiaire $preQ_1$ est ajouté au milieu. La culture ctrl est la culture non stressée, sans ajout de $preQ_1$, la culture MV est la culture stressée sans ajout de $preQ_1$.

Les ARNt issus de cultures stressées présentent des profils de migration semblant indiquer une proportion plus importante d'ARNt ne possédant plus de Q34 au court du stress oxydant. 30 min après l'ajout du précurseur de la queuosine $preQ_1$, les ARNt présentent de nouveau un profil électrophorétique similaire à ceux provenant de cellules cultivées en conditions normales. Ce profil se maintient à $TpreQ_1$+60 min et suggère une restauration de la voie de biosynthèse de la queuosine.

# III. Discussion

## 1. Mise en place de la méthode et cartographie des modifications

### i. Limites et méthodes complémentaires : le pouvoir de la coopération

La méthode de NanoLC-MS/MS choisie pour cette étude bénéficie d'une grande sensibilité et précision de mesure, permettant de détecter et localiser sur la séquence tous types de modifications connues. Cependant, elle présente plusieurs limites, principalement les informations fragmentaires obtenues ne permettant pas d'établir une cartographie complète des modifications présentes sur l'ensemble des ARNt.

L'utilisation de plusieurs RNases spécifiques permet d'améliorer par recoupement le recouvrement de séquence des ARNt. Cependant, seules les RNases T1 et A sont capables de digérer les ARNt directement à l'intérieur du gel de polyacrylamide. L'utilisation des RNases MC1 ou U2 par exemple, nécessite d'adapter la méthode de purification des ARNt. Pour cela, la purification d'un ARNt spécifique par hybridation avec un oligodésoxynucléotide biotinylé, suivie d'une chromatographie d'affinité peut permettre d'isoler un ARN ciblé qui n'a pas été détecté à la révélation du gel de polyacrylamide en 2D (*cf* § II. 4. iii.). La séparation des fragments d'ARNt digérés peut également être optimisée grâce à l'utilisation de l'électrophorèse capillaire afin de pouvoir détecter les fragments plus courts (Lechner *et al.*, 2020).

La pseudouridine est une modification de masse silencieuse et n'est pas détectable directement par cette méthode. Un traitement chimique au CMCT est possible mais lors des

tests réalisés, les pseudouridines n'ont pas pu être localisées sur les séquences suite au décrochage du groupement CMC lors de la fragmentation. Une altérnative possible est d'utiliser l'acrylonitrile qui semble plus stable en MS/MS (Mengel-Jørgensen and Kirpekar, 2002).

L'analyse par spectrométrie de masse des nucléosides issus de la digestion complète des ARNt suivi de la déphosphorylation des nucléotides fournit la composition globale en modifications des ARNt. Cette méthode ne nécessite pas de séparation ou de purification préalable des ARNt mais ne fournit pas d'informations concernant la position ou la séquence et permet la quantification relative entre différentes conditions des modifications présentes (Helm and Motorin, 2017; Galvanin *et al.*, 2020). Il est également possible comme alternative, d'utiliser l'approche de marquage SIL-IS in vivo en cultivant les bactéries avec du 13C-glucose comme source majeure de carbone pour faciliter la comparaison relative des modifications par LC-MS/MS (Kellner, Ochel, *et al.*, 2014). En dehors de la spectrométrie de masse, les différentes méthodes de RNA-Seq permettent de localiser certaines modifications spécifiques en fonction du traitement appliqué lors de la préparation des librairies. Les analyses quantitatives sont également possibles avec cette méthode.

Les analyses par des méthodes complémentaires permettent de compléter la cartographie des modifications établie et confirmer les résultats obtenus. La combinaison de différentes méthodes citées apporte une caractérisation plus robuste des modifications des ARNt et de la dynamique de celles-ci.

### ii. Cartographie des modifications des ARN non codants de *S. aureus*

Les données de RNA-Seq (HydraPsi-Seq, AlkAniline-Seq et RiboMethSeq) ont permis de confirmer la présence de modifications sur les ARNt de *S. aureus* et de compléter la carte partielle avec les pseudouridines. Les modifications présentes dans les ARNt de *S. aureus* diffèrent peu des modifications présentes dans d'autres bactéries à gram positif telles que *B. subtilis* ou *L. lactis* pour lesquels des cartographies existent (Vold, 1976; Puri, Wetzel, Saffert, W.Gaston, *et al.*, 2014; de Crécy-Lagard *et al.*, 2020). La cartographie des modifications des

ARNt de *S. aureus* demeure encore partielle. Afin de la compléter, une analyse des nucléosides présents sur les ARNt sera réalisée.

La présence de particularités des ARNt de *S.aureus* a été mise en évidence. Plus précisément, la présence d'ARNt isoaccepteurs de la glycine spécifiques impliqués dans la synthèse de la paroi cellulaire. Ces ARNt interviennent dans la constitution du pont pentapeptide spécifique du peptidoglycane des Staphylocoques via les complexe de proteines FemXAB (facteurs essentiels pour la méthicilline (Giannouli *et al.*, 2009; Rietmeyer *et al.*, 2021) (**Fig. 8A**). Ces $ARNt^{Gly}$, dits non protéinogéniques, présentent une séquence différente des $ARNt^{Gly}$ intervenants dans la traduction (protéinogéniques) et j'ai pu déterminer qu'ils ne possèdent pas la modification 5-méthoxyuridine ($mo^5U$) en 34 permettant le décodage des ARNm. Ils présentent également une boucle T particulière avec un G en position 55, L'absence de la Ψ55 peu inflencer la présence d'autres modifications, comme c'est le cas notamment dans l'$ARNt^{Phe}$ de *Saccharomyces cerevisiae* (Barraud *et al.*, 2019). Chacun de ces $ARNt^{Gly}$ ont été purifiés et analysé par spectrométrie de masse (**Fig. 8B**), confirmant l'absence de modifications dans les régions analysées. Une investigation complète est en cours à ce jour au laboratoire pour déterminer le rôle des modifications dans la discrimination de la machinerie traductionnelle et la redirection de ces ARNt vers la voie de biosynthèse correspondante.

A

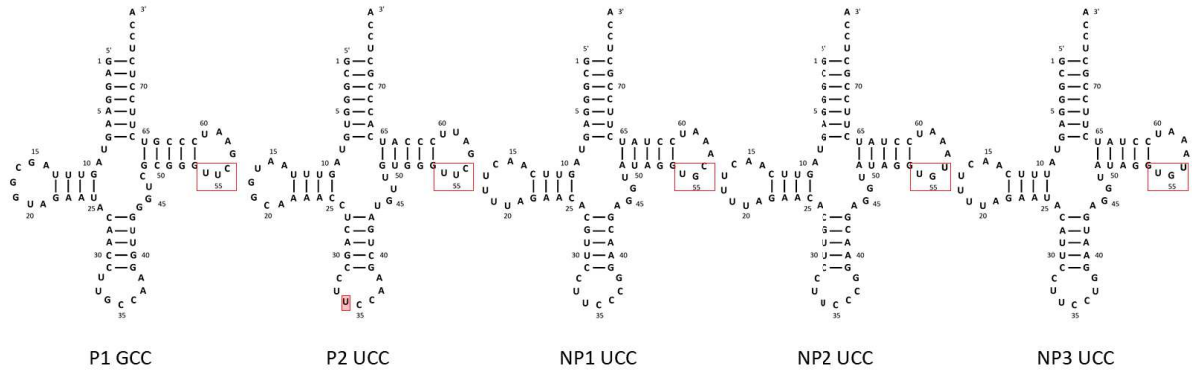


B

| Amino Acid | Antiocodon | | Acc-stem | | D-stem | D-loop | D-stem | | Ac-stem | Ac-loop | Ac-stem | V-region | T-stem | T-loop | T-stem | Acc-stem | | CCA |
|---|---|---|---|---|---|---|---|---|---|---|---|---|---|---|---|---|---|---|
| | | -1 | 1 | 8 | 10 | 14 | 22 | 26 | 27 | 32 | 39 | 44 | 49 | 53 | 61 | 66 | 73 | 74 |
| Gly P1 | GCC | - | GCAGAAG | UA | GUUC | AGCGGUA | GAAU | A | CAACC | UUGCCAA | GGUUG | GGGUC | GCGGG | UUCGAAU | CCCGU | CUUCUGC | U | CCA |
| Gly P2 | UCC | - | GCGGGUG | UA | GUUU | AAUGGCA | AAAC | C | UCAGC | CU5CCAA | GCUGA | UGUU | GUGGG | UUCGAUU | CCCAU | CACCCGC | U | CCA |
| Gly NP1 | UCC | - | GCGGGAG | UA | GUUC | AACUUUUA | GAAC | A | CGUUC | CUUCCCG | GAACG | AGGU | AUAGG | UGCAAAU | CCUAU | CUUCCGC | U | CCA |
| Gly NP2 | UCC | - | GCGGGAG | UA | GUUC | AACUUUUA | GAAC | A | CGUUC | CUUCCCG | GAACG | AGGU | AUAGG | UGUAAAU | CCUAU | CUUCCGC | U | CCA |
| Gly NP3 | UCC | - | GCGGGAG | UA | UUUC | AACUUUUA | GAAU | A | CAUUC | CUUCCUG | GAAUG | AGGU | AUAGG | UGUAAAU | CCUAU | CUUCCGC | U | CCA |

**Figure 8 : Séquences des ARNt$^{Gly}$ de *S. aureus*** adapté de (Giannouli *et al.*, 2009). **A)** P1 et P2 sont les isoaccepteurs protéinogéniques, l'ARNt P2 UCC possède un mo$^5$U en position 34 encadré en rouge. Les ARNt NP123 sont des ARNt non protéinogéniques, encadré en rouge la différence de séquence dans la boucle T. **B)** Dû a leur forte identité de séquence, il est difficile de les identifier spécifiquement un par un. NP1 et NP2 sont alors confondu dans nos analyses. Cependant, aucune modification n'a été détectée dans ces ARNt.

La présence d'une modification de masse inconnue a été établie dans l'ARNt de la Lysine (*cf* § II. 3. **Fig. S1**). Cependant, la caractérisation complète afin d'identifier cette nouvelle modification nécessite de plus amples investigations. Il est en effet possible de cultiver les bactéries en présence d'isotopes afin de déteminer la formule brute de la modification (Kellner, Neumann, *et al.*, 2014).

Il n'existe pas de cartographie globale des modifications présentes sur l'ensemble du ribosome de *S. aureus* à ce jour. Seulement 10 modifications ont pu être assignées pas la structure Cryo-EM du ribosome 70S (Golubev *et al.*, 2020). Les données de RNA-Seq des modifications dans les ARNr sont en cours de traitement par Roberto Bahena qui est doctorant au sein de l'équipe. Les résultats obtenus par cette méthode sur les ARNr sont en cours de confirmation par extension d'amorce (Motorin *et al.*, 2007). Pour caractériser certaines régions spécifiques des ARNr, une adaptation de la NanoLC-MS/MS peut être développée (*cf* § V. 3. **Fig. 13**). L'ARNr 16S a été très partiellement analysé par les différentes techniques mises en place (spectrométrie de masse et RNA-Seq), ce qui a permis de localiser

les modifications situées au niveau du site de décodage impliquant des interactions avec les ARNt et l'ARNm.

## 2. Réponse globale de *S. aureus* au stress oxydant

La transcriptomique différentielle et les analyses protéomiques ont permis d'établir une représentation globale de l'expression des gènes en condition de stress. Ci-après, Les changements observés seront discutés selon les voies métaboliques impliquées (**Annexe 1**). Il a été mentionné qu'une analyse de transcriptome sur micropuce de la réponse cellulaire de *S. aureus* (NCTC 8325) a déjà été rapportée (Chang *et al.*, 2006). L'étude a été conduite en début de phase exponentielle dans un milieu pauvre, ce qui diffère de notre étude réalisée en milieu riche et plus tard dans la phase de croissance de la bactérie. Cependant, les gènes de la réponse SOS et des mécanismes de réparation de l'ADN ont été retrouvés activés également. D'autres gènes, notamment de nombreux facteurs de virulence pour lesquels nous avons observé des variations significatives, n'ont pas été détectés dans ce rapport.

### i. Système SOS de réparation de l'ADN et gènes phagiques

Parmi les ROS, le radical hydroxyle hautement réactif (HO•) réagit avec l'ADN produisant environ 20 produits majeurs d'oxydation des bases ou des sucres de l'ADN, des clivages du brin, et des crosslinks d'ADN et protéines (Cadet and Wagner, 2013). Les dommages sur l'ADN altèrent la réplication et la transcription, causant la mort cellulaire et peut mener à des mutations. Lorsque la DNA polymérase est bloquée sur une lésion, l'hélicase continue de dérouler l'ADN, générant des régions d'ADN simple brin étendues qui vont être ciblées par les protéines du système SOS (Podlesek and Žgur Bertok, 2020). La réponse SOS entraine l'induction de multiples protéines qui renforcent l'intégrité de l'ADN. Cette réponse inclus également des facteurs qui sont des sources d'erreurs, ils vont permettre d'améliorer la survie et la continuité de la réplication en présence de dommages étendus de l'ADN, mais au prix d'une mutagénèse élevée. Dû à son potentiel mutagène, le système de réponse SOS est sujet à une régulation complexe (Maslowska *et al.*, 2019). L'activation du système SOS de

réparation de l'ADN est lié à l'inhibition du répresseur LexA qui va générer l'expression de nombreux gènes, notamment la surexpression de la protéine RecA (Ha *et al.*, 2020b) qui est observé dans nos analyses avec un FoldChange . La protéine RecA est connue pour stimuler l'autoclivage de LexA eu ainsi augmenter l'expression (Bisognano et al., 2004). Nous avons également observé une augmentation de l'expression de *uvrB*, codant pour un facteur requis pendant les étapes précoces de la réparation par excision des nucléotides qui va former un complexe ADN-protéine au niveau du site endommagé permettant l'incision (Gordienko and Rupp, 1997). De plus, de nombreuses protéines impliquées dans la synthèse des purines et des pyrimidines semblent confirmer la mise en place de réparation des acides nucléiques.

L'activation de l'expression de gènes prophagiques suite au stress oxydant était attendue, leur expression étant activée suite au déclenchement du système SOS de réparation de l'ADN (Maiques *et al.*, 2006). Les protéines prophagiques favorisent le transfert horizontal de l'ADN et peuvent entrainer l'acquisition par la bactérie de résistances. Ce transfert génétique entre les bactéries est habituellemnet induit par des stresseurs, comme les antibiotiques (Beaber *et al.*, 2004; Jutkina *et al.*, 2016), les métaux et biocides (Seier-Petersen *et al.*, 2014) et plus généralement par la réponse SOS (Andersson and Hughes, 2014). De plus il a été récemment observé que la diffusion chez *E. coli* de gènes de résistance via la conjugaison et aussi stimulée par le stress oxydant généré par les radiations UV (Chen *et al.*, 2019). Puisque la transduction conditionnée par les bacteriophages est considérée comme un des facteurs principaux des transferts de gènes horizontaux chez les Staphylocoques (Xia and Wolz, 2014; Stanczak-Mrozek *et al.*, 2015), il est possible que chez *S. aureus* le stress oxydant stimule le transfert de gènes via la transduction.

### ii. Détoxification des espèces réactives de l'oxygène

Les protéines AhpCF de détoxification des ROS sont très largement surexprimées, cependant, les analyses protéomiques réalisées n'ont pas montré de surexpression détectable des protéines Sod alors que l'analyse transcriptomique indique une surexpression de *sodM* dont l'expression est activée lors d'un manque de manganèse dans le milieu sans lien avec les conditions oxydantes rencontrées (Karavolos et al., 2003; Garcia et al., 2017). La

catalase KatA est légèrement surexprimée au niveau protéique alors que la transcription reste inchangée, suggérant une régulation au niveau traductionnel de son expression. L'expérience de ribosome profiling à haute résolution pourrait nous permettre de mieux comprendre s'il y a une différence d'efficacité de la traduction du gène *katA.*

### iii. Métabolisme des acides aminés

L'enzyme MetE impliquée dans la biosynthèse *de novo* de la méthionine à partir d'homocystéine ainsi que la sulfite réductase codée par le gène *cysJ* impliqué dans la biosynthèse de la cystéine sont surexprimées. L'expression de la thioredoxine permettant la réduction des thiols dans le cytoplasme est inchangée alors que la protéine régulatrice Spx, nécessaire à son expression est sous exprimée au niveau protéomique malgré une surexpression en transcriptomique.

### iv. Homéostasie du fer

De nombreuses protéines responsables de l'apport du fer sont largement surexprimées, illustrant l'importance vitale de celui-ci pour la survie de la bactérie en conditions oxydantes. Les staphyloferrines et les protéines Isd permettant l'import de celui-ci provenant de son environnement, ou des cellules de l'hôte. Dans un contexte d'infection, la production de ces protéines permettant l'internalisation par la cellule du fer présent dans l'hème ou la transferrine de l'hôte peut permettre à la bactérie de survivre à l'oxydation du Fer induit par les ROS.

### v. La voie de respiration en anaérobie

Les protéines impliquées dans la respiration anaérobie codées par les opérons *narGHWX* et *nasDEF* sont surexprimées au niveau transcriptionnel alors qu'elles sont moins exprimées en protéomique durant le stress oxydant. L'inhibition de l'expression de ses protéines peut s'expliquer par une absence de traduction des ARNm transcrits ou une traduction altérée qui

entrainerait la production de protéines instables et ainsi la dégradation de celles-ci. La surexpression de protéines chaperonnes impliquées dans le repliement semble corroborer la deuxième hypothèse. Cependant, La transcription de ces opérons depend de la présence ou non d'oxygène. En effet, la protéine NreB, qui est codé par l'opéron *narGHWX* et fait partie du régulon NreABC, est une kinase à cluster [4Fe-4S] qui va avoir un rôle de capteur de l'oxygène. En absence de $O_2$, le cluster est intact et l'enzyme est active, elle va s'autophosphoryler et transférer le phospore à NreC qui va pouvoir se lier à l'ADN pour activer l'expression des deux opérons le la voie de réduction du nitrate et du nitrite (Fedtke et al., 2002; Nilkens et al., 2014). En présence d'oxygène, le cluster [4Fe-4S] est dégradé et l'enzyme est inactivée. Dans nos conditions expérimentales de stress oxydant, NreC doit être inactive ce qui suggère que la transcription de l'opéron est activée par un autre facteur qui n'est pas caractérisé et qui n'entraine pas la production de protéines fonctionnelles. Ces résultats indiquent qu'il existe un système de régulation plus complexe de l'expression des opérons de la chaine de respiration anaérobie en lien avec le stress oxydant

### vi. L'implication des ARNt et des enzymes de modifications

Les enzymes de modifications des ARNt sont, bien que plus lègérement impactées, également surexprimés en transcriptomique et moins exprimées en protéomique. Les ARNt, plus spécifiquement l'ARNt$^{Tyr}$ sont moins exprimés pendant le stress oxydant. Chez E. coli, le stress induit par le $H_2O_2$ en milieu minimal entraine une diminution globale de la quantité de ARNt due à leur dégradation et engendrant l'inhibition de l'élongation de la traduction (Zhong et al., 2015). Alors que l'exposition au MV ne touche que l'ARNt$^{Gly}$, altérant le décodage des codons (Leiva et al., 2020). Chez E. coli, l'expression des ARNt peuvent moduler la réponse au stress oxydant. Il est possible que chez *S. aureus,* même si le niveau global d'ARNt n'est pas fortement impacté, des changements au niveau de leurs modifications puissent participer au contrôle traductionnel et à la réponse au stress oxydant.

### vii. La persistance de la bactérie privilégiée au détriment de la dissémination et de l'infection aiguë

Les mécanismes de survie et de réparation des dommages causés par les ROS sont privilégiés durant le stress oxydant au détriment de la production de toxines cytolytiques responsables d'infections aigües telles que les PSM ou les CHIPS. Dans le contexte d'une infection, cela est habituellement observé durant la colonisation des tissus dans lesquels *S. aureus* établit de nouvelles colonies grâce aux adhésines exprimées telles que la protéine SpA et le clumping factor B. D'un autre côté, le stress oxydant est habituellement rencontré lorsque *S. aureus* est internalisé dans les neutrophiles et les macrophages. *S. aureus* a été reconnue comme persistant à l'intérieur des phagocytes ou des cellules endothéliales sur des périodes prolongées (Hamill *et al.*, 1986). Dans ces conditions confinées, le système de quorum sensing Agr devrait normalement augmenter l'expression des toxins et exoprotéines (Carnes *et al.*, 2010). Cependant, chez les bactéries internalisées, il a été démontré que l'inactivation du régulateur Agr empêchant l'expression des facteurs de virulence dépendant du quorum sensing leur permet et persister sous forme de Small Colony Variants (SCV). Ces variants se développent plus lentement mais présentent une plus grande résistance aux antibiotiques, provoquant des infections chroniques (Sendi and Proctor, 2009; Young *et al.*, 2017). Lorsque Les conditions seront plus favorables ou la densité de cellules suffisante, les toxines seront produites afin de disséminer les bactéries et diffuser l'infection (Surewaard *et al.*, 2013; Bojer *et al.*, 2018).

## 3. Modifications des ARNt et stress oxydant

### i. Dynamique des modifications des ARNt durant le stress

En condition de stress oxydant, le profil de migration des ARNt sur gel de polyacrylamide est modifié pour la souche de laboratoire HG001 comme pour la souche clinique de *S.aureus* USA300. La migration des ARNt indique un changement dans l'état de modification de certains ARNt. L'absence de queuosine suggérée par le clivage par la RNAse T1 dans l'ARNt$^{Tyr}$

est confirmée par les profils de migration sur gel d'APB des 4 ARNt concernés. Les ARNt contenant une Q34 migrent à la même vitesse en condition de stress oxydant que les ARNt provenant d'une souche ne possédant pas de queuosine. Les analyses de 3 des ARNt purifiés par chromatographie d'affinité digérés par la RNase U2 montrent la présence de G34 non modifiés pour ces ARNt provenant de cultures stressées.

L'analyse par RNA-Seq en triplicats d'ARNt totaux issus de cultures stressées ou non est à ce jour en cours afin de déterminer si d'autres modifications sont affectées. Les enzymes de modification des ARN, plus spécifiquement les méthyltransférases, font partie des métalloenzymes à centre [4Fe-4S]. La présence de ROS peut donc entrainer leur inactivation et ainsi une diminution des méthylations des ARNt. Cependant aucun résultat obtenu lors de cette étude ne permet de le démontrer. Les 2'OMe présents en position 32 qui sont impliqués dans la réponse au stress oxydant chez *P. aeruginosa* n'ont pas été détectés par NanoLC-MS/MS chez *S. aureus*. De même, les $m^7G$ en position 46 ont été détectés dans peu d'ARNt, ne permettant pas de réaliser d'analyses sur de potentiels changements lors du stress.

### ii. Causes de l'absence de queuosine

L'analyse transcriptomique semble montrer une légère surexpression des enzymes impliquées dans la voie de biosynthèse de la queuosine malgré l'absence de celle-ci dans les ARNt. Ces résultats peuvent indiquer la chute de l'activité enzymatique des protéines produites. Les plus susceptibles d'être inactivées sont les enzymes contenant un cluster [4Fe-4S], il y en a 3 impliquées dans la synthèse de la queuosine : QueE, QueG et QueH. La 7-carboxy-7-deazaguanine synthase (QueE) utilise la SAM et catalyse la synthèse du CDG à partir du $CPH_4$ (**Fig. 7A**, étape 3) (McCarty *et al.*, 2013). *S. aureus* possède deux époxyqueuosine réductases (**Fig. 7**, étape8), QueG utilisant la cobalamine (Dowling *et al.*, 2016) et QueH qui semble être indépendante de la cobalamine (Zallot *et al.*, 2017).

L'ajout d'un intermédiaire de cette voie, le preQ1 permet de restaurer la présence de la queuosine sur les ARNt indiquant une possible inactivation d'une ou plusieurs enzymes en amont de cet intermédiaire. La réduction de l'époxyqueuosine (oQ) ne semble donc pas être

l'étape impactée par la présence des ROS. Comme deux enzymes sont capables de catalyser cette réaction, deux possibilités se présentent : soit les deux clusters ne sont pas sensibles aux ROS, soit leurs activités peuvent se compenser en cas d'inactivation de l'une des deux enzymes. L'enzyme QueE est potentiellement sensible à l'oxydation par les ROS, le fer apical (non coordiné par une cystéine du motif CXXXCXXC) du cluster peut être protégé de l'oxygène s'il est coordiné par un ligand ou à un autre acide aminé situé à proximité.

Cependant, cela ne semble pas être le cas pour QueE, le fer apical des enzymes à SAM doit être accessible pour permettre la coordination du SAM. Par exemple, l'enzyme QueE de *B. subtilis*, proche de celle de celle de *S.aureus* présente un fer très accessible (**Fig. 9**).

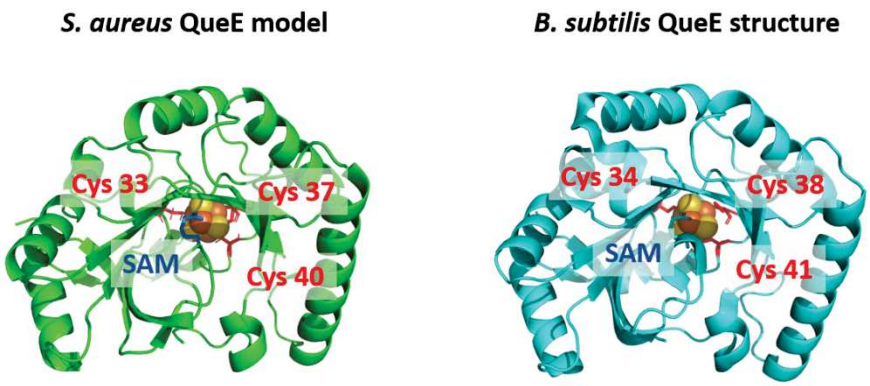


**Figure 9.** Comparaison structurelle entre la QueE de *S. aureus* modélisée par homologie est la structure obtenue par rayon X de *B. subtilis* (fichier pdb 5TH5; Bruender et al., 2017). Le motif spécifique pour la coordination du cluster [4Fe-4S] (en orange et jaune) est conservé. Il est composé de 3 résidus cystéine. Chez *B. subtilis,* cys 38 et cys 41 (chez *S. aureus,* cys 37 and cys 40 correspondants) sont assez proches our pouvoir former un pont disulfure si ils sont oxydés. Le 4ème fer du cluster interagit avec l'α-amino et l'α- carboxylate du SAM.

L'enzyme catalysant la synthèse du $preQ_1$ à partir du $preQ_0$, QueF (7-cyano-7-déazaguanine réductase NADPH dépendante) (**Fig. 7**, étape 5) possède une cystéine catalytique en position 57 chez *S. aureus* (**Fig. 10**).

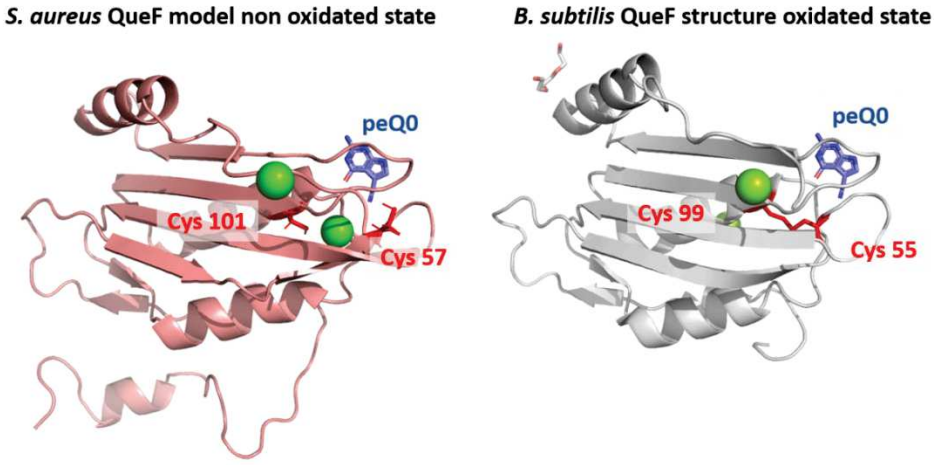


**Figure 10 : Comparaison structurale entre le modèle de QueF de *S. aureus* obtenu par homologie avec la structure aux rayons X de QueF de *B.subtilis* en état oxydé** (pdb file 5UDG; Mohammad et al., 2017). La Cys 55 de *B. subtilis* (correspondant à la Cys 57 chez *S. aureus*) se lie au substrat $preQ_0$, formant un intermédiaire thiomide. Ce résidu catalytique est sensible à l'oxydation et peut former un pont disulfure avec la Cys 99 (Cys 101 chez *S. aureus*). Le $preQ_0$ ne peut plus se fixer à QueF si la Cys 57 est oxydée, empêchant la formation de la queuosine.

Cette cystéine peut être protégée en conditions oxydantes par la formation d'un pont disulfure avec une deuxième cystéine se situant à proximité (Mohammad et al., 2017). Des analyses de LC-MS/MS ont été réalisées en alkylant les protéines avant la réduction des ponts disulfures mais les cystéines concernées n'ont pas pu être visualisées dû à la trop faible abondance de la protéine d'intérêt. La séparation préalable sur SDS-PAGE n'a pas permis d'éliminer suffisamment les protéines contaminantes. Afin d'enrichir l'échantillon pour l'analyse LC-MS/MS de QueF, il est possible d'exprimer la protéine portant une étiquette (flag-tag) avant purification par chromatographie d'affinité de type co-immunoprécipitation. Après élimination du MV par centrifugation des bactéries, aucune restauration de la queuosine n'a été observée sur gel de polyacrylamide, ce qui semble invalider l'hypothèse de l'inactivation réversible de QueF. De manière identique à $preQ_1$, l'ajout du substrat de QueF, $preQ_0$ au milieu de culture des bactéries cultivées en conditions oxydantes est en cours au laboratoire afin de tenter de restaurer la présence de queuosine.

### iii. Conséquences traductionnelles de l'absence de Q34

La queuosine est présente en position 34 des ARNt, la position wobble qui est impliquée dans le décodage des ARNm. L'altération de cette modification peut impacter la vitesse et la précision de la traduction des protéines contenant les 4 acides aminés dont l'incorporation dépend des ARNt qui ont perdu la queuosine.

La légère surexpression observée dans l'analyse transcriptomique des gènes de chaperonnes impliquées dans le repliement des protéines peut indiquer un problème d'agrégation des protéines dû à des variations de vitesse de traduction.

Afin d'étudier la vitesse de décodage des ARNm codon par codon, une expérience de ribosome profiling à haute résolution (hRibo-Seq) permet de révéler les sites de pause du ribosome. Un protocole établi pour *E. coli* (Mohammad *et al.*, 2019) a été adapté à l'étude de *S. aureus* au sein du laboratoire. Cette méthode consiste à immobiliser les ribosomes en cours de traduction grâce à la congélation directe des bactéries dans l'azote liquide en présence d'une concentration élevée de sels de magnésium. Après purification des polysomes, les portions d'ARNm qui ne sont pas protégés par la présence du ribosome sont digérées par une RNase spécifique (MNase) permettant de générer des fragments d'ARNm en cours de décodage. Le séquençage des fragments d'ARNm en cours de traduction permet de déterminer d'une par les gènes traduits spécifiquement durant les conditions données mais également d'obtenir un taux d'occupation des ribosomes le long des ARNm.

L'étape de digestion des ARNm est cruciale pour déterminer précisément les codons particuliers pour lesquels la vitesse de décodage est altérée. En effet, la digestion par la RNAse doit générer des fragments de longueur adaptée, correspondant à la position exacte du ribosome et permettant d'assigner un codon spécifique au site de décodage.

L'étude de l'impact des queuosines sur le décodage des ARNm chez les eucaryotes met en évidence des conséquences différentes de l'absence de queuosine sur la vitesse de décodage des codons contenants un C ou un U en 3' dépendant de l'organisme. La queuosine contribuant ainsi à l'harmonisation de la vitesse de la traduction de manière générale (Tuorto *et al.*, 2018; Müller *et al.*, 2019).

Les données préliminaires obtenues durant les tests réalisés au laboratoire semblent indiquer que chez *S. aureus*, spécialement pour l'ARNt$^{Tyr}$, l'absence de Q34, entraine une perte de vitesse de décodage des codons UAU durant le stress oxydant alors que la vitesse de décodage des codons UAC n'est pas impactée (**Fig. 11**).

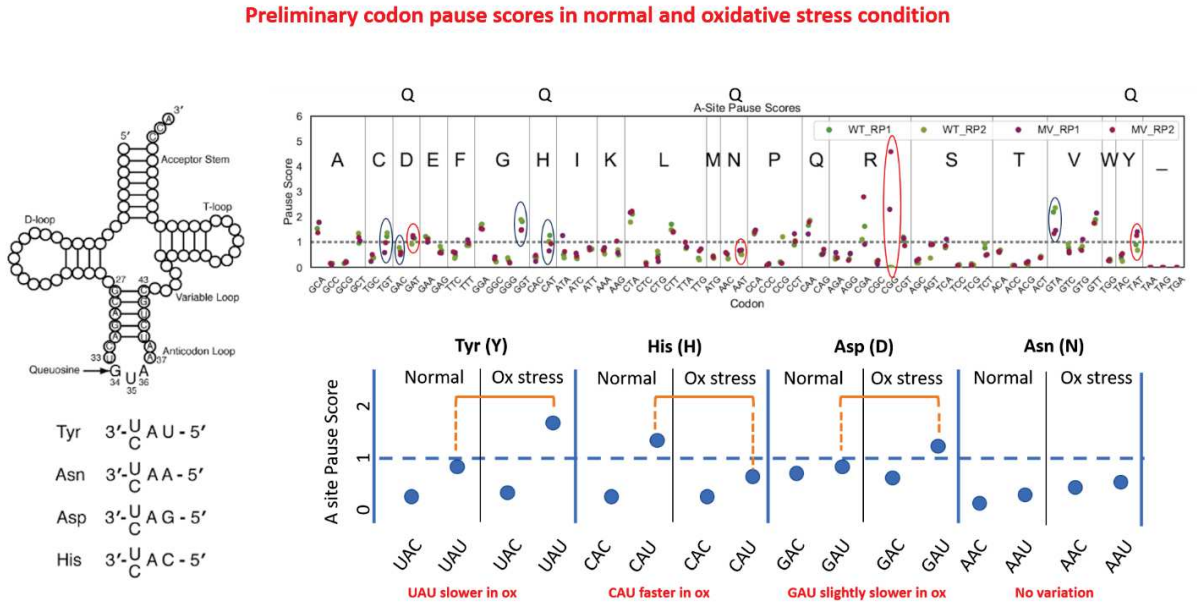


**Figure 11. Score de pause des codons dans le site A par analyse préliminaire de hRibo-seq** en condition normale (WT, en vert) et stress oxydant (MV, en rouge). Les scores de pauses ont été calculées selon Mohammad *et al.*, 2019. Des variations ont été obsérvées pour les codons synonymes des Cys (C), Asp (D), Gly (G), His (H), Asn (N), Arg (R), Val (V) et Tyr (Y). Les codons Asp (D), Asn (N) et Tyr (Y), et His (H) correspondent aux ARNt contenant une Q34 en condition normale et un G34 en stress oxydant. Parmis eux, les différences les plus importantes sont observées pour l'ARNt$^{Tyr}$ qui montre un décodage plus lent pour le codon UAU durant le stress oxydant.

Le protocole utilisé restreint le volume de culture qui peut être utilisé et dans les conditions de notre analyse, réalisée en fin de phase exponentielle (lorsque la traduction est déjà réduite), nous n'avons pas pu obtenir assez de fragments d'ARNm pour réaliser une analyse correcte et complète. Afin d'obtenir suffisamment d'ARNm en cours de traduction, les cellules doivent être en phase exponentielle et contenir un grand nombre de ribosomes matures et actifs. Cela implique pour nous d'induire le stress plus tôt dans la phase de croissance des bactéries et d'arrêter la culture plus tôt car dans les conditions présentées dans cette étude, de nombreux ribosomes se sont révélés être immatures ou inactifs. Un autre aspect qui peut être amélioré pour obtenir une meilleure résolution pour nos expériences de hRibo-seq est le choix de la RNase utilisée pour produire les fragments

d'ARNm protégés par le ribosome. L'utilisation de la MNase ne semble pas adaptée pour cette étude chez *S. aureus*, car la taille des fragments obtenus indique une dégradation non spécifique des extrémités des ARNm protégés par le ribosome. Cette étape de digestion est réalisée avec la RNase I pour les analyses de ribosome profiling chez les eucaryotes, cette procédure a été testées avec succès et sera donc mise en place au sein du laboratoire

Des perturbations dans la vitesse de traduction des protéines peut impacter le repliement de celles-ci et ainsi leur stabilité. Le décodage de certains ARNm, selon leur composition en codons spécifiques, peut donc participer à la régulation de l'expression de certaines protéines au niveau de la traduction. Cette analyse permettra d'étudier l'impact sur la vitesse de décodage de l'absence de la queuosine sur les 4 ARNt concernés et ainsi d'établir le rôle de cette modification dans l'adaptation de la bactérie au stress oxydant.

## IV. Conclusions

J'ai participé à la mise en place de la méthode d'UPLC-MS/MS qui, en association avec les méthodes de RNA-Seq, a permis d'établir les cartographies partielles des modifications présentes dans les ARN non codants de *S. aureus.* L'amélioration de cartographie est en cours avec l'utilisation de méthodes complémentaires permettant de la compléter et d'étendre cette analyse à d'autres ARN tels que les ARN régulateurs pour lesquels aucune modification n'a été caractérisée *chez S. aureus*

Cette cartographie m'a permis d'étudier leurs variations, en particulier dans les ARNt, lors du stress oxydant mimant la production de ROS par les cellules du système immunitaire lors de l'infection. J'ai ainsi pu mettre en évidence une altération de la queuosine des 4 ARNt possédant cette modification en position wobble de l'anticodon. De plus, l'ajout d'un intermédiaire de la voie de biosynthèse restaure la présence de la queuosine, apportant une indication sur la cause possible de l'absence de la modification

Ces résultats ont conduit à la mise en place de la méthode de ribosome profiling à haute résolution et son adaptation pour l'étude de *S.aureus*. Les premières analyses de l'impact sur la traduction de l'absence de cette modification sur les $ARNt^{Tyr}$ ont montré des résultats

encourageants. L'expérience de hRibo-Seq complète peut être réalisée afin d'élucider la fonction de la queuosine sur le décodage de l'ensemble des codons nécessitant cette modification. Les cultures contenant du $preQ_0$ ont été réalisées et peuvent être analysées afin de souligner une potentielle inactivation de l'enzyme QueF lors du stress oxydant.

La cartographie des modifications sur les ARN ribosomiques est en cours de réalisation, les données de RNA-Seq de ribosomes et d'ARNt provenant de bactéries soumises ou non au stress oxydant sont en cours d'analyse. Le projet se poursuit avec l'étude structurale de l'impact des variations des modifications des ARNt et ARNr sur l'ensemble de la machinerie traductionnelle qui est réalisée par Roberto Bahena, qui est actuellement en thèse.

L'analyse des modifications des $ARNt^{Gly}$ non protéinogéniques ne possédant pas de modifications a mené à la création d'un nouveau projet de recherche. L'étude structurale des différents isoaccepteurs de la glycine ainsi que de leurs interactions avec la machinerie traductionnelle (EFTU) ou la machinerie responsable du transfert des ARNt vers la paroi cellulaire telles que les protéines Fem (facteurs essentiels pour la résistance à la méthicilline) est en cours avec Hiroki Kanazawa actuellement en contrat post doctoral.

Cette approche mise en place pour l'étude des variations des modifications des ARN en réponse au stress oxydant et de leur impact traductionnel, pourra être appliquée à d'autres conditions environnementales rencontrées lors de l'infection. La combinaison des informations apportées par l'étude de la réponse du pathogène aux différents stress permettra d'améliorer notre compréhension du rôle des modifications durant l'infection.

# V. Matériels et méthodes

## 1. Produits et sondes utilisés

Les produits chimiques et milieux de culture utilisés proviennent de Sigma-Aldrich. Les enzymes utilisées proviennent de ThermoFischer Scientific.

Sondes utilisées :

| | probe for single tRNA purification | probe for Northern blotting |
|---|---|---|
| $tRNA^{Asp}_{GUC}$ | /5BiosG/GATCTCCTGCGTGACAGGCAGGCGTGTTAACCGCTACAC | GATCTCCTGCGTGACAGGCAGGCGTGTTAACCGCTACAC |
| $tRNA^{Asn}_{GUU}$ | /5BiosG/GACCGATCGGTTAACAGCCGATAGCTCTACCACTGAGC | GACCGATCGGTTAACAGCCGATAGCTCTACCACTGAGC |
| $tRNA^{His}_{GUG}$ | /5BiosG/GAATGTCGGAACCACAATCCGATGTGTTAACCACTTCAC | GAATGTCGGAACCACAATCCGATGTGTTAACCACTTCAC |
| $tRNA^{Tyr}_{GUA}$ | /5BiosG/CGAAGGAGCGGATTTACAGTCCGCCGCGTTTAGCCACTTCGC | CGAAGGAGCGGATTTACAGTCCGCCGCGTTTAGCCACTTCGC |
| tRNAGly P2 | /5Biosg/ATC AGC TTG GAA GGC TGA GGT TTT GCC ATT AAA CTA | / |
| tRNAGly NP1+NP2 | /5Biosg/TCG TTC CGG GAA GGA ACG TGT TCT AAA AGT TGA ACT A | / |
| tRNAGly NP3 | /5Biosg/TCA TTC CAG GAA GGA ATG TAT TCT AAG AGT TGA AAT A | / |
| rRNA pos | oligonucleotide for rRNA modifications MS analysis | |
| 1202-1241 | C GTGTGTAGCCCAAATCATAAGGGGCATGATGATTTGACG | |
| 1395-1440 | GGTGTTACAAACTCTCGTGG TGTGACGGGC GGTGTGTACAGACCC | |
| 1497-1542 | TCCAGCCGCACCTTCCGATACGGCTACCTTGTTACGACTTCACCCC | |

**Tableau 2 :** Oligonucléotides utilisés pour la purification des ARNt, les Northern blot et l'Analyse par NanoLC-MS/MS des modifications de l'ARNr 16S

## 2. Souches bactériennes et conditions de culture

### i. Souches

La souche principalement utilisée pour cette étude est la souche *S. aureus* HG001 de laboratoire, dérivée de la souche NCTC8325 contenant le gène *rsbU* restauré (Herbert *et al.*, 2010). La souche clinique MRSA (methicillin resistant *S.aureus*) *S. aureus* USA300 (Tenover and Goering, 2009) ainsi que la souche NE1885 provenant de la collection Nebraska qui en est dérivée seront également utilisées. La souche NE1885 possède un transposon contenant plusieurs codons stop en position 9 du gène *tgt* entrainant une absence de queuosine (Bose *et al.*, 2013).

### ii. Conditions de culture

Les cultures de bactéries non stressées sont réalisées dans les conditions publiées précédemment (*cf* § II. 2). Brièvement, une préculture sur la nuit est diluée à DO(600nm) = 0,05 dans 20 mL de BHI et est incubée à 37°C sous agitation à 180rpm durant 4h jusqu'à une $DO(600nm)_{finale}$ = 3.

Les cultures soumises au stress oxydant sont cultivées comme les bactéries non stressées pendant 120 min. A t= 120 min, 10mM final de méthylviologen est ajouté à la culture, les bactéries sont ensuite cultivées dans les conditions de température et d'agitation inchangées pendant 120 min jusqu'à atteindre une $DO(600nm)_{finale}$ = 2,5-3.

Pour l'étude de l'effet de l'intermédiaire $preQ_1$, le stress est appliqué par l'ajout de méthylviologen au milieu de culture après 90min d'incubation. Après 1h de croissance en condition de stress oxydant, le $preQ_1$ est ajouté à une concentration finale de 1µM, les cellules sont ensuite incubées dans les mêmes conditions de température et d'agitation.

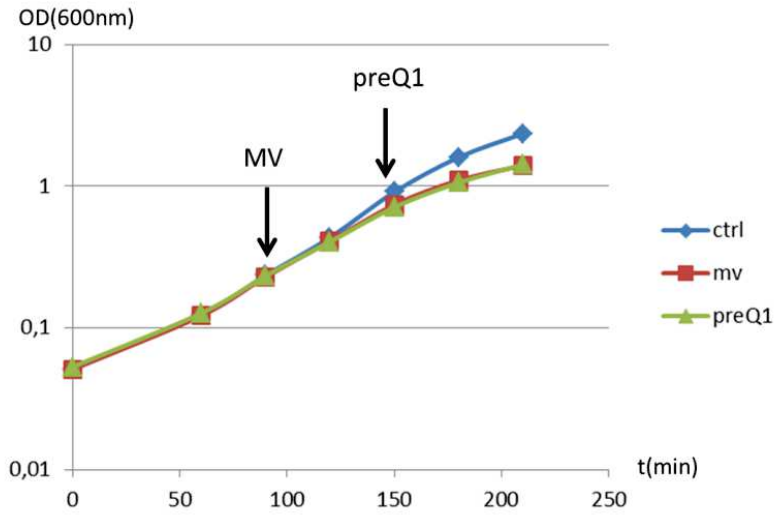


**Figure 12 :** Courbe de croissance des cultures de *S. aureus* HG001 cultivées en condition oxydante dont la queuosine est réstaurée par l'ajout de $preQ_1$.

### 3. Analyse par NanoLC-MS/MS de l'ARNr 16S

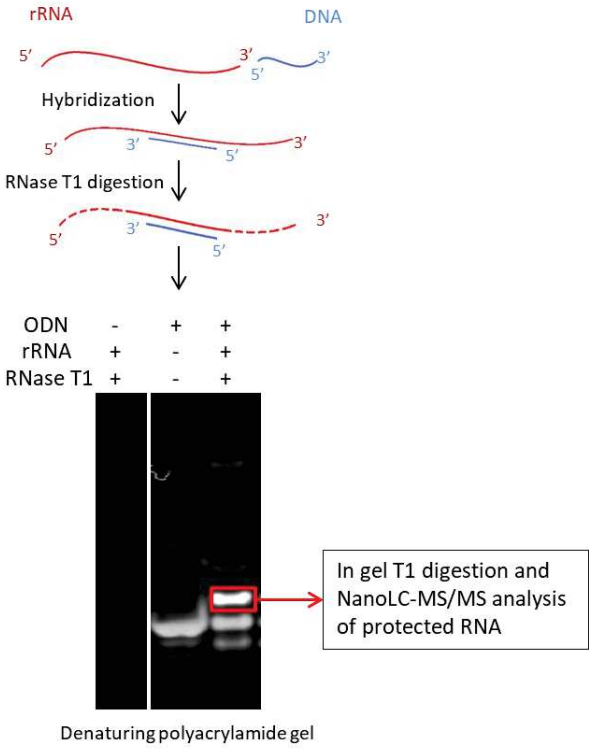


**Figure 13 : Adaptation de la méthode NanoLC-MS/MS à l'analyse des ARNr.** Brièvement, une partie ciblée de l'ARN est protégée par hybridation d'un oligodésoxynucléotide puis digérée avec la RNAse T1. Le duplexe ARN-ADN est ensuite séparé sur gel de polyacrylamide dénaturant avant une seconde digestion à la RNaseT1 et analyse NanoLC-MS/MS.

L'analyse est réalisée à partir d'ARNt totaux, préparés comme publié précédemment (*cf* § II. 2). 10 µg d'ARN totaux sont dénaturés en présence de l'oligonucléotide (**tableau 2**)dans un tampon cacodylate 10 mM ; 50 mM NaCl ; 25 mM KCl à 90°C pendant 5 min puis renaturés avec l'oligonucléotide d'ADN dans la glace pendant 30 min. L'ARN non protégé est ensuite digéré avec la RNase T1 à 37°C pendant 2h (100 mM Acétate d'ammonium). Les échantillons sont ensuite déposés sur gel de polyacrylamide 10%, 8M urée et migrés dans le TBE pendant 2h à10W constants.

Les ARN sont révélés par bromure d'éthidium, les bandes de gel sont découpées puis les ARN sont digérés en gel et analysés par NanoLC-MS/MS comme publié précédemment ((*cf* § II. 1).

### 4. Analyse transcriptomique

Les triplicats d'ARN totaux sont extraits suivant les protocoles publiés précédemment (*cf* § II. 2.). Brièvement, les cultures sont centrifugées à 3750 rpm et 4°C pendant 15min puis les cellules sont resuspendues dans 1mL de solution RNA Pro (MP biomedicals) et lysées mécaniquement au fastprep (MP biomedical) 2 fois 40s à vitesse maximale. Les ARN totaux sont extraits au chloroforme, puis précipités à l'éthanol et traités avec 1U de DNase I par µg d'acides nucléiques (estimés par mesure de l'absorbance à 260nm) pendant 45min à 37°C sans agitation. La DNase est éliminée par une nouvelle extraction au phénol/chloroforme/alcool isoamylique et les ARN sont précipités à l'éthanol. La concentration et la pureté des acides nucléiques sont mesurées par nanodrop avant la préparation des librairies et séquençage par la plateforme EpiRNA-Seq de Nancy. Les données sont traitées avec Galaxy comme détaillé dans (Lalaouna *et al.*, 2018) pour l'élimination des séquences des adaptateurs, le seuil de qualité, l'alignement sur le génome et le comptage des reads par feature annotée. Pour l'analyse différentielle, Deseq2 est utilisé.

### 5. Analyse protéomique

Les triplicats de protéines totales sont extraits de cellules resuspendues dans le tampon 50 mM Tris pH 8, 50 mM NaCl, 1% triton × 100 et lysée 40s au fastprep. Le dosage des protéines est réalisé par Bradford, les protéines (5 µg) sont précipitées au méthanol contenant 0,1 M d'acétate d'ammonium, puis réduites et alkylées (5 mM DTT, 10 mM iodoacetamide). Les protéines sont ensuite digérées à la trypsine puis les peptides (1µg) sont analysées par NanoLC-MS/MS sur un système NanoLC-2DPlus system couplé à un spectromètre de masse TripleTOF 5600 (ABSciex) (Chicher *et al.*, 2015).

## 6. Gel d'acide phénylboronique et Northern blot

Les gels de polyacrylamide contenant de l'acide phénylboronique ont été réalisées suivant les protocoles établis (Matuszek and Pan, 2019). Les ARN totaux (2µg) préalablement déacylés sont séparés sur gel de polyacrylamide, 12%, 8M urée, 0,5% APB pendant 3h30 à 13W constant. Les ARN sont ensuite transférés sur membrane de nitrocellulose Hybond N+ (GE Healthcare Life Sciences) par transfert semi-sec pendant 45 min à 10V (Trans-Blot semi-dry transfert cell, Biorad) et fixés par crosslink UV (Stratalinker 1800, Statagene). Les ARNt sont révélés par hybridation d'une sonde marquée au 32P (**Tableau 2**) et visualisés par autoradiographie.

## 7. Purification des ARNt

Les ARNt sont obtenus à partir d'extraits d'ARN totaux par filtration sur centricons 50 kDa (Amicon Ultra 0,5 mL, Millipore), 20 µg d'ARN total est déposé sur la membrane puis centrifugé 10 min, à 9000 rpm et température ambiante. Le filtrat est immédiatement précipité à -20°C durant la nuit avec 3 volumes d'éthanol contenant 0,1 M d'acétate d'ammonium. Après centrifugation 10 min à 13000 rpm et 4°C, le culot est rincé, séché puis repris dans 50 µL d'eau milliQ. 200 µL de résine streptavidine-sépharose sont préalablement incubée avec 400 µL de sonde spécifique biotinylée (7.5 µM) durant 30min à température ambiante puis rincée avec 400 µL de tampon (10mM Tris, HCl pH 7.5). Les ARNt sont incubés avec la résine streptavidine-sonde en présence de 900 mM de TEA-Cl et 0,1 mM d'EDTA pendant 5 min à 37°C. La résine est ensuite rincée 3 fois avec 400 µL de tampon. L'ARNt hybridé à la sonde est élué par chauffage à 60°C pendant 5 min suivi d'une centrifugation rapide (10 s, 13000 rpm, température ambiante). L'ARNt purifié est ensuite concentré par précipitation à l'éthanol (Yokogawa *et al.*, 2010).

### 8. Digestion à la RNAse U2 des ARNt purifiés.

La digestion des ARNt à la RNase U2 a été réalisée selon une adaptation de la méthode préalablement publiée (Wolff *et al.*, 2020). Brièvement, 20 ng d'ARNt purifié sont digérés avec 6 ng de RNase U2 produite au laboratoire dans 20 µL d'acétate d'ammonium 100mM à 37°C pendant 2h.

### 9. Modèlisation des structures de QueE et QueF de *S. aureus*

QueE et QueF *de S. aureus* ont été modélisées par homologie à l'aide du serveur tRosetta (Yang et al., 2020). L'alignement sur les modèles est amélioré par la réalisation d'alignement de séquence multiples (MSA : Multiple Sequence Alignment) utilisant les 1500 séquences disponibles pour chacune des deux protéines. Elles ont toutes deux été estimées comme étant de très haute confiance, avec des TM scores estimés de 0,91 pour QueE et 0,849 pour QueF. Le TM-score est une mesure permettant d'évaluer la similarité topologique des structures de protéines. Les valeurs de TM-score se situent entre 0 et 1, où 1 indique une parfaite correspondance entre deux structures. Les structures utilisées pour modéliser QueE sont les fichiers pdb 5TH5 (*B. subtilis*), 6NHL (*E. coli*), 4NJJ et 4NJH (*Burkholderia multivorans*). Celles utilisées pour modeliser QueF sont les fichiers pdb 4FGC, 4F8B et 5UDG (*B. subtilis*), 3S19 et 3UXJ (*Vibrio cholerae*).

### 10. Ribosome profiling à haute résolution

Les bactéries sont cultivées comme décrit précédemment. Les cultures (30 mL) sont congelées directement dans l'azote liquide avec le tampon de lyse (20mM Tris, HCl pH8 ; 150mM $MgCl_2$ ; 100 mM $NH_4Cl$ ; 5 mM $CaCl_2$ ; 0,1% NP40 ; 0,4%triton X100 ; 100 U de DNaseI/mL de culture). Les billes de cellules congelées sont ensuite lysées au Fastprep 5 x 40s à vitesse maximale en présence de billes en acier. Les lysats sont ensuite décongelés 1 h à température ambiante et directement centrifugés 20 min à 3750 rpm, 4°C. Le surnageant est clarifié par une deuxième centrifugation, à 8000rpm, 4°C pendant 20 min avant d'être

déposé sur 4mL de coussin de sucrose (20 mM Tris HCl, pH8 ; 10 mM $MgCl_2$ ; 0.5 M $NH_4Cl$ ; 0,5 mM EDTA ; 1,1M sucrose), puis ultracentrifugé 45000 rpm, 4°C, 3h30. Le culot est repris dans un tampon de resuspension (20 mM Tris HCl pH8 ; 10 mM $MgCl_2$ ; 5 mM $CaCl_2$ ; 0,1% NP40, 0,4% triton X100 ; 1 mM chloramphénicol) avant la digestion, ici à la MNase : 25 mM $CaCl_2$ ; 1000U MNase ; incubation à 25°C, 1 h, 1400 rpm. La digestion est arrêtée par l'ajout d'EGTA puis l'échantillon est déposé sur gradient de sucrose (5-50% ; 20 mM Tris, HCL pH7,5 ; 100mM $NH_4Cl$ ; 10 mM $MgCl_2$ ; 1mM DTT) et ultracentrifugé à 39000 rpm 4°C pendant 2h46. Les ribosomes 70S sont récupérés, les ARN sont extraits par phénol chaud, précipités puis déposés sur gel de polyacrylamide afin de purifier sur gel les fragments correspondant à une taille d'environ 28 nt et les séquencer. En parallèle, une partie de la culture est gardée pour réaliser l'analyse transcriptomique. Le traitement informatique des données de séquençage est réalisé en collaboration avec Béatrice Chane-Woon-Ming suivant la pipeline développée par Mohammad en 2019 (Mohammad and Buskirk, 2019).

# Références bibliographiques


Andersson, D.I. and Hughes, D. (2014) Microbiological effects of sublethal levels of antibiotics. *Nat Rev Microbiol* **12**: 465–478.

Antoine, L. and Wolff, P. (2020) Mapping of Posttranscriptional tRNA Modifications by Two-Dimensional Gel Electrophoresis Mass Spectrometry. *Methods Mol Biol Clifton NJ* **2113**: 101–110.

Antoine, L., Wolff, P., Westhof, E., Romby, P., and Marzi, S. (2019) Mapping post-transcriptional modifications in Staphylococcus aureus tRNAs by nanoLC/MSMS. *Biochimie* **164**: 60–69.

Arciola, C.R., Campoccia, D., Ravaioli, S., and Montanaro, L. (2015) Polysaccharide intercellular adhesin in biofilm: structural and regulatory aspects. *Front Cell Infect Microbiol* **5**:.

Ayadi, L., Motorin, Y., and Marchand, V. (2018) Quantification of 2'-O-Me Residues in RNA Using Next-Generation Sequencing (Illumina RiboMethSeq Protocol). *Methods Mol Biol Clifton NJ* **1649**: 29–48.

Barraud, P., Gato, A., Heiss, M., Catala, M., Kellner, S., and Tisné, C. (2019) Time-resolved NMR monitoring of tRNA maturation. *Nat Commun* **10**: 3373.

Beaber, J.W., Hochhut, B., and Waldor, M.K. (2004) SOS response promotes horizontal dissemination of antibiotic resistance genes. *Nature* **427**: 72–74.

Beasley, F.C., Vinés, E.D., Grigg, J.C., Zheng, Q., Liu, S., Lajoie, G.A., et al. (2009) Characterization of staphyloferrin A biosynthetic and transport mutants in Staphylococcus aureus. *Mol Microbiol* **72**: 947–963.

Berube, B.J. and Wardenburg, J.B. (2013) Staphylococcus aureus α-Toxin: Nearly a Century of Intrigue. *Toxins* **5**: 1140–1166.

Bisognano, C., Kelley, W.L., Estoppey, T., Francois, P., Schrenzel, J., Li, D., et al. (2004) A RecA-LexA-dependent Pathway Mediates Ciprofloxacin-induced Fibronectin Binding in Staphylococcus aureus*. *J Biol Chem* **279**: 9064–9071.

Bojer, M.S., Lindemose, S., Vestergaard, M., and Ingmer, H. (2018) Quorum Sensing-Regulated Phenol-Soluble Modulins Limit Persister Cell Populations in Staphylococcus aureus. *Front Microbiol* **9**: 255.

Bose, J.L., Fey, P.D., and Bayles, K.W. (2013) Genetic tools to enhance the study of gene function and regulation in Staphylococcus aureus. *Appl Environ Microbiol* **79**: 2218–2224.

Butala, M., Zgur-Bertok, D., and Busby, S.J.W. (2009) The bacterial LexA transcriptional repressor. *Cell Mol Life Sci CMLS* **66**: 82–93.

Cadet, J. and Wagner, J.R. (2013) DNA Base Damage by Reactive Oxygen Species, Oxidizing Agents, and UV Radiation. *Cold Spring Harb Perspect Biol* **5**: a012559.

Carnes, E.C., Lopez, D.M., Donegan, N.P., Cheung, A., Gresham, H., Timmins, G.S., and Brinker, C.J. (2010) Confinement-induced quorum sensing of individual Staphylococcus aureus bacteria. *Nat Chem Biol* **6**: 41–45.

Chang, W., Small, D.A., Toghrol, F., and Bentley, W.E. (2006) Global Transcriptome Analysis of Staphylococcus aureus Response to Hydrogen Peroxide. *J Bacteriol* **188**: 1648–1659.

Chen, X., Yin, H., Li, G., Wang, W., Wong, P.K., Zhao, H., and An, T. (2019) Antibiotic-resistance gene transfer in antibiotic-resistance bacteria under different light irradiation: Implications from oxidative stress and gene expression. *Water Res* **149**: 282–291.

Cheung, J., Beasley, F.C., Liu, S., Lajoie, G.A., and Heinrichs, D.E. (2009) Molecular characterization of staphyloferrin B biosynthesis in Staphylococcus aureus. *Mol Microbiol* **74**: 594–608.

Chicher, J., Simonetti, A., Kuhn, L., Schaeffer, L., Hammann, P., Eriani, G., and Martin, F. (2015) Purification of mRNA-programmed translation initiation complexes suitable for mass spectrometry analysis. *PROTEOMICS* **15**: 2417–2425.

Cho, K.H. and Caparon, M.G. (2008) tRNA Modification by GidA/MnmE Is Necessary for Streptococcus pyogenes Virulence: a New Strategy To Make Live Attenuated Strains. *Infect Immun* **76**: 3176–3186.

Cirz, R.T., Jones, M.B., Gingles, N.A., Minogue, T.D., Jarrahi, B., Peterson, S.N., and Romesberg, F.E. (2007) Complete and SOS-mediated response of Staphylococcus aureus to the antibiotic ciprofloxacin. *J Bacteriol* **189**: 531–539.

Clarke, S.R., Wiltshire, M.D., and Foster, S.J. (2004) IsdA of Staphylococcus aureus is a broad spectrum, iron-regulated adhesin. *Mol Microbiol* **51**: 1509–1519.

Clements, M.O., Watson, S.P., and Foster, S.J. (1999) Characterization of the major superoxide dismutase of Staphylococcus aureus and its role in starvation survival, stress resistance, and pathogenicity. *J Bacteriol* **181**: 3898–3903.

Cosgrove, K., Coutts, G., Jonsson, I.-M., Tarkowski, A., Kokai-Kun, J.F., Mond, J.J., and Foster, S.J. (2007) Catalase (KatA) and alkyl hydroperoxide reductase (AhpC) have compensatory roles in peroxide stress resistance and are required for survival, persistence, and nasal colonization in Staphylococcus aureus. *J Bacteriol* **189**: 1025–1035.

de Crécy-Lagard, V., Ross, R.L., Jaroch, M., Marchand, V., Eisenhart, C., Brégeon, D., et al. (2020) Survey and Validation of tRNA Modifications and Their Corresponding Genes in Bacillus subtilis sp Subtilis Strain 168. *Biomolecules* **10**:.

Davies, M.J. (2016) Protein oxidation and peroxidation. *Biochem J* **473**: 805–825.

Davies, M.J. (2005) The oxidative environment and protein damage. *Biochim Biophys Acta BBA - Proteins Proteomics* **1703**: 93–109.

Dean, R.T., Fu, S., Stocker, R., and Davies, M.J. (1997) Biochemistry and pathology of radical-mediated protein oxidation. *Biochem J* **324 ( Pt 1)**: 1–18.

Dowling, D., Miles, Z., Kohrer, C., Maiocco, S., Elliott, S., Bandarian, V., and Drennan, C. (2016) Molecular basis of cobalamin-dependent RNA modification. *Nucleic Acids Res* **44**:.

Dryla, A., Gelbmann, D., von Gabain, A., and Nagy, E. (2003) Identification of a novel iron regulated staphylococcal surface protein with haptoglobin-haemoglobin binding activity. *Mol Microbiol* **49**: 37–53.

Eidhin, D.N., Perkins, S., Francois, P., Vaudaux, P., Höök, M., and Foster, T.J. (1998) Clumping factor B (ClfB), a new surface-located fibrinogen-binding adhesin of Staphylococcus aureus. *Mol Microbiol* **30**: 245–257.

Elmwall, J., Kwiecinski, J., Na, M., Ali, A.A., Osla, V., Shaw, L.N., et al. (2017) Galectin-3 Is a Target for Proteases Involved in the Virulence of Staphylococcus aureus. *Infect Immun* **85**:.

Eltzschig, H.K. and Carmeliet, P. (2011) Hypoxia and inflammation. *N Engl J Med* **364**: 656–665.

Falugi, F., Kim, H.K., Missiakas, D.M., and Schneewind, O. (2013) Role of Protein A in the Evasion of Host Adaptive Immune Responses by Staphylococcus aureus. *mBio* **4**:.

Fang, F.C. (2004) Antimicrobial reactive oxygen and nitrogen species: concepts and controversies. *Nat Rev Microbiol* **2**: 820–832.

Fedtke, I., Kamps, A., Krismer, B., and Götz, F. (2002) The nitrate reductase and nitrite reductase operons and the narT gene of Staphylococcus carnosus are positively controlled by the novel two-component system NreBC. *J Bacteriol* **184**: 6624–6634.

Fey, P.D., Endres, J.L., Yajjala, V.K., Widhelm, T.J., Boissy, R.J., Bose, J.L., and Bayles, K.W. (2013) A Genetic Resource for Rapid and Comprehensive Phenotype Screening of Nonessential Staphylococcus aureus Genes. *mBio* **4**: e00537-12.

Galvanin, A., Vogt, L.-M., Grober, A., Freund, I., Ayadi, L., Bourguignon-Igel, V., et al. (2020) Bacterial tRNA 2'-O-methylation is dynamically regulated under stress conditions and modulates innate immune response. *Nucleic Acids Res* **48**: 12833–12844.

Garcia, Y.M., Barwinska-Sendra, A., Tarrant, E., Skaar, E.P., Waldron, K.J., and Kehl-Fie, T.E. (2017) A Superoxide Dismutase Capable of Functioning with Iron or Manganese Promotes the Resistance of Staphylococcus aureus to Calprotectin and Nutritional Immunity. *PLoS Pathog* **13**:.

Giannouli, S., Kyritsis, A., Malissovas, N., Becker, H.D., and Stathopoulos, C. (2009) On the role of an unusual tRNAGly isoacceptor in Staphylococcus aureus. *Biochimie* **91**: 344–351.

Golubev, A., Fatkhullin, B., Khusainov, I., Jenner, L., Gabdulkhakov, A., Validov, S., et al. (2020) Cryo-EM structure of the ribosome functional complex of the human pathogen Staphylococcus aureus at 3.2 Å resolution. *FEBS Lett* **594**: 3551–3567.

Gordienko, I. and Rupp, W.D. (1997) UvrAB activity at a damaged DNA site: is unpaired DNA present? *EMBO J* **16**: 880–888.

Grimaud, R., Ezraty, B., Mitchell, J.K., Lafitte, D., Briand, C., Derrick, P.J., and Barras, F. (2001) Repair of oxidized proteins. Identification of a new methionine sulfoxide reductase. *J Biol Chem* **276**: 48915–48920.

Ha, K.P., Clarke, R.S., Kim, G.-L., Brittan, J.L., Rowley, J.E., Mavridou, D.A.I., et al. (2020a) Staphylococcal DNA Repair Is Required for Infection. *mBio* **11**:.

Hamill, R.J., Vann, J.M., and Proctor, R.A. (1986) Phagocytosis of Staphylococcus aureus by cultured bovine aortic endothelial cells: model for postadherence events in endovascular infections. *Infect Immun* **54**: 833–836.

Hassan, H.M. (1984) Exacerbation of superoxide radical formation by paraquat. *Methods Enzymol* **105**: 523–532.

Heilmann, C., Niemann, S., Sinha, B., Herrmann, M., Kehrel, B.E., and Peters, G. (2004) Staphylococcus aureus fibronectin-binding protein (FnBP)-mediated adherence to platelets, and aggregation of platelets induced by FnBPA but not by FnBPB. *J Infect Dis* **190**: 321–329.

Helm, M. and Motorin, Y. (2017) Detecting RNA modifications in the epitranscriptome: predict and validate. *Nat Rev Genet* **18**: 275–291.

Herbert, S., Ziebandt, A.-K., Ohlsen, K., Schäfer, T., Hecker, M., Albrecht, D., et al. (2010) Repair of global regulators in Staphylococcus aureus 8325 and comparative analysis with other clinical isolates. *Infect Immun* **78**: 2877–2889.

Igloi, G.L. and Kössel, H. (1985) Affinity electrophoresis for monitoring terminal phosphorylation and the presence of queuosine in RNA. Application of polyacrylamide containing a covalently bound boronic acid. *Nucleic Acids Res* **13**: 6881–6898.

Imlay, J.A. (2006) Iron-sulphur clusters and the problem with oxygen. *Mol Microbiol* **59**: 1073–1082.

Jarry, T.M., Memmi, G., and Cheung, A.L. (2008) The expression of alpha-haemolysin is required for Staphylococcus aureus phagosomal escape after internalization in CFT-1 cells. *Cell Microbiol* **10**: 1801–1814.

Jutkina, J., Rutgersson, C., Flach, C.-F., and Joakim Larsson, D.G. (2016) An assay for determining minimal concentrations of antibiotics that drive horizontal transfer of resistance. *Sci Total Environ* **548–549**: 131–138.

Karavolos, M.H., Horsburgh, M.J., Ingham, E., and Foster, S.J. (2003) Role and regulation of the superoxide dismutases of Staphylococcus aureus. *Microbiol Read Engl* **149**: 2749–2758.

Kellner, S., Neumann, J., Rosenkranz, D., Lebedeva, S., Ketting, R.F., Zischler, H., et al. (2014) Profiling of RNA modifications by multiplexed stable isotope labelling. *Chem Commun Camb Engl* **50**: 3516–3518.

Kellner, S., Ochel, A., Thüring, K., Spenkuch, F., Neumann, J., Sharma, S., et al. (2014) Absolute and relative quantification of RNA modifications via biosynthetic isotopomers. *Nucleic Acids Res* **42**: e142.

Keyer, K. and Imlay, J.A. (1996) Superoxide accelerates DNA damage by elevating free-iron levels. *Proc Natl Acad Sci U S A* **93**: 13635–13640.

Koh, C.S. and Sarin, L.P. (2018) Transfer RNA modification and infection – Implications for pathogenicity and host responses. *Biochim Biophys Acta BBA - Gene Regul Mech* **1861**: 419–432.

Lalaouna, D., Desgranges, E., Caldelari, I., and Marzi, S. (2018) Chapter Sixteen - MS2-Affinity Purification Coupled With RNA Sequencing Approach in the Human Pathogen Staphylococcus aureus. In *Methods in Enzymology*. High-Density

Sequencing Applications in Microbial Molecular Genetics. Carpousis, A.J. (ed). Academic Press, pp. 393–411.

Lechner, A., Wolff, P., Leize-Wagner, E., and François, Y.-N. (2020) Characterization of Post-Transcriptional RNA Modifications by Sheathless Capillary Electrophoresis-High Resolution Mass Spectrometry. *Anal Chem* **92**: 7363–7370.

Leiva, L.E., Pincheira, A., Elgamal, S., Kienast, S.D., Bravo, V., Leufken, J., et al. (2020) Modulation of Escherichia coli Translation by the Specific Inactivation of tRNAGly Under Oxidative Stress. *Front Genet* **11**:.

Liu, G.Y., Essex, A., Buchanan, J.T., Datta, V., Hoffman, H.M., Bastian, J.F., et al. (2005) Staphylococcus aureus golden pigment impairs neutrophil killing and promotes virulence through its antioxidant activity. *J Exp Med* **202**: 209–215.

Liu, M., Tanaka, W.N., Zhu, H., Xie, G., Dooley, D.M., and Lei, B. (2008) Direct hemin transfer from IsdA to IsdC in the iron-regulated surface determinant (Isd) heme acquisition system of Staphylococcus aureus. *J Biol Chem* **283**: 6668–6676.

Lowy, F.D. (1998) Staphylococcus aureus Infections. *N Engl J Med* **339**: 520–532.

Luong, T.T. and Lee, C.Y. (2002) Overproduction of Type 8 Capsular Polysaccharide Augments Staphylococcus aureus Virulence. *Infect Immun* **70**: 3389–3395.

Maiques, E., Ubeda, C., Campoy, S., Salvador, N., Lasa, I., Novick, R.P., et al. (2006) beta-lactam antibiotics induce the SOS response and horizontal transfer of virulence factors in Staphylococcus aureus. *J Bacteriol* **188**: 2726–2729.

Marchand, V., Ayadi, L., Ernst, F.G.M., Hertler, J., Bourguignon-Igel, V., Galvanin, A., et al. (2018) AlkAniline-Seq: Profiling of m7 G and m3 C RNA Modifications at Single Nucleotide Resolution. *Angew Chem Int Ed Engl* **57**: 16785–16790.

Marchand, V., Blanloeil-Oillo, F., Helm, M., and Motorin, Y. (2016) Illumina-based RiboMethSeq approach for mapping of 2'-O-Me residues in RNA. *Nucleic Acids Res* **44**: e135.

Marchand, V., Pichot, F., Neybecker, P., Ayadi, L., Bourguignon-Igel, V., Wacheul, L., et al. (2020) HydraPsiSeq: a method for systematic and quantitative mapping of pseudouridines in RNA. *Nucleic Acids Res* **48**: e110.

Maslowska, K.H., Makiela-Dzbenska, K., and Fijalkowska, I.J. (2019) The SOS system: A complex and tightly regulated response to DNA damage. *Environ Mol Mutagen* **60**: 368–384.

Matuszek, Z. and Pan, T. (2019) Quantification of Queuosine Modification Levels in tRNA from Human Cells Using APB Gel and Northern Blot. *Bio-Protoc* **9**: e3191–e3191.

McCarty, R.M., Krebs, C., and Bandarian, V. (2013) Spectroscopic, steady-state kinetic, and mechanistic characterization of the radical SAM enzyme QueE, which catalyzes a complex cyclization reaction in the biosynthesis of 7-deazapurines. *Biochemistry* **52**: 188–198.

Mengel-Jørgensen, J. and Kirpekar, F. (2002) Detection of pseudouridine and other modifications in tRNA by cyanoethylation and MALDI mass spectrometry. *Nucleic Acids Res* **30**: e135.

Mohammad, F. and Buskirk, A.R. (2019) Protocol for Ribosome Profiling in Bacteria. *Bio-Protoc* **9**: e3468.

Mohammad, F., Green, R., and Buskirk, A.R. (2019) A systematically-revised ribosome profiling method for bacteria reveals pauses at single-codon resolution. *eLife* **8**: e42591.

Motorin, Y. and Helm, M. (2019) Methods for RNA Modification Mapping Using Deep Sequencing: Established and New Emerging Technologies. *Genes* **10**: 35.

Motorin, Y., Muller, S., Behm-Ansmant, I., and Branlant, C. (2007) Identification of modified residues in RNAs by reverse transcription-based methods. *Methods Enzymol* **425**: 21–53.

Müller, M., Legrand, C., Tuorto, F., Kelly, V.P., Atlasi, Y., Lyko, F., and Ehrenhofer-Murray, A.E. (2019) Queuine links translational control in eukaryotes to a micronutrient from bacteria. *Nucleic Acids Res* **47**: 3711–3727.

Muryoi, N., Tiedemann, M.T., Pluym, M., Cheung, J., Heinrichs, D.E., and Stillman, M.J. (2008) Demonstration of the Iron-regulated Surface Determinant (Isd) Heme Transfer Pathway in Staphylococcus aureus. *J Biol Chem* **283**: 28125–28136.

Nakatsuji, T., Chiang, H.-I., Jiang, S.B., Nagarajan, H., Zengler, K., and Gallo, R.L. (2013) The microbiome extends to subepidermal compartments of normal skin. *Nat Commun* **4**: 1431.

Nilkens, S., Koch-Singenstreu, M., Niemann, V., Götz, F., Stehle, T., and Unden, G. (2014) Nitrate/oxygen co-sensing by an NreA/NreB sensor complex of Staphylococcus carnosus. *Mol Microbiol* **91**: 381–393.

Oh, J., Byrd, A.L., Park, M., Kong, H.H., and Segre, J.A. (2016) Temporal Stability of the Human Skin Microbiome. *Cell* **165**: 854–866.

Otto, M. (2018) Staphylococcal Biofilms. *Microbiol Spectr* **6**:.

Park, R.-Y., Sun, H.-Y., Choi, M.-H., Bai, Y.-H., and Shin, S.-H. (2005) Staphylococcus aureus siderophore-mediated iron-acquisition system plays a dominant and essential role in the utilization of transferrin-bound iron. *J Microbiol Seoul Korea* **43**: 183–190.

Periasamy, S., Chatterjee, S.S., Cheung, G.Y.C., and Otto, M. (2012) Phenol-soluble modulins in staphylococci. *Commun Integr Biol* **5**: 275–277.

Pidwill, G.R., Gibson, J.F., Cole, J., Renshaw, S.A., and Foster, S.J. (2021) The Role of Macrophages in Staphylococcus aureus Infection. *Front Immunol* **11**: 620339.

Podlesek, Z. and Žgur Bertok, D. (2020) The DNA Damage Inducible SOS Response Is a Key Player in the Generation of Bacterial Persister Cells and Population Wide Tolerance. *Front Microbiol* **11**:.

Postma, B., Poppelier, M.J., van Galen, J.C., Prossnitz, E.R., van Strijp, J.A.G., de Haas, C.J.C., and van Kessel, K.P.M. (2004) Chemotaxis inhibitory protein of Staphylococcus aureus binds specifically to the C5a and formylated peptide receptor. *J Immunol Baltim Md 1950* **172**: 6994–7001.

Puri, P., Wetzel, C., Saffert, P., Gaston, K.W., Russell, S.P., Cordero Varela, J.A., et al. (2014) Systematic identification of tRNAome and its dynamics in Lactococcus lactis. *Mol Microbiol* **93**: 944–956.

Puri, P., Wetzel, C., Saffert, P., W.Gaston, K., Russell, S.P., Varela, J.A.C., et al. (2014) Systematic identification of tRNAome and its dynamics in Lactococcus lactis. *Mol Microbiol* **93**: 944–956.

Reniere, M.L., Ukpabi, G.N., Harry, S.R., Stec, D.F., Krull, R., Wright, D.W., et al. (2010) The IsdG-family of haem oxygenases degrades haem to a novel chromophore. *Mol Microbiol* **75**: 1529–1538.

Rietmeyer, L., Fix-Boulier, N., Le Fournis, C., Iannazzo, L., Kitoun, C., Patin, D., et al. (2021) Partition of tRNAGly isoacceptors between protein and cell-wall peptidoglycan synthesis in Staphylococcus aureus. *Nucleic Acids Res* **49**: 684–699.

Rooijakkers, S.H.M., Ruyken, M., Roon, J.V., Kessel, K.P.M.V., Strijp, J.A.G.V., and Wamel, W.J.B.V. (2006) Early expression of SCIN and CHIPS drives instant immune evasion by Staphylococcus aureus. *Cell Microbiol* **8**: 1282–1293.

Rozov, A., Demeshkina, N., Khusainov, I., Westhof, E., Yusupov, M., and Yusupova, G. (2016) Novel base-pairing interactions at the tRNA wobble position crucial for accurate reading of the genetic code. *Nat Commun* **7**: 10457.

Seier-Petersen, M.A., Jasni, A., Aarestrup, F.M., Vigre, H., Mullany, P., Roberts, A.P., and Agersø, Y. (2014) Effect of subinhibitory concentrations of four commonly used

biocides on the conjugative transfer of Tn916 in Bacillus subtilis. *J Antimicrob Chemother* **69**: 343–348.

Sendi, P. and Proctor, R.A. (2009) Staphylococcus aureus as an intracellular pathogen: the role of small colony variants. *Trends Microbiol* **17**: 54–58.

Shaw, L., Golonka, E., Potempa, J., and Foster, S.J. (2004) The role and regulation of the extracellular proteases of Staphylococcus aureus. *Microbiol Read Engl* **150**: 217–228.

Skaar, E.P., Gaspar, A.H., and Schneewind, O. (2004) IsdG and IsdI, heme-degrading enzymes in the cytoplasm of Staphylococcus aureus. *J Biol Chem* **279**: 436–443.

Smagur, J., Guzik, K., Bzowska, M., Kuzak, M., Zarebski, M., Kantyka, T., et al. (2009) Staphylococcal cysteine protease staphopain B (SspB) induces rapid engulfment of human neutrophils and monocytes by macrophages. *Biol Chem* **390**: 361–371.

Soong, G., Paulino, F., Wachtel, S., Parker, D., Wickersham, M., Zhang, D., et al. (2015) Methicillin-resistant Staphylococcus aureus adaptation to human keratinocytes. *mBio* **6**: e00289-15.

Spaan, A.N., van Strijp, J.A.G., and Torres, V.J. (2017) Leukocidins: Staphylococcal bi-component pore-forming toxins find their receptors. *Nat Rev Microbiol* **15**: 435–447.

Stanczak-Mrozek, K.I., Manne, A., Knight, G.M., Gould, K., Witney, A.A., and Lindsay, J.A. (2015) Within-host diversity of MRSA antimicrobial resistances. *J Antimicrob Chemother* **70**: 2191–2198.

Stojković, V., Noda-Garcia, L., Tawfik, D.S., and Fujimori, D.G. (2016) Antibiotic resistance evolved via inactivation of a ribosomal RNA methylating enzyme. *Nucleic Acids Res* **44**: 8897–8907.

Surewaard, B.G.J., de Haas, C.J.C., Vervoort, F., Rigby, K.M., DeLeo, F.R., Otto, M., et al. (2013) Staphylococcal alpha-phenol soluble modulins contribute to neutrophil lysis after phagocytosis. *Cell Microbiol* **15**: 1427–1437.

Syed, A.K., Reed, T.J., Clark, K.L., Boles, B.R., and Kahlenberg, J.M. (2015) Staphlyococcus aureus Phenol-Soluble Modulins Stimulate the Release of Proinflammatory Cytokines from Keratinocytes and Are Required for Induction of Skin Inflammation. *Infect Immun* **83**: 3428–3437.

Tenover, F.C. and Goering, R.V. (2009) Methicillin-resistant Staphylococcus aureus strain USA300: origin and epidemiology. *J Antimicrob Chemother* **64**: 441–446.

Torres, V.J., Pishchany, G., Humayun, M., Schneewind, O., and Skaar, E.P. (2006) Staphylococcus aureus IsdB is a hemoglobin receptor required for heme iron utilization. *J Bacteriol* **188**: 8421–8429.

Treffon, J., Chaves-Moreno, D., Niemann, S., Pieper, D.H., Vogl, T., Roth, J., and Kahl, B.C. (2020) Importance of superoxide dismutases A and M for protection of Staphylococcus aureus in the oxidative stressful environment of cystic fibrosis airways. *Cell Microbiol* **22**: e13158.

Tuorto, F., Legrand, C., Cirzi, C., Federico, G., Liebers, R., Müller, M., et al. (2018) Queuosine-modified tRNAs confer nutritional control of protein translation. *EMBO J* **37**: e99777.

Vold, B. (1976) Modified nucleosides of Bacillus subtilis transfer ribonucleic acids. *J Bacteriol* **127**: 258–267.

Wang, B. and Muir, T.W. (2016) Regulation of virulence in Staphylococcus aureus: molecular mechanisms and remaining puzzles. *Cell Chem Biol* **23**: 214–224.

Wertheim, H.F.L., Melles, D.C., Vos, M.C., van Leeuwen, W., van Belkum, A., Verbrugh, H.A., and Nouwen, J.L. (2005) The role of nasal carriage in Staphylococcus aureus infections. *Lancet Infect Dis* **5**: 751–762.

Wolff, P., Villette, C., Zumsteg, J., Heintz, D., Antoine, L., Chane-Woon-Ming, B., et al. (2020) Comparative patterns of modified nucleotides in individual tRNA species from a mesophilic and two thermophilic archaea. *RNA* **26**: 1957–1975.

Xia, G. and Wolz, C. (2014) Phages of Staphylococcus aureus and their impact on host evolution. *Infect Genet Evol J Mol Epidemiol Evol Genet Infect Dis* **21**: 593–601.

Yang, J., Anishchenko, I., Park, H., Peng, Z., Ovchinnikov, S., and Baker, D. (2020) Improved protein structure prediction using predicted interresidue orientations. *Proc Natl Acad Sci U S A* **117**: 1496–1503.

Yokogawa, T., Kitamura, Y., Nakamura, D., Ohno, S., and Nishikawa, K. (2010) Optimization of the hybridization-based method for purification of thermostable tRNAs in the presence of tetraalkylammonium salts. *Nucleic Acids Res* **38**: e89–e89.

Young, B.C., Wu, C.-H., Gordon, N.C., Cole, K., Price, J.R., Liu, E., et al. (2017) Severe infections emerge from commensal bacteria by adaptive evolution. *eLife* **6**: e30637.

Zallot, R., Ross, R., Chen, W.-H., Bruner, S.D., Limbach, P.A., and de Crécy-Lagard, V. (2017) Identification of a Novel Epoxyqueuosine Reductase Family by Comparative Genomics. *ACS Chem Biol* **12**: 844–851.

Zhong, J., Xiao, C., Gu, W., Du, G., Sun, X., He, Q.-Y., and Zhang, G. (2015) Transfer RNAs Mediate the Rapid Adaptation of Escherichia coli to Oxidative Stress. *PLoS Genet* **11**:.

Zhu, H., Xie, G., Liu, M., Olson, J.S., Fabian, M., Dooley, D.M., and Lei, B. (2008) Pathway for heme uptake from human methemoglobin by the iron-regulated surface determinants system of Staphylococcus aureus. *J Biol Chem* **283**: 18450–18460.

# Annexes

**Annexe 1 : Tableau de la transcription différentielle durant le stress oxydant**

Seuls les adjp<0,05 ont été conservés

**UP regulated genes from the differencial transcriptomics analysis in oxidative stress**

| id | gene | product | locus_tag_NCTC8325 | gene_NCTC8325 | log2FoldChange | padj |
|---|---|---|---|---|---|---|
| HG001_01893 | - | single-strand DNA-binding protein, phage | SAOUHSC_02071 | - | 5,424 | 2,51E-104 |
| HG001_01054 | carB | Carbamoyl-phosphate synthase large chain | SAOUHSC_01170 | carB | 5,412 | 9,50E-104 |
| HG001_01052 | pyrC | Dihydroorotase | SAOUHSC_01168 | pyrC | 5,305 | 1,73E-65 |
| HG001_01894 | - | Phage protein | SAOUHSC_02072 | - | 5,302 | 3,29E-106 |
| HG001_01055 | pyrF | Orotidine 5'-phosphate decarboxylase | SAOUHSC_01171 | - | 5,29 | 3,09E-126 |
| HG001_01053 | carA | Carbamoyl-phosphate synthase small chain | SAOUHSC_01169 | - | 5,282 | 6,93E-63 |
| HG001_01903 | - | Putative phage protein | SAOUHSC_02081 | - | 5,257 | 6,13E-84 |
| HG001_01051 | pyrB | Aspartate carbamoyltransferase | SAOUHSC_01166 | pyrB | 5,174 | 1,60E-52 |
| HG001_01904 | - | Putative phage regulatory protein | SAOUHSC_02083 | - | 5,132 | 1,51E-76 |
| HG001_01891 | - | Putative phage replication protein | SAOUHSC_02069 | - | 5,128 | 7,84E-104 |
| HG001_01895 | - | Bacteriophage Mu Gam like protein | SAOUHSC_02073 | - | 5,122 | 1,86E-101 |
| HG001_01898 | - | Phage protein | SAOUHSC_02076 | - | 5,035 | 5,50E-64 |
| HG001_01902 | - | Phage antirepressor protein KilAC domain protein | SAOUHSC_02080 | - | 5,024 | 1,44E-91 |
| HG001_01887 | - | Phage protein | SAOUHSC_02065 | - | 5,004 | 2,05E-91 |
| HG001_01885 | - | Phage protein | SAOUHSC_02063 | - | 4,979 | 1,29E-122 |
| HG001_01888 | - | Putative phage protein | SAOUHSC_02066 | - | 4,979 | 1,64E-111 |
| HG001_01056 | pyrE | Orotate phosphoribosyltransferase | SAOUHSC_01172 | pyrE | 4,966 | 1,35E-105 |
| HG001_01886 | - | Phage protein | SAOUHSC_02064 | - | 4,939 | 3,02E-104 |
| HG001_01889 | dnaC_2 | Replicative DNA helicase | SAOUHSC_02067 | - | 4,923 | 1,18E-111 |
| HG001_01884 | - | Putative phage regulatory protein; Helix-turn-helix domain protein | SAOUHSC_02062 | - | 4,889 | 3,62E-92 |
| HG001_01883 | - | Phage protein; PVL ORF-50-like family protein | SAOUHSC_02061 | - | 4,886 | 5,90E-94 |
| HG001_01900 | - | Phage protein | SAOUHSC_02078 | - | 4,885 | 1,40E-93 |
| HG001_01890 | - | Phage protein | SAOUHSC_02068 | - | 4,868 | 6,99E-99 |
| HG001_02016 | - | Phage protein | SAOUHSC_02213 | - | 4,856 | 5,76E-99 |
| HG001_01896 | - | Phage protein | SAOUHSC_02074 | - | 4,833 | 1,20E-88 |
| HG001_01901 | - | Putative phage protein | SAOUHSC_02079 | - | 4,811 | 2,42E-107 |
| HG001_01050 | pyrP | Uracil permease | SAOUHSC_01165 | - | 4,807 | 5,14E-46 |
| HG001_01875 | - | Transcriptional activator RinB (phage) | SAOUHSC_02053 | - | 4,754 | 1,21E-118 |
| HG001_01868 | - | Putative phage protein | SAOUHSC_02046 | - | 4,732 | 3,62E-66 |
| HG001_01880 | - | Putative phage protein | SAOUHSC_02058 | - | 4,7 | 1,30E-90 |
| HG001_01881 | - | Phage protein | SAOUHSC_02059 | - | 4,698 | 4,55E-98 |
| HG001_01870 | - | Phage portal protein%2C SPP1 Gp6-like | SAOUHSC_02048 | - | 4,694 | 1,57E-79 |
| HG001_01876 | - | Phage protein | SAOUHSC_02054 | - | 4,677 | 8,91E-80 |
| HG001_01882 | - | Phage protein | SAOUHSC_02060 | - | 4,659 | 8,31E-112 |
| HG001_01869 | - | Phage Mu protein F like protein | SAOUHSC_02047 | - | 4,631 | 3,92E-79 |
| HG001_01899 | - | Phage protein | SAOUHSC_02077 | - | 4,597 | 2,32E-83 |
| HG001_01873 | - | Transcriptional activator, phage-associated | SAOUHSC_02051 | - | 4,538 | 9,07E-91 |
| HG001_01878 | - | Putative phage protein | SAOUHSC_02056 | - | 4,536 | 2,16E-83 |
| HG001_02037 | - | Putative phage regulatory protein | SAOUHSC_02234 | - | 4,486 | 4,16E-70 |
| HG001_02032 | - | Phage protein | SAOUHSC_02228 | - | 4,457 | 4,05E-75 |
| HG001_01874 | - | Phage protein | SAOUHSC_02052 | - | 4,417 | 5,03E-104 |
| HG001_01383 | - | Phage protein | SAOUHSC_01550 | - | 4,412 | 8,41E-68 |
| HG001_02034 | - | AntA/AntB antirepressor | SAOUHSC_02229 | - | 4,402 | 3,05E-86 |
| HG001_02036 | - | Putative phage regulatory protein | SAOUHSC_02233 | - | 4,382 | 3,67E-72 |
| HG001_01877 | - | Phage protein | SAOUHSC_02055 | - | 4,379 | 1,19E-87 |
| HG001_02727 | glpE_3 | Thiosulfate sulfurtransferase GlpE | SAOUHSC_03024 | - | 4,351 | 4,32E-96 |
| HG001_02433 | narH | Respiratory nitrate reductase 1 beta chain | SAOUHSC_02680 | - | 4,276 | 1,58E-52 |
| HG001_02432 | narW | putative nitrate reductase molybdenum cofactor assembly chaperone NarW | SAOUHSC_02679 | - | 4,264 | 4,39E-51 |
| HG001_01897 | - | Phage protein | SAOUHSC_02075 | - | 4,223 | 3,08E-83 |
| HG001_01866 | - | Phage capsid family protein | SAOUHSC_02043 | - | 4,199 | 1,95E-57 |
| HG001_02033 | - | Phage antirepressor protein KilAC domain protein | SAOUHSC_02229 | - | 4,185 | 1,60E-83 |
| HG001_01867 | - | Putative phage head protein | SAOUHSC_02044 | - | 4,145 | 1,63E-61 |
| HG001_01871 | - | Phage terminase large subunit | SAOUHSC_02049 | - | 4,14 | 4,87E-53 |
| HG001_01865 | - | Phage protein | SAOUHSC_02042 | - | 4,118 | 9,34E-51 |
| HG001_01863 | - | Putative phage protein | SAOUHSC_02040 | - | 4,069 | 1,18E-53 |
| HG001_02023 | - | Putative phage nuclease | SAOUHSC_02219 | - | 4,043 | 5,11E-85 |
| HG001_01222 | dinB_1 | DNA polymerase IV | SAOUHSC_01363 | MucB | 4,037 | 1,46E-55 |
| HG001_01858 | - | Phage protein | SAOUHSC_02034 | - | 3,98 | 5,86E-61 |
| HG001_02031 | - | Putative phage protein | SAOUHSC_02227 | - | 3,978 | 1,83E-46 |
| HG001_02029 | - | Phage protein | SAOUHSC_02225 | - | 3,977 | 4,57E-80 |
| HG001_02025 | - | Phage protein | SAOUHSC_02221 | - | 3,951 | 6,11E-88 |
| HG001_01861 | - | Putative phage protein | SAOUHSC_02037 | - | 3,951 | 1,04E-58 |
| HG001_02017 | - | Putative phage protein | SAOUHSC_02214 | - | 3,883 | 2,85E-46 |
| HG001_02028 | - | Phage protein | SAOUHSC_02224 | - | 3,848 | 6,04E-45 |
| HG001_01386 | - | Phage protein; PVL orf 52-like protein; Phage phi 11 orf23 protein homolog | SAOUHSC_01553 | - | 3,847 | 2,70E-63 |
| HG001_02024 | - | Putative phage ssDNA binding protein | SAOUHSC_02220 | - | 3,831 | 7,83E-62 |
| HG001_01860 | - | Phage major tail protein 2 | SAOUHSC_02036 | - | 3,821 | 7,08E-64 |
| HG001_00085 | deoD | Purine nucleoside phosphorylase DeoD-type | SAOUHSC_00097 | - | 3,814 | 5,29E-33 |
| HG001_02026 | - | Putative phage protein | SAOUHSC_02222 | - | 3,813 | 2,07E-65 |
| HG001_02434 | narG | Respiratory nitrate reductase 1 alpha chain | SAOUHSC_02681 | - | 3,796 | 2,96E-40 |
| HG001_01859 | - | Phage protein | SAOUHSC_02035 | - | 3,769 | 1,37E-55 |
| HG001_01862 | - | Phage protein | SAOUHSC_02038 | - | 3,765 | 3,25E-54 |
| HG001_01872 | - | Terminase small subunit | SAOUHSC_02050 | - | 3,652 | 1,14E-36 |
| HG001_00308 | - | HTH-type transcriptional regulator | SAOUHSC_00347 | - | 3,647 | 5,13E-32 |
| HG001_02027 | - | Phage protein | SAOUHSC_02223 | - | 3,634 | 5,40E-53 |
| HG001_01057 | - | hypothetical protein; same operon as pyrP-pyrB-pyrC-carA-carB-pyrF-pyrE | SAOUHSC_01173 | - | 3,505 | 8,10E-45 |

| | | | | | | |
|---|---|---|---|---|---|---|
| HG001_01200 | - | hypothetical protein | SAOUHSC_01334 | - | 3,4 | 1,30E-23 |
| HG001_02435 | nasF | Uroporphyrinogen-III C-methyltransferase | SAOUHSC_02682 | - | 3,396 | 5,44E-37 |
| HG001_02020 | - | Phage protein | SAOUHSC_02217 | - | 3,323 | 8,20E-54 |
| HG001_02436 | nasE | Assimilatory nitrite reductase [NAD(P)H] small subunit | SAOUHSC_02683 | - | 3,321 | 1,65E-29 |
| HG001_01343 | - | Ferredoxin | SAOUHSC_01504 | - | 3,316 | 6,98E-40 |
| HG001_01214 | parC | DNA topoisomerase 4 subunit A | SAOUHSC_01352 | - | 3,261 | 8,08E-45 |
| HG001_02246 | aldC_1 | Alpha-acetolactate decarboxylase | SAOUHSC_02467 | - | 3,236 | 1,69E-21 |
| HG001_02437 | nasD | Nitrite reductase [NAD(P)H] | SAOUHSC_02684 | - | 3,201 | 1,42E-25 |
| HG001_02431 | narX | Nitrate reductase-like protein NarX | SAOUHSC_02678 | - | 3,187 | 3,92E-36 |
| HG001_01911 | queE_2 | 7-carboxy-7-deazaguanine synthase | SAOUHSC_02090 | - | 3,185 | 6,19E-61 |
| HG001_01856 | - | Phage tail protein | SAOUHSC_02031 | - | 3,181 | 1,69E-41 |
| HG001_01857 | - | hypothetical protein | SAOUHSC_02033 | - | 3,18 | 1,86E-38 |
| HG001_01855 | - | Prophage endopeptidase tail | SAOUHSC_02030 | - | 3,152 | 4,30E-43 |
| HG001_02018 | - | hypothetical protein | SAOUHSC_02215 | - | 3,119 | 2,24E-22 |
| HG001_02019 | dnaC_3 | DNA replication protein DnaC | SAOUHSC_02216 | - | 3,094 | 7,15E-45 |
| HG001_00086 | norB_2 | Quinolone resistance protein NorB | SAOUHSC_00099 | - | 3,013 | 7,19E-23 |
| HG001_01521 | der_3 | GTPase Der | SAOUHSC_01700 | - | 3,006 | 2,85E-48 |
| HG001_02629 | pyrD | Dihydroorotate dehydrogenase (quinone) | SAOUHSC_02909 | - | 2,959 | 6,09E-08 |
| HG001_01213 | parE | DNA topoisomerase 4 subunit B | SAOUHSC_01351 | - | 2,931 | 2,91E-45 |
| HG001_00807 | argH1 | Argininosuccinate lyase 1 | SAOUHSC_00898 | - | 2,89 | 2,12E-24 |
| HG001_02429 | nreB | Oxygen sensor histidine kinase NreB | SAOUHSC_02676 | - | 2,863 | 7,06112E-32 |
| HG001_02609 | isaA | putative transglycosylase IsaA precursor | SAOUHSC_02887 | - | 2,863 | 2,63E-30 |
| HG001_01522 | gph_2 | Phosphoglycolate phosphatase | SAOUHSC_01701 | - | 2,849 | 2,29E-45 |
| HG001_01854 | - | hypothetical protein | SAOUHSC_02029 | - | 2,844 | 3,92E-38 |
| HG001_02014 | - | PVL ORF-50-like family protein | SAOUHSC_02211 | - | 2,814 | 1,25E-27 |
| HG001_02166 | dps | General stress protein 20U | SAOUHSC_02381 | - | 2,778 | 1,86E-35 |
| HG001_01384 | - | hypothetical protein | SAOUHSC_01551 | - | 2,772 | 2,91E-22 |
| HG001_02483 | - | UDP-glucose 4-epimerase | SAOUHSC_02737 | - | 2,762 | 8,31E-35 |
| HG001_02015 | - | hypothetical protein | SAOUHSC_02212 | - | 2,76 | 1,41E-24 |
| HG001_01520 | aroE | Shikimate dehydrogenase | SAOUHSC_01699 | - | 2,724 | 3,56E-42 |
| HG001_02669 | clfB | Clumping factor B precursor | SAOUHSC_02963 | - | 2,698 | 6,72E-44 |
| HG001_01206 | sbcC | Nuclease SbcCD subunit C | SAOUHSC_01343 | - | 2,692 | 2,90E-40 |
| HG001_01518 | nadD | putative nicotinate-nucleotide adenylyltransferase | SAOUHSC_01697 | - | 2,659 | 1,10E-38 |
| HG001_02247 | alsS | Acetolactate synthase | SAOUHSC_02468 | - | 2,641 | 1,58E-14 |
| HG001_01250 | yheS_1 | putative ABC transporter ATP-binding protein YheS | SAOUHSC_01392 | - | 2,602 | 3,13E-29 |
| HG001_01519 | yhbY | RNA-binding protein YhbY | SAOUHSC_01698 | - | 2,596 | 2,07E-30 |
| HG001_02438 | shfC (nirR) | Sirohydrochlorin ferrochelatase | SAOUHSC_02685 | - | 2,585 | 3,49591E-19 |
| HG001_00937 | ythB | Putative cytochrome bd menaquinol oxidase subunit II | SAOUHSC_01032 | - | 2,584 | 6,91E-23 |
| HG001_02430 | - | hypothetical protein | SAOUHSC_02677 | - | 2,549 | 5,64788E-26 |
| HG001_00670 | nrdF | Ribonucleoside-diphosphate reductase subunit beta | SAOUHSC_00743 | nrdF | 2,532 | 5,81E-22 |
| HG001_02428 | nreC | Oxygen regulatory protein NreC | SAOUHSC_02675 | - | 2,512 | 1,59E-30 |
| HG001_02340 | hpxO | FAD-dependent urate hydroxylase | SAOUHSC_02579 | - | 2,511 | 2,42E-33 |
| HG001_01853 | - | hypothetical protein | SAOUHSC_02028 | - | 2,508 | 1,17E-27 |
| HG001_02654 | - | anaerobic ribonucleotide reductase-activating protein | SAOUHSC_02941 | - | 2,491 | 2,99E-23 |
| HG001_02108 | - | putative DEAD-box ATP-dependent RNA helicase | SAOUHSC_02316 | - | 2,477 | 6,34E-27 |
| HG001_01682 | bioB_1 | Biotin synthase | SAOUHSC_01877 | - | 2,453 | 3,48E-34 |
| HG001_02013 | - | hypothetical protein | SAOUHSC_02210 | - | 2,441 | 8,25E-18 |
| HG001_02657 | p2d | Precorrin-2 dehydrogenase | SAOUHSC_02945 | - | 2,411 | 1,29E-19 |
| HG001_00491 | azo1 | FMN-dependent NADPH-azoreductase | SAOUHSC_00543 | - | 2,408 | 5,19E-17 |
| HG001_02655 | nrdD | Anaerobic ribonucleoside-triphosphate reductase | SAOUHSC_02942 | - | 2,407 | 8,69E-18 |
| HG001_02154 | pyrG | CTP synthase | SAOUHSC_02368 | pyrG | 2,393 | 8,99E-22 |
| HG001_01107 | rpsB | 30S ribosomal protein S2 | - | - | 2,389 | 2,03E-27 |
| HG001_02006 | - | hypothetical protein | SAOUHSC_02203 | - | 2,385 | 7,01E-22 |
| HG001_00082 | sodM | Superoxide dismutase [Mn/Fe] 2 | SAOUHSC_00093 | - | 2,372 | 1,32E-34 |
| HG001_01850 | - | hypothetical protein | SAOUHSC_02025 | - | 2,354 | 1,71E-19 |
| HG001_01523 | mtnN | 5'-methylthioadenosine/S-adenosylhomocysteine nucleosidase | SAOUHSC_01702 | - | 2,349 | 3,00E-29 |
| HG001_01517 | - | putative nicotinate-nucleotide adenylyltransferase | SAOUHSC_01696 | - | 2,346 | 1,82E-24 |
| HG001_01925 | cobQ | Cobyric acid synthase | SAOUHSC_02106 | - | 2,329 | 1,16E-29 |
| HG001_01852 | - | hypothetical protein | SAOUHSC_02027 | - | 2,308 | 6,85E-22 |
| HG001_01092 | rplS | 50S ribosomal protein L19 | SAOUHSC_01211 | rplS | 2,297 | 5,73E-24 |
| HG001_02041 | xerC_3 | Tyrosine recombinase XerC | SAOUHSC_02239 | - | 2,297 | 9,53E-19 |
| HG001_02042 | hlb_2 | Phospholipase C precursor | - | - | 2,281 | 6,98E-20 |
| HG001_01215 | alsT_2 | Amino-acid carrier protein AlsT | SAOUHSC_01354 | - | 2,273 | 1,10E-25 |
| HG001_00139 | ptsG_1 | PTS system glucose-specific EIICBA component | SAOUHSC_00155 | - | 2,27 | 2,96E-05 |
| HG001_00019 | purA | Adenylosuccinate synthetase | SAOUHSC_00019 | - | 2,259 | 4,52562E-15 |
| HG001_01765 | hemY | Protoporphyrinogen oxidase | SAOUHSC_01960 | - | 2,248 | 1,57E-18 |
| HG001_01766 | hemH | Ferrochelatase | SAOUHSC_01961 | hemH | 2,233 | 2,42E-24 |
| HG001_01941 | - | Trp repressor protein | SAOUHSC_02125 | - | 2,207 | 2,38E-13 |
| HG001_01851 | - | hypothetical protein | SAOUHSC_02026 | - | 2,195 | 1,41E-12 |
| HG001_01137 | recA | Protein RecA | SAOUHSC_01262 | recA | 2,189 | 1,32E-20 |
| HG001_01939 | pcrA | ATP-dependent DNA helicase PcrA | SAOUHSC_02123 | - | 2,184 | 7,32E-27 |
| HG001_02012 | - | YopX protein | SAOUHSC_02209 | - | 2,168 | 1,58E-10 |
| HG001_00951 | ydcV | Inner membrane ABC transporter permease protein YdcV | SAOUHSC_01048 | - | 2,155 | 1,25E-14 |
| HG001_02145 | prfA | Peptide chain release factor 1 | SAOUHSC_02359 | prfA | 2,153 | 1,46E-22 |
| HG001_02424 | narT | putative nitrate transporter NarT | SAOUHSC_02671 | - | 2,148 | 0,000554689 |
| HG001_00808 | argG | Argininosuccinate synthase | SAOUHSC_00899 | - | 2,134 | 7,77E-12 |
| HG001_02005 | - | Transcriptional activator RinB | SAOUHSC_02202 | - | 2,129 | 1,46E-09 |
| HG001_01910 | xerC_2 | Tyrosine recombinase XerC | SAOUHSC_02089 | - | 2,121 | 6,78E-15 |
| HG001_00512 | - | hypothetical protein | SAOUHSC_00567 | - | 2,106 | 2,43E-16 |

| | | | | | |
|---|---|---|---|---|---|
| HG001_00659 | recQ_1 | ATP-dependent DNA helicase RecQ | SAOUHSC_00730 | - | 2,104 | 4,16E-29 |
| HG001_02008 | - | dUTPase | SAOUHSC_02205 | - | 2,103 | 8,88E-15 |
| HG001_02144 | prmC | Release factor glutamine methyltransferase | SAOUHSC_02358 | - | 2,098 | 9,52E-18 |
| HG001_02009 | - | hypothetical protein | SAOUHSC_02206 | - | 2,09 | 9,66E-13 |
| HG001_02004 | - | hypothetical protein | - | - | 2,09 | 1,02E-11 |
| HG001_00002 | dnaN | DNA polymerase III subunit beta | SAOUHSC_00002 | - | 2,088 | 1,57E-20 |
| HG001_02256 | truA | tRNA pseudouridine synthase A | SAOUHSC_02480 | truA | 2,083 | 4,31E-25 |
| HG001_01957 | - | YoID-like protein | SAOUHSC_02144 | - | 2,078 | 2,48E-10 |
| HG001_02123 | sceD | putative transglycosylase SceD precursor | SAOUHSC_02333 | - | 2,071 | 1,77E-15 |
| HG001_02003 | - | hypothetical protein | SAOUHSC_02200 | - | 2,062 | 4,14E-12 |
| HG001_02007 | - | hypothetical protein | SAOUHSC_02204 | - | 2,061 | 3,52E-10 |
| HG001_02658 | cysJ | Sulfite reductase [NADPH] flavoprotein alpha-component | SAOUHSC_02947 | - | 2,056 | 7,70E-15 |
| HG001_02411 | - | hypothetical protein | SAOUHSC_02656 | - | 2,046 | 8,86E-17 |
| HG001_01184 | nucH | Thermonuclease precursor | SAOUHSC_01316 | - | 2,044 | 5,01E-13 |
| HG001_00878 | - | hypothetical protein | SAOUHSC_00964 | - | 2,018 | 1,04E-14 |
| HG001_00959 | typA | GTP-binding protein TypA/BipA | SAOUHSC_01058 | - | 2,012 | 4,82E-20 |
| HG001_00005 | gyrB | DNA gyrase subunit B | SAOUHSC_00005 | - | 2,009 | 9,48E-24 |
| HG001_01938 | ligA | DNA ligase | SAOUHSC_02122 | - | 2,001 | 7,85E-21 |
| HG001_00060 | spa | Immunoglobulin G-binding protein A precursor | SAOUHSC_00069 | - | 1,993 | 1,52E-17 |
| HG001_02155 | rpoE | putative DNA-directed RNA polymerase subunit delta | SAOUHSC_02369 | - | 1,988 | 1,30E-24 |
| HG001_02253 | rpsI | 30S ribosomal protein S9 | SAOUHSC_02477 | rpsI | 1,964 | 2,69E-16 |
| HG001_01574 | mreC | Cell shape-determining protein MreC precursor | SAOUHSC_01759 | - | 1,96 | 2,51E-21 |
| HG001_02750 | rsmG | Ribosomal RNA small subunit methyltransferase G | SAOUHSC_03051 | gidB | 1,959 | 3,77E-16 |
| HG001_01933 | gatB_2 | Aspartyl/glutamyl-tRNA(Asn/Gln) amidotransferase subunit B | SAOUHSC_02116 | gatB | 1,941 | 6,58E-17 |
| HG001_01515 | tylM1 | dTDP-3-amino-3%2C6-dideoxy-alpha-D-glucopyranose N%2CN-dimethyltransferase | SAOUHSC_01694 | - | 1,94 | 4,98E-22 |
| HG001_02090 | - | Protein SprT-like protein | SAOUHSC_02296 | - | 1,936 | 1,20E-17 |
| HG001_02388 | emrB_1 | Multidrug export protein EmrB | SAOUHSC_02629 | - | 1,932 | 6,19E-20 |
| HG001_02751 | mnmG | tRNA uridine 5-carboxymethylaminomethyl modification enzyme MnmG | SAOUHSC_03052 | gidA | 1,927 | 2,97E-16 |
| HG001_00411 | - | hypothetical protein | SAOUHSC_00465 | - | 1,925 | 1,56E-20 |
| HG001_02010 | - | hypothetical protein | SAOUHSC_02207 | - | 1,919 | 2,22E-11 |
| HG001_01203 | - | hypothetical protein | SAOUHSC_01338 | - | 1,913 | 9,09E-14 |
| HG001_01048 | rluD_2 | Ribosomal large subunit pseudouridine synthase D | SAOUHSC_01163 | lspA | 1,91 | 9,54E-20 |
| HG001_01790 | tcyC_1 | L-cystine import ATP-binding protein TcyC | SAOUHSC_01990 | - | 1,898 | 2,77E-15 |
| HG001_01047 | lspA | Lipoprotein signal peptidase | SAOUHSC_01162 | lspA | 1,894 | 3,62E-15 |
| HG001_01995 | - | Phage capsid family protein | SAOUHSC_02191 | - | 1,888 | 2,26E-10 |
| HG001_01560 | apt | Adenine phosphoribosyltransferase | SAOUHSC_01743 | - | 1,886 | 5,58131E-18 |
| HG001_01791 | artQ | Arginine transport system permease protein ArtQ | SAOUHSC_01991 | - | 1,882 | 1,63E-17 |
| HG001_01479 | znuB | High-affinity zinc uptake system membrane protein ZnuB | SAOUHSC_01656 | - | 1,875 | 5,45E-17 |
| HG001_00324 | ahpC | Alkyl hydroperoxide reductase subunit C | SAOUHSC_00365 | - | 1,874 | 1,93E-18 |
| HG001_00067 | sbnC | Staphyloferrin B synthase | SAOUHSC_00077 | - | 1,869 | 5,02E-14 |
| HG001_00008 | hutH | Histidine ammonia-lyase | SAOUHSC_00008 | - | 1,865 | 2,86E-15 |
| HG001_01942 | purB | Adenylosuccinate lyase | SAOUHSC_02126 | - | 1,864 | 6,42238E-15 |
| HG001_00372 | mccB | Cystathionine gamma-lyase | SAOUHSC_00422 | - | 1,855 | 6,45E-15 |
| HG001_02257 | ecfT | Energy-coupling factor transporter transmembrane protein EcfT | SAOUHSC_02481 | - | 1,847 | 2,29E-16 |
| HG001_01992 | - | Phage head-tail joining protein | SAOUHSC_02188 | - | 1,846 | 4,65E-09 |
| HG001_02389 | emrK | putative multidrug resistance protein EmrK | SAOUHSC_02630 | - | 1,843 | 3,22E-19 |
| HG001_01339 | - | Glucosaminate ammonia-lyase | SAOUHSC_01499 | - | 1,842 | 1,57E-12 |
| HG001_02120 | thiD | Hydroxymethylpyrimidine/phosphomethylpyrimidine kinase | SAOUHSC_02330 | - | 1,833 | 1,31E-13 |
| HG001_02453 | - | hypothetical protein | SAOUHSC_02702 | - | 1,832 | 2,04E-10 |
| HG001_00468 | rplA | 50S ribosomal protein L1 | SAOUHSC_00519 | rplA | 1,827 | 6,91E-18 |
| HG001_01070 | stp | Serine/threonine phosphatase stp | SAOUHSC_01186 | - | 1,827 | 1,16E-14 |
| HG001_01573 | - | rod shape-determining protein MreD | SAOUHSC_01758 | - | 1,827 | 1,44E-13 |
| HG001_02754 | rpmH | 50S ribosomal protein L34 | SAOUHSC_03055 | rpmH | 1,826 | 1,87E-12 |
| HG001_01849 | atl_3 | Bifunctional autolysin precursor | SAOUHSC_02023 | - | 1,825 | 4,00E-18 |
| HG001_01571 | - | hypothetical protein | SAOUHSC_01756 | - | 1,817 | 9,94E-15 |
| HG001_00351 | hsdM | Type I restriction enzyme EcoKI M protein | SAOUHSC_00397 | - | 1,813 | 1,39E-14 |
| HG001_01311 | ponA | Penicillin-binding protein 1A/1B | SAOUHSC_01467 | recU | 1,795 | 7,85E-17 |
| HG001_01461 | gcvT | Aminomethyltransferase | SAOUHSC_01634 | gcvT | 1,793 | 1,02E-11 |
| HG001_01481 | nfo | putative endonuclease 4 | SAOUHSC_01658 | - | 1,788 | 2,77E-17 |
| HG001_00323 | ahpF | Alkyl hydroperoxide reductase subunit F | SAOUHSC_00364 | - | 1,785 | 7,15E-17 |
| HG001_00712 | cggR | Central glycolytic genes regulator | SAOUHSC_00794 | - | 1,782 | 2,46E-12 |
| HG001_00363 | yciC_1 | Putative metal chaperone YciC | SAOUHSC_00410 | - | 1,775 | 2,05E-11 |
| HG001_01691 | ribE | Riboflavin synthase | SAOUHSC_01888 | - | 1,773 | 3,31E-09 |
| HG001_02156 | bltD_2 | Spermine/spermidine acetyltransferase | SAOUHSC_02370 | - | 1,769 | 1,48E-12 |
| HG001_02243 | mepM_2 | Murein DD-endopeptidase MepM | SAOUHSC_02464 | - | 1,768 | 1,58E-17 |
| HG001_02282 | rplV | 50S ribosomal protein L22 | SAOUHSC_02507 | rplV | 1,745 | 2,26E-15 |
| HG001_00408 | ycfH | putative deoxyribonuclease YcfH | SAOUHSC_00462 | - | 1,743 | 4,29E-15 |
| HG001_01764 | ydeN | Putative hydrolase YdeN | SAOUHSC_01958 | - | 1,741 | 2,17E-11 |
| HG001_02443 | zinT | Metal-binding protein ZinT precursor | SAOUHSC_02690 | - | 1,737 | 8,57E-19 |
| HG001_02022 | - | hypothetical protein | - | - | 1,734 | 1,56E-06 |
| HG001_01634 | - | hypothetical protein | SAOUHSC_01823 | - | 1,723 | 8,68E-16 |
| HG001_01451 | cfiB_2 | 2-oxoglutarate carboxylase small subunit | SAOUHSC_01623 | - | 1,72 | 2,22E-14 |
| HG001_01934 | gatA | Glutamyl-tRNA(Gln) amidotransferase subunit A | SAOUHSC_02117 | gatA | 1,717 | 4,02E-11 |
| HG001_01142 | korB | 2-oxoglutarate oxidoreductase subunit KorB | SAOUHSC_01267 | - | 1,716 | 3,52E-09 |
| HG001_02352 | yifK | putative transport protein YifK | SAOUHSC_02590 | - | 1,709 | 7,42E-13 |
| HG001_01572 | rplU | 50S ribosomal protein L21 | SAOUHSC_01757 | rplU | 1,701 | 4,01E-16 |
| HG001_01382 | - | Transcriptional activator RinB | SAOUHSC_01549 | - | 1,701 | 2,86E-06 |
| HG001_02586 | pksG | Polyketide biosynthesis 3-hydroxy-3-methylglutaryl-ACP synthase PksG | SAOUHSC_02860 | - | 1,698 | 1,22E-14 |
| HG001_02280 | rplP | 50S ribosomal protein L16 | SAOUHSC_02505 | rplP | 1,696 | 3,18E-13 |

| | | | | | |
|---|---|---|---|---|---|
| HG001_01848 | - | hypothetical protein | SAOUHSC_02022 | - | 1,691 | 1,32E-13 |
| HG001_02446 | bdbD | Disulfide bond formation protein D precursor | SAOUHSC_02694 | - | 1,689 | 7,48E-17 |
| HG001_02420 | gltT | Proton/sodium-glutamate symport protein | SAOUHSC_02667 | - | 1,683 | 1,47E-12 |
| HG001_02287 | rplC | 50S ribosomal protein L3 | SAOUHSC_02512 | rplC | 1,68 | 6,59E-13 |
| HG001_01689 | ribH | 6%2C7-dimethyl-8-ribityllumazine synthase | SAOUHSC_01886 | ribH | 1,678 | 1,28E-09 |
| HG001_02258 | ecfA2 | Energy-coupling factor transporter ATP-binding protein EcfA2 | SAOUHSC_02482 | cbiO | 1,674 | 5,77E-15 |
| HG001_00475 | rplGB | Ribosome-associated protein L7Ae-like protein | SAOUHSC_00526 | - | 1,666 | 1,59E-10 |
| HG001_01846 | - | Bacteriophage holin | SAOUHSC_02020 | - | 1,665 | 5,32E-14 |
| HG001_01478 | zur | Zinc-specific metallo-regulatory protein | SAOUHSC_01655 | - | 1,662 | 5,53E-11 |
| HG001_01926 | murE_2 | UDP-N-acetylmuramoyl-L-alanyl-D-glutamate--2%2C6-diaminopimelate ligase | SAOUHSC_02107 | - | 1,66 | 3,56E-14 |
| HG001_00352 | - | Type I restriction modification DNA specificity domain protein | SAOUHSC_00398 | - | 1,66 | 7,19E-13 |
| HG001_02284 | rplB | 50S ribosomal protein L2 | SAOUHSC_02509 | rplB | 1,654 | 9,54E-14 |
| HG001_02285 | rplW | 50S ribosomal protein L23 | SAOUHSC_02510 | rplW | 1,649 | 7,01E-12 |
| HG001_01831 | - | Putative multidrug export ATP-binding/permease protein | SAOUHSC_02003 | - | 1,646 | 2,97E-16 |
| HG001_00941 | def | Peptide deformylase | SAOUHSC_01038 | def | 1,644 | 8,36E-15 |
| HG001_01535 | yhbU_1 | putative protease YhbU precursor | SAOUHSC_01716 | - | 1,639 | 4,45E-16 |
| HG001_00073 | sbnI | L-serine kinase | SAOUHSC_00083 | - | 1,639 | 9,52E-15 |
| HG001_02283 | rpsS | 30S ribosomal protein S19 | SAOUHSC_02508 | rpsS | 1,639 | 1,08E-13 |
| HG001_02286 | rplD | 50S ribosomal protein L4 | SAOUHSC_02511 | rplD | 1,638 | 1,28E-16 |
| HG001_01096 | sucC | Succinyl-CoA ligase [ADP-forming] subunit beta | SAOUHSC_01216 | sucC | 1,633 | 1,64E-12 |
| HG001_00949 | potA | Spermidine/putrescine import ATP-binding protein PotA | SAOUHSC_01046 | - | 1,63 | 1,16E-07 |
| HG001_02091 | rpsA_2 | 30S ribosomal protein S1 | SAOUHSC_02297 | - | 1,626 | 4,57E-11 |
| HG001_02752 | mnmE | tRNA modification GTPase MnmE | SAOUHSC_03053 | trmE | 1,624 | 2,36E-10 |
| HG001_01690 | ribBA | Riboflavin biosynthesis protein RibBA | SAOUHSC_01887 | - | 1,623 | 4,04E-09 |
| HG001_02635 | panD | Aspartate 1-decarboxylase precursor | SAOUHSC_02916 | - | 1,615 | 2,74E-13 |
| HG001_01337 | cmk | Cytidylate kinase | SAOUHSC_01496 | cmk | 1,612 | 3,25E-11 |
| HG001_01338 | ansA | putative L-asparaginase | SAOUHSC_01497 | - | 1,612 | 4,47E-10 |
| HG001_01631 | ackA | Acetate kinase | SAOUHSC_01820 | - | 1,611 | 8,50E-08 |
| HG001_01564 | tgt | Queuine tRNA-ribosyltransferase | SAOUHSC_01748 | tgt | 1,604 | 8,50E-13 |
| HG001_02652 | gloB_2 | Hydroxyacylglutathione hydrolase | SAOUHSC_02936 | - | 1,602 | 1,24E-10 |
| HG001_01516 | rsfS | Ribosomal silencing factor RsfS | SAOUHSC_01695 | - | 1,601 | 1,58E-15 |
| HG001_00936 | ythA | Putative cytochrome bd menaquinol oxidase subunit I | SAOUHSC_01031 | - | 1,599 | 1,10E-10 |
| HG001_00773 | - | hypothetical protein | SAOUHSC_00862 | - | 1,59 | 1,85E-12 |
| HG001_01683 | rsmH_2 | Ribosomal RNA small subunit methyltransferase H | SAOUHSC_01878 | - | 1,589 | 3,49E-07 |
| HG001_00061 | sarS | HTH-type transcriptional regulator SarS | SAOUHSC_00070 | - | 1,586 | 1,36E-13 |
| HG001_01937 | - | CamS sex pheromone cAM373 precursor | SAOUHSC_02121 | - | 1,573 | 4,16E-12 |
| HG001_00496 | folE2 | GTP cyclohydrolase FolE2 | SAOUHSC_00549 | - | 1,567 | 1,60E-14 |
| HG001_00407 | metG | Methionine--tRNA ligase | SAOUHSC_00461 | - | 1,553 | 1,43E-11 |
| HG001_00467 | rplK | 50S ribosomal protein L11 | SAOUHSC_00518 | rplK | 1,545 | 3,85E-12 |
| HG001_02560 | catE_2 | Catechol-2%2C3-dioxygenase | SAOUHSC_02828 | - | 1,542 | 9,12E-13 |
| HG001_00071 | sbnG | Citrate synthase | SAOUHSC_00081 | - | 1,542 | 1,07E-11 |
| HG001_02279 | rpmC | 50S ribosomal protein L29 | SAOUHSC_02504 | - | 1,541 | 8,58E-15 |
| HG001_00697 | uvrA | UvrABC system protein A | SAOUHSC_00780 | uvrA | 1,54 | 4,12E-15 |
| HG001_01735 | - | EcoKI restriction-modification system protein HsdS | SAOUHSC_01932 | - | 1,538 | 1,51E-11 |
| HG001_00879 | - | CAAX amino terminal protease self- immunity | SAOUHSC_00965 | - | 1,531 | 1,49E-11 |
| HG001_01158 | - | methionine gamma-lyase | SAOUHSC_01284 | - | 1,53 | 1,45E-11 |
| HG001_00469 | - | L10_leader | - | - | 1,525 | 3,10E-11 |
| HG001_02244 | - | putative hydrolase | SAOUHSC_02465 | - | 1,517 | 4,46E-11 |
| HG001_00068 | sbnD | Staphyloferrin B export protein | SAOUHSC_00078 | - | 1,513 | 6,73E-11 |
| HG001_02109 | murF | UDP-N-acetylmuramoyl-tripeptide--D-alanyl-D-alanine ligase | SAOUHSC_02317 | - | 1,513 | 4,28E-10 |
| HG001_02278 | rpsQ | 30S ribosomal protein S17 | SAOUHSC_02503 | rpsQ | 1,509 | 1,53E-11 |
| HG001_02423 | - | Acid shock protein | SAOUHSC_02670 | - | 1,507 | 4,26E-08 |
| HG001_00497 | mshB | 1D-myo-inositol 2-acetamido-2-deoxy-alpha-D-glucopyranoside deacetylase | SAOUHSC_00550 | - | 1,502 | 1,24E-10 |
| HG001_01499 | rpsU | 30S ribosomal protein S21 | SAOUHSC_01678 | rpsU | 1,501 | 4,82E-13 |
| HG001_02255 | - | L13_leader | - | - | 1,496 | 3,25E-09 |
| HG001_02148 | - | hypothetical protein | SAOUHSC_02362 | rho | 1,484 | 3,13E-11 |
| HG001_00867 | prfC | Peptide chain release factor 3 | SAOUHSC_00956 | prfC | 1,483 | 3,26E-10 |
| HG001_02439 | ytmI | putative N-acetyltransferase YtmI | SAOUHSC_02686 | - | 1,482 | 7,31E-09 |
| HG001_01767 | hemE | Uroporphyrinogen decarboxylase | SAOUHSC_01962 | hemE | 1,478 | 5,45E-13 |
| HG001_00072 | sbnH | 2-[(L-alanin-3-ylcarbamoyl)methyl]-2-hydroxybutanedioate decarboxylase | SAOUHSC_00082 | - | 1,477 | 1,97E-12 |
| HG001_00066 | sbnB | N-[(2S)-2-amino-2-carboxyethyl]-L-glutamate dehydrogenase | SAOUHSC_00076 | - | 1,472 | 9,94E-09 |
| HG001_00265 | - | alpha/beta hydrolase fold protein | SAOUHSC_00301 | - | 1,471 | 1,57E-10 |
| HG001_02119 | thiM | Hydroxyethylthiazole kinase | SAOUHSC_02329 | - | 1,471 | 1,52E-07 |
| HG001_01844 | - | putative sapT prophage toxin | SAOUHSC_02018 | - | 1,468 | 1,33E-09 |
| HG001_01792 | - | Phosphotransferase system%2C EIIC | SAOUHSC_01992 | - | 1,457 | 1,70E-10 |
| HG001_01994 | - | hypothetical protein | SAOUHSC_02190 | - | 1,454 | 1,78E-05 |
| HG001_02291 | topB | DNA topoisomerase 3 | SAOUHSC_02517 | - | 1,451 | 3,35E-11 |
| HG001_01905 | immR_1 | HTH-type transcriptional regulator ImmR | SAOUHSC_02084 | - | 1,451 | 2,38E-10 |
| HG001_00069 | sbnE | L-2,3-diaminopropanoate--citrate ligase | SAOUHSC_00079 | - | 1,444 | 3,86E-09 |
| HG001_02288 | rpsJ | 30S ribosomal protein S10 | SAOUHSC_02512a | - | 1,443 | 8,05E-09 |
| HG001_02636 | panC | Pantothenate synthetase | SAOUHSC_02918 | panC | 1,441 | 2,48E-12 |
| HG001_01151 | glpK | Glycerol kinase | SAOUHSC_01276 | glpK | 1,438 | 2,14E-09 |
| HG001_02157 | coaW | Type II pantothenate kinase | SAOUHSC_02371 | - | 1,438 | 9,09E-08 |
| HG001_01071 | prkC | Serine/threonine-protein kinase PrkC | SAOUHSC_01187 | - | 1,431 | 5,41E-10 |
| HG001_01514 | comEA | ComE operon protein 1 | SAOUHSC_01693 | - | 1,43 | 2,04E-08 |
| HG001_01310 | recU | Holliday junction resolvase RecU | SAOUHSC_01466 | recU | 1,426 | 2,34E-09 |
| HG001_00811 | spsB_1 | Signal peptidase IB | SAOUHSC_00902 | - | 1,425 | 2,71E-08 |
| HG001_02277 | rplN | 50S ribosomal protein L14 | SAOUHSC_02502 | rplN | 1,424 | 1,72E-12 |
| HG001_02682 | - | ABC-2 family transporter protein | SAOUHSC_02978 | - | 1,424 | 9,24E-12 |

| | | | | | |
|---|---|---|---|---|---|
| HG001_00819 | - | hypothetical protein | SAOUHSC_00910 | - | 1,422 | 2,89E-12 |
| HG001_01653 | fhs | Formate--tetrahydrofolate ligase | SAOUHSC_01845 | - | 1,419 | 1,14E-09 |
| HG001_01591 | clpX | ATP-dependent Clp protease ATP-binding subunit ClpX | SAOUHSC_01778 | clpX | 1,418 | 4,48E-12 |
| HG001_00197 | tagF | CDP-glycerol:poly(glycerophosphate) glycerophosphotransferase | SAOUHSC_00223 | - | 1,417 | 2,29E-11 |
| HG001_01635 | thiI | putative tRNA sulfurtransferase | SAOUHSC_01824 | - | 1,415 | 1,03E-11 |
| HG001_01482 | cshB | DEAD-box ATP-dependent RNA helicase CshB | SAOUHSC_01659 | - | 1,413 | 2,29E-11 |
| HG001_01736 | - | putative type I restriction enzymeP M protein | SAOUHSC_01933 | - | 1,412 | 3,19E-09 |
| HG001_01091 | trmD | tRNA (guanine-N(1)-)-methyltransferase | SAOUHSC_01210 | trmD | 1,409 | 2,36E-10 |
| HG001_01645 | ptsG_4 | PTS system glucose-specific EIICBA component | SAOUHSC_01836 | - | 1,409 | 2,85E-07 |
| HG001_00950 | potB | Spermidine/putrescine transport system permease protein PotB | SAOUHSC_01047 | - | 1,408 | 1,02E-06 |
| HG001_02275 | rplE | 50S ribosomal protein L5 | SAOUHSC_02500 | rplE | 1,402 | 2,21E-11 |
| HG001_00155 | azoR | FMN-dependent NADH-azoreductase | SAOUHSC_00173 | - | 1,402 | 1,59E-10 |
| HG001_01204 | - | hypothetical protein | SAOUHSC_01340 | - | 1,402 | 1,01E-08 |
| HG001_00517 | - | putative heme peroxidase | SAOUHSC_00573 | - | 1,396 | 2,01E-11 |
| HG001_01993 | - | Phage gp6-like head-tail connector protein | SAOUHSC_02189 | - | 1,393 | 0,002756727 |
| HG001_02276 | rplX | 50S ribosomal protein L24 | SAOUHSC_02501 | rplX | 1,39 | 1,75E-10 |
| HG001_01592 | tig | Trigger factor | SAOUHSC_01779 | tig | 1,387 | 9,40E-11 |
| HG001_01940 | pcrB | Heptaprenylglyceryl phosphate synthase | SAOUHSC_02124 | - | 1,381 | 3,78E-08 |
| HG001_01085 | smc | Chromosome partition protein Smc | SAOUHSC_01204 | - | 1,379 | 4,98E-11 |
| HG001_01141 | korA | 2-oxoglutarate oxidoreductase subunit KorA | SAOUHSC_01266 | - | 1,372 | 3,35E-06 |
| HG001_01205 | sbcD | Nuclease SbcCD subunit D | SAOUHSC_01341 | - | 1,371 | 2,58E-07 |
| HG001_01561 | recJ | Single-stranded-DNA-specific exonuclease RecJ | SAOUHSC_01744 | - | 1,366 | 2,90E-12 |
| HG001_00669 | nrdE2 | Ribonucleoside-diphosphate reductase subunit alpha 2 | SAOUHSC_00742 | nrdI | 1,363 | 7,99E-08 |
| HG001_02011 | - | hypothetical protein | SAOUHSC_02208 | - | 1,361 | 0,000139633 |
| HG001_00871 | ktrB_1 | Ktr system potassium uptake protein B | SAOUHSC_00959 | - | 1,355 | 9,75E-10 |
| HG001_01565 | queA | S-adenosylmethionine:tRNA ribosyltransferase-isomerase | SAOUHSC_01749 | queA | 1,35 | 1,96E-08 |
| HG001_02320 | fhuD_2 | Iron(3+)-hydroxamate-binding protein FhuD precursor | SAOUHSC_02554 | - | 1,349 | 9,45E-11 |
| HG001_01562 | secD | Protein translocase subunit SecD | SAOUHSC_01746 | - | 1,348 | 9,47E-09 |
| HG001_00658 | yjjK | putative ABC transporter ATP-binding protein YjjK | SAOUHSC_00729 | - | 1,344 | 8,80E-10 |
| HG001_02121 | tenA | Putative thiaminase-2 | SAOUHSC_02331 | - | 1,343 | 3,22E-11 |
| HG001_00993 | mutS2 | Endonuclease MutS2 | SAOUHSC_01099 | - | 1,341 | 1,28E-10 |
| HG001_02038 | lexA_3 | LexA repressor | SAOUHSC_02235 | - | 1,339 | 7,53E-11 |
| HG001_02274 | rpsN1 | 30S ribosomal protein S14 | SAOUHSC_02499 | rpsN | 1,335 | 2,96E-09 |
| HG001_02375 | mro | Aldose 1-epimerase precursor | SAOUHSC_02614 | - | 1,334 | 1,27E-08 |
| HG001_01509 | lepA | Elongation factor 4 | SAOUHSC_01688 | - | 1,332 | 2,76E-08 |
| HG001_00473 | rpoB | DNA-directed RNA polymerase subunit beta | SAOUHSC_00524 | rpoB | 1,33 | 3,07E-08 |
| HG001_00377 | - | hypothetical protein | SAOUHSC_00428 | - | 1,328 | 9,56E-10 |
| HG001_02142 | ptpB | Low molecular weight protein-tyrosine-phosphatase PtpB | SAOUHSC_02356 | - | 1,326 | 1,37E-06 |
| HG001_00070 | sbnF | 2-[(L-alanin-3-ylcarbamoyl)methyl]-3-(2-aminoethylcarbamoyl)-2-hydroxypropanoate synt | SAOUHSC_00080 | - | 1,324 | 5,34E-07 |
| HG001_01997 | - | Phage portal protein | SAOUHSC_02194 | - | 1,323 | 8,17E-05 |
| HG001_01907 | - | hypothetical protein | SAOUHSC_02086 | - | 1,322 | 1,10E-08 |
| HG001_01480 | znuC_2 | High-affinity zinc uptake system ATP-binding protein ZnuC | SAOUHSC_01657 | - | 1,32 | 3,39E-07 |
| HG001_00490 | ywpJ_1 | Putative phosphatase YwpJ | SAOUHSC_00542 | - | 1,318 | 8,39E-08 |
| HG001_01439 | - | hypothetical protein | SAOUHSC_01610 | - | 1,317 | 8,45E-10 |
| HG001_01829 | hemL2 | Glutamate-1-semialdehyde 2%2C1-aminomutase 2 | SAOUHSC_02000 | - | 1,312 | 1,00E-08 |
| HG001_00790 | - | Na+/H+ antiporter family protein | SAOUHSC_00880 | - | 1,308 | 5,41E-06 |
| HG001_01024 | yfnB | Putative HAD-hydrolase YfnB | SAOUHSC_01137 | - | 1,307 | 7,96E-09 |
| HG001_01788 | trmL | tRNA (cytidine(34)-2'-O)-methyltransferase | SAOUHSC_01988 | - | 1,301 | 1,85E-08 |
| HG001_01110 | frr | Ribosome-recycling factor | SAOUHSC_01236 | frr | 1,301 | 8,66E-08 |
| HG001_01534 | udk | Uridine kinase | SAOUHSC_01715 | - | 1,298 | 2,62E-10 |
| HG001_01847 | - | hypothetical protein | SAOUHSC_02021 | - | 1,298 | 6,09E-08 |
| HG001_00001 | dnaA | Chromosomal replication initiator protein DnaA | SAOUHSC_00001 | dnaA | 1,297 | 1,34E-09 |
| HG001_02290 | pbuG | Guanine/hypoxanthine permease PbuG | SAOUHSC_02516 | - | 1,288 | 7,46E-07 |
| HG001_01991 | - | hypothetical protein | SAOUHSC_02187 | - | 1,284 | 0,001099013 |
| HG001_00801 | - | Putative peptidyl-prolyl cis-trans isomerase | SAOUHSC_00891 | - | 1,281 | 4,59E-10 |
| HG001_00656 | kipA_1 | KipI antagonist | SAOUHSC_00727 | - | 1,279 | 9,23E-10 |
| HG001_01781 | liaR | Transcriptional regulatory protein LiaR | SAOUHSC_01980 | - | 1,277 | 2,06E-08 |
| HG001_00654 | - | hypothetical protein | SAOUHSC_00724 | - | 1,275 | 1,60E-08 |
| HG001_02753 | rnpA | Ribonuclease P protein component | SAOUHSC_03054 | rnpA | 1,275 | 5,73E-05 |
| HG001_00499 | nagB_1 | Glucosamine-6-phosphate deaminase | SAOUHSC_00552 | - | 1,274 | 3,52E-10 |
| HG001_01090 | rimM | Ribosome maturation factor RimM | SAOUHSC_01209 | rimM | 1,272 | 2,35E-08 |
| HG001_01996 | - | Caudovirus prohead protease | SAOUHSC_02193 | - | 1,269 | 0,000998902 |
| HG001_00943 | pdhA | Pyruvate dehydrogenase E1 component subunit alpha | SAOUHSC_01040 | - | 1,268 | 8,46E-09 |
| HG001_01089 | rpsP | 30S ribosomal protein S16 | SAOUHSC_01208 | rpsP | 1,265 | 6,80E-07 |
| HG001_02382 | fni | Isopentenyl-diphosphate delta-isomerase | SAOUHSC_02623 | - | 1,263 | 7,86E-09 |
| HG001_01208 | opuD_1 | Glycine betaine transporter OpuD | SAOUHSC_01346 | - | 1,26 | 2,14E-06 |
| HG001_01288 | - | hypothetical protein | SAOUHSC_01436 | - | 1,259 | 8,13E-09 |
| HG001_01988 | - | hypothetical protein | SAOUHSC_02184 | - | 1,259 | 0,000131299 |
| HG001_02174 | czcD_2 | Cadmium%2C cobalt and zinc/H(+)-K(+) antiporter | SAOUHSC_02389 | - | 1,256 | 5,80E-08 |
| HG001_02293 | glcU_2 | putative glucose uptake protein GlcU | SAOUHSC_02520 | - | 1,256 | 2,41E-07 |
| HG001_00027 | yfkN_1 | Trifunctional nucleotide phosphoesterase protein YfkN precursor | SAOUHSC_00025 | - | 1,252 | 6,87E-07 |
| HG001_00028 | rlmH | Ribosomal RNA large subunit methyltransferase H | SAOUHSC_00027 | - | 1,247 | 2,75E-08 |
| HG001_02143 | ywlC_2 | Threonylcarbamoyl-AMP synthase | SAOUHSC_02357 | - | 1,244 | 1,72E-07 |
| HG001_02642 | davT | 5-aminovalerate aminotransferase DavT | SAOUHSC_02924 | - | 1,239 | 6,63E-06 |
| HG001_01484 | trmK | tRNA (adenine(22)-N(1))-methyltransferase | SAOUHSC_01661 | - | 1,236 | 3,25E-09 |
| HG001_02210 | - | hypothetical protein | SAOUHSC_02425 | - | 1,236 | 6,23E-06 |
| HG001_02272 | rplF | 50S ribosomal protein L6 | SAOUHSC_02496 | rplF | 1,235 | 2,98E-09 |
| HG001_00137 | yecD | Isochorismatase family protein YecD | SAOUHSC_00152 | - | 1,23 | 2,28E-06 |
| HG001_00498 | - | hypothetical protein | SAOUHSC_00551 | - | 1,229 | 1,89E-06 |

| | | | | | | |
|---|---|---|---|---|---|---|
| HG001_00138 | ipdC | Indole-3-pyruvate decarboxylase | SAOUHSC_00153 | - | 1,229 | 3,85E-06 |
| HG001_00417 | prs_1 | Ribose-phosphate pyrophosphokinase | SAOUHSC_00472 | - | 1,225 | 1,20E-07 |
| HG001_02273 | rpsH | 30S ribosomal protein S8 | SAOUHSC_02498 | rpsH | 1,221 | 4,91E-09 |
| HG001_01146 | - | Thiamine-precursor transporter protein (ThiW) | SAOUHSC_01271 | - | 1,22 | 1,83E-08 |
| HG001_00812 | spsB_2 | Signal peptidase IB | SAOUHSC_00903 | - | 1,22 | 6,64E-08 |
| HG001_00310 | ssb_1 | Single-stranded DNA-binding protein ssb | SAOUHSC_00349 | - | 1,214 | 7,79E-08 |
| HG001_01449 | - | hypothetical protein | SAOUHSC_01621 | nusB | 1,207 | 8,07E-08 |
| HG001_02559 | - | Acetyltransferase (GNAT) family protein | SAOUHSC_02827 | - | 1,207 | 3,61E-06 |
| HG001_00299 | metE | 5-methyltetrahydropteroyltriglutamate--homocysteine methyltransferase | SAOUHSC_00338 | - | 1,201 | 1,59E-07 |
| HG001_02585 | mvaA | 3-hydroxy-3-methylglutaryl-coenzyme A reductase | SAOUHSC_02859 | - | 1,198 | 2,10E-08 |
| HG001_00944 | pdhB | Pyruvate dehydrogenase E1 component subunit beta | SAOUHSC_01041 | - | 1,197 | 3,51E-07 |
| HG001_01446 | - | Farnesyl diphosphate synthase | SAOUHSC_01618 | - | 1,193 | 4,99E-07 |
| HG001_02207 | - | Haemolysin-III related | SAOUHSC_02422 | - | 1,192 | 6,17E-09 |
| HG001_01452 | accB_1 | Biotin carboxyl carrier protein of acetyl-CoA carboxylase | SAOUHSC_01624 | - | 1,19 | 1,70E-08 |
| HG001_02030 | - | hypothetical protein | SAOUHSC_02226 | - | 1,19 | 5,52E-05 |
| HG001_01906 | - | hypothetical protein | SAOUHSC_02085 | - | 1,189 | 1,62E-06 |
| HG001_01109 | pyrH | Uridylate kinase | SAOUHSC_01235 | pyrH | 1,188 | 7,15E-06 |
| HG001_01712 | metK | S-adenosylmethionine synthase | SAOUHSC_01909 | - | 1,187 | 4,90E-08 |
| HG001_01681 | mdtH | Multidrug resistance protein MdtH | SAOUHSC_01876 | - | 1,185 | 1,09E-07 |
| HG001_01132 | phbB | Acetoacetyl-CoA reductase | SAOUHSC_01257 | - | 1,185 | 2,67E-06 |
| HG001_02421 | - | hypothetical protein | SAOUHSC_02668 | - | 1,185 | 2,63E-05 |
| HG001_02208 | - | putative uridylyltransferase | SAOUHSC_02423 | - | 1,184 | 1,20E-07 |
| HG001_01990 | - | hypothetical protein | SAOUHSC_02186 | - | 1,179 | 0,00182997 |
| HG001_01235 | femB | Aminoacyltransferase FemB | SAOUHSC_01374 | - | 1,174 | 2,25E-07 |
| HG001_02372 | lyrA | Lysostaphin resistance protein A | SAOUHSC_02611 | - | 1,173 | 9,52E-08 |
| HG001_01989 | - | Bacterial Ig-like domain (group 2) | SAOUHSC_02185 | - | 1,172 | 6,28E-07 |
| HG001_01912 | - | putative acyl-CoA thioester hydrolase | SAOUHSC_02091 | - | 1,17 | 5,82E-08 |
| HG001_00065 | sbnA | putative siderophore biosynthesis protein SbnA | SAOUHSC_00075 | - | 1,17 | 0,000501837 |
| HG001_01460 | gcvPA | putative glycine dehydrogenase (decarboxylating) subunit 1 | SAOUHSC_01633 | - | 1,168 | 1,59E-05 |
| HG001_00004 | recF | DNA replication and repair protein RecF | SAOUHSC_00004 | recF | 1,166 | 6,04E-09 |
| HG001_02383 | corA | Magnesium transport protein CorA | SAOUHSC_02624 | - | 1,164 | 2,66E-07 |
| HG001_02203 | ylxH | Flagellum site-determining protein YlxH | SAOUHSC_02417 | - | 1,161 | 1,85E-07 |
| HG001_00118 | aldA | Putative aldehyde dehydrogenase AldA | SAOUHSC_00132 | - | 1,161 | 1,55E-06 |
| HG001_01692 | ribD | Riboflavin biosynthesis protein RibD | SAOUHSC_01889 | - | 1,16 | 1,76E-06 |
| HG001_01334 | gpsA | Glycerol-3-phosphate dehydrogenase [NAD(P)+] | SAOUHSC_01491 | gpsA | 1,156 | 3,00E-06 |
| HG001_02118 | thiE | Thiamine-phosphate synthase | SAOUHSC_02328 | thiE | 1,155 | 2,18E-05 |
| HG001_01059 | - | hypothetical protein | SAOUHSC_01175 | - | 1,151 | 1,08E-07 |
| HG001_01620 | accA | Acetyl-coenzyme A carboxylase carboxyl transferase subunit alpha | SAOUHSC_01808 | - | 1,151 | 1,21E-07 |
| HG001_00476 | rpsL | 30S ribosomal protein S12 | SAOUHSC_00527 | rpsL | 1,15 | 8,47E-06 |
| HG001_01769 | - | Bacterial ABC transporter protein EcsB | SAOUHSC_01966 | - | 1,148 | 1,95E-06 |
| HG001_00821 | clpB_1 | Chaperone protein ClpB | SAOUHSC_00912 | - | 1,144 | 5,03E-07 |
| HG001_01145 | - | hypothetical protein | SAOUHSC_01270 | - | 1,143 | 2,04E-08 |
| HG001_02607 | oatA_2 | O-acetyltransferase OatA | SAOUHSC_02885 | - | 1,14 | 3,32E-06 |
| HG001_01447 | xseB | Exodeoxyribonuclease 7 small subunit | SAOUHSC_01619 | - | 1,139 | 9,95E-05 |
| HG001_00326 | tcyP | L-cystine uptake protein TcyP | SAOUHSC_00367 | - | 1,134 | 8,75E-08 |
| HG001_02270 | rpsE | 30S ribosomal protein S5 | SAOUHSC_02494 | rpsE | 1,133 | 7,69E-09 |
| HG001_01448 | xseA | Exodeoxyribonuclease 7 large subunit | SAOUHSC_01620 | xseA | 1,128 | 5,09E-09 |
| HG001_00641 | corC | Magnesium and cobalt efflux protein CorC | SAOUHSC_00711 | - | 1,123 | 4,05E-06 |
| HG001_01639 | rpsD | 30S ribosomal protein S4 | SAOUHSC_01829 | rpsD | 1,121 | 1,96E-08 |
| HG001_01095 | rnhB | Ribonuclease HII | SAOUHSC_01215 | rnhB | 1,121 | 1,30E-06 |
| HG001_02748 | - | hypothetical protein | SAOUHSC_03048 | - | 1,121 | 6,74E-06 |
| HG001_01636 | iscS_2 | Cysteine desulfurase | SAOUHSC_01825 | - | 1,121 | 1,38E-05 |
| HG001_00870 | - | Serine protease HtrA-like protein | SAOUHSC_00958 | - | 1,119 | 3,52E-05 |
| HG001_01843 | - | putative phage protein 2 of sapT operon | SAOUHSC_02017 | - | 1,117 | 2,82E-06 |
| HG001_01391 | - | hypothetical protein | SAOUHSC_01558 | - | 1,115 | 0,000846604 |
| HG001_00992 | polX | DNA polymerase/3'-5' exonuclease PolX | SAOUHSC_01098 | - | 1,111 | 2,71E-08 |
| HG001_01069 | rlmN | putative dual-specificity RNA methyltransferase RlmN | SAOUHSC_01185 | - | 1,111 | 4,03E-07 |
| HG001_00655 | kipI_1 | Kinase A inhibitor | SAOUHSC_00726 | - | 1,108 | 1,75E-07 |
| HG001_00428 | ftsH | ATP-dependent zinc metalloprotease FtsH | SAOUHSC_00486 | - | 1,101 | 1,57E-07 |
| HG001_02526 | - | putative lipoprotein precursor | SAOUHSC_02789 | - | 1,098 | 6,92E-05 |
| HG001_01983 | - | hypothetical protein | SAOUHSC_02178 | - | 1,098 | 0,000787174 |
| HG001_02068 | - | putative inner membrane protein | SAOUHSC_02272 | - | 1,097 | 5,34E-05 |
| HG001_02298 | femX | Lipid II:glycine glycyltransferase | SAOUHSC_02527 | - | 1,096 | 8,84E-07 |
| HG001_01140 | - | Calcineurin-like phosphoesterase | SAOUHSC_01265 | - | 1,094 | 4,57E-06 |
| HG001_00424 | divIC | Cell division protein DivIC | SAOUHSC_00482 | - | 1,087 | 5,13E-06 |
| HG001_02147 | rpmE2 | 50S ribosomal protein L31 type B | SAOUHSC_02361 | rpmE2 | 1,086 | 1,51E-07 |
| HG001_01300 | der_1 | GTPase Der | SAOUHSC_01455 | - | 1,085 | 1,46E-05 |
| HG001_00772 | lipA_1 | Lipoyl synthase | SAOUHSC_00861 | - | 1,081 | 4,80E-08 |
| HG001_01044 | ileS | Isoleucine--tRNA ligase | SAOUHSC_01159 | ileS | 1,079 | 0,000184868 |
| HG001_02449 | tcyC_2 | L-cystine import ATP-binding protein TcyC | SAOUHSC_02697 | - | 1,078 | 4,12E-06 |
| HG001_01315 | asnS | Asparagine--tRNA ligase | SAOUHSC_01471 | asnC | 1,075 | 1,61E-05 |
| HG001_01413 | Int-Tn | Transposase from transposon Tn916 | SAOUHSC_01582 | - | 1,071 | 2,88E-06 |
| HG001_01475 | rpmG2_2 | 50S ribosomal protein L33 2 | SAOUHSC_01651 | rpmG | 1,064 | 0,000111302 |
| HG001_00399 | tmk | Thymidylate kinase | SAOUHSC_00451 | tmk | 1,061 | 4,06E-06 |
| HG001_00305 | ykuT | putative MscS family protein YkuT | SAOUHSC_00344 | - | 1,061 | 2,21E-05 |
| HG001_00780 | patA_1 | Peptidoglycan O-acetyltransferase | SAOUHSC_00870 | - | 1,059 | 3,81E-06 |
| HG001_02749 | noc | Nucleoid occlusion protein | SAOUHSC_03049 | - | 1,058 | 9,40E-07 |
| HG001_01607 | coaE | Dephospho-CoA kinase | SAOUHSC_01795 | coaE | 1,057 | 1,39E-06 |
| HG001_01953 | rutB | Peroxyureidoacrylate/ureidoacrylate amidohydrolase RutB | SAOUHSC_02139 | - | 1,057 | 1,24E-05 |

| | | | | | | |
|---|---|---|---|---|---|---|
| HG001_00474 | rpoC | DNA-directed RNA polymerase subunit beta' | SAOUHSC_00525 | - | 1,053 | 3,59E-06 |
| HG001_00311 | rpsR | 30S ribosomal protein S18 | SAOUHSC_00350 | rpsR | 1,046 | 1,58E-05 |
| HG001_00146 | - | hypothetical protein | SAOUHSC_00163 | - | 1,046 | 6,37E-05 |
| HG001_01536 | yhbU_2 | putative protease YhbU precursor | SAOUHSC_01717 | - | 1,044 | 2,20E-07 |
| HG001_01102 | trmFO | Methylenetetrahydrofolate--tRNA-(uracil-5-)-methyltransferase TrmFO | SAOUHSC_01223 | gid | 1,043 | 3,65E-06 |
| HG001_01715 | - | Transposase IS200 like protein | SAOUHSC_01911 | - | 1,042 | 1,69E-06 |
| HG001_02039 | - | hypothetical protein | SAOUHSC_02237 | - | 1,042 | 4,26E-05 |
| HG001_02630 | - | hypothetical protein | SAOUHSC_02910 | - | 1,042 | 0,001620305 |
| HG001_02310 | - | tRNA-Gln(ttg) | - | - | 1,04 | 0,002666821 |
| HG001_01596 | rpmI | 50S ribosomal protein L35 | SAOUHSC_01785 | rpmI | 1,037 | 2,31E-07 |
| HG001_00393 | dnaX_1 | DNA polymerase III subunit tau | SAOUHSC_00442 | - | 1,034 | 4,83E-07 |
| HG001_02117 | yidC | Membrane protein insertase YidC precursor | SAOUHSC_02327 | - | 1,034 | 1,04E-05 |
| HG001_02527 | srmB | ATP-dependent RNA helicase SrmB | SAOUHSC_02790 | - | 1,034 | 3,15E-05 |
| HG001_01342 | - | hypothetical protein | SAOUHSC_01503 | - | 1,028 | 7,79E-05 |
| HG001_02315 | modA | Molybdate-binding periplasmic protein precursor | SAOUHSC_02549 | - | 1,024 | 6,61E-07 |
| HG001_01124 | rpsO | 30S ribosomal protein S15 | SAOUHSC_01250 | rpsO | 1,024 | 2,79E-06 |
| HG001_00510 | ung | Uracil-DNA glycosylase | SAOUHSC_00564 | - | 1,024 | 0,000840362 |
| HG001_01299 | ypcP | 5'-3' exonuclease | SAOUHSC_01454 | - | 1,021 | 6,35E-05 |
| HG001_01629 | ald2 | Alanine dehydrogenase 2 | SAOUHSC_01818 | - | 1,02 | 1,41E-06 |
| HG001_02450 | tcyB | L-cystine transport system permease protein TcyB | SAOUHSC_02698 | - | 1,02 | 0,000167666 |
| HG001_02481 | - | hypothetical protein | SAOUHSC_02733 | - | 1,018 | 4,27E-06 |
| HG001_02306 | moaD | Molybdopterin synthase sulfur carrier subunit | SAOUHSC_02538 | - | 1,015 | 6,84E-05 |
| HG001_01049 | pyrR | Bifunctional protein PyrR | SAOUHSC_01164 | - | 1,013 | 0,000496863 |
| HG001_01144 | miaB | (Dimethylallyl)adenosine tRNA methylthiotransferase MiaB | SAOUHSC_01269 | - | 1,011 | 6,46E-06 |
| HG001_00675 | - | CHY zinc finger | SAOUHSC_00751 | - | 1,011 | 6,49E-06 |
| HG001_01097 | sucD | Succinyl-CoA ligase [ADP-forming] subunit alpha | SAOUHSC_01218 | - | 1,007 | 6,24E-06 |
| HG001_01908 | - | hypothetical protein | SAOUHSC_02087 | - | 1,006 | 1,32E-06 |
| HG001_01450 | - | hypothetical protein | SAOUHSC_01622 | - | 1,003 | 3,84E-06 |
| HG001_01913 | pepS | Aminopeptidase PepS | SAOUHSC_02092 | - | 1,003 | 1,30E-05 |
| HG001_00771 | yfkN_3 | Trifunctional nucleotide phosphoesterase protein YfkN precursor | SAOUHSC_00860 | - | 1,002 | 1,76E-06 |
| HG001_01566 | ruvB | Holliday junction ATP-dependent DNA helicase RuvB | SAOUHSC_01750 | ruvB | 1,001 | 2,72E-05 |

**DOWN regulated genes from the differencial transcriptomics analysis in oxidative stress**

| id | gene | product | locus_tag_NCTC8325 | gene_NCTC8325 | log2FoldChange | padj |
|---|---|---|---|---|---|---|
| HG001_01009 | hly | Alpha-hemolysin precursor | SAOUHSC_01121 | - | -4,933 | 7,31E-95 |
| HG001_00100 | cap8A_1 | Capsular polysaccharide type 8 biosynthesis protein cap8A | SAOUHSC_00114 | - | -4,313 | 1,48E-50 |
| HG001_00099 | adhE | Aldehyde-alcohol dehydrogenase | SAOUHSC_00113 | - | -3,985 | 1,68E-54 |
| HG001_00101 | ywqD_1 | Tyrosine-protein kinase YwqD | SAOUHSC_00115 | - | -3,82 | 4,93E-46 |
| HG001_01030 | ftsL | Cell division protein FtsL | SAOUHSC_01144 | - | -3,572 | 1,09E-52 |
| HG001_02245 | - | 65 kDa membrane protein precursor | - | - | -3,498 | 7,36E-32 |
| HG001_00102 | ywqE_1 | Tyrosine-protein phosphatase YwqE | SAOUHSC_00116 | - | -3,459 | 4,35E-38 |
| HG001_00570 | psaA | Manganese ABC transporter substrate-binding lipoprotein precursor | SAOUHSC_00634 | - | -3,302 | 4,90E-40 |
| HG001_00103 | pglF | UDP-N-acetyl-alpha-D-glucosamine C6 dehydratase | SAOUHSC_00117 | - | -3,2 | 1,99E-39 |
| HG001_02045 | dapE | putative succinyl-diaminopimelate desuccinylase | SAOUHSC_02244 | - | -3,098 | 4,16E-35 |
| HG001_00209 | bglA | Aryl-phospho-beta-D-glucosidase BglA | SAOUHSC_00236 | - | -3,079 | 3,93E-22 |
| HG001_01028 | mraZ | Protein MraZ | SAOUHSC_01142 | - | -3,059 | 8,47E-48 |
| HG001_00264 | lip2 | Lipase 2 precursor | SAOUHSC_00300 | - | -2,999 | 3,65E-33 |
| HG001_00206 | lrgB | Antiholin-like protein LrgB | SAOUHSC_00233 | - | -2,985 | 5,26E-07 |
| HG001_00358 | lpl2 | putative lipoprotein precursor | SAOUHSC_00405 | - | -2,962 | 3,88E-41 |
| HG001_00331 | xpt | Xanthine phosphoribosyltransferase | SAOUHSC_00372 | - | -2,96 | 5,87E-31 |
| HG001_00544 | adh | Alcohol dehydrogenase | SAOUHSC_00608 | adhA | -2,958 | 9,55E-47 |
| HG001_01680 | - | T-box | - | - | -2,95 | 4,37E-37 |
| HG001_02709 | lipA_2 | Lipase 1 precursor | SAOUHSC_03006 | - | -2,917 | 2,96E-27 |
| HG001_00571 | mntB | Manganese transport system membrane protein MntB | SAOUHSC_00636 | - | -2,907 | 3,21E-40 |
| HG001_02640 | ldh2 | L-lactate dehydrogenase 2 | SAOUHSC_02922 | - | -2,845 | 9,55E-43 |
| HG001_00710 | - | RsaH | - | - | -2,802 | 6,38E-21 |
| HG001_00104 | capD | UDP-glucose 4-epimerase | SAOUHSC_00118 | - | -2,8 | 1,10E-29 |
| HG001_01029 | rsmH_1 | Ribosomal RNA small subunit methyltransferase H | SAOUHSC_01143 | mraW | -2,787 | 5,63E-50 |
| HG001_00055 | - | Oleate hydratase | SAOUHSC_00061 | - | -2,771 | 9,85E-37 |
| HG001_02756 | - | RsaG | - | - | -2,762 | 2,92E-16 |
| HG001_01172 | - | hypothetical protein | SAOUHSC_01303 | - | -2,749 | 2,42E-21 |
| HG001_00318 | - | Transglycosylase associated protein | SAOUHSC_00358 | - | -2,721 | 5,70E-41 |
| HG001_01548 | - | hypothetical protein | SAOUHSC_01729 | - | -2,699 | 4,62E-48 |
| HG001_00359 | - | hypothetical protein | SAOUHSC_00406 | - | -2,659 | 1,15E-29 |
| HG001_01297 | tdcB | L-threonine dehydratase catabolic TdcB | SAOUHSC_01451 | - | -2,654 | 1,59E-22 |
| HG001_00106 | wbpI | UDP-2%2C3-diacetamido-2%2C3-dideoxy-D-glucuronate 2-epimerase | SAOUHSC_00120 | - | -2,572 | 4,15E-30 |
| HG001_02103 | kdpC | Potassium-transporting ATPase C chain | SAOUHSC_02310 | - | -2,54 | 1,77E-27 |
| HG001_00107 | vatD | Streptogramin A acetyltransferase | SAOUHSC_00121 | - | -2,527 | 2,76E-23 |
| HG001_00105 | fcl | GDP-L-fucose synthase | SAOUHSC_00119 | - | -2,525 | 1,10E-29 |
| HG001_00827 | - | 65 kDa membrane protein precursor | - | - | -2,514 | 9,85E-28 |
| HG001_01684 | rot | HTH-type transcriptional regulator rot | SAOUHSC_01879 | - | -2,499 | 2,44E-25 |
| HG001_02221 | - | Transposase DDE domain protein | SAOUHSC_02437 | - | -2,477 | 1,78E-19 |
| HG001_00561 | mrpA | Na(+)/H(+) antiporter subunit A | SAOUHSC_00625 | - | -2,462 | 8,59E-28 |
| HG001_01296 | steT | Serine/threonine exchanger SteT | SAOUHSC_01450 | - | -2,455 | 1,71E-29 |
| HG001_02181 | glmS | Glutamine--fructose-6-phosphate aminotransferase [isomerizing] | SAOUHSC_02399 | - | -2,402 | 3,78E-28 |
| HG001_02105 | kdpA | Potassium-transporting ATPase A chain | SAOUHSC_02312 | - | -2,4 | 1,65E-22 |
| HG001_00241 | - | hypothetical protein | SAOUHSC_00272 | - | -2,382 | 5,63E-20 |
| HG001_00274 | - | PTS system ascorbate-specific transporter subunits IICB | SAOUHSC_00311 | - | -2,378 | 7,71E-22 |
| HG001_02104 | kdpB | Potassium-transporting ATPase B chain | SAOUHSC_02311 | - | -2,371 | 3,10E-18 |
| HG001_01630 | - | Putative universal stress protein | SAOUHSC_01819 | - | -2,37 | 2,62E-31 |
| HG001_01610 | - | hypothetical protein | SAOUHSC_01798 | - | -2,361 | 1,04E-22 |
| HG001_02514 | ahpD | Alkyl hydroperoxide reductase AhpD | SAOUHSC_02774 | - | -2,352 | 2,77E-23 |
| HG001_00273 | ulaA | Ascorbate-specific permease IIC component UlaA | SAOUHSC_00310 | ulaA | -2,348 | 3,96E-23 |
| HG001_00562 | mrpB | Na(+)/H(+) antiporter subunit B | SAOUHSC_00626 | - | -2,342 | 4,97E-17 |
| HG001_00360 | - | hypothetical protein | SAOUHSC_00407 | - | -2,333 | 8,89E-24 |
| HG001_00556 | sarA | Transcriptional regulator SarA | SAOUHSC_00620 | - | -2,33 | 2,30E-20 |
| HG001_02040 | - | hypothetical protein | SAOUHSC_02238 | - | -2,32 | 6,72E-25 |
| HG001_02107 | kdpE | KDP operon transcriptional regulatory protein KdpE | SAOUHSC_02315 | - | -2,315 | 2,96E-19 |
| HG001_02677 | isaB | Immunodominant staphylococcal antigen B precursor | SAOUHSC_02972 | - | -2,292 | 2,65E-22 |
| HG001_00899 | sspA | Glutamyl endopeptidase precursor | SAOUHSC_00988 | - | -2,286 | 1,08E-22 |
| HG001_00847 | - | RsaE | - | - | -2,284 | 2,58E-06 |
| HG001_01412 | - | hypothetical protein | SAOUHSC_01580 | - | -2,282 | 5,01E-24 |
| HG001_00725 | - | hypothetical protein | SAOUHSC_00808 | - | -2,258 | 6,01E-20 |
| HG001_02494 | - | hypothetical protein | SAOUHSC_02753 | - | -2,239 | 5,45E-25 |
| HG001_02359 | malP | PTS system maltose-specific EIICB component | SAOUHSC_02597 | - | -2,234 | 2,88E-26 |
| HG001_01744 | - | hypothetical protein | SAOUHSC_01945 | - | -2,233 | 2,77E-16 |
| HG001_00120 | - | hypothetical protein | SAOUHSC_00134 | - | -2,232 | 4,58E-20 |
| HG001_00108 | - | hypothetical protein | SAOUHSC_00122 | - | -2,231 | 3,19E-21 |
| HG001_01075 | rpmB | 50S ribosomal protein L28 | SAOUHSC_01191 | rpmB | -2,228 | 1,21E-23 |
| HG001_02398 | - | FtsX-like permease family protein | SAOUHSC_02641 | - | -2,222 | 1,28E-18 |
| HG001_00564 | mnhD1_1 | Na(+)/H(+) antiporter subunit D1 | SAOUHSC_00628 | - | -2,22 | 1,74E-24 |
| HG001_00275 | cmtB | Mannitol-specific cryptic phosphotransferase enzyme IIA component | SAOUHSC_00312 | - | -2,216 | 3,56E-20 |
| HG001_00898 | sspB | Staphopain B precursor | SAOUHSC_00987 | - | -2,208 | 4,30E-17 |
| HG001_02337 | - | hypothetical protein | SAOUHSC_02575 | - | -2,199 | 3,98E-20 |
| HG001_00563 | mrpC | Na(+)/H(+) antiporter subunit C | SAOUHSC_00627 | - | -2,185 | 7,06E-20 |
| HG001_02182 | - | glmS | - | - | -2,182 | 1,02E-14 |
| HG001_00724 | - | hypothetical protein | SAOUHSC_00806 | - | -2,175 | 5,66E-22 |

| | | | | | | |
|---|---|---|---|---|---|---|
| HG001_00545 | - | hypothetical protein | SAOUHSC_00609 | - | -2,173 | 0,000132078 |
| HG001_01340 | ebpS | Elastin-binding protein EbpS | SAOUHSC_01501 | - | -2,155 | 3,66E-22 |
| HG001_00573 | ideR | Iron-dependent repressor IdeR | SAOUHSC_00638 | mntR | -2,129 | 8,63E-19 |
| HG001_00897 | sspC | Staphostatin B | SAOUHSC_00986 | - | -2,128 | 5,00E-17 |
| HG001_02588 | clpL | ATP-dependent Clp protease ATP-binding subunit ClpL | SAOUHSC_02862 | - | -2,125 | 2,50E-18 |
| HG001_02057 | - | RNAIII | SAOUHSC_02260 | - | -2,116 | 3,71E-27 |
| HG001_01958 | - | hypothetical protein | SAOUHSC_02145 | - | -2,11 | 2,54E-23 |
| HG001_02125 | - | hypothetical protein | SAOUHSC_02335 | - | -2,099 | 1,64E-14 |
| HG001_02737 | - | hypothetical protein | SAOUHSC_03035 | - | -2,098 | 1,87E-19 |
| HG001_00248 | - | hypothetical protein | SAOUHSC_00280 | - | -2,097 | 4,44E-17 |
| HG001_00482 | hchA | Molecular chaperone Hsp31 and glyoxalase 3 | SAOUHSC_00533 | - | -2,073 | 6,43E-21 |
| HG001_01747 | - | Thermophilic serine proteinase precursor | SAOUHSC_01949 | - | -2,065 | 1,07E-15 |
| HG001_01772 | - | hypothetical protein | SAOUHSC_01969 | - | -2,06 | 5,73E-24 |
| HG001_00889 | - | hypothetical protein | SAOUHSC_00977 | - | -2,032 | 1,15E-14 |
| HG001_01064 | - | hypothetical protein | SAOUHSC_01180 | - | -2,012 | 9,99E-13 |
| HG001_01978 | sak | Staphylokinase precursor | SAOUHSC_02171 | - | -2,003 | 2,33E-19 |
| HG001_02222 | - | Alkaline shock protein 23 | SAOUHSC_02441 | - | -2,001 | 9,35E-17 |
| HG001_01237 | - | hypothetical protein | SAOUHSC_01376 | - | -1,978 | 1,20E-22 |
| HG001_00316 | - | Peptidase propeptide and YPEB domain protein | SAOUHSC_00356 | - | -1,978 | 1,39E-15 |
| HG001_00046 | plc | 1-phosphatidylinositol phosphodiesterase precursor | SAOUHSC_00051 | - | -1,97 | 2,79E-21 |
| HG001_02062 | agrA | Accessory gene regulator protein A | SAOUHSC_02265 | - | -1,967 | 1,79E-14 |
| HG001_02060 | - | Staphylococcal AgrD protein | SAOUHSC_02262 | - | -1,962 | 6,81E-14 |
| HG001_00740 | - | hypothetical protein | SAOUHSC_00825 | - | -1,942 | 2,73E-16 |
| HG001_02225 | opuD_2 | Glycine betaine transporter OpuD | SAOUHSC_02444 | - | -1,94 | 1,98E-17 |
| HG001_01065 | - | TM2 domain protein | SAOUHSC_01181 | - | -1,94 | 3,89E-16 |
| HG001_00361 | - | hypothetical protein | SAOUHSC_00408 | - | -1,936 | 1,56E-15 |
| HG001_01746 | yxlF_2 | putative ABC transporter ATP-binding protein YxlF | SAOUHSC_01948 | - | -1,934 | 4,04E-14 |
| HG001_01298 | ald1 | Alanine dehydrogenase 1 | SAOUHSC_01452 | - | -1,927 | 5,01E-13 |
| HG001_02330 | sarR | HTH-type transcriptional regulator SarR | SAOUHSC_02566 | - | -1,925 | 2,59E-13 |
| HG001_02601 | crtN | Dehydrosqualene desaturase | SAOUHSC_02877 | - | -1,921 | 8,97E-18 |
| HG001_02347 | - | RsaOG | - | - | -1,92 | 1,06E-12 |
| HG001_01612 | phoP | Alkaline phosphatase synthesis transcriptional regulatory protein PhoP | SAOUHSC_01800 | - | -1,919 | 1,99E-20 |
| HG001_02458 | hlgC | Gamma-hemolysin component C precursor | SAOUHSC_02709 | - | -1,911 | 6,49E-19 |
| HG001_01445 | argR_1 | Arginine repressor | SAOUHSC_01617 | - | -1,91 | 4,66E-16 |
| HG001_00565 | mrpE | Na(+)/H(+) antiporter subunit E | SAOUHSC_00629 | - | -1,909 | 9,27E-16 |
| HG001_00744 | - | hypothetical protein | SAOUHSC_00830 | - | -1,898 | 4,89E-10 |
| HG001_01495 | ybeZ | PhoH-like protein | SAOUHSC_01673 | - | -1,893 | 1,72E-19 |
| HG001_00567 | mrpG | Na(+)/H(+) antiporter subunit G | SAOUHSC_00632 | - | -1,891 | 7,48E-16 |
| HG001_01955 | alkH | Aldehyde dehydrogenase | SAOUHSC_02142 | - | -1,887 | 2,51E-15 |
| HG001_00058 | - | hypothetical protein | SAOUHSC_00065 | - | -1,881 | 4,25E-19 |
| HG001_02397 | hrtA_2 | Putative hemin import ATP-binding protein HrtA | SAOUHSC_02640 | - | -1,876 | 8,24E-11 |
| HG001_01216 | glcT | GlcA/glcB genes antiterminator | SAOUHSC_01356 | - | -1,871 | 3,05E-15 |
| HG001_01364 | - | hypothetical protein | SAOUHSC_01527 | - | -1,871 | 3,52E-09 |
| HG001_00109 | - | hypothetical protein | SAOUHSC_00123 | - | -1,862 | 9,54E-17 |
| HG001_00227 | esxA | Virulence factor EsxA | SAOUHSC_00257 | - | -1,858 | 1,52E-17 |
| HG001_00566 | mrpF | Na(+)/H(+) antiporter subunit F | SAOUHSC_00632 | - | -1,851 | 2,38E-13 |
| HG001_02365 | yghA | putative oxidoreductase YghA | SAOUHSC_02604 | - | -1,849 | 3,51E-16 |
| HG001_00169 | pflB | Formate acetyltransferase | SAOUHSC_00187 | - | -1,839 | 9,01E-16 |
| HG001_01751 | gdmA | Lantibiotic gallidermin precursor | SAOUHSC_01953 | - | -1,836 | 2,24E-13 |
| HG001_02303 | sarV | HTH-type transcriptional regulator SarV | SAOUHSC_02532 | - | -1,834 | 1,02E-10 |
| HG001_02106 | kdpD | Sensor protein KdpD | SAOUHSC_02314 | - | -1,818 | 2,02E-16 |
| HG001_00330 | - | Purine | - | - | -1,807 | 4,69E-05 |
| HG001_01032 | mraY | Phospho-N-acetylmuramoyl-pentapeptide-transferase | SAOUHSC_01146 | mraY | -1,804 | 2,57E-19 |
| HG001_00902 | slyA_2 | Transcriptional regulator SlyA | SAOUHSC_00992 | - | -1,799 | 1,23E-11 |
| HG001_00759 | - | CsbD-like protein | SAOUHSC_00845 | - | -1,797 | 8,91E-21 |
| HG001_00560 | xerD_2 | Tyrosine recombinase XerD | SAOUHSC_00624 | - | -1,786 | 3,23E-16 |
| HG001_01704 | tal | Transaldolase | SAOUHSC_01901 | - | -1,785 | 5,82E-13 |
| HG001_01173 | - | hypothetical protein | SAOUHSC_01304 | - | -1,783 | 4,77E-10 |
| HG001_02061 | dpiB | Sensor histidine kinase DpiB | SAOUHSC_02264 | - | -1,782 | 1,04E-09 |
| HG001_02223 | - | hypothetical protein | SAOUHSC_02442 | - | -1,781 | 3,39E-15 |
| HG001_02059 | agrB | Accessory gene regulator protein B | SAOUHSC_02261 | - | -1,78 | 2,62E-12 |
| HG001_01363 | - | hypothetical protein | SAOUHSC_01526 | - | -1,779 | 2,76E-06 |
| HG001_02495 | ybbL | putative ABC transporter ATP-binding protein YbbL | SAOUHSC_02754 | - | -1,778 | 5,45E-17 |
| HG001_00414 | yabJ | Enamine/imine deaminase | SAOUHSC_00468 | - | -1,767 | 5,40E-18 |
| HG001_00110 | - | hypothetical protein | SAOUHSC_00124 | - | -1,764 | 5,05E-13 |
| HG001_01174 | - | hypothetical protein | SAOUHSC_01305 | - | -1,758 | 6,40E-08 |
| HG001_02627 | - | hypothetical protein | SAOUHSC_02907 | - | -1,755 | 7,58E-07 |
| HG001_01031 | pbpB | Penicillin-binding protein 2B | SAOUHSC_01145 | - | -1,753 | 1,13E-15 |
| HG001_01581 | - | T-box | - | - | -1,751 | 1,14E-13 |
| HG001_00728 | clfA | Clumping factor A precursor | SAOUHSC_00812 | - | -1,737 | 4,36E-13 |
| HG001_00572 | znuC_1 | High-affinity zinc uptake system ATP-binding protein ZnuC | SAOUHSC_00637 | - | -1,736 | 1,75E-12 |
| HG001_02332 | - | hypothetical protein | SAOUHSC_02569 | - | -1,731 | 3,38E-13 |
| HG001_01802 | - | tRNA-Tyr(gta) | SAOUHSC_T00057 | - | -1,726 | 8,71E-09 |
| HG001_02112 | - | hypothetical protein | SAOUHSC_02320 | - | -1,718 | 4,31E-13 |
| HG001_02195 | - | tRNA-Tyr(gta) | SAOUHSC_T00058 | - | -1,709 | 1,71E-08 |

| | | | | | |
|---|---|---|---|---|---|
| HG001_02626 | - | hypothetical protein | SAOUHSC_02906 | - | -1,707 | 9,64E-08 |
| HG001_00929 | - | hypothetical protein | SAOUHSC_01024 | - | -1,703 | 1,77E-15 |
| HG001_01729 | - | hypothetical protein | SAOUHSC_01925 | - | -1,702 | 7,03E-05 |
| HG001_02379 | yhaI | Inner membrane protein YhaI | SAOUHSC_02620 | - | -1,699 | 7,78E-15 |
| HG001_01952 | pfbA | Plasmin and fibronectin-binding protein A precursor | SAOUHSC_02138 | - | -1,689 | 1,21E-14 |
| HG001_01544 | yrrB | TPR repeat-containing protein YrrB | SAOUHSC_01724 | - | -1,689 | 6,62E-11 |
| HG001_00111 | cap5L | putative glycosyl transferase | SAOUHSC_00125 | - | -1,68 | 1,13E-15 |
| HG001_00174 | fadA | 3-ketoacyl-CoA thiolase | SAOUHSC_00195 | - | -1,676 | 9,15E-07 |
| HG001_01917 | - | hypothetical protein | SAOUHSC_02097 | - | -1,675 | 2,90E-13 |
| HG001_01043 | - | T-box | - | - | -1,666 | 1,53E-11 |
| HG001_00267 | limB_1 | Limonene 1%2C2-monooxygenase | SAOUHSC_00304 | - | -1,663 | 5,78E-14 |
| HG001_01287 | thyA | Thymidylate synthase | SAOUHSC_01435 | thyA | -1,66 | 1,91E-14 |
| HG001_01361 | - | Phage tail protein | SAOUHSC_01524 | - | -1,659 | 1,82E-09 |
| HG001_02507 | nikA | Nickel-binding periplasmic protein precursor | SAOUHSC_02767 | - | -1,658 | 5,40E-12 |
| HG001_02603 | crtQ | 4%2C4'-diaponeurosporenoate glycosyltransferase | SAOUHSC_02880 | - | -1,657 | 9,84E-12 |
| HG001_00329 | - | hypothetical protein | SAOUHSC_00371 | - | -1,652 | 2,45E-13 |
| HG001_02697 | - | hypothetical protein | SAOUHSC_02994 | - | -1,651 | 3,15E-14 |
| HG001_00709 | - | Epimerase family protein | SAOUHSC_00792 | - | -1,651 | 3,78E-13 |
| HG001_02410 | - | Ferredoxin--NADP reductase | SAOUHSC_02654 | - | -1,649 | 1,26E-13 |
| HG001_02459 | hlgB | Gamma-hemolysin component B precursor | SAOUHSC_02710 | - | -1,643 | 4,60E-15 |
| HG001_00184 | ldh1 | L-lactate dehydrogenase 1 | SAOUHSC_00206 | - | -1,643 | 4,46E-09 |
| HG001_00625 | mgrA | HTH-type transcriptional regulator MgrA | SAOUHSC_00694 | - | -1,638 | 1,53E-12 |
| HG001_00617 | - | hypothetical protein | SAOUHSC_00686 | - | -1,635 | 4,47E-12 |
| HG001_02399 | hssR | Heme response regulator HssR | SAOUHSC_02643 | - | -1,63 | 1,25E-12 |
| HG001_00175 | fadN | putative 3-hydroxyacyl-CoA dehydrogenase | SAOUHSC_00196 | - | -1,63 | 2,14E-06 |
| HG001_01444 | recN | DNA repair protein RecN | SAOUHSC_01615 | - | -1,619 | 5,84E-16 |
| HG001_00214 | degA | HTH-type transcriptional regulator DegA | SAOUHSC_00242 | - | -1,616 | 4,49E-12 |
| HG001_02093 | rsbW | Serine-protein kinase RsbW | SAOUHSC_02299 | - | -1,61 | 8,53E-13 |
| HG001_00503 | proP | Proline/betaine transporter | SAOUHSC_00556 | - | -1,608 | 7,89E-14 |
| HG001_01841 | - | hypothetical protein | SAOUHSC_02014 | - | -1,606 | 3,35E-09 |
| HG001_01731 | - | Transposase | SAOUHSC_01928 | - | -1,605 | 1,71E-11 |
| HG001_00130 | psf-1 | 4'-phosphopantetheinyl transferase psf-1 | SAOUHSC_00145 | - | -1,599 | 1,64E-12 |
| HG001_02545 | - | hypothetical protein | SAOUHSC_02812 | - | -1,599 | 3,25E-12 |
| HG001_01745 | - | ABC-2 family transporter protein | SAOUHSC_01947 | - | -1,592 | 5,42E-10 |
| HG001_02520 | - | hypothetical protein | SAOUHSC_02781 | - | -1,591 | 7,96E-13 |
| HG001_01730 | - | hypothetical protein | SAOUHSC_01926 | - | -1,589 | 4,49E-12 |
| HG001_00074 | - | hypothetical protein | SAOUHSC_00084 | - | -1,585 | 3,81E-10 |
| HG001_00741 | - | hypothetical protein | SAOUHSC_00826 | - | -1,584 | 2,66E-11 |
| HG001_01175 | - | hypothetical protein | SAOUHSC_01306 | - | -1,58 | 0,00276172 |
| HG001_02415 | sacX | Negative regulator of SacY activity | SAOUHSC_02661 | - | -1,573 | 9,24E-14 |
| HG001_01414 | - | hypothetical protein | SAOUHSC_01583 | - | -1,562 | 7,43E-12 |
| HG001_02406 | - | putative lipoprotein precursor | SAOUHSC_02650 | - | -1,56 | 1,91E-11 |
| HG001_01362 | - | Glycyl-glycine endopeptidase ALE-1 precursor | SAOUHSC_01525 | - | -1,558 | 8,74E-16 |
| HG001_00415 | spoVG | Putative septation protein SpoVG | SAOUHSC_00469 | - | -1,553 | 3,09E-13 |
| HG001_00678 | - | hypothetical protein | SAOUHSC_00754 | - | -1,546 | 6,31E-12 |
| HG001_00738 | - | hypothetical protein | SAOUHSC_00823 | - | -1,536 | 1,36E-05 |
| HG001_00303 | - | T-box | - | - | -1,514 | 1,16E-06 |
| HG001_02734 | - | hypothetical protein | SAOUHSC_03032 | - | -1,513 | 3,76E-09 |
| HG001_00726 | - | hypothetical protein | SAOUHSC_00810 | - | -1,51 | 3,14E-09 |
| HG001_01659 | - | hypothetical protein | SAOUHSC_01854 | - | -1,506 | 9,22E-12 |
| HG001_00707 | - | tRNA-Arg(ccg) | SAOUHSC_T0005 | - | -1,503 | 0,031150464 |
| HG001_00176 | acdA | Acyl-CoA dehydrogenase | SAOUHSC_00197 | - | -1,5 | 4,39E-06 |
| HG001_02326 | ureE | Urease accessory protein UreE | SAOUHSC_02562 | ureE | -1,499 | 8,19E-10 |
| HG001_00663 | - | Putative 5'(3')-deoxyribonucleotidase | SAOUHSC_00734 | - | -1,495 | 1,34E-09 |
| HG001_00607 | sarX | HTH-type transcriptional regulator SarX | SAOUHSC_00674 | - | -1,492 | 6,69E-10 |
| HG001_01654 | acsA_1 | Acetyl-coenzyme A synthetase | SAOUHSC_01846 | - | -1,488 | 1,86E-09 |
| HG001_02368 | hutU | Urocanate hydratase | SAOUHSC_02607 | - | -1,484 | 4,65E-09 |
| HG001_00828 | - | hypothetical protein | SAOUHSC_00919 | - | -1,48 | 1,87E-11 |
| HG001_02404 | lctP_2 | L-lactate permease | SAOUHSC_02648 | - | -1,468 | 2,76E-08 |
| HG001_00690 | yvyD | Putative sigma-54 modulation protein | SAOUHSC_00767 | - | -1,463 | 2,90E-11 |
| HG001_02735 | nixA | High-affinity nickel-transport protein NixA | SAOUHSC_03033 | - | -1,46 | 2,10E-11 |
| HG001_01927 | ftnA | Ferritin | SAOUHSC_02108 | - | -1,45 | 7,51E-13 |
| HG001_00528 | - | hypothetical protein | SAOUHSC_00586 | - | -1,45 | 9,08E-09 |
| HG001_02367 | hutI | Imidazolonepropionase | SAOUHSC_02606 | - | -1,45 | 1,31E-07 |
| HG001_01428 | proC | Pyrroline-5-carboxylate reductase | SAOUHSC_01597 | - | -1,448 | 3,98E-10 |
| HG001_01711 | - | hypothetical protein | SAOUHSC_01908 | - | -1,447 | 1,50E-11 |
| HG001_01171 | - | hypothetical protein | SAOUHSC_01301 | - | -1,445 | 0,007144881 |
| HG001_02162 | - | hypothetical protein | SAOUHSC_02376 | - | -1,444 | 1,50E-11 |
| HG001_00736 | - | hypothetical protein | SAOUHSC_00821 | - | -1,442 | 2,29E-08 |
| HG001_00047 | - | putative lipoprotein precursor | SAOUHSC_00052 | - | -1,441 | 7,53E-08 |
| HG001_00618 | - | Acetyltransferase (GNAT) family protein | SAOUHSC_00687 | - | -1,439 | 3,28E-08 |
| HG001_01336 | rpsA_1 | 30S ribosomal protein S1 | SAOUHSC_01493 | rpsA | -1,438 | 9,56E-13 |
| HG001_01004 | - | hypothetical protein | SAOUHSC_01113 | - | -1,431 | 2,16E-08 |
| HG001_00332 | pucK | Uric acid permease PucK | SAOUHSC_00373 | - | -1,429 | 5,92E-06 |
| HG001_02544 | ywaC | GTP pyrophosphokinase YwaC | SAOUHSC_02811 | - | -1,424 | 3,25E-11 |

| | | | | | |
|---|---|---|---|---|---|
| HG001_01740 splC | Serine protease SplC precursor | SAOUHSC_01939 | - | -1,419 | 2,47E-06 |
| HG001_01974 scn_3 | Staphylococcal complement inhibitor precursor | SAOUHSC_02167 | - | -1,417 | 7,20E-08 |
| HG001_00986 - | T-box | - | - | -1,414 | 1,11E-09 |
| HG001_02543 zntR | HTH-type transcriptional regulator ZntR | SAOUHSC_02810 | - | -1,41 | 2,68E-12 |
| HG001_00131 yagU | Inner membrane protein YagU | SAOUHSC_00146 | - | -1,409 | 9,97E-13 |
| HG001_00362 - | hypothetical protein | SAOUHSC_00409 | - | -1,403 | 4,73E-07 |
| HG001_02172 yhfK | putative sugar epimerase YhfK | SAOUHSC_02387 | - | -1,401 | 4,59E-10 |
| HG001_01728 - | hypothetical protein | SAOUHSC_01923 | - | -1,401 | 7,46E-08 |
| HG001_02324 ureB | Urease subunit beta | SAOUHSC_02559 | ureB | -1,398 | 7,41E-07 |
| HG001_01524 - | hypothetical protein | SAOUHSC_01704 | - | -1,397 | 0,004196363 |
| HG001_02163 pdp | Pyrimidine-nucleoside phosphorylase | SAOUHSC_02377 | - | -1,393 | 1,15E-10 |
| HG001_02094 rsbV | Anti-sigma-B factor antagonist | SAOUHSC_02300 | - | -1,39 | 1,11E-10 |
| HG001_00553 - | hypothetical protein | SAOUHSC_00617 | - | -1,389 | 1,30E-09 |
| HG001_02418 ydaG | General stress protein 26 | SAOUHSC_02665 | - | -1,385 | 3,81E-10 |
| HG001_00126 - | hypothetical protein | SAOUHSC_00141 | - | -1,384 | 3,63E-10 |
| HG001_00247 - | hypothetical protein | SAOUHSC_00279 | - | -1,383 | 1,05E-08 |
| HG001_01255 dapB | 4-hydroxy-tetrahydrodipicolinate reductase | SAOUHSC_01397 | - | -1,381 | 7,81E-10 |
| HG001_01163 - | hypothetical protein | SAOUHSC_01290 | - | -1,38 | 0,004802171 |
| HG001_01787 nagB_2 | Glucosamine-6-phosphate deaminase | SAOUHSC_01987 | - | -1,379 | 4,97E-11 |
| HG001_01611 phoR | Alkaline phosphatase synthesis sensor protein PhoR | SAOUHSC_01799 | - | -1,376 | 4,07E-11 |
| HG001_00743 argO | Arginine exporter protein ArgO | SAOUHSC_00828 | - | -1,373 | 1,21E-06 |
| HG001_00634 tetA_2 | Tetracycline resistance protein%2C class B | SAOUHSC_00703 | - | -1,371 | 5,57E-10 |
| HG001_01256 dapH | 2%2C3%2C4%2C5-tetrahydropyridine-2%2C6-dicarboxylate N-acetyltransferase | SAOUHSC_01398 | - | -1,367 | 1,20E-09 |
| HG001_00605 - | Inhibitor of apoptosis-promoting Bax1 | SAOUHSC_00672 | - | -1,365 | 1,33E-09 |
| HG001_01186 - | hypothetical protein | SAOUHSC_01318 | - | -1,365 | 1,56E-08 |
| HG001_00990 zapA | Cell division protein ZapA | SAOUHSC_01096 | - | -1,363 | 1,51E-07 |
| HG001_00835 oppF_1 | Oligopeptide transport ATP-binding protein OppF | SAOUHSC_00926 | - | -1,359 | 2,68E-07 |
| HG001_02164 deoC2 | Deoxyribose-phosphate aldolase 2 | SAOUHSC_02379 | - | -1,357 | 8,55E-13 |
| HG001_02666 - | hypothetical protein | - | - | -1,356 | 1,27E-09 |
| HG001_01129 phnF | putative transcriptional regulator PhnF | SAOUHSC_01254 | - | -1,353 | 4,60E-09 |
| HG001_02676 aur | Zinc metalloproteinase aureolysin precursor | SAOUHSC_02971 | - | -1,349 | 1,89E-07 |
| HG001_00516 - | RsaA | - | - | -1,346 | 6,30E-09 |
| HG001_02409 - | Acetyltransferase (GNAT) family protein | SAOUHSC_02653 | - | -1,346 | 0,000139451 |
| HG001_02407 paiA | Protease synthase and sporulation negative regulatory protein PAI 1 | SAOUHSC_02651 | - | -1,344 | 4,64E-08 |
| HG001_02363 - | SAM | - | - | -1,344 | 8,59E-08 |
| HG001_00850 yjbI | Group 2 truncated hemoglobin YjbI | SAOUHSC_00939 | - | -1,34 | 1,68E-10 |
| HG001_00891 - | Acetyltransferase (GNAT) family protein | SAOUHSC_00979 | - | -1,339 | 2,03E-06 |
| HG001_01660 - | hypothetical protein | SAOUHSC_01855 | - | -1,336 | 1,87E-11 |
| HG001_01192 - | hypothetical protein | SAOUHSC_01324 | - | -1,335 | 6,09E-07 |
| HG001_00170 pflA | Pyruvate formate-lyase-activating enzyme | SAOUHSC_00188 | - | -1,334 | 8,75E-07 |
| HG001_00249 focA | putative formate transporter 1 | SAOUHSC_00281 | - | -1,334 | 1,31E-05 |
| HG001_00568 nhaK_1 | Sodium%2C potassium%2C lithium and rubidium/H(+) antiporter | SAOUHSC_00633 | - | -1,332 | 3,61E-11 |
| HG001_01834 - | hypothetical protein | SAOUHSC_02006 | - | -1,33 | 2,35E-11 |
| HG001_00606 melR_1 | Melibiose operon regulatory protein | SAOUHSC_00673 | - | -1,329 | 1,23E-09 |
| HG001_02325 ureC | Urease subunit alpha | SAOUHSC_02561 | ureC | -1,329 | 9,64E-08 |
| HG001_01360 - | Prophage endopeptidase tail | SAOUHSC_01523 | - | -1,324 | 1,76E-07 |
| HG001_00954 - | hypothetical protein | SAOUHSC_01051 | - | -1,321 | 1,72E-07 |
| HG001_00554 - | hypothetical protein | SAOUHSC_00618 | - | -1,32 | 7,25E-09 |
| HG001_00802 yugI_2 | General stress protein 13 | SAOUHSC_00892 | - | -1,318 | 4,37E-09 |
| HG001_01223 - | prephenate dehydrogenase | SAOUHSC_01364 | - | -1,317 | 5,00E-09 |
| HG001_02678 - | hypothetical protein | SAOUHSC_02973 | - | -1,317 | 8,46E-09 |
| HG001_02351 ybbH_3 | putative HTH-type transcriptional regulator YbbH | SAOUHSC_02589 | - | -1,314 | 1,04E-07 |
| HG001_00183 hmp | Flavohemoprotein | SAOUHSC_00204 | - | -1,312 | 1,40E-05 |
| HG001_01909 - | hypothetical protein | SAOUHSC_02088 | - | -1,309 | 6,86E-06 |
| HG001_00836 dppE | Dipeptide-binding protein DppE precursor | SAOUHSC_00927 | - | -1,309 | 1,00E-05 |
| HG001_02732 yflS | Putative malate transporter YflS | SAOUHSC_03030 | - | -1,306 | 6,81E-12 |
| HG001_01033 murD | UDP-N-acetylmuramoylalanine--D-glutamate ligase | SAOUHSC_01147 | murD | -1,306 | 1,01E-08 |
| HG001_00704 aroK_1 | Shikimate kinase | SAOUHSC_00787 | - | -1,306 | 1,42E-08 |
| HG001_00112 epsL | putative sugar transferase EpsL | SAOUHSC_00126 | - | -1,304 | 4,34E-08 |
| HG001_01756 - | tRNA-Ser(gga) | SAOUHSC_T00050 | - | -1,294 | 0,00428682 |
| HG001_00178 ydiF | Acetate CoA-transferase YdiF | SAOUHSC_00199 | - | -1,291 | 3,53E-05 |
| HG001_00129 grsB | Gramicidin S synthase 2 | SAOUHSC_00144 | - | -1,287 | 4,56E-08 |
| HG001_01333 hup | DNA-binding protein HU | SAOUHSC_01490 | - | -1,286 | 1,02E-09 |
| HG001_01971 - | 65 kDa membrane protein precursor | SAOUHSC_02160 | - | -1,284 | 5,92E-06 |
| HG001_02680 manP | PTS system mannose-specific EIIBCA component | SAOUHSC_02975 | - | -1,283 | 8,48E-09 |
| HG001_02719 - | Polysaccharide deacetylase | SAOUHSC_03016 | - | -1,281 | 9,40E-07 |
| HG001_02600 dapL | LL-diaminopimelate aminotransferase | SAOUHSC_02876 | - | -1,276 | 3,98E-09 |
| HG001_01164 - | hypothetical protein | SAOUHSC_01292 | - | -1,275 | 0,01572951 |
| HG001_02124 ssb_2 | Single-stranded DNA-binding protein ssb | SAOUHSC_02334 | - | -1,273 | 2,08E-06 |
| HG001_01007 - | hypothetical protein | SAOUHSC_01119 | - | -1,266 | 4,66E-05 |
| HG001_00113 galE | UDP-glucose 4-epimerase | SAOUHSC_00127 | - | -1,265 | 5,66E-09 |
| HG001_01347 - | hypothetical protein | SAOUHSC_01510 | - | -1,264 | 0,004493515 |
| HG001_01415 - | hypothetical protein | SAOUHSC_01584 | - | -1,259 | 1,47E-06 |
| HG001_01542 - | T-box | - | - | -1,256 | 4,68E-05 |
| HG001_00529 - | hypothetical protein | SAOUHSC_00587 | - | -1,254 | 1,17E-06 |

| | | | | | |
|---|---|---|---|---|---|
| HG001_01254 | dapA | 4-hydroxy-tetrahydrodipicolinate synthase | SAOUHSC_01396 | -1,253 | 2,90E-08 |
| HG001_02331 | - | hypothetical protein | SAOUHSC_02568 | -1,243 | 1,44E-08 |
| HG001_02506 | nikB_2 | Nickel transport system permease protein NikB | SAOUHSC_02766 | -1,234 | 1,11E-05 |
| HG001_01759 | - | tRNA-Gly(tcc) | SAOUHSC_T00022 | -1,225 | 0,000540677 |
| HG001_01786 | - | hypothetical protein | SAOUHSC_01986 | -1,212 | 3,05E-08 |
| HG001_02354 | - | hypothetical protein | SAOUHSC_02592 | -1,212 | 2,81E-06 |
| HG001_01295 | norB_4 | Quinolone resistance protein NorB | SAOUHSC_01448 | -1,21 | 6,49E-06 |
| HG001_00953 | - | hypothetical protein | SAOUHSC_01050 | -1,208 | 2,62E-08 |
| HG001_01556 | - | T-box | - | -1,208 | 1,06E-05 |
| HG001_00834 | oppD_1 | Oligopeptide transport ATP-binding protein OppD | SAOUHSC_00925 | -1,208 | 2,34E-05 |
| HG001_01665 | ytpP | Thioredoxin-like protein YtpP | SAOUHSC_01860 | -1,207 | 2,01E-09 |
| HG001_01742 | splA | Serine protease SplA precursor | SAOUHSC_01942 | -1,207 | 0,000610276 |
| HG001_01365 | - | Bacterial Ig-like domain (group 2) | SAOUHSC_01528 | -1,195 | 2,05E-06 |
| HG001_00048 | - | putative lipoprotein precursor | SAOUHSC_00053 | -1,192 | 1,21E-06 |
| HG001_02292 | - | hypothetical protein | SAOUHSC_02519 | -1,19 | 6,11E-07 |
| HG001_02489 | opuCA | Carnitine transport ATP-binding protein OpuCA | SAOUHSC_02744 | -1,189 | 5,16E-06 |
| HG001_00864 | ugtP | Processive diacylglycerol beta-glucosyltransferase | SAOUHSC_00953 | -1,186 | 1,09E-08 |
| HG001_02044 | - | putative leukocidin-like protein 2 precursor | SAOUHSC_02243 | -1,186 | 2,83E-06 |
| HG001_01018 | - | hypothetical protein | SAOUHSC_01131 | -1,184 | 0,000125426 |
| HG001_01260 | - | hypothetical protein | SAOUHSC_01402 | -1,184 | 0,013374835 |
| HG001_01238 | nikE | Nickel import ATP-binding protein NikE | SAOUHSC_01377 | -1,182 | 4,27E-07 |
| HG001_00268 | gcvH_1 | Glycine cleavage system H protein | SAOUHSC_00305 | -1,179 | 2,04E-06 |
| HG001_01332 | - | Heptaprenyl diphosphate synthase (HEPPP synthase) subunit 1 | SAOUHSC_01488 | -1,179 | 3,22E-06 |
| HG001_01494 | ybeY | Endoribonuclease YbeY | SAOUHSC_01672 | -1,175 | 9,41E-09 |
| HG001_00952 | potD | Spermidine/putrescine-binding periplasmic protein precursor | SAOUHSC_01049 | -1,173 | 3,67E-08 |
| HG001_01463 | aroK_2 | Shikimate kinase | SAOUHSC_01635 | -1,168 | 5,44E-07 |
| HG001_02371 | hutG | Formimidoylglutamase | SAOUHSC_02610 | -1,162 | 2,41E-08 |
| HG001_00059 | lctP_1 | L-lactate permease | SAOUHSC_00067 | -1,162 | 1,45E-06 |
| HG001_02364 | - | hypothetical protein | SAOUHSC_02603 | -1,158 | 6,53E-06 |
| HG001_00021 | - | tRNA-Asp(gtc) | SAOUHSC_T00011 | -1,158 | 0,000389585 |
| HG001_01553 | - | 6S | - | -1,155 | 0,000116541 |
| HG001_00826 | - | putative kinase inhibitor | SAOUHSC_00917 | -1,155 | 0,000367906 |
| HG001_02327 | ureF | Urease accessory protein UreF | SAOUHSC_02563 | -1,14 | 1,55E-06 |
| HG001_01211 | - | Iron-sulphur cluster biosynthesis | SAOUHSC_01349 | -1,14 | 8,82E-06 |
| HG001_02625 | - | hypothetical protein | SAOUHSC_02905 | -1,139 | 0,001100864 |
| HG001_00708 | clpP | ATP-dependent Clp protease proteolytic subunit | SAOUHSC_00790 | -1,137 | 5,17E-08 |
| HG001_01455 | - | hypothetical protein | SAOUHSC_01627 | -1,136 | 0,000103352 |
| HG001_01657 | ccpA | Catabolite control protein A | SAOUHSC_01850 | -1,134 | 4,30E-07 |
| HG001_01757 | - | tRNA-Glu(ttc) | SAOUHSC_T00019 | -1,134 | 0,006684315 |
| HG001_01826 | perR | Peroxide-responsive repressor PerR | SAOUHSC_01997 | -1,132 | 1,18E-06 |
| HG001_01694 | - | hypothetical protein | SAOUHSC_01890 | -1,13 | 1,77E-07 |
| HG001_01762 | - | tRNA-Asp(gtc) | SAOUHSC_T00012 | -1,129 | 0,000404503 |
| HG001_00261 | ybbH_2 | putative HTH-type transcriptional regulator YbbH | SAOUHSC_00297 | -1,128 | 3,10E-07 |
| HG001_01602 | - | T-box | SAOUHSC_01789 | -1,127 | 6,79E-07 |
| HG001_00647 | - | Electron transfer DM13 | SAOUHSC_00717 | -1,124 | 1,27E-05 |
| HG001_01808 | - | tRNA-Asp(gtc) | SAOUHSC_T00014 | -1,123 | 0,000512416 |
| HG001_02197 | - | tRNA-Glu(ttc) | SAOUHSC_T00020 | -1,121 | 0,0067847 |
| HG001_01737 | splF | Serine protease SplF precursor | SAOUHSC_01935 | -1,119 | 0,000404393 |
| HG001_00706 | whiA | Putative sporulation transcription regulator WhiA | SAOUHSC_00789 | -1,115 | 4,52E-07 |
| HG001_01202 | tkt | Transketolase | SAOUHSC_01337 | -1,114 | 1,46E-07 |
| HG001_02572 | - | hypothetical protein | SAOUHSC_02842 | -1,113 | 0,012071358 |
| HG001_01436 | pepT_2 | Peptidase T | SAOUHSC_01606 | -1,112 | 1,22E-06 |
| HG001_01650 | mrcA | Penicillin-binding protein 1A | SAOUHSC_01840 | -1,11 | 3,48E-05 |
| HG001_02353 | - | hypothetical protein | SAOUHSC_02591 | -1,109 | 5,68E-07 |
| HG001_00439 | - | tRNA-Gly(gcc) | SAOUHSC_T00021 | -1,103 | 0,000712167 |
| HG001_01805 | - | tRNA-Asp(gtc) | SAOUHSC_T00013 | -1,102 | 0,000698607 |
| HG001_00985 | - | Putative TrmH family tRNA/rRNA methyltransferase | SAOUHSC_01091 | -1,099 | 3,49E-07 |
| HG001_02422 | sarZ | HTH-type transcriptional regulator SarZ | SAOUHSC_02669 | -1,099 | 1,11E-05 |
| HG001_01221 | - | putative tautomerase | SAOUHSC_01362 | -1,095 | 1,27E-06 |
| HG001_00868 | - | yybP-ykoY | - | -1,095 | 0,00142821 |
| HG001_01498 | - | hypothetical protein | SAOUHSC_01677 | -1,093 | 1,75E-08 |
| HG001_00679 | - | hypothetical protein | SAOUHSC_00755 | -1,093 | 2,12E-07 |
| HG001_01165 | - | hypothetical protein | SAOUHSC_01293 | -1,093 | 0,046553567 |
| HG001_01627 | gloB_1 | Hydroxyacylglutathione hydrolase | SAOUHSC_01815 | -1,089 | 9,83E-07 |
| HG001_02688 | secA_2 | Protein translocase subunit SecA | SAOUHSC_02985 | -1,086 | 5,76E-07 |
| HG001_01750 | - | hypothetical protein | SAOUHSC_01952 | -1,086 | 2,88E-06 |
| HG001_01453 | efp | Elongation factor P | SAOUHSC_01625 | -1,084 | 3,07E-08 |
| HG001_01253 | asd | Aspartate-semialdehyde dehydrogenase | SAOUHSC_01395 | -1,082 | 5,10E-07 |
| HG001_00035 | fccB | Sulfide dehydrogenase [flavocytochrome c] flavoprotein chain precursor | SAOUHSC_00037 | -1,082 | 1,33E-05 |
| HG001_00163 | - | Xylose isomerase-like TIM barrel | SAOUHSC_00181 | -1,082 | 3,25E-05 |
| HG001_00502 | gph_1 | Phosphoglycolate phosphatase | SAOUHSC_00555 | -1,082 | 0,000428418 |
| HG001_00806 | glpQ1_1 | putative glycerophosphoryl diester phosphodiesterase 1 | SAOUHSC_00897 | -1,079 | 7,50E-06 |
| HG001_00994 | trxA_2 | Thioredoxin | SAOUHSC_01100 | -1,078 | 9,11E-07 |
| HG001_01249 | cvfB | Conserved virulence factor B | SAOUHSC_01391 | -1,076 | 1,07E-06 |
| HG001_01426 | - | hypothetical protein | SAOUHSC_01595 | -1,074 | 0,013872178 |

| | | | | | |
|---|---|---|---|---|---|
| HG001_02574 | lipR_2 | Putative acetyl-hydrolase LipR precursor | SAOUHSC_02844 | - | -1,07 | 9,83E-07 |
| HG001_01258 | alr2 | Alanine racemase 2 | SAOUHSC_01400 | - | -1,069 | 1,81E-05 |
| HG001_01824 | - | tRNA-Ile(gat) | SAOUHSC_T00028 | - | -1,066 | 0,002328113 |
| HG001_01456 | - | hypothetical protein | SAOUHSC_01628 | - | -1,064 | 0,001185038 |
| HG001_00758 | metQ_2 | Methionine-binding lipoprotein MetQ precursor | SAOUHSC_00844 | - | -1,062 | 0,000103352 |
| HG001_00495 | tagE_2 | putative poly(glycerol-phosphate) alpha-glucosyltransferase | SAOUHSC_00548 | - | -1,06 | 2,16E-07 |
| HG001_02647 | hmoB | Heme-degrading monooxygenase HmoB | SAOUHSC_02930 | - | -1,058 | 2,79E-07 |
| HG001_02343 | - | hypothetical protein | SAOUHSC_02581 | - | -1,058 | 6,24E-05 |
| HG001_02226 | - | Zinc-type alcohol dehydrogenase-like protein | SAOUHSC_02445 | - | -1,055 | 1,20E-07 |
| HG001_00114 | wbpA | UDP-N-acetyl-D-glucosamine 6-dehydrogenase | SAOUHSC_00128 | - | -1,052 | 8,31E-07 |
| HG001_00321 | - | hypothetical protein | SAOUHSC_00362 | - | -1,048 | 1,42E-06 |
| HG001_00694 | yfbR | 5'-deoxynucleotidase YfbR | SAOUHSC_00774 | - | -1,047 | 9,13E-06 |
| HG001_01811 | - | tRNA-Met(cat) | SAOUHSC_T00041 | - | -1,044 | 0,002973751 |
| HG001_02419 | - | hypothetical protein | SAOUHSC_02666 | - | -1,042 | 2,49E-05 |
| HG001_00401 | dnaX_2 | DNA polymerase III subunit tau | SAOUHSC_00454 | - | -1,041 | 8,09E-06 |
| HG001_01977 | - | Bacterial SH3 domain protein | SAOUHSC_02170 | - | -1,04 | 0,000180039 |
| HG001_00958 | - | hypothetical protein | SAOUHSC_01055a | - | -1,038 | 1,44E-05 |
| HG001_00182 | - | hypothetical protein | SAOUHSC_00203 | - | -1,038 | 4,52E-05 |
| HG001_02686 | gtf2 | Glycosyltransferase-stabilizing protein Gtf2 | SAOUHSC_02983 | - | -1,036 | 5,89E-05 |
| HG001_00340 | qorB | Quinone oxidoreductase 2 | SAOUHSC_00382 | - | -1,035 | 9,37E-06 |
| HG001_02097 | mazE | Antitoxin MazE | SAOUHSC_02304 | - | -1,031 | 4,06E-06 |
| HG001_02604 | crtP | Diapolycopene oxygenase | SAOUHSC_02881 | - | -1,031 | 1,94E-05 |
| HG001_00727 | - | hypothetical protein | SAOUHSC_00811 | - | -1,031 | 0,000125921 |
| HG001_02530 | - | hypothetical protein | SAOUHSC_02794 | - | -1,028 | 0,00222342 |
| HG001_01814 | - | tRNA-Arg(acg) | SAOUHSC_T0007 | - | -1,027 | 0,007388761 |
| HG001_00626 | yciC_2 | Putative metal chaperone YciC | SAOUHSC_00695 | - | -1,026 | 3,19E-05 |
| HG001_00357 | - | putative lipoprotein precursor | SAOUHSC_00404 | - | -1,025 | 0,000831451 |
| HG001_00436 | - | tRNA-Val(tac) | SAOUHSC_T00059 | - | -1,025 | 0,002443889 |
| HG001_01578 | comC | Type 4 prepilin-like proteins leader peptide-processing enzyme | SAOUHSC_01764 | - | -1,025 | 0,03007429 |
| HG001_02236 | lacR | Lactose phosphotransferase system repressor | SAOUHSC_02456 | - | -1,023 | 4,93E-06 |
| HG001_01820 | - | tRNA-Val(tac) | SAOUHSC_T00060 | - | -1,023 | 0,002914399 |
| HG001_00621 | - | hypothetical protein | SAOUHSC_00690 | - | -1,022 | 2,56E-06 |
| HG001_01366 | - | Phage major tail protein | SAOUHSC_01529 | - | -1,022 | 5,07E-05 |
| HG001_01749 | nisC | Nisin biosynthesis protein NisC | SAOUHSC_01951 | - | -1,018 | 0,000168582 |
| HG001_00443 | - | tRNA-Ala(tgc) | SAOUHSC_T0001 | - | -1,018 | 0,001977909 |
| HG001_01647 | htrA | Serine protease Do-like HtrA | SAOUHSC_01838 | - | -1,016 | 5,59E-06 |
| HG001_00520 | galK_1 | Galactokinase | SAOUHSC_00577 | - | -1,016 | 1,07E-05 |
| HG001_01017 | - | hypothetical protein | SAOUHSC_01130 | - | -1,015 | 1,25E-06 |
| HG001_00210 | rebM | Demethylrebeccamycin-D-glucose O-methyltransferase | SAOUHSC_00237 | - | -1,015 | 0,002756727 |
| HG001_00437 | - | tRNA-Thr(tgt) | SAOUHSC_T00053 | - | -1,014 | 0,005170704 |
| HG001_00507 | - | hypothetical protein | SAOUHSC_00560 | - | -1,014 | 0,008070658 |
| HG001_00824 | ywlC_1 | Threonylcarbamoyl-AMP synthase | SAOUHSC_00915 | - | -1,01 | 0,011835025 |
| HG001_01294 | ebh_1 | Extracellular matrix-binding protein ebh precursor | SAOUHSC_01447 | - | -1,009 | 1,21E-06 |
| HG001_01359 | - | hypothetical protein | SAOUHSC_01522 | - | -1,008 | 0,007891537 |
| HG001_01699 | - | hypothetical protein | SAOUHSC_01896 | - | -1,007 | 7,34E-05 |
| HG001_02088 | - | tRNA-Gly(tcc) | SAOUHSC_T00025 | - | -1,005 | 0,002847856 |
| HG001_00253 | hrtA_1 | Putative hemin import ATP-binding protein HrtA | SAOUHSC_00287 | - | -1,004 | 1,03E-05 |
| HG001_01738 | splE | Serine protease SplE precursor | SAOUHSC_01936 | - | -1,003 | 0,010082431 |
| HG001_01251 | - | Lysine | - | - | -1 | 2,32E-05 |

**Annexe 2 : Tableau de l'expression différentielle des protéines durant le stress oxydant :**

Liste de tous les gènes activés ou inhibés durant le stress oxydant.

| UP regulated genes from the differencial proteomics analysis in oxidative stress | | | |
|---|---|---|---|
| accession | description | LogFC (MV/WT) | adjp |
| HG001_01897 | HG001_01897\|gene_NONE\|hypothetical protein | 9,14 | 1,96E-43 |
| HG001_01902 | HG001_01902\|gene_NONE\|Phage antirepressor protein KilAC domain protein | 9,03 | 5,76E-54 |
| HG001_00066 | HG001_00066\|gene_ala\|Alanine dehydrogenase | 8,63 | 5,62E-28 |
| HG001_01894 | HG001_01894\|gene_NONE\|hypothetical protein | 7,72 | 8,10E-24 |
| HG001_00070 | HG001_00070\|gene_iucC_2\|Aerobactin synthase | 7,41 | 3,27E-19 |
| HG001_01895 | HG001_01895\|gene_NONE\|Bacteriophage Mu Gam like protein | 7,35 | 2,61E-18 |
| HG001_01899 | HG001_01899\|gene_NONE\|hypothetical protein | 7,22 | 7,52E-17 |
| HG001_00299 | HG001_00299\|gene_metE\|5-methyltetrahydropteroyltriglutamate--homocysteine methyltransferase | 7,16 | 7,63E-12 |
| HG001_00071 | HG001_00071\|gene_garL\|5-keto-4-deoxy-D-glucarate aldolase | 6,79 | 1,54E-12 |
| HG001_01880 | HG001_01880\|gene_NONE\|hypothetical protein | 6,23 | 1,47E-08 |
| HG001_00072 | HG001_00072\|gene_btrK\|L-glutamyl-[BtrI acyl-carrier protein] decarboxylase | 6,11 | 7,21E-08 |
| HG001_01879 | HG001_01879\|gene_dut_2\|Deoxyuridine 5'-triphosphate nucleotidohydrolase | 5,91 | 6,65E-07 |
| HG001_01893 | HG001_01893\|gene_NONE\|hypothetical protein | 5,81 | 2,24E-29 |
| HG001_01867 | HG001_01867\|gene_NONE\|hypothetical protein | 5,68 | 6,87E-06 |
| HG001_00069 | HG001_00069\|gene_iucA_1\|N(2)-citryl-N(6)-acetyl-N(6)-hydroxylysine synthase | 5,59 | 1,37E-05 |
| HG001_01873 | HG001_01873\|gene_NONE\|hypothetical protein | 5,50 | 2,76E-05 |
| HG001_00073 | HG001_00073\|gene_NONE\|ParB-like nuclease domain protein | 5,50 | 2,76E-05 |
| HG001_01900 | HG001_01900\|gene_NONE\|hypothetical protein | 5,30 | 1,17E-04 |
| HG001_00067 | HG001_00067\|gene_iucC_1\|Aerobactin synthase | 5,19 | 2,32E-04 |
| HG001_00218 | HG001_00218\|gene_NONE\|Penicillin acylase precursor | 5,07 | 4,70E-04 |
| HG001_01891 | HG001_01891\|gene_NONE\|hypothetical protein | 4,93 | 9,83E-04 |
| HG001_01232 | HG001_01232\|gene_trpB\|Tryptophan synthase beta chain | 4,79 | 2,09E-03 |
| HG001_01883 | HG001_01883\|gene_NONE\|PVL ORF-50-like family protein | 4,44 | 8,53E-03 |
| HG001_01866 | HG001_01866\|gene_NONE\|Phage capsid family protein | 4,23 | 1,64E-02 |
| HG001_00064 | HG001_00064\|gene_yfiY\|putative siderophore-binding lipoprotein YfiY precursor | 3,99 | 8,34E-81 |
| HG001_01859 | HG001_01859\|gene_NONE\|Phage protein | 3,98 | 3,18E-02 |
| HG001_01886 | HG001_01886\|gene_NONE\|hypothetical protein | 3,98 | 3,18E-02 |
| HG001_01884 | HG001_01884\|gene_NONE\|Helix-turn-helix domain protein | 3,68 | 6,59E-02 |
| HG001_02384 | HG001_02384\|gene_lcdH\|L-carnitine dehydrogenase | 3,68 | 6,59E-02 |
| HG001_00977 | HG001_00977\|gene_isdB\|Iron-regulated surface determinant protein B precursor | 3,68 | 6,59E-02 |
| HG001_02135 | HG001_02135\|gene_atpE\|ATP synthase subunit c | 3,30 | 1,23E-01 |
| HG001_02215 | HG001_02215\|gene_NONE\|Alanine racemase | 3,30 | 1,23E-01 |
| HG001_00300 | HG001_00300\|gene_yitJ\|Bifunctional homocysteine S-methyltransferase/5,10-methylenetetrahydrofolate reductase | 3,30 | 1,23E-01 |
| HG001_00269 | HG001_00269\|gene_ymdB\|O-acetyl-ADP-ribose deacetylase | 3,30 | 1,23E-01 |
| HG001_01860 | HG001_01860\|gene_NONE\|Phage major tail protein 2 | 3,30 | 1,23E-01 |
| HG001_01877 | HG001_01877\|gene_NONE\|hypothetical protein | 3,30 | 1,23E-01 |
| HG001_02727 | HG001_02727\|gene_glpE_3\|Thiosulfate sulfurtransferase GlpE | 3,20 | 2,44E-09 |
| HG001_00979 | HG001_00979\|gene_isdC\|Iron-regulated surface determinant protein C precursor | 2,79 | 2,32E-01 |
| HG001_02367 | HG001_02367\|gene_hutI\|Imidazolonepropionase | 2,79 | 2,32E-01 |
| HG001_02216 | HG001_02216\|gene_iucA_2\|N(2)-citryl-N(6)-acetyl-N(6)-hydroxylysine synthase | 2,79 | 2,32E-01 |
| HG001_01865 | HG001_01865\|gene_NONE\|hypothetical protein | 2,79 | 2,32E-01 |
| HG001_00365 | HG001_00365\|gene_NONE\|hypothetical protein | 2,79 | 2,32E-01 |
| HG001_00302 | HG001_00302\|gene_metI\|Cystathionine gamma-synthase/O-acetylhomoserine (thiol)-lyase | 2,79 | 2,32E-01 |
| HG001_00065 | HG001_00065\|gene_sbnA\|putative siderophore biosynthesis protein SbnA | 2,79 | 2,32E-01 |
| HG001_01769 | HG001_01769\|gene_NONE\|Bacterial ABC transporter protein EcsB | 2,79 | 2,32E-01 |
| HG001_01887 | HG001_01887\|gene_NONE\|hypothetical protein | 2,79 | 2,32E-01 |
| HG001_01890 | HG001_01890\|gene_NONE\|hypothetical protein | 2,79 | 2,32E-01 |
| HG001_01049 | HG001_01049\|gene_pyrR\|Bifunctional protein PyrR | 2,76 | 4,52E-09 |
| HG001_02166 | HG001_02166\|gene_dps\|General stress protein 20U | 2,71 | 1,02E-27 |
| HG001_02214 | HG001_02214\|gene_yfmC_2\|Fe(3+)-citrate-binding protein YfmC precursor | 2,62 | 4,81E-52 |
| HG001_01910 | HG001_01910\|gene_xerC_2\|Tyrosine recombinase XerC | 2,45 | 1,19E-01 |
| HG001_02629 | HG001_02629\|gene_pyrD\|Dihydroorotate dehydrogenase (quinone) | 2,33 | 6,96E-12 |
| HG001_00586 | HG001_00586\|gene_yusV_1\|putative siderophore transport system ATP-binding protein YusV | 2,24 | 6,82E-02 |
| HG001_02658 | HG001_02658\|gene_cysJ\|Sulfite reductase [NADPH] flavoprotein alpha-component | 2,03 | 1,30E-11 |
| HG001_00116 | HG001_00116\|gene_isdI\|Heme oxygenase (staphylobilin-producing) 2 | 2,02 | 5,34E-05 |
| HG001_01901 | HG001_01901\|gene_NONE\|hypothetical protein | 1,98 | 4,11E-01 |
| HG001_01227 | HG001_01227\|gene_trpE\|Anthranilate synthase component 1 | 1,98 | 4,11E-01 |
| HG001_01579 | HG001_01579\|gene_fgs\|Folylpolyglutamate synthase | 1,98 | 4,11E-01 |
| HG001_02668 | HG001_02668\|gene_NONE\|S-formylglutathione hydrolase | 1,98 | 4,11E-01 |
| HG001_02600 | HG001_02600\|gene_dapL\|LL-diaminopimelate aminotransferase | 1,98 | 4,11E-01 |
| HG001_01949 | HG001_01949\|gene_nos\|Nitric oxide synthase oxygenase | 1,98 | 4,11E-01 |
| HG001_02029 | HG001_02029\|gene_NONE\|hypothetical protein | 1,98 | 4,11E-01 |
| HG001_02034 | HG001_02034\|gene_NONE\|AntA/AntB antirepressor | 1,98 | 4,11E-01 |
| HG001_02352 | HG001_02352\|gene_yifK\|putative transport protein YifK | 1,98 | 4,11E-01 |
| HG001_02409 | HG001_02409\|gene_NONE\|Acetyltransferase (GNAT) family protein | 1,98 | 4,11E-01 |

| | | |
|---|---|---|
| HG001_01870 HG001_01870\|gene_NONE\|Phage portal protein, SPP1 Gp6-like | 1,98 | 4,11E-01 |
| HG001_00984 HG001_00984\|gene_isdG\|Heme oxygenase (staphylobilin-producing) 1 | 1,98 | 4,11E-01 |
| HG001_01015 HG001_01015\|gene_argF\|Ornithine carbamoyltransferase | 1,98 | 4,11E-01 |
| HG001_01200 HG001_01200\|gene_NONE\|hypothetical protein | 1,98 | 4,11E-01 |
| HG001_02420 HG001_02420\|gene_gltT\|Proton/sodium-glutamate symport protein | 1,98 | 4,11E-01 |
| HG001_01903 HG001_01903\|gene_NONE\|hypothetical protein | 1,98 | 4,11E-01 |
| HG001_02024 HG001_02024\|gene_NONE\|hypothetical protein | 1,98 | 4,11E-01 |
| HG001_02731 HG001_02731\|gene_NONE\|DinB superfamily protein | 1,98 | 4,11E-01 |
| HG001_00277 HG001_00277\|gene_slyA_1\|Transcriptional regulator SlyA | 1,98 | 4,11E-01 |
| HG001_01177 HG001_01177\|gene_NONE\|hypothetical protein | 1,98 | 4,11E-01 |
| HG001_00525 HG001_00525\|gene_NONE\|Transcriptional regulator | 1,98 | 4,11E-01 |
| HG001_02639 HG001_02639\|gene_aldC_2\|Alpha-acetolactate decarboxylase | 1,98 | 4,11E-01 |
| HG001_02423 HG001_02423\|gene_NONE\|Acid shock protein | 1,98 | 4,11E-01 |
| HG001_00981 HG001_00981\|gene_isdE\|High-affinity heme uptake system protein IsdE precursor | 1,98 | 4,11E-01 |
| HG001_00324 HG001_00324\|gene_ahpC\|Alkyl hydroperoxide reductase subunit C | 1,92 | 4,00E-77 |
| HG001_00799 HG001_00799\|gene_mnhA1\|Na(+)/H(+) antiporter subunit A1 | 1,90 | 2,99E-01 |
| HG001_02609 HG001_02609\|gene_isaA\|putative transglycosylase IsaA precursor | 1,88 | 5,26E-02 |
| HG001_00323 HG001_00323\|gene_ahpF\|Alkyl hydroperoxide reductase subunit F | 1,86 | 3,84E-51 |
| HG001_02123 HG001_02123\|gene_sceD\|putative transglycosylase SceD precursor | 1,79 | 4,36E-02 |
| HG001_01025 HG001_01025\|gene_NONE\|putative N-acetyltransferase | 1,74 | 1,46E-01 |
| HG001_02597 HG001_02597\|gene_copA\|Copper-exporting P-type ATPase A | 1,74 | 1,46E-01 |
| HG001_00752 HG001_00752\|gene_NONE\|hypothetical protein | 1,69 | 1,53E-02 |
| HG001_00978 HG001_00978\|gene_isdA\|Iron-regulated surface determinant protein A precursor | 1,66 | 1,01E-04 |
| HG001_00375 HG001_00375\|gene_metQ_1\|putative D-methionine-binding lipoprotein MetQ precursor | 1,65 | 1,23E-01 |
| HG001_00927 HG001_00927\|gene_ykoE\|Putative HMP/thiamine permease protein YkoE | 1,57 | 2,12E-01 |
| HG001_02507 HG001_02507\|gene_nikA\|Nickel-binding periplasmic protein precursor | 1,57 | 1,48E-02 |
| HG001_01912 HG001_01912\|gene_NONE\|putative acyl-CoA thioester hydrolase | 1,53 | 4,35E-01 |
| HG001_02673 HG001_02673\|gene_arcB\|Ornithine carbamoyltransferase, catabolic | 1,53 | 4,35E-01 |
| HG001_00674 HG001_00674\|gene_yclQ\|putative ABC transporter solute-binding protein YclQ precursor | 1,45 | 5,00E-15 |
| HG001_00696 HG001_00696\|gene_uvrB\|UvrABC system protein B | 1,44 | 2,47E-02 |
| HG001_00298 HG001_00298\|gene_kynB\|Kynurenine formamidase | 1,43 | 3,54E-01 |
| HG001_01024 HG001_01024\|gene_yfnB\|Putative HAD-hydrolase YfnB | 1,43 | 3,54E-01 |
| HG001_00186 HG001_00186\|gene_rihA\|Pyrimidine-specific ribonucleoside hydrolase RihA | 1,39 | 2,99E-01 |
| HG001_00712 HG001_00712\|gene_cggR\|Central glycolytic genes regulator | 1,39 | 2,99E-01 |
| HG001_00747 HG001_00747\|gene_fbiB\|Coenzyme F420:L-glutamate ligase | 1,37 | 2,46E-01 |
| HG001_01137 HG001_01137\|gene_recA\|Protein RecA | 1,36 | 5,99E-05 |
| HG001_02247 HG001_02247\|gene_alsS\|Acetolactate synthase | 1,32 | 3,80E-06 |
| HG001_00490 HG001_00490\|gene_ywpJ_1\|Putative phosphatase YwpJ | 1,28 | 8,12E-05 |
| HG001_02276 HG001_02276\|gene_rplX\|50S ribosomal protein L24 | 1,27 | 1,38E-04 |
| HG001_02246 HG001_02246\|gene_aldC_1\|Alpha-acetolactate decarboxylase | 1,26 | 6,63E-10 |
| HG001_01052 HG001_01052\|gene_pyrC\|Dihydroorotase | 1,22 | 8,22E-09 |
| HG001_02320 HG001_02320\|gene_fhuD_2\|Iron(3+)-hydroxamate-binding protein FhuD precursor | 1,18 | 2,08E-09 |
| HG001_01119 HG001_01119\|gene_rplGA\|putative ribosomal protein YlxQ | 1,18 | 4,09E-01 |
| HG001_00328 HG001_00328\|gene_NONE\|hypothetical protein | 1,13 | 4,56E-01 |
| HG001_00476 HG001_00476\|gene_rpsL\|30S ribosomal protein S12 | 1,10 | 2,66E-03 |
| HG001_00491 HG001_00491\|gene_azo1\|FMN-dependent NADPH-azoreductase | 1,05 | 6,55E-04 |
| HG001_00761 HG001_00761\|gene_yurY\|Vegetative protein 296 | 1,04 | 6,61E-06 |
| HG001_01499 HG001_01499\|gene_rpsU\|30S ribosomal protein S21 | 1,03 | 1,27E-03 |
| HG001_02752 HG001_02752\|gene_mnmE\|tRNA modification GTPase MnmE | 1,02 | 2,12E-01 |
| HG001_02228 HG001_02228\|gene_NONE\|hypothetical protein | 1,01 | 6,28E-01 |
| HG001_02190 HG001_02190\|gene_disA\|DNA integrity scanning protein DisA | 1,01 | 6,28E-01 |
| HG001_00411 HG001_00411\|gene_NONE\|hypothetical protein | 1,01 | 6,28E-01 |
| HG001_02649 HG001_02649\|gene_betA\|Oxygen-dependent choline dehydrogenase | 1,01 | 6,28E-01 |
| HG001_00379 HG001_00379\|gene_bltD_1\|Spermine/spermidine acetyltransferase | 1,01 | 6,28E-01 |
| HG001_02259 HG001_02259\|gene_ecfA1\|Energy-coupling factor transporter ATP-binding protein EcfA1 | 1,01 | 6,28E-01 |

**DOWN regulated genes from the differencial proteomics analysis in oxidative stress**

| accession | description | LogFC (MV/WT) | adjp |
|---|---|---|---|
| HG001_00725 | HG001_00725\|gene_NONE\|hypothetical protein | -7,12 | 1,82E-14 |
| HG001_02120 | HG001_02120\|gene_thiD\|Hydroxymethylpyrimidine/phosphomethylpyrimidine kinase | -5,83 | 5,64E-06 |
| HG001_00734 | HG001_00734\|gene_cspA_1\|Cold shock protein CspA | -5,71 | 4,91E-04 |
| HG001_00291 | HG001_00291\|gene_NONE\|hypothetical protein | -5,56 | 4,83E-05 |
| HG001_02681 | HG001_02681\|gene_yvyI\|Putative mannose-6-phosphate isomerase YvyI | -5,40 | 1,34E-04 |
| HG001_01211 | HG001_01211\|gene_NONE\|Iron-sulphur cluster biosynthesis | -5,22 | 3,90E-04 |
| HG001_00803 | HG001_00803\|gene_NONE\|NADH oxidase | -5,13 | 6,61E-04 |
| HG001_01144 | HG001_01144\|gene_miaB\|(Dimethylallyl)adenosine tRNA methylthiotransferase MiaB | -5,02 | 1,32E-03 |
| HG001_02534 | HG001_02534\|gene_sasG\|Surface protein G precursor | -4,91 | 2,09E-03 |
| HG001_02529 | HG001_02529\|gene_pgcA\|Phosphoglucomutase | -4,79 | 3,37E-03 |
| HG001_01115 | HG001_01115\|gene_polC_1\|DNA polymerase III PolC-type | -4,79 | 3,37E-03 |
| HG001_00422 | HG001_00422\|gene_mazG\|Nucleoside triphosphate pyrophosphohydrolase/pyrophosphatase MazG | -4,79 | 3,37E-03 |
| HG001_00774 | HG001_00774\|gene_NONE\|hypothetical protein | -4,79 | 3,37E-03 |
| HG001_01953 | HG001_01953\|gene_rutB\|Peroxyureidoacrylate/ureidoacrylate amidohydrolase RutB | -4,66 | 5,75E-03 |
| HG001_02343 | HG001_02343\|gene_NONE\|hypothetical protein | -4,56 | 4,13E-08 |
| HG001_00480 | HG001_00480\|gene_yxeP_2\|putative hydrolase YxeP | -4,51 | 9,85E-03 |
| HG001_00923 | HG001_00923\|gene_purH\|Bifunctional purine biosynthesis protein PurH | -4,51 | 9,85E-03 |
| HG001_00163 | HG001_00163\|gene_NONE\|Xylose isomerase-like TIM barrel | -4,51 | 9,85E-03 |
| HG001_00223 | HG001_00223\|gene_NONE\|hypothetical protein | -4,51 | 9,85E-03 |
| HG001_01432 | HG001_01432\|gene_malL\|Oligo-1,6-glucosidase | -4,35 | 1,64E-02 |
| HG001_00170 | HG001_00170\|gene_pflA\|Pyruvate formate-lyase-activating enzyme | -4,35 | 1,64E-02 |
| HG001_01129 | HG001_01129\|gene_phnF\|putative transcriptional regulator PhnF | -4,35 | 1,64E-02 |
| HG001_00317 | HG001_00317\|gene_NONE\|hypothetical protein | -4,17 | 2,68E-02 |
| HG001_02432 | HG001_02432\|gene_narW\|putative nitrate reductase molybdenum cofactor assembly chaperone NarW | -4,17 | 2,68E-02 |
| HG001_01917 | HG001_01917\|gene_NONE\|hypothetical protein | -4,17 | 2,68E-02 |
| HG001_02540 | HG001_02540\|gene_gntT\|High-affinity gluconate transporter | -4,17 | 2,68E-02 |
| HG001_00161 | HG001_00161\|gene_ycjS_1\|putative oxidoreductase YcjS | -3,96 | 4,63E-02 |
| HG001_02150 | HG001_02150\|gene_yodB\|HTH-type transcriptional regulator YodB | -3,96 | 4,63E-02 |
| HG001_00694 | HG001_00694\|gene_yfbR\|5'-deoxynucleotidase YfbR | -3,96 | 4,63E-02 |
| HG001_01034 | HG001_01034\|gene_divIB\|Cell division protein DivIB | -3,96 | 4,63E-02 |
| HG001_01645 | HG001_01645\|gene_ptsG_4\|PTS system glucose-specific EIICBA component | -3,96 | 4,63E-02 |
| HG001_02344 | HG001_02344\|gene_NONE\|Putative formate dehydrogenase | -3,93 | 1,23E-21 |
| HG001_01549 | HG001_01549\|gene_NONE\|CsbD-like protein | -3,84 | 1,17E-04 |
| HG001_00768 | HG001_00768\|gene_NONE\|Nitronate monooxygenase | -3,72 | 7,39E-02 |
| HG001_00999 | HG001_00999\|gene_murI\|Glutamate racemase | -3,72 | 7,39E-02 |
| HG001_00598 | HG001_00598\|gene_graR_1\|Response regulator protein GraR | -3,72 | 7,39E-02 |
| HG001_01028 | HG001_01028\|gene_mraZ\|Protein MraZ | -3,72 | 7,39E-02 |
| HG001_00180 | HG001_00180\|gene_gsiB\|Glutathione-binding protein GsiB precursor | -3,72 | 7,39E-02 |
| HG001_00142 | HG001_00142\|gene_NONE\|PTS system EIIBC component | -3,72 | 7,39E-02 |
| HG001_02625 | HG001_02625\|gene_NONE\|hypothetical protein | -3,72 | 7,39E-02 |
| HG001_01255 | HG001_01255\|gene_dapB\|4-hydroxy-tetrahydrodipicolinate reductase | -3,72 | 7,39E-02 |
| HG001_01150 | HG001_01150\|gene_glpF\|Glycerol uptake facilitator protein | -3,72 | 7,39E-02 |
| HG001_02424 | HG001_02424\|gene_narT\|putative nitrate transporter NarT | -3,72 | 7,39E-02 |
| HG001_01724 | HG001_01724\|gene_NONE\|Telomeric repeat-binding factor 2 | -3,71 | 7,39E-02 |
| HG001_02099 | HG001_02099\|gene_acpS\|Holo-[acyl-carrier-protein] synthase | -3,71 | 7,39E-02 |
| HG001_01612 | HG001_01612\|gene_phoP\|Alkaline phosphatase synthesis transcriptional regulatory protein PhoP | -3,42 | 1,23E-01 |
| HG001_00916 | HG001_00916\|gene_purC\|Phosphoribosylaminoimidazole-succinocarboxamide synthase | -3,42 | 1,23E-01 |
| HG001_00826 | HG001_00826\|gene_NONE\|putative kinase inhibitor | -3,42 | 1,23E-01 |
| HG001_01319 | HG001_01319\|gene_pimB\|GDP-mannose-dependent alpha-(1-6)-phosphatidylinositol monomannoside mannosy | -3,42 | 1,23E-01 |
| HG001_00724 | HG001_00724\|gene_NONE\|hypothetical protein | -3,42 | 1,23E-01 |
| HG001_01351 | HG001_01351\|gene_NONE\|hypothetical protein | -3,42 | 1,23E-01 |
| HG001_00449 | HG001_00449\|gene_pdxT\|Glutamine amidotransferase subunit PdxT | -3,42 | 1,23E-01 |
| HG001_00793 | HG001_00793\|gene_mnhG1\|Na(+)/H(+) antiporter subunit G1 | -3,42 | 1,23E-01 |
| HG001_00206 | HG001_00206\|gene_lrgB\|Antiholin-like protein LrgB | -3,42 | 1,23E-01 |
| HG001_00392 | HG001_00392\|gene_NONE\|Acetyltransferase (GNAT) family protein | -3,42 | 1,23E-01 |
| HG001_01537 | HG001_01537\|gene_NONE\|Putative O-methyltransferase/MSMEI_4947 | -3,42 | 1,23E-01 |
| HG001_02483 | HG001_02483\|gene_NONE\|UDP-glucose 4-epimerase | -3,42 | 1,23E-01 |
| HG001_01079 | HG001_01079\|gene_fapR\|Transcription factor FapR | -3,42 | 1,23E-01 |
| HG001_01666 | HG001_01666\|gene_pepA_2\|Glutamyl aminopeptidase | -3,42 | 2,68E-05 |
| HG001_02592 | HG001_02592\|gene_ydfJ\|Membrane protein YdfJ | -3,25 | 6,71E-08 |
| HG001_00395 | HG001_00395\|gene_recR\|Recombination protein RecR | -3,05 | 2,00E-01 |
| HG001_01694 | HG001_01694\|gene_NONE\|hypothetical protein | -3,05 | 2,00E-01 |
| HG001_00274 | HG001_00274\|gene_NONE\|PTS system ascorbate-specific transporter subunits IICB | -3,05 | 2,00E-01 |
| HG001_01919 | HG001_01919\|gene_vraS\|Sensor protein VraS | -3,05 | 2,00E-01 |

| | | |
|---|---|---|
| HG001_01216 HG001_01216\|gene_glcT\|GlcA/glcB genes antiterminator | -3,05 | 2,00E-01 |
| HG001_00494 HG001_00494\|gene_tagE_1\|putative poly(glycerol-phosphate) alpha-glucosyltransferase | -3,05 | 2,00E-01 |
| HG001_02500 HG001_02500\|gene_gltB_2\|Glutamate synthase [NADPH] large chain precursor | -3,05 | 2,00E-01 |
| HG001_00262 HG001_00262\|gene_nanE\|Putative N-acetylmannosamine-6-phosphate 2-epimerase | -3,05 | 2,00E-01 |
| HG001_01908 HG001_01908\|gene_NONE\|hypothetical protein | -3,05 | 2,00E-01 |
| HG001_01164 HG001_01164\|gene_NONE\|hypothetical protein | -3,05 | 2,00E-01 |
| HG001_02308 HG001_02308\|gene_mobB\|Molybdopterin-guanine dinucleotide biosynthesis adapter protein | -3,05 | 2,00E-01 |
| HG001_01066 HG001_01066\|gene_def1\|Peptide deformylase 1 | -3,05 | 2,00E-01 |
| HG001_01299 HG001_01299\|gene_ypcP\|5'-3' exonuclease | -3,05 | 2,00E-01 |
| HG001_01501 HG001_01501\|gene_mtaB_2\|Threonylcarbamoyladenosine tRNA methylthiotransferase MtaB | -3,05 | 2,00E-01 |
| HG001_00784 HG001_00784\|gene_NONE\|hypothetical protein | -3,05 | 2,00E-01 |
| HG001_00162 HG001_00162\|gene_ycjS_2\|putative oxidoreductase YcjS | -3,05 | 2,00E-01 |
| HG001_00921 HG001_00921\|gene_purM\|Phosphoribosylformylglycinamidine cyclo-ligase | -3,05 | 2,00E-01 |
| HG001_02576 HG001_02576\|gene_NONE\|hypothetical protein | -3,05 | 2,00E-01 |
| HG001_02442 HG001_02442\|gene_NONE\|hypothetical protein | -3,05 | 2,00E-01 |
| HG001_00885 HG001_00885\|gene_NONE\|hypothetical protein | -3,05 | 2,00E-01 |
| HG001_02634 HG001_02634\|gene_cocE\|Cocaine esterase | -3,05 | 2,00E-01 |
| HG001_00736 HG001_00736\|gene_NONE\|hypothetical protein | -3,05 | 2,00E-01 |
| HG001_01470 HG001_01470\|gene_NONE\|putative metallo-hydrolase | -3,05 | 2,00E-01 |
| HG001_01087 HG001_01087\|gene_NONE\|putative DNA-binding protein | -3,05 | 2,00E-01 |
| HG001_00627 HG001_00627\|gene_ydhF\|Oxidoreductase YdhF | -3,05 | 2,00E-01 |
| HG001_01674 HG001_01674\|gene_rsuA\|Ribosomal small subunit pseudouridine synthase A | -3,05 | 2,00E-01 |
| HG001_02126 HG001_02126\|gene_fabZ\|3-hydroxyacyl-[acyl-carrier-protein] dehydratase FabZ | -3,05 | 2,00E-01 |
| HG001_01697 HG001_01697\|gene_arsC2\|Arsenate-mycothiol transferase ArsC2 | -3,05 | 2,00E-01 |
| HG001_02680 HG001_02680\|gene_manP\|PTS system mannose-specific EIIBCA component | -3,04 | 6,72E-04 |
| HG001_00940 HG001_00940\|gene_NONE\|hypothetical protein | -2,93 | 2,20E-02 |
| HG001_00541 HG001_00541\|gene_mshD_1\|Mycothiol acetyltransferase | -2,93 | 2,20E-02 |
| HG001_00331 HG001_00331\|gene_xpt\|Xanthine phosphoribosyltransferase | -2,84 | 8,52E-08 |
| HG001_00410 HG001_00410\|gene_rsmA\|Ribosomal RNA small subunit methyltransferase A | -2,81 | 3,33E-02 |
| HG001_00118 HG001_00118\|gene_aldA\|Putative aldehyde dehydrogenase AldA | -2,81 | 3,33E-02 |
| HG001_01513 HG001_01513\|gene_tadA_2\|tRNA-specific adenosine deaminase | -2,77 | 4,33E-03 |
| HG001_01905 HG001_01905\|gene_immR_1\|HTH-type transcriptional regulator ImmR | -2,69 | 6,50E-03 |
| HG001_00420 HG001_00420\|gene_mfd\|Transcription-repair-coupling factor | -2,67 | 5,36E-02 |
| HG001_01661 HG001_01661\|gene_murC\|UDP-N-acetylmuramate--L-alanine ligase | -2,61 | 1,00E-02 |
| HG001_00145 HG001_00145\|gene_hsdR\|Type-1 restriction enzyme R protein | -2,57 | 2,96E-04 |
| HG001_02434 HG001_02434\|gene_narG\|Respiratory nitrate reductase 1 alpha chain | -2,56 | 1,47E-13 |
| HG001_02038 HG001_02038\|gene_lexA_3\|LexA repressor | -2,55 | 2,99E-01 |
| HG001_00032 HG001_00032\|gene_csoR_1\|Copper-sensing transcriptional repressor CsoR | -2,55 | 2,99E-01 |
| HG001_01551 HG001_01551\|gene_rarA\|Replication-associated recombination protein A | -2,55 | 2,99E-01 |
| HG001_02090 HG001_02090\|gene_NONE\|Protein SprT-like protein | -2,55 | 2,99E-01 |
| HG001_02542 HG001_02542\|gene_ydfH\|putative HTH-type transcriptional regulator YdfH | -2,55 | 2,99E-01 |
| HG001_01298 HG001_01298\|gene_ald1\|Alanine dehydrogenase 1 | -2,55 | 2,99E-01 |
| HG001_02487 HG001_02487\|gene_opuCC\|Carnitine transport binding protein OpuCC precursor | -2,55 | 2,99E-01 |
| HG001_01961 HG001_01961\|gene_NONE\|hypothetical protein | -2,55 | 2,99E-01 |
| HG001_01132 HG001_01132\|gene_phbB\|Acetoacetyl-CoA reductase | -2,55 | 2,99E-01 |
| HG001_00406 HG001_00406\|gene_rsmI\|Ribosomal RNA small subunit methyltransferase I | -2,55 | 2,99E-01 |
| HG001_00228 HG001_00228\|gene_NONE\|hypothetical protein | -2,55 | 2,99E-01 |
| HG001_00029 HG001_00029\|gene_NONE\|hypothetical protein | -2,55 | 2,99E-01 |
| HG001_01136 HG001_01136\|gene_cinA\|Putative competence-damage inducible protein | -2,55 | 2,99E-01 |
| HG001_01145 HG001_01145\|gene_NONE\|hypothetical protein | -2,55 | 2,99E-01 |
| HG001_00914 HG001_00914\|gene_purE\|N5-carboxyaminoimidazole ribonucleotide mutase | -2,55 | 2,99E-01 |
| HG001_02178 HG001_02178\|gene_NONE\|SAP domain protein | -2,55 | 2,99E-01 |
| HG001_00609 HG001_00609\|gene_NONE\|hypothetical protein | -2,55 | 2,99E-01 |
| HG001_02686 HG001_02686\|gene_gtf2\|Glycosyltransferase-stabilizing protein Gtf2 | -2,55 | 2,99E-01 |
| HG001_01931 HG001_01931\|gene_NONE\|putative RNA methyltransferase | -2,55 | 2,99E-01 |
| HG001_00568 HG001_00568\|gene_nhaK_1\|Sodium, potassium, lithium and rubidium/H(+) antiporter | -2,55 | 2,99E-01 |
| HG001_01163 HG001_01163\|gene_NONE\|hypothetical protein | -2,55 | 2,99E-01 |
| HG001_01676 HG001_01676\|gene_NONE\|Ferredoxin--NADP reductase | -2,55 | 2,99E-01 |
| HG001_00904 HG001_00904\|gene_yjcF\|putative N-acetyltransferase YjcF | -2,55 | 2,99E-01 |
| HG001_02141 HG001_02141\|gene_NONE\|hypothetical protein | -2,55 | 2,99E-01 |
| HG001_01833 HG001_01833\|gene_yfhQ\|putative A/G-specific adenine glycosylase YfhQ | -2,55 | 2,99E-01 |
| HG001_00767 HG001_00767\|gene_tlyC\|Hemolysin C | -2,55 | 2,99E-01 |
| HG001_00919 HG001_00919\|gene_purL\|Phosphoribosylformylglycinamidine synthase 2 | -2,55 | 2,99E-01 |
| HG001_02545 HG001_02545\|gene_NONE\|hypothetical protein | -2,55 | 2,99E-01 |
| HG001_00175 HG001_00175\|gene_fadN\|putative 3-hydroxyacyl-CoA dehydrogenase | -2,55 | 2,99E-01 |
| HG001_00616 HG001_00616\|gene_NONE\|hypothetical protein | -2,55 | 2,99E-01 |

| | | |
|---|---|---|
| HG001_00746 HG001_00746\|gene_aroD\|3-dehydroquinate dehydratase | -2,55 | 2,99E-01 |
| HG001_01669 HG001_01669\|gene_trmB\|tRNA (guanine-N(7)-)-methyltransferase | -2,55 | 2,99E-01 |
| HG001_01543 HG001_01543\|gene_recD2\|ATP-dependent RecD-like DNA helicase | -2,55 | 2,99E-01 |
| HG001_00540 HG001_00540\|gene_ywqN_2\|Putative NAD(P)H-dependent FMN-containing oxidoreductase YwqN | -2,55 | 2,99E-01 |
| HG001_00185 HG001_00185\|gene_ptsG_2\|PTS system glucose-specific EIICBA component | -2,55 | 2,99E-01 |
| HG001_00926 HG001_00926\|gene_ykoD_1\|Putative HMP/thiamine import ATP-binding protein YkoD | -2,55 | 2,99E-01 |
| HG001_00633 | -2,55 | 2,99E-01 |
| HG001_00378 HG001_00378\|gene_nudC\|NADH pyrophosphatase | -2,55 | 2,99E-01 |
| HG001_01664 HG001_01664\|gene_NONE\|hypothetical protein | -2,55 | 2,99E-01 |
| HG001_00305 HG001_00305\|gene_ykuT\|putative MscS family protein YkuT | -2,55 | 2,99E-01 |
| HG001_02429 HG001_02429\|gene_nreB\|Oxygen sensor histidine kinase NreB | -2,55 | 2,99E-01 |
| HG001_01682 HG001_01682\|gene_bioB_1\|Biotin synthase | -2,55 | 2,99E-01 |
| HG001_00811 HG001_00811\|gene_spsB_1\|Signal peptidase IB | -2,55 | 2,99E-01 |
| HG001_00377 HG001_00377\|gene_NONE\|hypothetical protein | -2,55 | 2,99E-01 |
| HG001_01217 HG001_01217\|gene_tqsA\|AI-2 transport protein TqsA | -2,55 | 2,99E-01 |
| HG001_01842 HG001_01842\|gene_NONE\|putative phage protein 3 of sapT operon | -2,55 | 2,99E-01 |
| HG001_02480 HG001_02480\|gene_nhaK_2\|Sodium, potassium, lithium and rubidium/H(+) antiporter | -2,55 | 2,99E-01 |
| HG001_01040 HG001_01040\|gene_NONE\|YGGT family protein | -2,55 | 2,99E-01 |
| HG001_02035 HG001_02035\|gene_NONE\|hypothetical protein | -2,55 | 2,99E-01 |
| HG001_00120 HG001_00120\|gene_NONE\|hypothetical protein | -2,55 | 2,99E-01 |
| HG001_01667 HG001_01667\|gene_NONE\|Peptidase propeptide and YPEB domain protein | -2,55 | 2,99E-01 |
| HG001_00125 HG001_00125\|gene_NONE\|hypothetical protein | -2,55 | 2,99E-01 |
| HG001_00660 HG001_00660\|gene_opuBA\|Choline transport ATP-binding protein OpuBA | -2,43 | 2,30E-02 |
| HG001_01478 HG001_01478\|gene_zur\|Zinc-specific metallo-regulatory protein | -2,19 | 1,80E-01 |
| HG001_01069 HG001_01069\|gene_rlmN\|putative dual-specificity RNA methyltransferase RlmN | -2,19 | 1,80E-01 |
| HG001_02183 HG001_02183\|gene_mtlA\|PTS system mannitol-specific EIICB component | -2,18 | 1,80E-01 |
| HG001_00387 HG001_00387\|gene_treA\|Trehalose-6-phosphate hydrolase | -2,18 | 1,80E-01 |
| HG001_01449 HG001_01449\|gene_NONE\|hypothetical protein | -2,18 | 2,04E-02 |
| HG001_00358 HG001_00358\|gene_lpl2\|putative lipoprotein precursor | -2,13 | 1,19E-04 |
| HG001_00579 HG001_00579\|gene_tagX\|Putative glycosyltransferase TagX | -2,12 | 7,39E-02 |
| HG001_01788 HG001_01788\|gene_trmL\|tRNA (cytidine(34)-2'-O)-methyltransferase | -2,12 | 7,39E-02 |
| HG001_01495 HG001_01495\|gene_ybeZ\|PhoH-like protein | -2,12 | 7,39E-02 |
| HG001_02433 HG001_02433\|gene_narH\|Respiratory nitrate reductase 1 beta chain | -2,06 | 2,56E-04 |
| HG001_00018 HG001_00018\|gene_dnaC_1\|Replicative DNA helicase | -2,00 | 1,08E-01 |
| HG001_00819 HG001_00819\|gene_NONE\|hypothetical protein | -1,98 | 2,47E-01 |
| HG001_01827 HG001_01827\|gene_ghrB_2\|Glyoxylate/hydroxypyruvate reductase B | -1,98 | 2,47E-01 |
| HG001_00412 HG001_00412\|gene_ispE\|4-diphosphocytidyl-2-C-methyl-D-erythritol kinase | -1,98 | 2,47E-01 |
| HG001_00857 HG001_00857\|gene_kefC\|Glutathione-regulated potassium-efflux system protein KefC | -1,98 | 2,47E-01 |
| HG001_01091 HG001_01091\|gene_trmD\|tRNA (guanine-N(1)-)-methyltransferase | -1,98 | 2,47E-01 |
| HG001_00594 HG001_00594\|gene_aes\|Acetyl esterase | -1,98 | 2,47E-01 |
| HG001_00402 HG001_00402\|gene_NONE\|hypothetical protein | -1,98 | 2,47E-01 |
| HG001_00865 HG001_00865\|gene_murE_1\|UDP-N-acetylmuramoyl-L-alanyl-D-glutamate--L-lysine ligase | -1,94 | 1,65E-04 |
| HG001_01775 HG001_01775\|gene_yhaM\|3'-5' exoribonuclease YhaM | -1,88 | 3,47E-02 |
| HG001_01118 HG001_01118\|gene_NONE\|hypothetical protein | -1,87 | 1,50E-01 |
| HG001_00576 HG001_00576\|gene_tagH_1\|Teichoic acids export ATP-binding protein TagH | -1,87 | 1,50E-01 |
| HG001_01783 HG001_01783\|gene_rluD_3\|Ribosomal large subunit pseudouridine synthase D | -1,85 | 1,95E-02 |
| HG001_02693 HG001_02693\|gene_sraP\|Serine-rich adhesin for platelets precursor | -1,83 | 8,66E-02 |
| HG001_02588 HG001_02588\|gene_clpL\|ATP-dependent Clp protease ATP-binding subunit ClpL | -1,81 | 8,88E-14 |
| HG001_00849 HG001_00849\|gene_NONE\|hypothetical protein | -1,78 | 4,42E-01 |
| HG001_01643 HG001_01643\|gene_serA\|D-3-phosphoglycerate dehydrogenase | -1,78 | 4,42E-01 |
| HG001_00084 HG001_00084\|gene_treR_1\|Trehalose operon transcriptional repressor | -1,78 | 4,42E-01 |
| HG001_02238 HG001_02238\|gene_NONE\|hypothetical protein | -1,78 | 4,42E-01 |
| HG001_01967 HG001_01967\|gene_ytrB_2\|ABC transporter ATP-binding protein YtrB | -1,78 | 4,42E-01 |
| HG001_01030 HG001_01030\|gene_ftsL\|Cell division protein FtsL | -1,78 | 4,42E-01 |
| HG001_02185 HG001_02185\|gene_mtlF\|Mannitol-specific phosphotransferase enzyme IIA component | -1,78 | 4,42E-01 |
| HG001_00709 HG001_00709\|gene_NONE\|Epimerase family protein | -1,78 | 4,42E-01 |
| HG001_01308 HG001_01308\|gene_NONE\|hypothetical protein | -1,78 | 4,42E-01 |
| HG001_01675 HG001_01675\|gene_ytgP_2\|putative cell division protein YtgP | -1,78 | 4,42E-01 |
| HG001_02541 HG001_02541\|gene_xylB\|Xylulose kinase | -1,78 | 4,42E-01 |
| HG001_00653 HG001_00653\|gene_pabB\|Aminodeoxychorismate synthase component 1 | -1,78 | 4,42E-01 |
| HG001_02304 HG001_02304\|gene_moaA\|Cyclic pyranopterin monophosphate synthase | -1,78 | 4,42E-01 |
| HG001_01158 HG001_01158\|gene_NONE\|methionine gamma-lyase | -1,78 | 4,42E-01 |
| HG001_01520 HG001_01520\|gene_aroE\|Shikimate dehydrogenase | -1,78 | 4,42E-01 |
| HG001_01642 HG001_01642\|gene_NONE\|Soluble hydrogenase 42 kDa subunit | -1,78 | 4,42E-01 |
| HG001_01159 HG001_01159\|gene_glnR\|HTH-type transcriptional regulator GlnR | -1,78 | 4,42E-01 |
| HG001_02258 HG001_02258\|gene_ecfA2\|Energy-coupling factor transporter ATP-binding protein EcfA2 | -1,78 | 4,42E-01 |

| | | |
|---|---|---|
| HG001_02521 HG001_02521\|gene_NONE\|putative lipoprotein precursor | -1,78 | 4,42E-01 |
| HG001_01654 HG001_01654\|gene_acsA_1\|Acetyl-coenzyme A synthetase | -1,78 | 4,42E-01 |
| HG001_00447 HG001_00447\|gene_gabR\|HTH-type transcriptional regulatory protein GabR | -1,78 | 4,42E-01 |
| HG001_01944 HG001_01944\|gene_NONE\|Staphostatin A | -1,78 | 4,42E-01 |
| HG001_01770 HG001_01770\|gene_ecsA\|ABC-type transporter ATP-binding protein EcsA | -1,78 | 4,42E-01 |
| HG001_02377 HG001_02377\|gene_NONE\|ABC-2 family transporter protein | -1,78 | 4,42E-01 |
| HG001_00744 HG001_00744\|gene_NONE\|hypothetical protein | -1,78 | 4,42E-01 |
| HG001_02495 HG001_02495\|gene_ybbL\|putative ABC transporter ATP-binding protein YbbL | -1,78 | 4,42E-01 |
| HG001_00844 HG001_00844\|gene_mecA\|Adapter protein MecA | -1,78 | 4,42E-01 |
| HG001_01326 HG001_01326\|gene_aroB\|3-dehydroquinate synthase | -1,78 | 4,42E-01 |
| HG001_00052 HG001_00052\|gene_yxeP_1\|putative hydrolase YxeP | -1,78 | 4,42E-01 |
| HG001_02570 HG001_02570\|gene_sdhB\|L-serine dehydratase, beta chain | -1,78 | 4,42E-01 |
| HG001_02359 HG001_02359\|gene_malP\|PTS system maltose-specific EIICB component | -1,78 | 4,42E-01 |
| HG001_00092 HG001_00092\|gene_phnD\|Phosphate-import protein PhnD precursor | -1,78 | 4,42E-01 |
| HG001_01410 HG001_01410\|gene_NONE\|hypothetical protein | -1,78 | 4,42E-01 |
| HG001_00522 HG001_00522\|gene_galK_2\|Galactokinase | -1,78 | 4,42E-01 |
| HG001_01176 HG001_01176\|gene_ltaE\|Low specificity L-threonine aldolase | -1,78 | 4,42E-01 |
| HG001_01530 HG001_01530\|gene_accB_2\|Biotin carboxyl carrier protein of acetyl-CoA carboxylase | -1,78 | 4,42E-01 |
| HG001_01945 HG001_01945\|gene_NONE\|hypothetical protein | -1,78 | 4,42E-01 |
| HG001_02485 HG001_02485\|gene_norB_5\|Quinolone resistance protein NorB | -1,78 | 4,42E-01 |
| HG001_01037 HG001_01037\|gene_NONE\|Laccase domain protein | -1,78 | 4,42E-01 |
| HG001_00656 HG001_00656\|gene_kipA_1\|KipI antagonist | -1,78 | 4,42E-01 |
| HG001_02422 HG001_02422\|gene_sarZ\|HTH-type transcriptional regulator SarZ | -1,78 | 4,42E-01 |
| HG001_01011 HG001_01011\|gene_NONE\|hypothetical protein | -1,78 | 4,42E-01 |
| HG001_00718 HG001_00718\|gene_NONE\|hypothetical protein | -1,78 | 4,42E-01 |
| HG001_00554 HG001_00554\|gene_NONE\|hypothetical protein | -1,78 | 4,42E-01 |
| HG001_01608 HG001_01608\|gene_mutM\|Formamidopyrimidine-DNA glycosylase | -1,78 | 4,42E-01 |
| HG001_01095 HG001_01095\|gene_rnhB\|Ribonuclease HII | -1,78 | 4,42E-01 |
| HG001_00972 HG001_00972\|gene_rsmD\|Ribosomal RNA small subunit methyltransferase D | -1,78 | 4,42E-01 |
| HG001_02157 HG001_02157\|gene_coaW\|Type II pantothenate kinase | -1,78 | 4,42E-01 |
| HG001_01084 HG001_01084\|gene_rnc\|Ribonuclease 3 | -1,78 | 4,42E-01 |
| HG001_00025 HG001_00025\|gene_yycI\|Two-component system YycFG regulatory protein | -1,78 | 4,42E-01 |
| HG001_01365 HG001_01365\|gene_NONE\|Bacterial Ig-like domain (group 2) | -1,78 | 4,42E-01 |
| HG001_01540 HG001_01540\|gene_NONE\|hypothetical protein | -1,78 | 4,42E-01 |
| HG001_02628 HG001_02628\|gene_NONE\|Fructosamine kinase | -1,78 | 4,42E-01 |
| HG001_01604 HG001_01604\|gene_dnaB\|Replication initiation and membrane attachment protein | -1,78 | 4,42E-01 |
| HG001_00806 HG001_00806\|gene_glpQ1_1\|putative glycerophosphoryl diester phosphodiesterase 1 | -1,78 | 4,42E-01 |
| HG001_01792 HG001_01792\|gene_NONE\|Phosphotransferase system, EIIC | -1,78 | 4,42E-01 |
| HG001_02063 HG001_02063\|gene_iolC\|5-dehydro-2-deoxygluconokinase | -1,78 | 4,42E-01 |
| HG001_00461 HG001_00461\|gene_mrnC\|Mini-ribonuclease 3 | -1,78 | 4,42E-01 |
| HG001_00894 HG001_00894\|gene_menD\|2-succinyl-5-enolpyruvyl-6-hydroxy-3-cyclohexene-1-carboxylate synthase | -1,78 | 4,42E-01 |
| HG001_00520 HG001_00520\|gene_galK_1\|Galactokinase | -1,78 | 4,42E-01 |
| HG001_01218 HG001_01218\|gene_mprF\|Phosphatidylglycerol lysyltransferase | -1,78 | 4,42E-01 |
| HG001_01536 HG001_01536\|gene_yhbU_2\|putative protease YhbU precursor | -1,78 | 4,42E-01 |
| HG001_01518 HG001_01518\|gene_nadD\|putative nicotinate-nucleotide adenylyltransferase | -1,78 | 4,42E-01 |
| HG001_00989 HG001_00989\|gene_rnhC\|Ribonuclease HIII | -1,78 | 4,42E-01 |
| HG001_00027 HG001_00027\|gene_yfkN_1\|Trifunctional nucleotide phosphoesterase protein YfkN precursor | -1,78 | 4,42E-01 |
| HG001_01297 HG001_01297\|gene_tdcB\|L-threonine dehydratase catabolic TdcB | -1,78 | 4,42E-01 |
| HG001_02611 HG001_02611\|gene_NONE\|DNA-binding transcriptional regulator EnvR | -1,78 | 4,42E-01 |
| HG001_01135 HG001_01135\|gene_pgsA\|CDP-diacylglycerol--glycerol-3-phosphate 3-phosphatidyltransferase | -1,78 | 4,42E-01 |
| HG001_02101 HG001_02101\|gene_NONE\|Bacterial membrane flanked domain protein | -1,78 | 4,42E-01 |
| HG001_00564 HG001_00564\|gene_mnhD1_1\|Na(+)/H(+) antiporter subunit D1 | -1,78 | 4,42E-01 |
| HG001_02616 HG001_02616\|gene_NONE\|hypothetical protein | -1,78 | 4,42E-01 |
| HG001_00054 HG001_00054\|gene_NONE\|Na+/Pi-cotransporter | -1,78 | 4,42E-01 |
| HG001_00610 HG001_00610\|gene_NONE\|hypothetical protein | -1,78 | 4,42E-01 |
| HG001_01831 HG001_01831\|gene_NONE\|Putative multidrug export ATP-binding/permease protein | -1,78 | 4,42E-01 |
| HG001_00780 HG001_00780\|gene_patA_1\|Peptidoglycan O-acetyltransferase | -1,78 | 4,42E-01 |
| HG001_01262 HG001_01262\|gene_NONE\|hypothetical protein | -1,78 | 4,42E-01 |
| HG001_02383 HG001_02383\|gene_corA\|Magnesium transport protein CorA | -1,78 | 4,42E-01 |
| HG001_01207 HG001_01207\|gene_mscL\|Large-conductance mechanosensitive channel | -1,78 | 4,42E-01 |
| HG001_02599 HG001_02599\|gene_ldhD_2\|D-lactate dehydrogenase | -1,78 | 4,42E-01 |
| HG001_00247 HG001_00247\|gene_NONE\|hypothetical protein | -1,78 | 4,42E-01 |
| HG001_01535 HG001_01535\|gene_yhbU_1\|putative protease YhbU precursor | -1,78 | 4,42E-01 |
| HG001_02608 HG001_02608\|gene_NONE\|Acetyltransferase (GNAT) family protein | -1,78 | 4,42E-01 |
| HG001_00099 HG001_00099\|gene_adhE\|Aldehyde-alcohol dehydrogenase | -1,78 | 4,42E-01 |
| HG001_01032 HG001_01032\|gene_mraY\|Phospho-N-acetylmuramoyl-pentapeptide-transferase | -1,78 | 4,42E-01 |

| | | |
|---|---|---|
| HG001_02726 HG001_02726\|gene_NONE\|Lactonase drp35 | -1,78 | 4,42E-01 |
| HG001_02593 HG001_02593\|gene_NONE\|hypothetical protein | -1,78 | 4,42E-01 |
| HG001_00974 HG001_00974\|gene_NONE\|hypothetical protein | -1,78 | 4,42E-01 |
| HG001_01480 HG001_01480\|gene_znuC_2\|High-affinity zinc uptake system ATP-binding protein ZnuC | -1,78 | 4,42E-01 |
| HG001_00664 HG001_00664\|gene_NONE\|Putative lipid kinase | -1,78 | 4,42E-01 |
| HG001_00553 HG001_00553\|gene_NONE\|hypothetical protein | -1,77 | 1,54E-02 |
| HG001_00967 HG001_00967\|gene_NONE\|Cysteine-rich secretory protein family protein | -1,73 | 3,26E-01 |
| HG001_02489 HG001_02489\|gene_opuCA\|Carnitine transport ATP-binding protein OpuCA | -1,73 | 3,26E-01 |
| HG001_02115 HG001_02115\|gene_cls_2\|Cardiolipin synthase | -1,73 | 3,26E-01 |
| HG001_00668 HG001_00668\|gene_nrdI\|Protein NrdI | -1,73 | 3,26E-01 |
| HG001_01063 HG001_01063\|gene_priA\|Primosomal protein N' | -1,73 | 3,26E-01 |
| HG001_02326 HG001_02326\|gene_ureE\|Urease accessory protein UreE | -1,73 | 3,26E-01 |
| HG001_02319 HG001_02319\|gene_rihB\|Pyrimidine-specific ribonucleoside hydrolase RihB | -1,73 | 3,26E-01 |
| HG001_02373 HG001_02373\|gene_rpiA\|Ribose-5-phosphate isomerase A | -1,73 | 3,26E-01 |
| HG001_00304 HG001_00304\|gene_spo0C\|Chromosome-partitioning protein Spo0J | -1,73 | 3,26E-01 |
| HG001_02631 HG001_02631\|gene_NONE\|hypothetical protein | -1,73 | 3,26E-01 |
| HG001_01424 HG001_01424\|gene_nudF\|ADP-ribose pyrophosphatase | -1,73 | 3,26E-01 |
| HG001_00686 HG001_00686\|gene_yigZ\|IMPACT family member YigZ | -1,73 | 3,26E-01 |
| HG001_00818 HG001_00818\|gene_yidA\|Sugar phosphatase YidA | -1,72 | 2,04E-01 |
| HG001_00705 HG001_00705\|gene_NONE\|Gluconeogenesis factor | -1,72 | 2,04E-01 |
| HG001_01237 HG001_01237\|gene_NONE\|hypothetical protein | -1,72 | 2,04E-01 |
| HG001_00463 HG001_00463\|gene_NONE\|YacP-like NYN domain protein | -1,72 | 2,04E-01 |
| HG001_02615 HG001_02615\|gene_azoB\|NAD(P)H azoreductase | -1,72 | 2,05E-01 |
| HG001_01085 HG001_01085\|gene_smc\|Chromosome partition protein Smc | -1,72 | 1,23E-01 |
| HG001_00022 HG001_00022\|gene_walR\|Transcriptional regulatory protein WalR | -1,72 | 6,91E-02 |
| HG001_01279 HG001_01279\|gene_NONE\|Acetyltransferase (GNAT) family protein | -1,72 | 3,76E-02 |
| HG001_00319 HG001_00319\|gene_gpmA_1\|2,3-bisphosphoglycerate-dependent phosphoglycerate mutase | -1,72 | 7,06E-02 |
| HG001_02062 HG001_02062\|gene_agrA\|Accessory gene regulator protein A | -1,61 | 1,65E-01 |
| HG001_01407 HG001_01407\|gene_lexA_2\|LexA repressor | -1,58 | 4,11E-03 |
| HG001_01959 HG001_01959\|gene_NONE\|Acyl-coenzyme A:6-aminopenicillanic acid acyl-transferase | -1,56 | 2,80E-01 |
| HG001_00493 HG001_00493\|gene_sdrD\|Serine-aspartate repeat-containing protein D precursor | -1,53 | 2,68E-05 |
| HG001_01116 HG001_01116\|gene_rimP\|Ribosome maturation factor RimP | -1,47 | 7,39E-02 |
| HG001_01939 HG001_01939\|gene_pcrA\|ATP-dependent DNA helicase PcrA | -1,45 | 5,72E-02 |
| HG001_02527 HG001_02527\|gene_srmB\|ATP-dependent RNA helicase SrmB | -1,45 | 5,81E-02 |
| HG001_00366 HG001_00366\|gene_NONE\|hypothetical protein | -1,44 | 4,42E-01 |
| HG001_00181 HG001_00181\|gene_NONE\|hypothetical protein | -1,44 | 4,42E-01 |
| HG001_02125 HG001_02125\|gene_NONE\|hypothetical protein | -1,44 | 4,42E-01 |
| HG001_01419 HG001_01419\|gene_scpB\|Segregation and condensation protein B | -1,44 | 4,42E-01 |
| HG001_01837 HG001_01837\|gene_NONE\|hypothetical protein | -1,44 | 4,42E-01 |
| HG001_01606 HG001_01606\|gene_gapA2\|Glyceraldehyde-3-phosphate dehydrogenase 2 | -1,44 | 4,42E-01 |
| HG001_01257 HG001_01257\|gene_yxeP_3\|putative hydrolase YxeP | -1,44 | 4,42E-01 |
| HG001_01268 HG001_01268\|gene_cobT\|Aerobic cobaltochelatase subunit CobT | -1,44 | 4,42E-01 |
| HG001_01448 HG001_01448\|gene_xseA\|Exodeoxyribonuclease 7 large subunit | -1,44 | 4,42E-01 |
| HG001_01074 HG001_01074\|gene_thiN\|Thiamine pyrophosphokinase | -1,38 | 3,46E-01 |
| HG001_01219 HG001_01219\|gene_msrA1\|Peptide methionine sulfoxide reductase MsrA 1 | -1,38 | 3,46E-01 |
| HG001_00252 HG001_00252\|gene_NONE\|FtsX-like permease family protein | -1,36 | 2,83E-01 |
| HG001_02446 HG001_02446\|gene_bdbD\|Disulfide bond formation protein D precursor | -1,35 | 2,84E-01 |
| HG001_00359 HG001_00359\|gene_NONE\|hypothetical protein | -1,34 | 2,18E-01 |
| HG001_01585 HG001_01585\|gene_hemB\|Delta-aminolevulinic acid dehydratase | -1,32 | 2,99E-02 |
| HG001_00843 HG001_00843\|gene_spxA\|Regulatory protein Spx | -1,29 | 2,97E-03 |
| HG001_01587 HG001_01587\|gene_hemC\|Porphobilinogen deaminase | -1,27 | 9,47E-02 |
| HG001_00867 HG001_00867\|gene_prfC\|Peptide chain release factor 3 | -1,26 | 1,23E-01 |
| HG001_02121 HG001_02121\|gene_tenA\|Putative thiaminase-2 | -1,25 | 1,00E-02 |
| HG001_02408 HG001_02408\|gene_yhfP\|Putative quinone oxidoreductase YhfP | -1,23 | 2,81E-01 |
| HG001_00640 HG001_00640\|gene_nagA\|N-acetylglucosamine-6-phosphate deacetylase | -1,23 | 2,81E-01 |
| HG001_00641 HG001_00641\|gene_corC\|Magnesium and cobalt efflux protein CorC | -1,23 | 2,81E-01 |
| HG001_00238 HG001_00238\|gene_yezG_1\|putative antitoxin YezG | -1,22 | 7,39E-02 |
| HG001_00782 HG001_00782\|gene_NONE\|DltD central region | -1,22 | 2,14E-02 |
| HG001_01451 HG001_01451\|gene_cfiB_2\|2-oxoglutarate carboxylase small subunit | -1,22 | 9,25E-02 |
| HG001_02189 HG001_02189\|gene_NONE\|YbbR-like protein | -1,21 | 9,25E-02 |
| HG001_01332 HG001_01332\|gene_NONE\|Heptaprenyl diphosphate synthase (HEPPP synthase) subunit 1 | -1,21 | 3,44E-01 |
| HG001_00836 HG001_00836\|gene_dppE\|Dipeptide-binding protein DppE precursor | -1,21 | 3,44E-01 |
| HG001_02667 HG001_02667\|gene_slyA_3\|Transcriptional regulator SlyA | -1,21 | 3,44E-01 |
| HG001_02382 HG001_02382\|gene_fni\|Isopentenyl-diphosphate delta-isomerase | -1,19 | 6,82E-02 |
| HG001_02095 HG001_02095\|gene_rsbU\|Phosphoserine phosphatase RsbU | -1,17 | 2,06E-01 |
| HG001_02537 HG001_02537\|gene_gtaB\|UTP--glucose-1-phosphate uridylyltransferase | -1,17 | 4,42E-01 |

| | | | |
|---|---|---|---|
| HG001_01950 | HG001_01950\|gene_pheA\|P-protein | -1,17 | 4,42E-01 |
| HG001_00211 | HG001_00211\|gene_rbsK\|Ribokinase | -1,17 | 4,42E-01 |
| HG001_00699 | HG001_00699\|gene_lgt\|Prolipoprotein diacylglyceryl transferase | -1,17 | 4,42E-01 |
| HG001_00781 | HG001_00781\|gene_dltC\|D-alanine--poly(phosphoribitol) ligase subunit 2 | -1,17 | 4,42E-01 |
| HG001_01254 | HG001_01254\|gene_dapA\|4-hydroxy-tetrahydrodipicolinate synthase | -1,17 | 4,42E-01 |
| HG001_00183 | HG001_00183\|gene_hmp\|Flavohemoprotein | -1,17 | 2,97E-03 |
| HG001_02428 | HG001_02428\|gene_nreC\|Oxygen regulatory protein NreC | -1,17 | 4,42E-01 |
| HG001_00931 | HG001_00931\|gene_rlmI\|Ribosomal RNA large subunit methyltransferase I | -1,17 | 4,42E-01 |
| HG001_02551 | HG001_02551\|gene_yxlF_5\|putative ABC transporter ATP-binding protein YxlF | -1,17 | 4,42E-01 |
| HG001_00432 | HG001_00432\|gene_folB\|Dihydroneopterin aldolase | -1,17 | 4,42E-01 |
| HG001_01128 | HG001_01128\|gene_ftsK\|DNA translocase FtsK | -1,15 | 2,71E-01 |
| HG001_01280 | HG001_01280\|gene_NONE\|putative CtpA-like serine protease | -1,12 | 6,45E-02 |
| HG001_00199 | HG001_00199\|gene_gutB_2\|Sorbitol dehydrogenase | -1,12 | 1,21E-01 |
| HG001_01776 | HG001_01776\|gene_NONE\|Leucine-rich repeats of kinetochore protein Cenp-F/LEK1 | -1,11 | 2,34E-04 |
| HG001_01714 | HG001_01714\|gene_pckA\|Phosphoenolpyruvate carboxykinase [ATP] | -1,11 | 9,00E-03 |
| HG001_00679 | HG001_00679\|gene_NONE\|hypothetical protein | -1,11 | 3,31E-01 |
| HG001_01603 | HG001_01603\|gene_dnaI\|Primosomal protein DnaI | -1,11 | 3,34E-01 |
| HG001_01452 | HG001_01452\|gene_accB_1\|Biotin carboxyl carrier protein of acetyl-CoA carboxylase | -1,10 | 1,48E-01 |
| HG001_02646 | HG001_02646\|gene_acsA_2\|Acetyl-coenzyme A synthetase | -1,10 | 8,88E-04 |
| HG001_02118 | HG001_02118\|gene_thiE\|Thiamine-phosphate synthase | -1,10 | 6,13E-02 |
| HG001_00544 | HG001_00544\|gene_adh\|Alcohol dehydrogenase | -1,10 | 2,42E-04 |
| HG001_01624 | HG001_01624\|gene_nrnA_2\|Bifunctional oligoribonuclease and PAP phosphatase NrnA | -1,09 | 2,59E-01 |
| HG001_00998 | HG001_00998\|gene_frdB\|Fumarate reductase iron-sulfur subunit | -1,08 | 2,00E-01 |
| HG001_01261 | HG001_01261\|gene_cspA_2\|Cold shock protein CspA | -1,07 | 2,30E-02 |
| HG001_01031 | HG001_01031\|gene_pbpB\|Penicillin-binding protein 2B | -1,07 | 2,77E-02 |
| HG001_02436 | HG001_02436\|gene_nasE\|Assimilatory nitrite reductase [NAD(P)H] small subunit | -1,07 | 1,46E-01 |
| HG001_01148 | HG001_01148\|gene_mutL\|DNA mismatch repair protein MutL | -1,07 | 5,82E-01 |
| HG001_02614 | HG001_02614\|gene_NONE\|Glyoxalase-like domain protein | -1,07 | 5,82E-01 |
| HG001_01779 | HG001_01779\|gene_NONE\|hypothetical protein | -1,07 | 5,82E-01 |
| HG001_02045 | HG001_02045\|gene_dapE\|putative succinyl-diaminopimelate desuccinylase | -1,07 | 5,82E-01 |
| HG001_01692 | HG001_01692\|gene_ribD\|Riboflavin biosynthesis protein RibD | -1,07 | 5,82E-01 |
| HG001_01473 | HG001_01473\|gene_gluP\|Rhomboid protease GluP | -1,07 | 5,82E-01 |
| HG001_00515 | HG001_00515\|gene_NONE\|hypothetical protein | -1,07 | 5,82E-01 |
| HG001_01539 | HG001_01539\|gene_yrrK\|Putative Holliday junction resolvase | -1,07 | 5,82E-01 |
| HG001_01058 | HG001_01058\|gene_NONE\|3-demethylubiquinone-9 3-methyltransferase | -1,07 | 5,82E-01 |
| HG001_01197 | HG001_01197\|gene_guaC\|GMP reductase | -1,07 | 5,82E-01 |
| HG001_00352 | HG001_00352\|gene_NONE\|Type I restriction modification DNA specificity domain protein | -1,07 | 5,82E-01 |
| HG001_02346 | HG001_02346\|gene_suhB_2\|Inositol-1-monophosphatase | -1,07 | 5,82E-01 |
| HG001_02430 | HG001_02430\|gene_NONE\|hypothetical protein | -1,07 | 5,82E-01 |
| HG001_00851 | HG001_00851\|gene_NONE\|CYTH domain protein | -1,07 | 5,82E-01 |
| HG001_02421 | HG001_02421\|gene_NONE\|hypothetical protein | -1,06 | 5,82E-01 |
| HG001_01206 | HG001_01206\|gene_sbcC\|Nuclease SbcCD subunit C | -1,06 | 5,82E-01 |
| HG001_00575 | HG001_00575\|gene_tagA\|Putative N-acetylmannosaminyltransferase | -1,06 | 5,82E-01 |
| HG001_02745 | HG001_02745\|gene_cspLA\|Cold shock-like protein CspLA | -1,06 | 5,82E-01 |
| HG001_00542 | HG001_00542\|gene_NONE\|HD domain protein | -1,06 | 5,82E-01 |
| HG001_02094 | HG001_02094\|gene_rsbV\|Anti-sigma-B factor antagonist | -1,06 | 1,05E-01 |
| HG001_00872 | HG001_00872\|gene_yfkN_4\|Trifunctional nucleotide phosphoesterase protein YfkN precursor | -1,05 | 4,35E-01 |
| HG001_00243 | HG001_00243\|gene_yezG_3\|putative antitoxin YezG | -1,05 | 4,35E-01 |
| HG001_00386 | HG001_00386\|gene_treB\|PTS system trehalose-specific EIIBC component | -1,05 | 4,35E-01 |
| HG001_01487 | HG001_01487\|gene_yqfL\|Putative pyruvate, phosphate dikinase regulatory protein | -1,05 | 4,35E-01 |
| HG001_00376 | HG001_00376\|gene_sle1_1\|N-acetylmuramoyl-L-alanine amidase sle1 precursor | -1,04 | 3,19E-01 |
| HG001_00698 | HG001_00698\|gene_hprK\|HPr kinase/phosphorylase | -1,04 | 1,34E-01 |
| HG001_00728 | HG001_00728\|gene_clfA\|Clumping factor A precursor | -1,02 | 1,27E-01 |
| HG001_02181 | HG001_02181\|gene_glmS\|Glutamine--fructose-6-phosphate aminotransferase [isomerizing] | -1,01 | 1,75E-04 |
| HG001_02021 | HG001_02021\|gene_NONE\|hypothetical protein | -1,01 | 6,59E-02 |
| HG001_01918 | HG001_01918\|gene_vraR\|Response regulator protein VraR | -1,01 | 2,35E-01 |

**Annexe 3 : Tableau de l'expression différentielle selon les voies métaboliques impliquées.**

| Pyrimidine deoxyribonucleotides de novo biosyntheis | | | | | Diff. Transcriptomics MV/ctr | | Diff. Proteomics MV/ctr | |
|---|---|---|---|---|---|---|---|---|
| id | gene | product | locus_tag_NCTC8325 | gene_NCTC8325 | log2FoldChange | padj | log2FoldChange | padj |
| HG001_01054 | carB | Carbamoyl-phosphate synthase large chain | SAOUHSC_01170 | carB | 5,41 | 9,50E-104 | 0,12 | 7,76E-01 |
| HG001_01052 | pyrC | Dihydroorotase | SAOUHSC_01168 | pyrC | 5,31 | 1,73E-65 | 1,22 | 8,22E-09 |
| HG001_01055 | pyrF | Orotidine 5'-phosphate decarboxylase | SAOUHSC_01171 | - | 5,29 | 3,09E-126 | 0,59 | 2,47E-01 |
| HG001_01053 | carA | Carbamoyl-phosphate synthase small chain | SAOUHSC_01169 | - | 5,28 | 6,93E-63 | 0,67 | 1,04E-01 |
| HG001_01051 | pyrB | Aspartate carbamoyltransferase | SAOUHSC_01166 | pyrB | 5,17 | 1,60E-52 | 0,09 | 9,09E-01 |
| HG001_01056 | pyrE | Orotate phosphoribosyltransferase | SAOUHSC_01172 | pyrE | 4,97 | 1,35E-105 | 0,83 | 9,18E-02 |
| HG001_01050 | pyrP | Uracil permease | SAOUHSC_01165 | - | 4,81 | 5,14E-46 | 0,90 | 3,77E-01 |
| HG001_01057 | - | hypothetical protein; same operon as pyrP-pyrB-pyrC-carA-carB-pyrF-pyrI | SAOUHSC_01173 | - | 3,51 | 8,10E-45 | ND | ND |
| HG001_00399 | tmk | Thymidylate kinase | SAOUHSC_00451 | tmk | 1,06 | 4,06E-06 | 0,27 | 8,80E-01 |
| HG001_00669 | nrdE2 | Ribonucleoside-diphosphate reductase subunit alpha 2 | SAOUHSC_00742 | nrdI | 1,36 | 7,99E-08 | 0,40 | 8,71E-02 |
| HG001_00670 | nrdF | Ribonucleoside-diphosphate reductase subunit beta | SAOUHSC_00743 | nrdF | 2,53 | 5,81E-22 | 0,51 | 2,13E-02 |
| HG001_01049 | pyrR | Bifunctional protein PyrR | SAOUHSC_01164 | - | 1,01 | 0,000496863 | 2,76 | 4,52E-09 |
| HG001_01109 | pyrH | Uridylate kinase | SAOUHSC_01235 | pyrH | 1,19 | 7,15E-06 | -0,67 | 2,35E-01 |
| HG001_01337 | cmk | Cytidylate kinase | SAOUHSC_01496 | cmk | 1,61 | 3,25E-11 | -0,10 | 8,52E-01 |
| HG001_01534 | udk | Uridine kinase | SAOUHSC_01715 | - | 1,30 | 2,62E-10 | -0,66 | 6,45E-01 |
| HG001_02154 | pyrG | CTP synthase | SAOUHSC_02368 | pyrG | 2,39 | 8,99E-22 | -0,35 | 3,37E-01 |
| HG001_02629 | pyrD | Dihydroorotate dehydrogenase (quinone) | SAOUHSC_02909 | - | 2,96 | 6,09E-08 | 2,33 | 6,96E-12 |

| Purine deoxyribonucleotides de novo biosyntheis | | | | | Diff. Transcriptomics MV/ctr | | Diff. Proteomics MV/ctr | |
|---|---|---|---|---|---|---|---|---|
| id | gene | product | locus_tag_NCTC8325 | gene_NCTC8325 | log2FoldChange | padj | log2FoldChange | padj |
| HG001_00085 | deoD | Purine nucleoside phosphorylase DeoD-type | SAOUHSC_00097 | - | 3,81 | 5,29E-33 | ND | ND |
| HG001_00019 | purA | Adenylosuccinate synthetase | SAOUHSC_00019 | - | 2,26 | 4,52562E-15 | 0,05 | 9,57E-01 |
| HG001_01560 | apt | Adenine phosphoribosyltransferase | SAOUHSC_01743 | - | 1,89 | 5,58131E-18 | -0,37 | 7,86E-01 |
| HG001_01942 | purB | Adenylosuccinate lyase | SAOUHSC_02126 | - | 1,86 | 6,42238E-15 | -0,34 | 2,32E-01 |
| HG001_02655 | nrdD | Anaerobic ribonucleoside-triphosphate reductase | SAOUHSC_02942 | - | 2,41 | 8,69131E-18 | 0,27 | 8,69E-01 |

| Phage genes | | | | | Diff. Transcriptomics MV/ctr | | Diff. Proteomics MV/ctr | |
|---|---|---|---|---|---|---|---|---|
| id | gene | product | locus_tag_NCTC8325 | gene_NCTC8325 | log2FoldChange | padj | log2FoldChange | padj |
| HG001_01894 | - | Phage protein | SAOUHSC_02072 | - | 5,30 | 3,29E-106 | 7,72 | 8,10E-24 |
| HG001_01903 | - | Putative phage protein | SAOUHSC_02081 | - | 5,26 | 6,13E-84 | 1,98 | 4,11E-01 |
| HG001_01904 | - | Putative phage regulatory protein | SAOUHSC_02083 | - | 5,13 | 1,51E-76 | ND | ND |
| HG001_01891 | - | Putative phage replication protein | SAOUHSC_02069 | - | 5,13 | 7,84E-104 | 4,93 | 9,83E-04 |
| HG001_01895 | - | Bacteriophage Mu Gam like protein | SAOUHSC_02073 | - | 5,12 | 1,86E-101 | 7,35 | 2,61E-18 |
| HG001_01898 | - | Phage protein | SAOUHSC_02076 | - | 5,04 | 5,50E-64 | ND | ND |
| HG001_01902 | - | Phage antirepressor protein KilAC domain protein | SAOUHSC_02080 | - | 5,02 | 1,44E-91 | 9,03 | 5,76E-54 |
| HG001_01887 | - | Phage protein | SAOUHSC_02065 | - | 5,00 | 2,05E-91 | 2,79 | 2,32E-01 |
| HG001_01888 | - | Putative phage protein | SAOUHSC_02066 | - | 4,98 | 1,64E-111 | ND | ND |
| HG001_01885 | - | Phage protein | SAOUHSC_02063 | - | 4,98 | 1,29E-122 | ND | ND |
| HG001_01886 | - | Phage protein | SAOUHSC_02064 | - | 4,94 | 3,02E-104 | 3,98 | 3,18E-02 |
| HG001_01884 | - | Putative phage regulatory protein; Helix-turn-helix domain protein | SAOUHSC_02062 | - | 4,89 | 3,62E-92 | 3,68 | 6,59E-02 |
| HG001_01883 | - | Phage protein; PVL ORF-50-like family protein | SAOUHSC_02061 | - | 4,89 | 5,90E-94 | 4,44 | 8,53E-03 |
| HG001_01900 | - | Phage protein | SAOUHSC_02078 | - | 4,89 | 1,40E-93 | 5,30 | 1,17E-04 |
| HG001_01890 | - | Phage protein | SAOUHSC_02068 | - | 4,87 | 6,99E-99 | 2,79 | 2,32E-01 |
| HG001_02016 | - | Phage protein | SAOUHSC_02213 | - | 4,86 | 5,76E-99 | ND | ND |
| HG001_01896 | - | Phage protein | SAOUHSC_02074 | - | 4,83 | 1,20E-88 | ND | ND |
| HG001_01901 | - | Putative phage protein | SAOUHSC_02079 | - | 4,81 | 2,42E-107 | 1,98 | 4,11E-01 |
| HG001_01875 | - | Transcriptional activator RinB (phage) | SAOUHSC_02053 | - | 4,75 | 1,21E-118 | ND | ND |
| HG001_01868 | - | Putative phage protein | SAOUHSC_02046 | - | 4,73 | 3,62E-66 | ND | ND |
| HG001_01880 | - | Putative phage protein | SAOUHSC_02058 | - | 4,70 | 1,30E-90 | 6,23 | 1,47E-08 |
| HG001_01881 | - | Phage protein | SAOUHSC_02059 | - | 4,70 | 4,55E-98 | ND | ND |
| HG001_01870 | - | Phage portal protein%2C SPP1 Gp6-like | SAOUHSC_02048 | - | 4,69 | 1,57E-79 | 1,98 | 4,11E-01 |
| HG001_01876 | - | Phage protein | SAOUHSC_02054 | - | 4,68 | 8,91E-80 | ND | ND |
| HG001_01882 | - | Phage protein | SAOUHSC_02060 | - | 4,66 | 8,31E-112 | ND | ND |
| HG001_01869 | - | Phage Mu protein F like protein | SAOUHSC_02047 | - | 4,63 | 3,92E-79 | ND | ND |
| HG001_01899 | - | Phage protein | SAOUHSC_02077 | - | 4,60 | 2,32E-83 | 7,22 | 7,52E-17 |
| HG001_01873 | - | Transcriptional activator, phage-associated | SAOUHSC_02051 | - | 4,54 | 9,07E-91 | 5,50 | 2,76E-05 |
| HG001_01878 | - | Putative phage protein | SAOUHSC_02056 | - | 4,54 | 2,16E-83 | ND | ND |
| HG001_02037 | - | Putative phage regulatory protein | SAOUHSC_02234 | - | 4,49 | 4,16E-70 | ND | ND |
| HG001_02032 | - | Phage protein | SAOUHSC_02228 | - | 4,46 | 4,05E-75 | ND | ND |
| HG001_01874 | - | Phage protein | SAOUHSC_02052 | - | 4,42 | 5,03E-104 | ND | ND |
| HG001_01383 | - | Phage protein | SAOUHSC_01550 | - | 4,41 | 8,41E-68 | ND | ND |
| HG001_02034 | - | AntA/AntB antirepressor | SAOUHSC_02229 | - | 4,40 | 3,05E-86 | 1,98 | 4,11E-01 |
| HG001_02036 | - | Putative phage regulatory protein | SAOUHSC_02233 | - | 4,38 | 3,67E-72 | ND | ND |
| HG001_01877 | - | Phage protein | SAOUHSC_02055 | - | 4,38 | 1,19E-87 | 3,30 | 1,23E-01 |
| HG001_01897 | - | Phage protein | SAOUHSC_02075 | - | 4,22 | 3,08E-83 | 9,14 | 1,96E-43 |
| HG001_01866 | - | Phage capsid family protein | SAOUHSC_02043 | - | 4,20 | 1,95E-57 | 4,23 | 1,64E-02 |
| HG001_02033 | - | Phage antirepressor protein KilAC domain protein | SAOUHSC_02229 | - | 4,19 | 1,60E-83 | ND | ND |
| HG001_01867 | - | Putative phage head protein | SAOUHSC_02044 | - | 4,15 | 1,63E-61 | 5,68 | 6,87E-06 |
| HG001_01871 | - | Phage terminase large subunit | SAOUHSC_02049 | - | 4,14 | 4,87E-53 | ND | ND |
| HG001_01865 | - | Phage protein | SAOUHSC_02042 | - | 4,12 | 9,34E-51 | 2,79 | 2,32E-01 |
| HG001_01863 | - | Putative phage protein | SAOUHSC_02040 | - | 4,07 | 1,18E-53 | ND | ND |
| HG001_02023 | - | Putative phage nuclease | SAOUHSC_02219 | - | 4,04 | 5,11E-85 | ND | ND |
| HG001_01858 | - | Phage protein | SAOUHSC_02034 | - | 3,98 | 5,86E-61 | ND | ND |
| HG001_02031 | - | Putative phage protein | SAOUHSC_02227 | - | 3,98 | 1,83E-46 | ND | ND |
| HG001_02029 | - | Phage protein | SAOUHSC_02225 | - | 3,98 | 4,57E-80 | 1,98 | 4,11E-01 |
| HG001_01861 | - | Putative phage protein | SAOUHSC_02037 | - | 3,95 | 1,04E-58 | ND | ND |
| HG001_02025 | - | Phage protein | SAOUHSC_02221 | - | 3,95 | 6,11E-88 | ND | ND |
| HG001_02017 | - | Putative phage protein | SAOUHSC_02214 | - | 3,88 | 2,85E-46 | ND | ND |
| HG001_02028 | - | Phage protein | SAOUHSC_02224 | - | 3,85 | 6,04E-45 | ND | ND |
| HG001_01386 | - | Phage protein; PVL orf 52-like protein; Phage phi 11 orf23 protein homolc | SAOUHSC_01553 | - | 3,85 | 2,70E-63 | ND | ND |
| HG001_02024 | - | Putative phage ssDNA binding protein | SAOUHSC_02220 | - | 3,83 | 7,83E-62 | 1,98 | 4,11E-01 |
| HG001_01860 | - | Phage major tail protein 2 | SAOUHSC_02036 | - | 3,82 | 7,08E-64 | 3,30 | 1,23E-01 |

| | | | | | | | | |
|---|---|---|---|---|---|---|---|---|
| HG001_02026 | - | Putative phage protein | SAOUHSC_02222 | - | 3,81 | 2,07E-65 | ND | ND |
| HG001_01859 | - | Phage protein | SAOUHSC_02035 | - | 3,77 | 1,37E-55 | 3,98 | 3,18E-02 |
| HG001_01862 | - | Phage protein | SAOUHSC_02038 | - | 3,77 | 3,25E-54 | ND | ND |
| HG001_01872 | - | Terminase small subunit | SAOUHSC_02050 | - | 3,65 | 1,14E-36 | ND | ND |
| HG001_02027 | - | Phage protein | SAOUHSC_02223 | - | 3,63 | 5,40E-53 | ND | ND |
| HG001_02020 | - | Phage protein | SAOUHSC_02217 | - | 3,32 | 8,20E-54 | ND | ND |

| DNA repair | | | | | Diff. Transcriptomics MV/ctr | | Diff. Proteomics MV/ctr | |
|---|---|---|---|---|---|---|---|---|
| id | gene | product | locus_tag_NCTC8325 | gene_NCTC8325 | log2FoldChange | padj | log2FoldChange | padj |
| HG001_01889 | dnaC_2 | Replicative DNA helicase | SAOUHSC_02067 | - | 4,92 | 1,18E-111 | ND | ND |
| HG001_01222 | dinB_1 | DNA polymerase IV | SAOUHSC_01363 | MucB | 4,04 | 1,46E-55 | ND | ND |
| HG001_00018 | dnaB | Replicative DNA helicase | SAOUHSC_00018 | - | 0,51 | 0,052192362 | -2,00 | 1,08E-01 |
| HG001_00004 | recF | DNA replication and repair protein RecF | SAOUHSC_00004 | recF | 1,17 | 6,04E-09 | ND | ND |
| HG001_00310 | ssb_1 | Single-stranded DNA-binding protein ssb | SAOUHSC_00349 | - | 1,21 | 7,79E-08 | 0,57 | 2,83E-01 |
| HG001_00510 | ung | Uracil-DNA glycosylase | SAOUHSC_00564 | - | 1,02 | 0,000840362 | -0,66 | 6,45E-01 |
| HG001_00659 | recQ_1 | ATP-dependent DNA helicase RecQ | SAOUHSC_00730 | - | 2,10 | 4,16E-29 | ND | ND |
| HG001_00697 | uvrA | UvrABC system protein A | SAOUHSC_00780 | uvrA | 1,54 | 4,12E-15 | 0,27 | 8,18E-01 |
| HG001_00992 | polX | DNA polymerase/3'-5' exonuclease PolX | SAOUHSC_01098 | - | 1,11 | 2,71E-08 | -0,37 | 7,86E-01 |
| HG001_00993 | mutS2 | Endonuclease MutS2 | SAOUHSC_01099 | - | 1,34 | 1,28E-10 | -0,86 | 3,26E-01 |
| HG001_01095 | rnhB | Ribonuclease HII | SAOUHSC_01215 | rnhB | 1,12 | 1,30E-06 | -1,78 | 4,42E-01 |
| HG001_01137 | recA | Protein RecA | SAOUHSC_01262 | recA | 2,19 | 1,32E-20 | 1,36 | 5,99E-05 |
| HG001_01205 | sbcD | Nuclease SbcCD subunit D | SAOUHSC_01341 | - | 1,37 | 2,58E-07 | ND | ND |
| HG001_01310 | recU | Holliday junction resolvase RecU | SAOUHSC_01466 | recU | 1,43 | 2,34E-09 | ND | ND |
| HG001_01481 | nfo | putative endonuclease 4 | SAOUHSC_01658 | - | 1,79 | 2,77E-17 | -0,20 | 7,91E-01 |
| HG001_01514 | comEA | ComE operon protein 1 | SAOUHSC_01693 | - | 1,43 | 2,04E-08 | ND | ND |
| HG001_01561 | recJ | Single-stranded-DNA-specific exonuclease RecJ | SAOUHSC_01744 | - | 1,37 | 2,90E-12 | -0,03 | 9,83E-01 |
| HG001_01566 | ruvB | Holliday junction ATP-dependent DNA helicase RuvB | SAOUHSC_01750 | ruvB | 1,00 | 2,72E-05 | ND | ND |
| HG001_01938 | ligA | DNA ligase | SAOUHSC_02122 | - | 2,00 | 7,85E-21 | -0,48 | 2,00E-01 |
| HG001_01939 | pcrA | ATP-dependent DNA helicase PcrA | SAOUHSC_02123 | - | 2,18 | 7,32E-27 | -1,45 | 5,72E-02 |

| Nitrate and Nitrite reduction. Porfirines biosisnthesis, anaerobic respiratory chain | | | | | Diff. Transcriptomics MV/ctr | | Diff. Proteomics MV/ctr | |
|---|---|---|---|---|---|---|---|---|
| id | gene | product | locus_tag_NCTC8325 | gene_NCTC8325 | log2FoldChange | padj | log2FoldChange | padj |
| HG001_02438 | shfC (nirR) | Sirohydrochlorin ferrochelatase | SAOUHSC_02685 | nirR | 2,59 | 3,49591E-19 | ND | ND |
| HG001_02437 | nasD | Nitrite reductase [NAD(P)H] large subunit - similar to tRNA U-34 5-methyl | SAOUHSC_02684 | nasD | 3,20 | 1,42E-25 | -0,35 | 4,19E-01 |
| HG001_02436 | nasE | Nitrite reductase [NAD(P)H] small subunit | SAOUHSC_02683 | nasE | 3,32 | 1,65E-29 | -1,07 | 1,46E-01 |
| HG001_02435 | nasF | Uroporphyrinogen-III C-methyltransferase - similar to queE | SAOUHSC_02682 | nasF | 3,40 | 5,44181E-37 | 0,66 | 5,51E-01 |
| | | | | | | | | |
| HG001_02434 | narG | Respiratory nitrate reductase 1 alpha chain - molybdopterin [4Fe-4S] clust | SAOUHSC_02681 | narG | 3,80 | 2,96E-40 | -2,56 | 1,47E-13 |
| HG001_02433 | narH | Respiratory nitrate reductase 1 beta chain - [4Fe-4S] cluster | SAOUHSC_02680 | narH | 4,28 | 1,58E-52 | -2,06 | 2,56E-04 |
| HG001_02432 | narW | Nitrate reductase molybdenum cofactor assembly chaperone | SAOUHSC_02679 | narJ | 4,26 | 4,39E-51 | -4,17 | 2,68E-02 |
| HG001_02431 | narX | Respiratory nitrate reductase subunit gamma | SAOUHSC_02678 | narI | 3,19 | 3,92E-36 | ND | ND |
| HG001_02430 | nreA | Nitrogen fixation regulatory protein | SAOUHSC_02677 | nreA | 2,55 | 5,64788E-26 | -1,07 | 5,82E-01 |
| HG001_02429 | nreB | Oxygen sensor  two-component histidine kinase [4Fe-4S] cluster | SAOUHSC_02676 | nreB | 2,86 | 7,06112E-32 | -2,55 | 2,99E-01 |
| HG001_02428 | nreC | Oxygen regulatory protein regulator transcription factor of the two comp | SAOUHSC_02675 | nreC | 2,51 | 1,59378E-30 | -1,17 | 4,42E-01 |
| | | | | | | | | |
| HG001_02344 | - | Putative formate dehydrogenase | SAOUHSC_02582 | fdhA | -0,69 | 0,002489064 | -3,93 | 1,23E-21 |
| HG001_02343 | - | Putative formate dehydrogenase | SAOUHSC_02581 | - | -1,06 | 6,23554E-05 | -4,56 | 4,13E-08 |
| | | | | | | | | |
| HG001_02424 | narT | putative nitrate transporter NarT | SAOUHSC_02671 | - | 2,15 | 0,000554689 | -3,72 | 7,39E-02 |

| Regulation of respiratory chain | | | | | Diff. Transcriptomics MV/ctr | | Diff. Proteomics MV/ctr | |
|---|---|---|---|---|---|---|---|---|
| id | gene | product | locus_tag_NCTC8325 | gene_NCTC8325 | log2FoldChange | padj | log2FoldChange | padj |
| HG001_02428 | nreC | Oxygen regulatory protein NreC | SAOUHSC_02675 | - | 2,51 | 1,59E-30 | -1,17 | 4,42E-01 |
| HG001_02069 | rex | Redox-sensing transcriptional repressor Rex | SAOUHSC_02273 | - | -0,25 | 0,272186609 | 0,05 | 9,53E-01 |

| Protein Folding | | | | | Diff. Transcriptomics MV/ctr | | Diff. Proteomics MV/ctr | |
|---|---|---|---|---|---|---|---|---|
| id | gene | product | locus_tag_NCTC8325 | gene_NCTC8325 | log2FoldChange | padj | log2FoldChange | padj |
| HG001_00429 | hslO | 33 kDa chaperonin | SAOUHSC_00487 | hslO | 0,95 | 8,36E-06 | 0,01 | 9,85E-01 |
| HG001_00821 | clpB_1 | Chaperone protein ClpB | SAOUHSC_00912 | - | 1,14 | 5,03E-07 | 0,09 | 8,73E-01 |
| HG001_01504 | dnaJ | Chaperone protein DnaJ | SAOUHSC_01682 | - | 0,72 | 0,000696191 | -0,31 | 5,20E-01 |
| HG001_01506 | grpE | Protein GrpE | SAOUHSC_01684 | - | 0,74 | 0,00066207 | 0,23 | 4,42E-01 |
| HG001_01591 | clpX | ATP-dependent Clp protease ATP-binding subunit ClpX | SAOUHSC_01778 | clpX | 1,42 | 4,48E-12 | 0,70 | 4,11E-03 |
| HG001_01592 | tig | Trigger factor | SAOUHSC_01779 | tig | 1,39 | 9,40E-11 | 0,90 | 5,36E-05 |

| tRNA modification | | | | | Diff. Transcriptomics MV/ctr | | Diff. Proteomics MV/ctr | |
|---|---|---|---|---|---|---|---|---|
| id | gene | product | locus_tag_NCTC8325 | gene_NCTC8325 | log2FoldChange | padj | log2FoldChange | padj |
| HG001_02727 | glpE_3 | Thiosulfate sulfurtransferase GlpE | SAOUHSC_03024 | - | 4,35 | 4,32E-96 | 3,20 | 2,44E-09 |
| HG001_01911 | queE_2 | 7-carboxy-7-deazaguanine synthase | SAOUHSC_02090 | - | 3,19 | 6,19E-61 | 0,93 | 5,04E-01 |
| HG001_02256 | truA | tRNA pseudouridine synthase A | SAOUHSC_02480 | truA | 2,08 | 4,31E-25 | -0,63 | 7,17E-01 |
| HG001_02751 | mnmG | tRNA uridine 5-carboxymethylaminomethyl modification enzyme MnmG | SAOUHSC_03052 | gidA | 1,93 | 2,97E-16 | 0,65 | 5,36E-02 |
| HG001_02752 | mnmE | tRNA modification GTPase MnmE | SAOUHSC_03053 | trmE | 1,62 | 2,36E-10 | 1,02 | 2,12E-01 |
| HG001_01564 | tgt | Queuine tRNA-ribosyltransferase | SAOUHSC_01748 | tgt | 1,60 | 8,50E-13 | -0,75 | 2,61E-01 |
| HG001_01635 | thiI | putative tRNA sulfurtransferase | SAOUHSC_01824 | - | 1,42 | 1,03E-11 | -0,60 | 4,98E-01 |
| HG001_01091 | trmD | tRNA (guanine-N(1)-)-methyltransferase | SAOUHSC_01210 | trmD | 1,41 | 2,36E-10 | -1,98 | 2,47E-01 |
| HG001_01565 | queA | S-adenosylmethionine:tRNA ribosyltransferase-isomerase | SAOUHSC_01749 | queA | 1,35 | 1,96E-08 | 0,15 | 9,06E-01 |
| HG001_01788 | trmL | tRNA (cytidine(34)-2'-O)-methyltransferase | SAOUHSC_01988 | - | 1,30 | 1,85E-08 | -2,12 | 7,39E-02 |
| HG001_01484 | trmK | tRNA (adenine(22)-N(1))-methyltransferase | SAOUHSC_01661 | - | 1,24 | 3,25E-09 | 0,20 | 8,25E-01 |
| HG001_01102 | trmFO | Methylenetetrahydrofolate--tRNA-(uracil-5-)-methyltransferase TrmFO | SAOUHSC_01223 | gid | 1,04 | 3,65E-06 | 0,05 | 9,33E-01 |
| HG001_01144 | miaB | (Dimethylallyl)adenosine tRNA methylthiotransferase MiaB | SAOUHSC_01269 | - | 1,01 | 6,46E-06 | -5,02 | 1,32E-03 |
| HG001_01552 | tcdA | tRNA threonylcarbamoyladenosine dehydratase | SAOUHSC_01735 | - | 0,88 | 0,000111308 | -0,78 | 3,93E-01 |
| HG001_02072 | tsaD | tRNA N6-adenosine threonylcarbamoyltransferase | SAOUHSC_02277 | gcp | 0,75 | 0,000378128 | -0,87 | 5,13E-01 |

| | | | | | | | | |
|---|---|---|---|---|---|---|---|---|
| HG001_01500 | mtaB_1 | Threonylcarbamoyladenosine tRNA methylthiotransferase MtaB | SAOUHSC_01679 | - | 0,69 | 0,001185038 | ND | ND |
| HG001_00404 | yfiC | tRNA1(Val) (adenine(37)-N6)-methyltransferase | SAOUHSC_00457 | - | 0,58 | 0,023934541 | ND | ND |
| HG001_00462 | - | Putative TrmH family tRNA/rRNA methyltransferase | SAOUHSC_00513 | - | -0,43 | 0,074696654 | -0,51 | 4,42E-01 |
| HG001_02075 | tsaE | tRNA threonylcarbamoyladenosine biosynthesis protein TsaE | SAOUHSC_02280 | - | -0,83 | 0,016585893 | ND | ND |
| HG001_01122 | truB | tRNA pseudouridine synthase B | SAOUHSC_01248 | - | -0,90 | 4,08E-05 | 0,44 | 6,84E-01 |
| HG001_00036 | dus_2 | putative tRNA-dihydrouridine synthase | SAOUHSC_00039 | - | -0,98 | 4,87E-06 | 0,66 | 5,51E-01 |
| HG001_00985 | - | Putative TrmH family tRNA/rRNA methyltransferase | SAOUHSC_01091 | - | -1,10 | 3,49E-07 | -0,04 | 9,76E-01 |
| HG001_01537 | trmR | Putative O-methyltransferase/MSMEI_4947 tRNA 5-hydroxyuridine meth | SAOUHSC_01718 | - | 0,94 | 0,004417914 | -3,42 | 1,23E-01 |
| HG001_00666 | queF | NADPH-dependent 7-cyano-7-deazaguanine reductase | SAOUHSC_00739 | - | 0,60 | 0,00815737 | 0,49 | 4,42E-01 |
| HG001_01789 | queG | Epoxyqueuosine reductase | SAOUHSC_01989 | - | 0,54 | 0,030211245 | ND | ND |
| HG001_00496 | folE2 | GTP cyclohydrolase FolE2 | SAOUHSC_00549 | - | 1,57 | 1,60E-14 | 0,50 | 3,56E-01 |
| HG001_01154 | miaA | tRNA dimethylallyltransferase | SAOUHSC_01280 | miaA | 0,33 | 0,196377884 | 0,02 | 9,85E-01 |
| HG001_00650 | queD | 6-carboxy-5%2C6%2C7%2C8-tetrahydropterin synthase | SAOUHSC_00720 | - | -0,10 | 0,750041318 | 0,83 | 4,42E-01 |
| HG001_00649 | queE_1 | 7-carboxy-7-deazaguanine synthase | SAOUHSC_00719 | - | 0,39 | 0,083379277 | ND | ND |
| HG001_00651 | queC | 7-cyano-7-deazaguanine synthase | SAOUHSC_00721 | - | 0,04 | 0,872388212 | -0,28 | 8,73E-01 |

| Fermentation | | | | | Diff. Transcriptomics MV/ctr | | Diff. Proteomics MV/ctr | |
|---|---|---|---|---|---|---|---|---|
| id | gene | product | locus_tag_NCTC8325 | gene_NCTC8325 | log2FoldChange | padj | log2FoldChange | padj |
| HG001_02246 | aldC_1 | Alpha-acetolactate decarboxylase | SAOUHSC_02467 | - | 3,24 | 1,69E-21 | 1,26 | 6,63E-10 |

| Detoxifying enzymes | | | | | Diff. Transcriptomics MV/ctr | | Diff. Proteomics MV/ctr | |
|---|---|---|---|---|---|---|---|---|
| id | gene | product | locus_tag_NCTC8325 | gene_NCTC8325 | log2FoldChange | padj | log2FoldChange | padj |
| HG001_00082 | sodM | Superoxide dismutase [Mn/Fe] 2 | SAOUHSC_00093 | - | 2,37 | 1,32E-34 | -0,18 | 7,14E-01 |
| HG001_01477 | sodA | Superoxide dismutase [Mn/Fe] 1 | SAOUHSC_01653 | - | 0,47 | 0,05143839 | 0,34 | 3,51E-01 |
| HG001_01194 | katA | Catalase | SAOUHSC_01327 | - | -0,499 | 0,052458991 | 0,91 | 3,55E-04 |
| HG001_01633 | tpx | putative thiol peroxidase | SAOUHSC_01822 | tpx | 0,445 | 0,051341102 | 0,20 | 6,15E-01 |
| HG001_00324 | ahpC | Alkyl hydroperoxide reductase subunit C | SAOUHSC_00365 | - | 1,87 | 1,93E-18 | 1,92 | 4,00E-77 |
| HG001_00323 | ahpF | Alkyl hydroperoxide reductase subunit F | SAOUHSC_00364 | - | 1,79 | 7,15E-17 | 1,86 | 3,84E-51 |
| HG001_02514 | ahpD | Alkyl hydroperoxide reductase AhpD | SAOUHSC_02774 | - | -2,35 | 2,77E-23 | -0,67 | 2,59E-01 |
| HG001_00183 | hmp | Flavohemoprotein | SAOUHSC_00204 | - | -1,31 | 1,40E-05 | -1,17 | 2,97E-03 |
| HG001_02602 | crtM | Dehydrosqualene synthase | SAOUHSC_02879 | - | -1,57 | NA | ND | ND |
| HG001_02601 | crtN | Dehydrosqualene desaturase | SAOUHSC_02877 | - | -1,92 | 8,97E-18 | -0,66 | 6,45E-01 |

| Regulation of detoxifying enzymes | | | | | Diff. Transcriptomics MV/ctr | | Diff. Proteomics MV/ctr | |
|---|---|---|---|---|---|---|---|---|
| id | gene | product | locus_tag_NCTC8325 | gene_NCTC8325 | log2FoldChange | padj | log2FoldChange | padj |
| HG001_01826 | perR | Peroxide-responsive repressor PerR | SAOUHSC_01997 | - | -1,13 | 1,18E-06 | ND | ND |
| HG001_02092 | sigB | RNA polymerase sigma-B factor | SAOUHSC_02298 | - | -0,94 | 5,31E-06 | -0,91 | 2,71E-01 |
| HG001_01423 | fur | Ferric uptake regulation protein | SAOUHSC_01592 | - | -0,447 | 0,080768103 | 0,53 | 3,07E-01 |
| HG001_00556 | sarA | Transcriptional regulator SarA | SAOUHSC_00620 | - | -2,33 | 2,30E-20 | 0,31 | 2,99E-01 |

| Metal homeostasis | | | | | Diff. Transcriptomics MV/ctr | | Diff. Proteomics MV/ctr | |
|---|---|---|---|---|---|---|---|---|
| id | gene | product | locus_tag_NCTC8325 | gene_NCTC8325 | log2FoldChange | padj | log2FoldChange | padj |
| HG001_00116 | isdI | Heme oxygenase (staphylobilin-producing) 2 | SAOUHSC_00130 | - | -0,663 | 0,020844767 | 2,02 | 5,34E-05 |
| HG001_00981 | isdE | High-affinity heme uptake system protein IsdE precursor | SAOUHSC_01085 | - | -0,86 | 0,006277875 | 1,98 | 4,11E-01 |
| HG001_02320 | fhuD_2 | Iron(3+)-hydroxamate-binding protein FhuD precursor | SAOUHSC_02554 | - | 1,35 | 9,45E-11 | 1,18 | 2,08E-09 |
| HG001_02047 | fhuD_1 | Iron(3+)-hydroxamate-binding protein FhuD precursor | SAOUHSC_02246 | - | -0,81 | 0,044043942 | ND | ND |
| HG001_01927 | ftnA | Ferritin | SAOUHSC_02108 | - | -1,45 | 7,51E-13 | 0,16 | 6,45E-01 |
| HG001_00625 | mgrA | HTH-type transcriptional regulator MgrA | SAOUHSC_00694 | - | -1,64 | 1,53E-12 | -0,23 | 7,11E-01 |
| HG001_01527 | mntH_2 | Divalent metal cation transporter MntH | SAOUHSC_01707 | - | -0,88 | 0,001151062 | ND | ND |
| HG001_00065 | sbnA | putative siderophore biosynthesis protein SbnA | SAOUHSC_00075 | - | 1,17 | 0,000501837 | 2,79 | 2,32E-01 |
| HG001_00066 | sbnB | N-[(2S)-2-amino-2-carboxyethyl]-L-glutamate dehydrogenase | SAOUHSC_00076 | - | 1,47 | 9,94E-09 | 8,63 | 5,62E-28 |
| HG001_00067 | sbnC | Staphyloferrin B synthase | SAOUHSC_00077 | - | 1,87 | 5,02E-14 | 5,19 | 2,32E-04 |
| HG001_00068 | sbnD | Staphyloferrin B export protein | SAOUHSC_00078 | - | 1,51 | 6,73E-11 | ND | ND |
| HG001_00069 | sbnE | L-2,3-diaminopropanoate--citrate ligase | SAOUHSC_00079 | - | 1,44 | 3,86E-09 | 5,59 | 1,37E-05 |
| HG001_00070 | sbnF | 2-[(L-alanin-3-ylcarbamoyl)methyl]-3-(2-aminoethylcarbamoyl)-2-hydroxy | SAOUHSC_00080 | - | 1,32 | 5,34E-07 | 7,41 | 3,27E-19 |
| HG001_00071 | sbnG | Citrate synthase | SAOUHSC_00081 | - | 1,54 | 1,07E-11 | 6,79 | 1,54E-12 |
| HG001_00072 | sbnH | 2-[(L-alanin-3-ylcarbamoyl)methyl]-2-hydroxybutanedioate decarboxylase | SAOUHSC_00082 | - | 1,48 | 1,97E-12 | 6,11 | 7,21E-08 |
| HG001_00073 | sbnI | L-serine kinase | SAOUHSC_00083 | - | 1,64 | 9,52E-15 | 5,50 | 2,76E-05 |
| HG001_00573 | ideR | Iron-dependent repressor IdeR | SAOUHSC_00638 | mntR | -2,13 | 8,63E-19 | -0,58 | 5,48E-01 |
| HG001_00572 | **mntA** | High-affinity zinc uptake system ATP-binding protein ZnuC | SAOUHSC_00637 | - | -1,74 | 1,75E-12 | 0,03 | 9,71E-01 |
| HG001_00571 | **mntB** | Manganese transport system membrane protein MntB | SAOUHSC_00636 | - | -2,91 | 3,21E-40 | ND | ND |
| HG001_00570 | **mntC** | Manganese ABC transporter substrate-binding lipoprotein precursor | SAOUHSC_00634 | - | -3,30 | 4,90E-40 | 0,34 | 9,47E-02 |

| Electron transport chain | | | | | Diff. Transcriptomics MV/ctr | | Diff. Proteomics MV/ctr | |
|---|---|---|---|---|---|---|---|---|
| id | gene | product | locus_tag_NCTC8325 | gene_NCTC8325 | log2FoldChange | padj | log2FoldChange | padj |
| HG001_01585 | hemB | Delta-aminolevulinic acid dehydratase | SAOUHSC_01772 | - | 0,579 | 0,019809775 | -1,32 | 2,99E-02 |

| Transcription regulator | | | | | Diff. Transcriptomics MV/ctr | | Diff. Proteomics MV/ctr | |
|---|---|---|---|---|---|---|---|---|
| id | gene | product | locus_tag_NCTC8325 | gene_NCTC8325 | log2FoldChange | padj | log2FoldChange | padj |
| HG001_00022 | walR | Transcriptional regulatory protein WalR | SAOUHSC_00020 | - | 0,292 | 0,211077335 | -1,72 | 6,91E-02 |
| HG001_02667 | slyA_3 | Transcriptional regulator SlyA | SAOUHSC_02961 | - | 0,671 | 0,007078829 | -1,21 | 3,44E-01 |
| HG001_00061 | sarS | HTH-type transcriptional regulator SarS | SAOUHSC_00070 | - | 1,59 | 1,36E-13 | 0,05 | 9,33E-01 |
| HG001_02422 | sarZ | HTH-type transcriptional regulator SarZ | SAOUHSC_02669 | - | -1,10 | 1,11E-05 | -1,78 | 4,42E-01 |
| HG001_00607 | sarX | HTH-type transcriptional regulator SarX | SAOUHSC_00674 | - | -1,49 | 6,69E-10 | -0,93 | 2,86E-01 |
| HG001_02303 | sarV | HTH-type transcriptional regulator SarV | SAOUHSC_02532 | - | -1,83 | 1,02E-10 | ND | ND |
| HG001_02330 | sarR | HTH-type transcriptional regulator SarR | SAOUHSC_02566 | - | -1,93 | 2,59E-13 | -0,71 | 2,00E-01 |
| HG001_00556 | sarA | Transcriptional regulator SarA | SAOUHSC_00620 | - | -2,33 | 2,30E-20 | 0,31 | 2,99E-01 |

| Ethanol degradation | Diff. Transcriptomics MV/ctr | Diff. Proteomics MV/ctr |
|---|---|---|

| id | gene | product | locus_tag_NCTC8325 | gene_NCTC8325 | log2FoldChange | padj | log2FoldChange | padj |
|---|---|---|---|---|---|---|---|---|
| HG001_00118 | aldA | Putative aldehyde dehydrogenase AldA | SAOUHSC_00132 | - | 1,16 | 1,55433E-06 | -2,81 | 3,33E-02 |
| HG001_00099 | adhE | Aldehyde-alcohol dehydrogenase | SAOUHSC_00113 | - | **-3,99** | 1,68476E-54 | -1,78 | 4,42E-01 |
| HG001_00544 | adh | Alcohol dehydrogenase | SAOUHSC_00608 | adhA | **-2,96** | 9,54629E-47 | -1,10 | 2,42E-04 |
| HG001_01654 | acsA_1 | Acetyl-coenzyme A synthetase | SAOUHSC_01846 | - | **-1,49** | 1,85733E-09 | -1,78 | 4,42E-01 |
| HG001_01955 | alkH | Aldehyde dehydrogenase | SAOUHSC_02142 | - | **-1,89** | 2,51113E-15 | -0,31 | 4,11E-01 |

| tRNA charging | | | | | Diff. Transcriptomics MV/ctr | | Diff. Proteomics MV/ctr | |
|---|---|---|---|---|---|---|---|---|
| id | gene | product | locus_tag_NCTC8325 | gene_NCTC8325 | log2FoldChange | padj | log2FoldChange | padj |
| HG001_00407 | metG | Methionine--tRNA ligase | SAOUHSC_00461 | - | **1,55** | 1,42641E-11 | -0,10 | 7,39E-01 |
| HG001_01315 | asnS | Asparagine--tRNA ligase | SAOUHSC_01471 | asnC | **1,08** | 1,60743E-05 | -0,32 | 0,0861312 |
| HG001_01044 | ileS | Isoleucine--tRNA ligase | SAOUHSC_01159 | ileS | **1,08** | 0,000184868 | 0,07 | 0,6020900 |
| HG001_01679 | leuS | Leucine--tRNA ligase | SAOUHSC_01875 | leuS | **0,95** | 0,000494718 | 0,22 | 0,1775016 |
| HG001_00434 | lysS | Lysine--tRNA ligase | SAOUHSC_00493 | lysS | 0,683 | 0,004966781 | 0,30 | 0,0657212 |
| HG001_00547 | argS | Arginine--tRNA ligase | SAOUHSC_00611 | argS | 0,603 | 0,007896657 | 0,12 | 0,3623763 |
| HG001_01114 | proS | Proline--tRNA ligase | SAOUHSC_01240 | - | **0,80** | 0,000847588 | -0,23 | 0,2029304 |
| HG001_00457 | gltX | Glutamate--tRNA ligase | SAOUHSC_00509 | gltX | 0,472 | 0,055358849 | -0,02 | 0,9104106 |
| HG001_01601 | thrS | Threonine--tRNA ligase | SAOUHSC_01788 | thrS | -0,45 | 0,061656411 | -0,24 | 0,3307554 |
| HG001_01555 | hisS | Histidine--tRNA ligase | SAOUHSC_01738 | hisS | -0,686 | 0,011301763 | -0,51 | 0,1148211 |
| HG001_00010 | serS | Serine--tRNA ligase | SAOUHSC_00009 | - | **-0,80** | 0,000790321 | -0,08 | 0,6029672 |
| HG001_00842 | trpS | Tryptophan--tRNA ligase | SAOUHSC_00933 | - | **-0,97** | 8,54628E-05 | -0,54 | 0,0255249 |

Université de Strasbourg

**Laura ANTOINE**

École Doctorale des Sciences de la Vie et de la Santé STRASBOURG

# Caractérisation des modifications post-transcriptionnelles des ARN non codants chez *Staphylococcus aureus* en réponse à divers stress environnementaux : analyse dynamique et fonctionnelle

Les modifications post-transcriptionnelles des ARN sont impliquées dans de nombreux processus biologiques. Elles sont constitutives ou modulées en réponse à des processus adaptatifs et remplissent de nombreuses fonctions. La cartographie des modifications dans les ARN du pathogène *S. aureus*, responsable d'un grand nombre d'infections de gravité variable et touchant un large éventail de tissus, reste encore peu connue ainsi que leurs implications dans l'adaptation de la bactérie à son environnement, notamment lors de l'infection.

Cette étude a pour but principal dans un premier temps d'établir une cartographie des modifications présentes dans les ARN non codants, plus spécifiquement dans les ARNt de *S. aureus* puis de révéler la dynamique des modifications en adaptation à différentes conditions environnementales rencontrées par la bactérie lors de l'infection.

Enfin, l'étude des causes ainsi que des conséquences traductionnelles des changements observés pourra être réalisée afin de déterminer le potentiel rôle des modifications post-transcriptionnelles dans l'adaptation aux stress

Mots clés : Modifications post-transcriptionnelles, *Staphylococcus aureus*, adaptation au stress

RNA post-transcriptionnal modifications are involved in numerous biological processes. They are constitutive or modulated in response to adaptive processes and play multiple functions. The mapping of RNA modifications on the pathogen *S. aureus*, responsible for several infections of variable severity and targeting several tissues, is still poorly known, as well as their involvement in the host adaptation processes.

This study aims to produce a first map of modifications that are present on *S. aureus* non coding RNAs, especially *S.aureus* tRNA and to reveal the dynamics of some of these modifications in a stress condition encountered during the infection.

Finally, the mechanisms promoting different modification levels and the impact that these variations might have on the translation processes could be studied.

Keywords : Post-transcriptionnal modifications, *Staphylococcus aureus*, stress adaptation.